

THE JOURNAL OF PHYSICAL CHEMISTRY

(Registered in U. S. Patent Office)

Thor L. Smith: Application of Ice Calorimetry to Chemical Kinetics.....	385
Mack F. Hughes and George Richard Hill: Rate Law and Mechanism for the Oxidation of Carbon Monoxide over a Vanadium Oxide Catalyst.....	388
Robert S. Hansen, Frederick A. Miller and Sherril D. Christian: Activity Coefficients of Components in the Systems Water-Acetic Acid, Water-Propionic Acid and Water- <i>n</i> -Butyric Acid at 25°.....	391
Thomas D. Waugh, Harold F. Walton and John A. Laswick: Ionization Constants of Some Organomercuric Hydroxides and Halides.....	395
F. H. Healey, Yung-Fang Yu and J. J. Chessick: The Detection of Hydrophilic Heterogeneities on a Carbon Surface..	399
John D. Ferry, Malcolm L. Williams and Edwin R. Fitzgerald: Electrical Relaxation Distribution Functions in Polymers and their Temperature Dependence.....	403
Marvin L. Granstrom and Bernd Kahn: The Adsorption of Cesium in Low Concentration by Paper.....	408
Francis J. Hughes and Don S. Martin, Jr.: Kinetics of the Oxidation of Selenious Acid by Hydrogen Peroxide.....	410
J. Calvin Giddings and Henry Eyring: A Molecular Dynamic Theory of Chromatography.....	416
Leo Brewer and John Margrave: The Vapor Pressures of Lithium and Sodium Oxides.....	421
T. M. Reed, III: The Theoretical Energies of Mixing for Fluorocarbon-Hydrocarbon Mixtures.....	425
T. M. Reed, III: The Ionization Potential and the Polarizability of Molecules.....	428
Kōzō Shinoda: The Critical Micelle Concentrations in Aqueous Solutions of Potassium Alkyl Malonates.....	432
Sidney A. Greenberg and David Sinclair: The Polymerization of Silicic Acid.....	435
Joseph J. Jasper and George B. Miller: The Vapor Pressure of Monofluoroacetic Acid.....	441
E. L. Dougherty, Jr., and H. G. Drickamer: Thermal Diffusion and Molecular Motion in Liquids.....	443
Burton J. Thamer: The Spectrophotometric Determination of Dissociation Constants of Dibasic Acids. Methods Using a Minimum Amount of Data.....	450
E. P. Doane and H. G. Drickamer: The Effect of Pressure on the Solubility of Solids in Non-polar Liquids.....	454
C. W. Hoerr, R. A. Reck, Geraldine B. Corcoran and H. J. Harwood: Solubility Characteristics of Several Long-chain Methyl Alkyl Ketones in Common Organic Solvents.....	457
Paul B. Weisz: Chemical Reactivity of CF ₄ and C ₂ F ₄ Induced by Electrical Discharge.....	464
Leon J. Vieland and Ralph P. Seward: The Electrical Conductance of Weak Acids in Anhydrous Hydrazine.....	466
Erwin Fishman: Self-Diffusion in Liquid Normal Pentane and Normal Heptane.....	469
Gert Ehrlich: On the Kinetics of Chemisorption.....	473
Note: Joel R. Gutmann: The Exchange Reaction between Deuterium and Methylamines on Iron Powder.....	478
Communication to the Editor: Kenneth G. A. Pankhurst: Monolayer Structure as Revealed by Electron Microscopy.....	480

THE JOURNAL OF PHYSICAL CHEMISTRY

(Registered in U. S. Patent Office)

W. ALBERT NOYES, JR., EDITOR

ALLEN D. BLISS

ASSISTANT EDITORS

ARTHUR C. BOND

EDITORIAL BOARD

R. P. BELL

PAUL M. DOTY

S. C. LIND

E. J. BOWEN

G. D. HALSEY, JR.

H. W. MELVILLE

R. E. CONNICK

J. W. KENNEDY

W. O. MILLIGAN

R. W. DODSON

E. A. MOELWYN-HUGHES

Published monthly by the American Chemical Society at 20th and Northampton Sts., Easton, Pa.

Entered as second-class matter at the Post Office at Easton, Pennsylvania.

The *Journal of Physical Chemistry* is devoted to the publication of selected symposia in the broad field of physical chemistry and to other contributed papers.

Manuscripts originating in the British Isles, Europe and Africa should be sent to F. C. Tompkins, The Faraday Society, 6 Gray's Inn Square, London W. C. 1, England.

Manuscripts originating elsewhere should be sent to W. Albert Noyes, Jr., Department of Chemistry, University of Rochester, Rochester 3, N. Y.

Correspondence regarding accepted copy, proofs and reprints should be directed to Assistant Editor, Allen D. Bliss, Department of Chemistry, Simmons College, 300 The Fenway, Boston 15, Mass.

Business Office: Alden H. Emery, Executive Secretary, American Chemical Society, 1155 Sixteenth St., N. W., Washington 6, D. C.

Advertising Office: Reinhold Publishing Corporation, 430 Park Avenue, New York 22, N. Y.

Articles must be submitted in duplicate, typed and double spaced. They should have at the beginning a brief Abstract, in no case exceeding 300 words. Original drawings should accompany the manuscript. Lettering at the sides of graphs (black on white or blue) may be pencilled in, and will be typeset. Figures and tables should be held to a minimum consistent with adequate presentation of information. Photographs will not be printed on glossy paper except by special arrangement. All footnotes and references to the literature should be numbered consecutively and placed in the manuscript at the proper places. Initials of authors referred to in citations should be given. Nomenclature should conform to that used in *Chemical Abstracts*, mathematical characters marked for italic, Greek letters carefully made or annotated, and subscripts and superscripts clearly shown. Articles should be written as briefly as possible consistent with clarity and should avoid historical background unnecessary for specialists.

Symposium papers should be sent in all cases to Secretaries of Divisions sponsoring the symposium, who will be responsible for their transmittal to the Editor. The Secretary of the Division by agreement with the Editor will specify a time after which symposium papers cannot be accepted. The Editor reserves the right to refuse to publish symposium articles, for valid scientific reasons. Each symposium paper may not exceed four printed pages (about sixteen double spaced typewritten pages) in length except by prior arrangement with the Editor.

Remittances and orders for subscriptions and for single copies, notices of changes of address and new professional connections, and claims for missing numbers should be sent to the American Chemical Society, 1155 Sixteenth St., N. W., Washington 6, D. C. Changes of address for the *Journal of Physical Chemistry* must be received on or before the 30th of the preceding month.

Claims for missing numbers will not be allowed (1) if received more than sixty days from date of issue (because of delivery hazards, no claims can be honored from subscribers in Central Europe, Asia, or Pacific Islands other than Hawaii), (2) if loss was due to failure of notice of change of address to be received before the date specified in the preceding paragraph, or (3) if the reason for the claim is "missing from files."

Subscription Rates: to members of the American Chemical Society, \$8.00 for 1 year, \$15.00 for 2 years, \$22.00 for 3 years; to non-members, \$10.00 for 1 year, \$18.00 for 2 years, \$26.00 for 3 years. Postage free to countries in the Pan American Union; Canada, \$0.40; all other countries, \$1.20. \$12.50 per volume, foreign postage \$1.20, Canadian postage \$0.40; special rates for A.C.S. members supplied on request. Single copies, current volume, \$1.00; foreign postage, \$0.15; Canadian postage \$0.05. Back issue rates (starting with Vol. 56): \$15.00 per volume, foreign postage \$1.20, Canadian, \$0.40; \$1.50 per issue, foreign postage \$0.15, Canadian postage \$0.05.

The American Chemical Society and the Editors of the *Journal of Physical Chemistry* assume no responsibility for the statements and opinions advanced by contributors to THIS JOURNAL.

The American Chemical Society also publishes *Journal of the American Chemical Society*, *Chemical Abstracts*, *Industrial and Engineering Chemistry*, *Chemical and Engineering News*, *Analytical Chemistry*, and *Journal of Agricultural and Food Chemistry*. Rates on request.

THE JOURNAL OF PHYSICAL CHEMISTRY

(Registered in U. S. Patent Office) (Copyright, 1955, by the American Chemical Society)

VOLUME 59

MAY 17, 1955

NUMBER 5

APPLICATION OF ICE CALORIMETRY TO CHEMICAL KINETICS

BY THOR L. SMITH¹

Contribution from Experiment Station, Hercules Powder Company, Wilmington, Delaware

Received September 13, 1954

Rate constants of slow reactions can be determined by measuring the rate of heat evolution with an ice calorimeter. This method is especially valuable for measuring rates of heterogeneous reactions, since the usual physical and chemical methods for following homogeneous reactions are often inapplicable. As illustrative examples, the determination of the rate constant for the hydrolysis and alcoholysis of acetic anhydride and for the fibrous acetylation of cellulose are described. Rate constants accurate to 5% or better were calculated from the measured rates of heat evolution.

Introduction

Various modifications of the Bunsen ice calorimeter² have been used to measure a wide variety of thermochemical quantities,³⁻⁸ but to date it appears that such calorimeters have not been employed in kinetic studies. This investigation was made to demonstrate that rate constants at 0° of certain reactions, both homogeneous and heterogeneous, can be evaluated with satisfactory accuracy by measuring the rate of heat evolution with an ice calorimeter. The calorimetric technique is especially valuable for measuring rates of heterogeneous reactions, since many of the usual physical methods of following the extent of reactions are inapplicable to two phase systems, and chemical methods are tedious and require the obtaining of representative samples for analysis.

Experimental

Apparatus.—The calorimeter assembly, shown schematically in Fig. 1, is constructed of glass. Its main components are an outer jacket A, a cap B and an inner, Dewar-type vessel C. The cap and outer jacket have ground-glass flanges which are held together securely with a metal

clamp (not shown). The cap has a Tru-bore bearing H, a tube for adding reagents F and another tube G, through which passes a short piece of rubber tubing I, which connects the inner vessel with a semi-microburet J. The inner vessel is held in place by a spacer E, which is asbestos tape sealed in place with an asphalt sealing cement. The Dewar-type inner vessel and attached buret are filled with gas-free distilled water. The protrusions M serve to hold the ice mantle N in place, increase the rate of heat transfer, and act as breaker bars when a slurry is being stirred in the calorimeter. Some type of drying agent L is placed in the bottom of the outer jacket to keep the air in the annular space dry and prevent fogging of the glass surfaces.

Procedure.—The calorimeter is placed in a cold water-bath or a 0–5° room until the water in the calorimeter is in the vicinity of 0°. Then, the cap and stirrer K are removed from the calorimeter and a stream of cold air or nitrogen is directed into the bottom of the inner vessel. The cold air is produced by passing air through a coil of copper tubing immersed in a Dry Ice-acetone bath. As a mantle of ice starts to freeze around the inner glass wall, the tube admitting the cold air is raised several inches so that ice will freeze higher in the calorimeter. An ice mantle like the one sketched in Fig. 1 can be formed readily.

After the mantle is frozen, the desired materials are added to the calorimeter, the cap with stirrer is fastened in position, the semi-microburet attached and filled with water, and the apparatus placed in a 0° bath of crushed ice and water. If the bath is well insulated and has a suitable cover, calorimetric measurements can be extended over long periods. The stirrer K is attached to an electronically controlled d.c. motor⁹ which should be set at low speeds, as the heat generated by the stirrer is appreciable.

The rate of heat leakage into the calorimeter is established by taking volume readings on the buret with time. In the absence of stirring, the heat leakage is often about 0.10 cal./min. or less. If a slurry is agitated by the stirrer at 1–2 revolutions per second, the heat leakage is about 0.20 cal./minute or higher.

After the rate of heat leakage is established, the reagent or catalyst, cooled to 0°, needed in order to start the chemi-

(1) Jet Propulsion Laboratory, California Institute of Technology, Pasadena, California.

(2) R. Bunsen, *Ann. Physik.*, **141**, 1 (1870).

(3) (a) D. C. Ginnings and R. J. Corruccini, *J. Research Natl. Bur. Standards*, **38**, 583 (1947); (b) H. T. Spengler and W. S. Tamplin, *Anal. Chem.*, **24**, 941 (1952).

(4) W. A. Patrick and C. E. Greider, *THIS JOURNAL*, **29**, 1031 (1925).

(5) D. C. Ginnings, T. B. Douglas and A. F. Ball, *J. Research Natl. Bur. Standards*, **45**, 23 (1950).

(6) W. Heiber and F. Mühlbauer, *Z. anorg. allgem. Chem.*, **186**, 97 (1930).

(7) W. Swietoslawski, "Microcalorimetry," Reinhold Publ. Corp., New York, N. Y., 1946, pp. 66–69.

(8) W. Heiber and E. Reindl, *Z. Elektrochem.*, **46**, 556 (1940).

(9) Electronic Controlled GT-21 Laboratory Mixer, manufactured by G. H. Heller Co., Baltimore, Maryland.

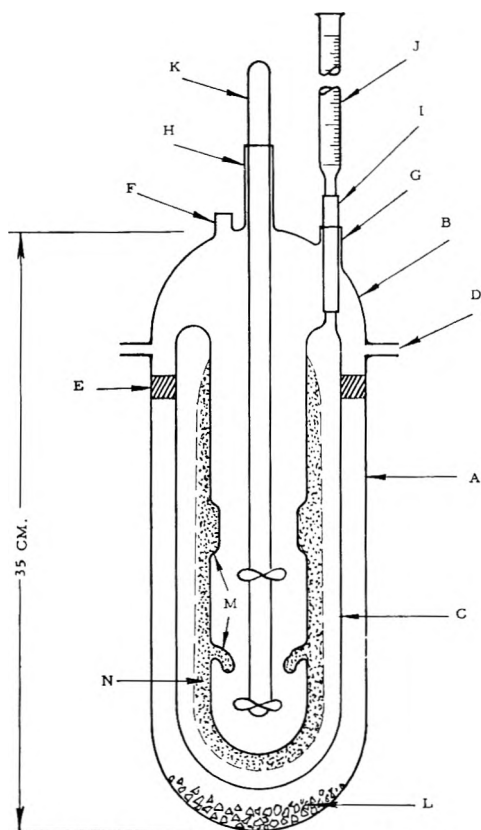


Fig. 1.—Schematic diagram of ice calorimeter.

cal reaction is added. Volume readings on the buret are then taken periodically. If the reaction can be followed to completion or if some reagent can be added to stop the reaction when desired, a rate of heat leakage at the end of the reaction can be obtained.

The rate of hydrolysis and alcoholysis of acetic anhydride and the heat of dilution of sulfuric acid, discussed below, were measured in a larger calorimeter of slightly different design than the one shown in Fig. 1. The heat leakage into this larger model was greater than into the model shown in Fig. 1, which was used to measure the heterogeneous acetylation of cellulose, also discussed below.

Materials.—Reagent grade acetic anhydride containing by analysis 99.3% anhydride was used in the hydrolysis and alcoholysis reaction.

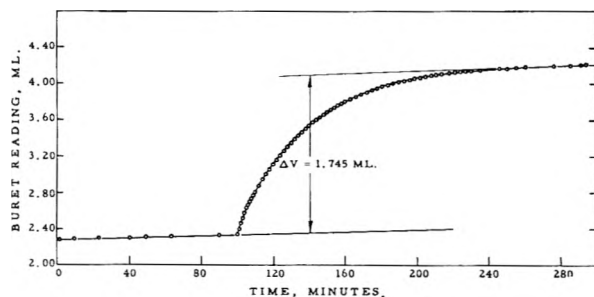


Fig. 2.—Buret reading-time curve obtained from hydrolysis of acetic anhydride.

Du Pont synthetic methanol which contained about 0.1% water by Karl Fischer analysis was used.

An acetylation grade wood pulp which had been finely cut in a Wiley mill was used in the fibrous acetylation reaction.

Hydrolysis of Acetic Anhydride.—After an ice mantle was frozen, 350 g. of water was placed in the calorimeter and volume-time readings were taken for 100 minutes in order to establish the rate of heat leakage. Then, 10.8 g. of 99.3% acetic anhydride, cooled to 0°, was added, giving

a 0.3 M solution. Volume-time readings were taken periodically for 200 minutes. The resulting rate data are shown in Fig. 2. The pre-reaction heat leakage was 0.53 cal./minute and the post-reaction heat leakage 0.62 cal./minute. Better agreement could have been obtained between the two heat leakage rates using the calorimeter described above, instead of the earlier model.

Alcoholysis of Acetic Anhydride.—The same procedure was followed as for the hydrolysis of acetic anhydride. Three hundred and fifty grams of methanol containing 0.2% pyridine as catalyst for the alcoholysis was placed in the calorimeter. After the rate of heat leakage was established, 10.8 g. of 99.3% acetic anhydride was added, giving a 0.28 M solution. The mixing of anhydride with methanol is accompanied by a positive heat of mixing which accounts for the sudden volume change, shown in Fig. 3, that occurred upon the addition of anhydride. The volume-time readings were taken periodically for 430 minutes and are shown in Fig. 3.

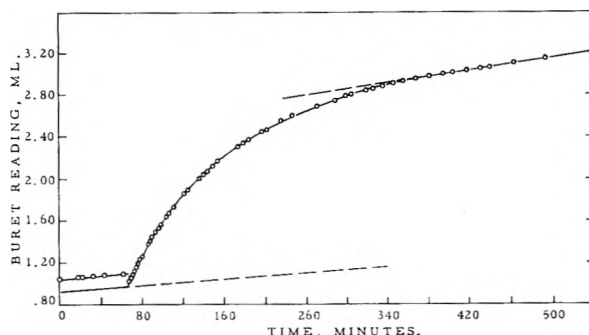


Fig. 3.—Buret reading-time curve obtained from pyridine-catalyzed alcoholysis of acetic anhydride.

Fibrous Acetylation of Cellulose.—Five grams of acetylation grade wood pulp which had been pretreated by steeping in acetic acid vapors for several days was placed in the calorimeter along with 150 g. of acetic anhydride. The stirring motor was set at 1.6 revolutions per second. The rate of heat leakage was found to be 0.023 cal./min. Next, a solution of methanesulfonic acid in acetic anhydride was added, giving a 0.0032 M solution of methanesulfonic acid which catalyzed the fibrous acetylation. Volume-time readings were taken periodically for about 570 minutes at which time an acetic acid solution of sodium acetate was added to neutralize the methanesulfonic acid catalyst. A post-reaction heat leakage of 0.024 cal./min. was measured, which is sensibly the same as the pre-reaction rate of heat leakage. The volume-time readings are shown in Fig. 4; the addition of the sodium acetate solution caused a sudden volume change since the solution had not been cooled to 0°.

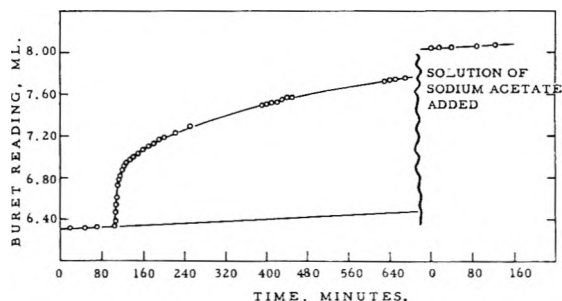


Fig. 4.—Buret reading-time curve obtained from fibrous acetylation of cellulose.

Heat of Dilution of H₂SO₄.—The heat of dilution of H₂SO₄ from 66.1 to 27.1% was measured by adding 138 g. of 66.1% H₂SO₄ to 200 g. of water in the calorimeter, producing a 27.1% solution. A heat of dilution of 5,370 cal./mole was obtained which agrees closely with 5,350 cal./mole calculated from the relative apparent molal heat contents of H₂SO₄ at 25° and heat capacity data of Craig and Vinal.¹⁰

(10) D. N. Craig and George W. Vinal, *J. Research Natl. Bur. Standards*, **24**, 475 (1940).

The temperature decrease with time of the 27.1% H₂SO₄ solution prepared in the calorimeter was measured with a copper-constantan thermocouple and could be expressed by the relation $T = T_0 e^{-0.33t}$, where T and T_0 are expressed in degrees centigrade and t in minutes. From this relation, the rate of heat transfer under specified conditions can be calculated.

Results

Hydrolysis of Acetic Anhydride.—The hydrolysis of acetic anhydride in dilute solution is a pseudo-unimolecular reaction with a half-life of 26 minutes.¹¹ Thus, the experimental rate data, shown in Fig. 2, can be expressed by the equation

$$\frac{V_t - V_\infty}{V_0 - V_\infty} = e^{-kt} \quad (1)$$

where k is the rate constant, t the time, V_t , V_0 and V_∞ are the volume readings at time t , zero time and infinite time, respectively. All volume readings must be corrected for the volume change caused solely by the heat leakage into the calorimeter. Thus, $V_t = V'_t - V_d$ where V'_t is the actual volume reading at time t and V_d the volume obtained by extrapolating the line representing heat leakage.

There is some uncertainty in measuring V_0 and V_∞ directly. The observed value of V_0 may be in error due to the heat of mixing of reagents, while values of V_∞ often cannot be obtained accurately due to the slow reaction rate near the completion of the reaction. However, the method of Guggenheim¹² can be used to calculate k without knowing V_0 and V_∞ .

Guggenheim showed that the following equation can be derived readily from equation 1

$$\ln(V_{t+\tau} - V_t) = \ln(V_\infty - V_0)(1 - e^{-k\tau}) - kt \quad (2)$$

where τ is an arbitrary constant, preferably more than twice the half-life of the reaction.

Figure 5 shows a Guggenheim plot, derived from the data shown in Fig. 2, using τ equal to 60 minutes. The slope of the line gives a half-life of 26.7 minutes. A duplicate experiment gave a half-life of 25.0 minutes. Thus, the half-life from either experiment differs by 4% from the value determined dilatometrically.¹¹

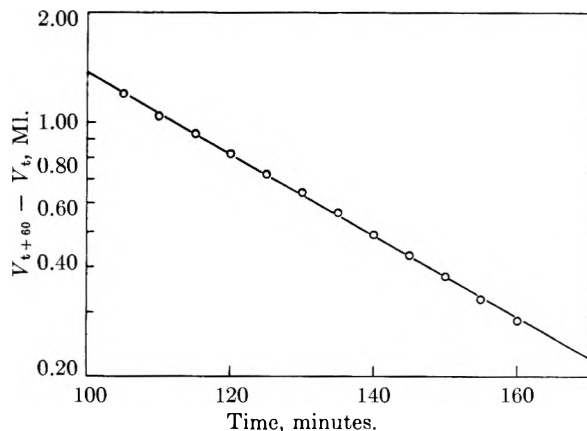


Fig. 5.—Guggenheim plot of rate data for hydrolysis of acetic anhydride.

The heat of hydrolysis can also be calculated from the data shown in Fig. 2. The total volume

(11) Martin Kilpatrick, *J. Am. Chem. Soc.*, **60**, 2891 (1928).

(12) E. A. Guggenheim, *Phil. Mag.*, Vol. II, 7th series, 538 (1926).

change during the reaction is 1.745 ml., but part of this volume change is caused by the heat of mixing of anhydride with water. Since the half-life of the reaction was found to be 26.7 minutes, the volume change during the last half of the reaction, *i.e.*, 0.82 ml., can be used to calculate the reaction heat. Since a total of 10.8 g. of 99.3% acetic anhydride was hydrolyzed, the heat of reaction is calculated to be 13,700 cal./mole, using 0.0906 ml./g. for the volume change when ice melts and 79.7 cal./g. for the heat of fusion of ice. In the duplicate experiment, the heat of reaction was found to be 14,100 cal./mole. The heat for the hydrolysis reaction at 30° has been reported¹³ to be 13,960 cal./mole.

Alcoholysis of Acetic Anhydride.—The rate data for the reaction of acetic anhydride with methanol containing 0.2% pyridine as catalyst are shown in Fig. 3. A Guggenheim plot of these data, setting τ equal to 100 minutes, is shown in Fig. 6. The half-life is 64.0 minutes and a duplicate experiment gave 65.0 minutes.

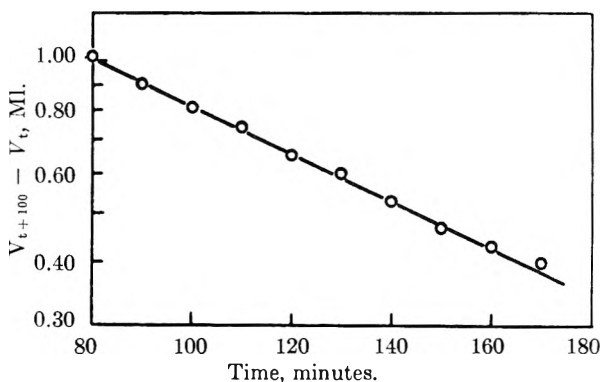


Fig. 6.—Guggenheim plot of rate data for pyridine-catalyzed alcoholysis of acetic anhydride.

The rate of the alcoholysis was measured in a 25-ml. dilatometer and the half-life was found to be 62.0 minutes. Thus, the agreement between the results obtained by the two methods is 3–5%.

The heat of alcoholysis was calculated from the data of the two experiments to be 14,800 and 15,400 cal./mole.

Fibrous Acetylation of Cellulose.—Perhaps the most valuable use of the calorimeter in kinetics is for the study of heterogeneous reactions. As a typical example, data for the acetylation of wood-pulp cellulose is shown in Fig. 4.

Part of the heat released following the addition of methanedisulfonic acid is due to the acid-catalyzed reaction of acetic anhydride with the water in the wood pulp. Consequently, only the data obtained 30 minutes subsequently to adding the catalyst were analyzed. The Guggenheim plot, with τ equal to 400 minutes, gave a straight line whose slope corresponded to a half-life of 172 minutes. No reliable rate data obtained by an independent method are available for comparison.

Discussion

It has been demonstrated that rate constants of certain homogeneous and heterogeneous reactions

(13) J. B. Conn, G. B. Kistiakowsky, R. M. Roberts and E. A. Smith, *J. Am. Chem. Soc.*, **64**, 1747 (1942).

can be measured accurately and conveniently using an ice calorimeter. Only one factor limits the applicability of the calorimetric method: The rate of heat transfer from a reaction mixture into the ice mantle must be large compared with the rate of heat evolution from the chemical reaction. When this condition is fulfilled, the temperature of the reaction mixture will remain close to 0°, and the rate of ice melting will be directly proportional to the rate of the reaction.

The rate of heat transfer in the calorimeter used to measure the rate of hydrolysis and alcoholysis of acetic anhydride can be calculated from temperature-time data obtained while measuring the heat of dilution of sulfuric acid. Using the equation found, $T = T_0 e^{-0.33t}$ (see Experimental Section), the heat transfer rate from the calorimeter containing 340 g. of 27.1% H₂SO₄ at 0.5° is calculated

to be 44 cal./minute. In the hydrolysis of acetic anhydride, the rate of heat formation at the beginning of the reaction, calculated from the rate constant and the amount present, was 37 cal./minute. Thus, even at the beginning of the reaction, the temperature should remain less than 0.5°. Actually, a single junction copper-constantan thermocouple placed in the reaction mixture indicated that sensibly no temperature increase occurred.

Although chemical reactions do not take place isothermally in an ice calorimeter, the temperature rise often can be kept below 0.5° by proper choice of reagent concentration and by constructing the inner tube of the calorimeter of metal. Unless highly precise data are desired, a temperature rise of 0.5° is not serious, since less than 5% error will be introduced in the rate constant if the activation energy is 15 kcal./mole.

RATE LAW AND MECHANISM FOR THE OXIDATION OF CARBON MONOXIDE OVER A VANADIUM OXIDE CATALYST^{1,2}

BY MACK F. HUGHES² AND GEORGE RICHARD HILL

Contribution from the Department of Fuel Technology, University of Utah, Salt Lake City, Utah

Received September 28, 1954

A flow system has been employed to study the kinetics of the oxidation of carbon monoxide over a vanadium oxide catalyst. The concentration of oxygen and carbon dioxide had no effect on the rate of oxidation, but the partial pressure effect of carbon monoxide resulted in a dependence similar to a unimolecular surface reaction. A mechanism is proposed which consists of the following steps: adsorption of carbon monoxide, desorption of carbon dioxide, oxygen regeneration of the catalyst. The heats of activation for the adsorption and desorption steps were 28.4 and 6.2 kcal. per mole, respectively. Assuming the entropy of activation for the desorption step to be zero, it was found that there were 20 active sites per square centimeter. The entropy of activation for the desorption of carbon monoxide was -39 cal. deg.⁻¹ mole⁻¹. This entropy was calculated on the basis of one gram of catalyst or 240 square meters of surface area.

Introduction

Vanadium oxide-type catalysts are extensively used for the selective catalytic oxidation of hydrocarbons. This type of catalyst is also employed in most of the contact sulfuric acid plants. A great deal of research has been carried out to develop better vanadium oxide catalysts and to determine their optimum operating conditions for a specific reaction. Most of this research has been carried out from an empirical approach. However, a few investigators have attacked this catalytic problem from a fundamental standpoint. Notable among the fundamental work is that of Simard,³ whose recent results showed that the active surface of a vanadium oxide catalyst consisted of a dynamic system of V⁴⁺, V⁵⁺ and O⁻² ions. At most, these ions were associated in three forms, namely, V₂O₄, V₂O_{4.34}, (V₁₂O₂₆) and V₂O₅. These observations agree with the thermodynamic⁴ and

crystallographic⁵ properties of the vanadium-oxygen system.

The purpose of this investigation was to determine the part that the vanadium oxide plays in a catalytic oxidation process. To accomplish this, a kinetic investigation of the catalytic oxidation of carbon monoxide was carried out and a reaction mechanism was postulated which explained the kinetic data.

Experimental

1. **Materials.**—The catalyst was a pelletized vanadium oxide catalyst (Code No. 903) supplied by Davison Chemical Company. The surface area of the catalyst was 240 m.²/g.; it was determined by the B.E.T. method⁶ using water. In the calculation, 10.8 Å.² was the value used for the molecular area of a water molecule. The carbon monoxide was obtained from the Matheson Company. This gas was of sufficient purity to use without further treatment, as was demonstrated by analysis with the infrared spectrometer. Also, the rate of the reaction was not affected by additional drying of the carbon monoxide or by adding carbon dioxide to the reactant mixture. Air was the source of oxygen in all runs except when the effect of oxygen concentration was being studied. The air was cleaned by passing it through silica gel, sulfuric acid and Ascarite columns.

2. **Apparatus.**—The reactor consisted of a preheating coil and a reaction chamber. The preheating coil was made out of 0.8 cm. Pyrex tubing and was 55 cm. long; this was sufficient to heat the reactants to the reaction tem-

(1) This paper is based on a portion of a thesis submitted by Mack F. Hughes in partial fulfillment of the requirements for the degree of Doctor of Philosophy in the Graduate School of the University of Utah, August, 1954. This investigation was supported in part by the University of Utah Research Committee and in part by the Office of Naval Research.

(2) California Research Corporation.

(3) G. L. Simard, presented at the Conference on Catalysts, American Association for the Advancement of Science, Colby, N. H., June 1951.

(4) N. P. Allen, O. Kubaschewski and O. von Goldbeck, *J. Electrochem. Soc.*, **98**, 417 (1951).

(5) F. Aebi, *Helv. Chim. Acta*, **31**, 8 (1948).

(6) S. Brunauer, P. H. Emmett and E. Teller, *J. Am. Chem. Soc.*, **60**, 309 (1938).

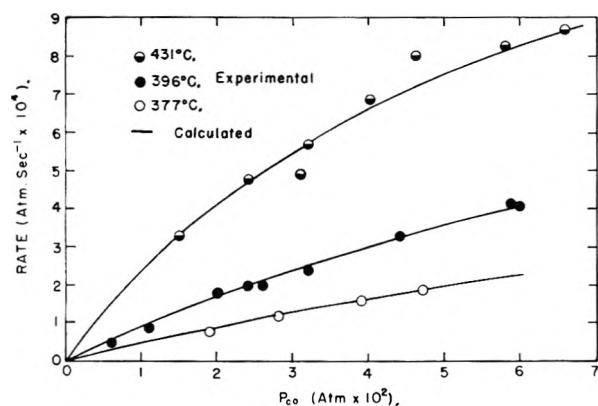


Fig. 1.—Rate of carbon dioxide formation versus P_{CO} .

perature before leaving the preheater. A Pyrex cylinder filled with glass spheres was included in the preheater to ensure that the reactants were at the reaction temperature. The reaction chamber was rectangular in shape. It was only 0.9 cm. thick, which was the length of two catalyst pellets. With this type of design the heat of the reaction could be liberated efficiently, since the maximum distance from the center of the reaction bed to the liquid bath was only 0.45 cm. At the base of the reaction chamber was a rectangular fritted glass disc, which supported the catalyst and evenly dispersed the reactants over the catalyst. The temperature of the reaction was measured by a chromel-alumel thermocouple suspended in the catalyst bed. The entire reactor was heated by a molten metal bath.

A low melting alloy, American Smelting and Refining Company No. 158-194, was employed in the metal-bath. The temperature of the metal-bath was measured and controlled by a Brown Temperature Controller-Recorder. The accuracy of the temperature readings is estimated to be $\pm 1^\circ$. With this reactor design, there was no detectable temperature differences between the catalyst bed and the metal bath.

3. Procedure.—As the catalyst was coming to operating temperature, the rate of flow and composition of the reactant mixture were set at the values at which the experiment was to be carried out. In general the rate of flow was either 250 or 500 ml. min.^{-1} at 25° and 65 cm. It was necessary to limit the initial concentration of carbon monoxide to 0-10 volume per cent. since higher concentrations caused the activity of the catalyst to decrease by overreducing the vanadium oxide.

Before any rate measurements were made, the system was brought to a steady state condition. This was accomplished by pretreating the catalyst for eight hours under the conditions that the rate measurements were to be made. This time was found to be sufficient for the catalyst to attain steady state conditions. Since the system was at operating conditions at the end of the pretreatment period, a sample of the products was withdrawn. To accomplish this, a gas sampling bulb and connecting tube filled with acidified water were connected to the manifold, and the sample was allowed to displace the water. The same procedure was used to transfer the sample from the sample bulb to the Fisher Precision Gas-Analysis Unit, where analysis was made for carbon dioxide, oxygen and carbon monoxide. During the time the sample was being withdrawn, the following readings were taken: Barometric pressure, pressure in the reactor, temperature of the catalyst bed, temperature of the metal-bath and the rate of flow of carbon monoxide, air and the products. In all cases the flow rate was corrected to 0° and 76 cm. of Hg, and the rate of carbon dioxide formation was calculated at this condition.

Results

To determine the effect of the partial pressure of carbon monoxide in the reactants, a series of rate isotherms were made at three different temperatures. The results of these studies are presented in Fig. 1. The partial pressure of carbon monoxide versus rate curves are typical rate curves for surface reactions involving one molecule of a single

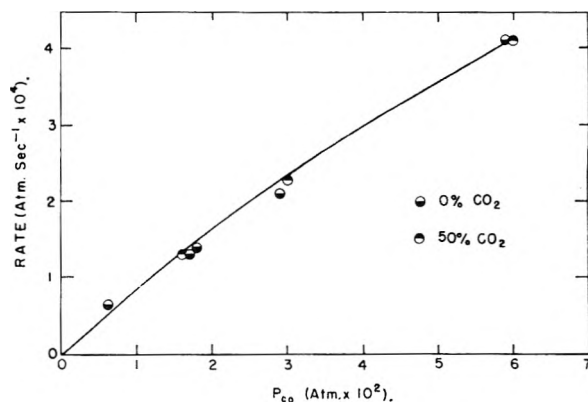


Fig. 2.—Rate of carbon dioxide formation versus P_{CO} with 0% CO_2 and 50% CO_2 in the reaction mixture.

reactant. The points are experimental results and the solid lines are calculated.

No appreciable change in the rate of carbon monoxide oxidation took place when the partial pressure of oxygen in the reactant mixture was varied. The oxygen concentration was varied by changing the oxygen-nitrogen ratio in the reactant mixture. The partial pressure range of oxygen investigated was from 0.008 to 0.64 atm. It is evident from these results that the rate of carbon dioxide formation is independent of oxygen concentration down to a partial pressure of 0.008 atm.

Two rate isotherms were made to determine the effect of carbon dioxide concentration on the rate of the reaction (Fig. 2). Both runs were made at 396° . For one isotherm the reaction mixture contained no carbon dioxide, while the reaction mixture for the other isotherm was 50% carbon dioxide by volume. For a given carbon monoxide concentration, both isotherms yielded the same rate of carbon dioxide formation.

Discussion

Under the conditions of these experiments, the oxidation of carbon monoxide on a vanadia catalyst was found to obey a rate law which is typical for a unimolecular surface reaction (Fig. 1). That is

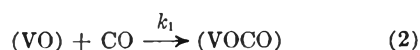
$$\text{rate} = \frac{AP_{CO}}{1 + BP_{CO}} \quad (1)$$

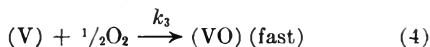
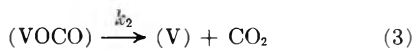
where A and B are empirical constants and P_{CO} is the partial pressure of carbon monoxide in the reactant mixture. Values obtained for A , B and A/B are tabulated in Table I. These values correspond to a surface area of $9.6 \times 10^3 \text{ m.}^2$ or 40 g. of catalyst.

TABLE I
EXPERIMENTAL RATE CONSTANTS FOR THE OXIDATION OF CARBON MONOXIDE ON A VANADIA CATALYST

Temp., $^\circ\text{C.}$	A , $\text{sec.}^{-1} \times 10^3$	B , atm.^{-1}	A/B , $\text{atm. sec.}^{-1} \times 10^3$
377	4.8	4.2	1.1
396	9.3	6.3	1.5
431	27.8	16.7	1.7

A mechanism that accounts for the experimentally observed facts is





In these equations, the parentheses indicate a surface species. VOCO is a species produced by the adsorption of carbon monoxide on a VO surface site. V is a surface site deficient in oxygen due to the desorption of carbon dioxide, and k_1 , k_2 and k_3 are the specific reaction rate constants for the adsorption, desorption and oxygen regeneration processes, respectively. Since the catalyst maintained its activity, and the rate of oxidation was independent of oxygen concentration, the oxygen regeneration step must be much faster than the steps indicated by equations 2 and 3. This mechanism yields a surface which is essentially composed of two species—VO and VOCO.

According to this mechanism, the rate of carbon dioxide formation is proportional to the number of VOCO sites and may be written as

$$\text{Rate} = k_2 k' \theta \quad (5)$$

In this equation, θ represents the fraction of the surface occupied by VOCO sites, and k' is a constant which includes the fraction of VOCO sites which are capable of decomposing at any instant and also includes a conversion factor for changing the fraction of the surface covered to the true surface concentration. In order to obtain an expression for θ which can be determined experimentally, the steady state treatment may be used.

According to the steady state hypothesis, the concentration of the adsorbed species is invariant with time, *i.e.*, $d\theta/dt = 0$. Thus, the species (VOCO) is being produced by the adsorption process at the same rate it is being removed by the desorption process. Hence

$$\frac{d\theta}{dt} = k_1 k' (1 - \theta) P_{\text{CO}} - k_2 k' \theta = 0 \quad (6)$$

where $(1 - \theta)$ is the fraction of the surface covered by VO sites. The specific reaction rate constants, k_1 and k_2 , are functions of θ of an unknown type. However, these constants will be assumed independent of θ in the subsequent treatment.

On the assumption that the rate constants are independent of θ , the expression for θ becomes

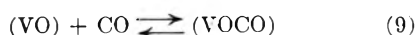
$$\theta = \frac{k_1 P_{\text{CO}}}{k_2 + k_1 P_{\text{CO}}} \quad (7)$$

Therefore, the rate law for the oxidation of carbon monoxide becomes

$$\text{rate} = \frac{k_1 k' P_{\text{CO}}}{1 + (k_1/k_2) P_{\text{CO}}} \quad (8)$$

This equation is of the same form as equation 1. According to this mechanism, A is equal to $k_1 k'$ and B is equal to k_1/k_2 .

An equilibrium treatment yielded to a rate expression similar to equation 1. Therefore, this treatment was considered to elucidate the experimental results. In the equilibrium treatment the first reaction (equation 2) was assumed to be in a state of equilibrium, *i.e.*



In this case the expression for the rate is

$$\text{rate} = \frac{k_2 k' K P_{\text{CO}}}{1 + K P_{\text{CO}}} \quad (10)$$

where K is the equilibrium constant for the adsorption reaction. If this mechanism is correct, $A \equiv k_2 k' K$ and $B \equiv K$.

It is evident from the values of B in Table I that the equilibrium constant increases with temperature. This indicates that for a given pressure of carbon monoxide the amount of carbon monoxide adsorbed increases with an increase in temperature. For this to be true the adsorption process would be endothermic. Such a process would not occur. Therefore, the equilibrium mechanism can be ruled out. Similar non-equilibrium results have been observed in the copper oxide, carbon monoxide and oxygen system.^{7,8}

Attempts were also made to explain the experimental results by other mechanisms. Assuming the desorption of carbon dioxide (equation 3) to be at equilibrium resulted in a rate law which was dependent on the carbon dioxide concentration. Experimentally, the rate was independent of the carbon dioxide concentration.

A mechanism which involved the diffusion of oxygen atoms on the surface of the catalyst yielded a rate expression similar to equation 1. For this mechanism, A/B is equal to $k_{1d} k_2 / (k_{1d} + k_2)$. Here, k_{1d} is the specific reaction rate constant for a diffusion step— $(\text{V}'\text{O}) + (\text{V}) \rightarrow (\text{VO}) + (\text{V}')$. In this reaction the primed sites are surface sites that will not react with carbon monoxide. If the rate of the reaction was influenced by the diffusion step, a plot of $\log A/B$ vs. $1/T$ would be linear only when very special conditions exist. Yet this plot was linear in the temperature range investigated.

Another mechanism of interest is one in which the rate of desorption of carbon monoxide is significant. This mechanism resulted in the rate law

$$\text{rate} = \frac{k_1 k' P_{\text{CO}}}{1 + \frac{k_{-1}}{k_2} + \frac{k_1 P_{\text{CO}}}{k_2}} \quad (11)$$

In this equation, k_{-1} is the rate constant for desorption of carbon monoxide, *i.e.*, $(\text{VOCO}) \xrightarrow{k_{-1}} (\text{VO}) + \text{CO}$, and the other constants have the same definitions as before. According to this mechanism, the values for A in Table I are equal to $k' k_1 k_2 / (k_2 + k_{-1})$. Therefore, plotting these values versus $1/T$ would yield a straight line only when the heats of activation for the desorption of CO and CO₂ were essentially the same or when $k \gg k_{-1}$. The latter case reduces to the mechanism shown by equations 2, 3 and 4. From the heats and entropies of activation for the adsorption of CO (eq. 2) and desorption of CO₂ (eq. 3) it may be seen that the heats of activation for the desorption of CO and CO₂ would not be the same. Since a plot of $\log A$ vs. $1/T$ is linear, this mechanism does not explain the experimental results.

Considering the mechanism shown in equations 2, 3 and 4 to be correct and employing the absolute reaction rate theory the constant, k' , and the heats and entropies of activation for steps 1 and 2 may

(7) W. E. Garnor, T. J. Gray and E. S. Stone, *Faraday Soc. Disc.*, No. 8, 246, 298 (1950).

(8) G. M. Schwab, *ibid.*, No. 8, 298 (1950).

be evaluated. According to the absolute reaction rate theory⁹

$$k_1 = \kappa \frac{kT}{h} \exp\left(\frac{-\Delta H_1^\ddagger}{RT}\right) \exp\left(\frac{\Delta S_1^\ddagger}{R}\right) \quad (12)$$

In this equation, k_1 is the rate constant; k , Boltzmann's constant; h , Planck's constant; T , absolute temperature; κ , transmission coefficient, R , the gas constant; ΔH_1^\ddagger and ΔS_1^\ddagger are the heat and entropy of activation for the adsorption process, respectively. A plot of $\log k_1 k_2 / T$ vs. $1/T$ was linear. From the slope of this line the heat of activation, ΔH_1^\ddagger was found to be 28.4 kcal. per mole.

The heat of activation for the desorption of carbon dioxide, ΔH_2^\ddagger , was determined from the $\log k_1/k_2(\log B)$ versus $1/T$ plot. The slope of the line is equal to $-(\Delta H_1^\ddagger - \Delta H_2^\ddagger)/4.576$. This yielded a value of 22.2 kcal. per mole for $(\Delta H_1^\ddagger - \Delta H_2^\ddagger)$; therefore, ΔH_2^\ddagger is 6.2 kcal./mole.

The entropies of activation for the two reactions—adsorption and desorption processes—cannot be calculated directly from equation 12 because the factors in the products $k_1 k'$ and $k_2 k'$ cannot be separated. However, it is interesting to note what the magnitude of k' and ΔS_1^\ddagger should be in terms of the proposed mechanism. In order to do this a value for ΔS_2^\ddagger has to be assumed.

(9) S. Glasstone, K. J. Laidler and H. Eyring, "The Theory of Rate Processes," McGraw-Hill Book Co., Inc., New York, N. Y., 1941.

The value of ΔS_2^\ddagger should be very small since it represents the entropy change in going from an adsorbed molecule to an activated complex on the surface. Therefore, ΔS_2^\ddagger was assumed to be zero in this semi-quantitative analysis of k' and ΔS_1^\ddagger .

Using the absolute reaction rate theory expression for k_2 , in equation 5 one obtains

$$\text{rate} = \kappa \frac{kT}{h} k' \theta \exp\left(\frac{-\Delta H_2^\ddagger}{RT}\right) \exp\left(\frac{\Delta S_2^\ddagger}{R}\right) \quad (13)$$

The units of k' are molecules/cm.² if the rate of the reaction is measured in molecules cm.⁻² sec.⁻¹. Assuming κ to be unity, ΔS_2^\ddagger to equal zero, and under the conditions that rate equals 8.5×10^{-4} atm. sec.⁻¹ (3.2×10^{10} mole cm.⁻² sec.⁻¹), $T = 431^\circ$ and $\theta = 0.5$, k' was found to be 20 molecules cm.⁻². For $V_2O_{4.34}$, Aebi³ found the O-O distance along the octahedron edges to be 2.7 to 3.3 Å. He also found that the O-O distance was essentially the same in V_2O_5 as in $V_2O_{4.34}$. Assuming all the oxygen atoms on the surface to be this distance apart, the surface would have approximately 10^{15} surface sites per square cm. Since the number of surface sites is so much greater than k' , it suggests that only very special type sites enter into the reaction. By knowing k' and ΔH_1^\ddagger , the entropy of activation for the adsorption process, ΔS_1^\ddagger was calculated to be -39 cal. deg.⁻¹ mole⁻¹. This is on the basis of one gram of catalyst or 240 square meters of surface.

ACTIVITY COEFFICIENTS OF COMPONENTS IN THE SYSTEMS WATER-ACETIC ACID, WATER-PROPIONIC ACID AND WATER-*n*-BUTYRIC ACID AT 25°¹

BY ROBERT S. HANSEN, FREDERICK A. MILLER² AND SHERRIL D. CHRISTIAN

Institute for Atomic Research and Department of Chemistry, Iowa State College, Ames, Iowa

Received October 18, 1954

Activity coefficients of components in the systems water-acetic acid, water-propionic acid and water-*n*-butyric acid have been determined at 25° from experimental partial pressure measurements. Activity coefficient functions self consistent according to the Gibbs-Duhem equation are obtained from these data which represent the data in each system over the entire concentration range. The representations appear to be very satisfactory over the entire concentration range for the systems water-acetic acid and water-*n*-butyric acid, but less satisfactory in the water-propionic acid systems at propionic acid mole fractions in excess of 0.3. Activity coefficients for water in fatty acid have been inferred from total vapor pressure measurements over the acid-rich portions of the concentration range for the systems water-*n*-valeric acid, water-*n*-caproic acid and water-*n*-heptylic acid. These results have been combined with the other activity results and solubility measurements to establish the limiting increment per -CH₂- group to the specific free energy of fatty acid at infinite dilution in water as 870 cal. per mole.

Introduction

Activities of aqueous solutions of the lower aliphatic acids valid at solution freezing temperatures have been obtained from freezing point depression data by Jones and Bury,³ and activities of these same systems have been measured at 34.45° by Giacalone, Accasina and Carnesi⁴ using a wet bulb thermometer technique. Both investiga-

tions were limited to the water-rich portion of the concentration range, and the second piece of work appears to be neither extensive nor highly accurate. The purpose of the present work was to obtain complete activity data for all components of these systems over the entire concentration range and to obtain the specific free energies of these components at infinite dilution.

Experimental

Partial pressures of both components in each of the systems water-acetic acid, water-propionic acid and water-*n*-butyric acid were determined at from 14 to 20 concentrations covering the entire concentration range. Determinations were performed using the apparatus and techniques

(1) Contribution No. 355. Work was performed in the Ames Laboratory of the Atomic Energy Commission.

(2) Based in part upon a dissertation submitted by Frederick A. Miller to the Graduate School, Iowa State College, in partial fulfillment of the requirements for the degree of Doctor of Philosophy, 1953.

(3) E. R. Jones and C. R. Bury, *Phil. Mag.*, **4**, 481 (1927).

(4) A. Giacalone, F. Accasina and G. Carnesi, *Gazz. chim. ital.*, **72**, 109 (1942).

described by Hansen and Miller.⁵ The partial pressures were obtained at $25.00 \pm 0.02^\circ$.

Total pressures were measured at selected concentrations in the acid-rich portions of the concentration range for the systems water-*n*-valeric acid, water-*n*-caproic acid and water-*n*-heptylic acid, and these pressures were ascribed entirely to water. In these measurements, a 25- to 100-ml. reservoir containing the sample was connected to a precision-bore mercury manometer and to a vacuum line. The sample was outgassed with shaking for 5-10 minutes, then allowed to come to pressure equilibrium. The flask was kept in a water-bath at $25.00 \pm 0.02^\circ$ during the experiment, and the manometer and connections between flask and manometer were maintained at higher temperature by means of heating coils to prevent condensation. When the pressure determination was completed, an aliquot of the sample was removed and water concentration was determined by Karl Fischer titration using the dead-stop end-point technique. Solubilities of water in organic acids were also determined by Karl Fischer titration of the acid saturated with water.

The water used was redistilled from alkaline permanganate solution; the fatty acids were Baker and Adamson reagent grade acetic acid, Eastman Kodak Co. white label propionic, *n*-butyric, *n*-valeric and *n*-heptylic acids, and Eastman practical grade *n*-caproic acid. The acetic, propionic, butyric and valeric acids were purified by distillation through a 30-plate Oldershaw column at 10-1 reflux ratios; the caproic and heptylic acids were purified by simple distillation. The fatty acid fractions used had boiling ranges as follows (corrected to 760 mm.): acetic acid, 118.20-118.33°; propionic acid, 141.44-141.61°; *n*-butyric acid, 164.0-164.2°; *n*-valeric acid, 186.1-186.4°; *n*-caproic acid, 203-205°; *n*-heptylic acid, 223-224°.

Treatment of Data

Resolution of experimental total pressure and condensate mole fraction data in terms of component partial pressures and fugacities is complicated in fatty acid systems by the extensive association of fatty acids in the vapor phase.

Let P_1 , P_2 and P_3 be the partial pressures of fatty acid monomer, dimer and trimer in the vapor phase; n_1 , n_2 and n_3 , the corresponding moles of condensate; P_w and n_w , the partial pressure and moles of water in condensate; P_T , the total pressure, and X_A , the experimental mole fraction acid in the condensate (in which all acid is counted as monomer). Evidently

$$X_A = \frac{n_1 + 2n_2 + 3n_3}{n_1 + 2n_2 + 3n_3 + n_w} = \frac{P_1 + 2P_2 + 3P_3}{P_1 + 2P_2 + 3P_3 + P_w} = \frac{P_1 + 2P_2 + 3P_3}{P_T + P_2 + 2P_3} \quad (1)$$

Let K_2 and K_3 be the equilibrium constants for formation of dimer and trimer from monomer, respectively. Substitution in (1) leads to

$$K_3(3 - 2X_A)P_1^3 + K_2(2 - X_A)P_1^2 + P_1 - X_AP_T = 0 \quad (2)$$

which may be solved for P_1 .

Let f_A be the fatty acid fugacity and $P_A = P_1 + P_2 + P_3$, the total fatty acid partial pressure. Then

$$\ln \frac{f_A}{P_A} = \int_0^{P_A} \left(\frac{\bar{V}_A}{RT} - 1/P_A \right) dP_A \quad (3)$$

If it is assumed that deviations from ideality are due solely to the indicated associations then

$$\ln \frac{f_A}{P_A} = \int_0^{P_A} \left(\frac{1}{P_1 + 2P_2 + 3P_3} - \frac{1}{P_A} \right) dP_A \quad (4)$$

$$= \int_0^{P_A} \left(\frac{1}{P_1 + 2K_2P_1^2 + 3K_3P_1^3} - \frac{1}{P_A} \right) dP_A \quad (5)$$

(5) R. S. Hansen and F. A. Miller, *THIS JOURNAL*, **58**, 193 (1954).

$$= \int_0^{P_A} \left(\frac{1}{P_1(dP_A/dP_1)} - \frac{1}{P_A} \right) dP_A = \ln P_1/P_A \quad (6)$$

whence

$$f_A = P_1 \quad (7)$$

Monomer pressures were calculated from eq. 2 using equilibrium constants obtained from the work of MacDougall in the case of acetic acid^{6a} and propionic acid^{6b} and from the data of Lundin, Harris and Nash⁷ in the case of *n*-butyric acid.

Constants used for calculations were: for acetic acid, $K_2 = 1.63 \text{ mm.}^{-1}$, $K_3 = 0.0016 \text{ mm.}^{-2}$; for propionic acid, $K_2 = 3.92 \text{ mm.}^{-1}$, $K_3 = 0.074 \text{ mm.}^{-2}$; for butyric acid, $K_2 = 1.27 \text{ mm.}^{-1}$. Equilibrium constants in the latter two systems were evaluated by extrapolation of data at higher temperatures. The progression of these constants is such as to cause some concern for their accuracy. Allen and Caldin⁸ have recently summarized work on fatty acid association. Thermodynamic quantities tabulated by these authors led to free energies of dimerization for acetic acid at 25° ranging from -3.95 to -4.30 kcal., and representing work of four different groups. The work of MacDougall (selected because his experiments were performed at 25°) corresponded to a free energy of dimerization of -4.20 kcal. at 25°. On this basis the dimerization constant used is probably correct to within 15%. The situation with respect to propionic acid is much less satisfactory in that the free energy of dimerization calculated from MacDougall's work, -4.8 kcal., differs from that calculated from the work of Taylor and Bruton,⁹ -4.35 kcal., sufficiently that dimerization constants calculated differ by a factor of two. Lundin, Harris and Nash⁷ appear to have presented the only data available on the dimerization of butyric acid.

The uncertainties in dimerization constants lead to considerably smaller relative uncertainties in activity coefficients. For example, considering dimerization only, the fatty acid activity referred to pure liquid fatty acid as standard state is given by

$$a_A = \frac{f_A}{f_A^\circ} = \frac{P_1}{P_1^\circ} = \frac{1}{2 - X_A} \frac{\sqrt{1 + 4K_2(2 - X_A)X_AP_T} - 1}{\sqrt{1 + 4K_2P_T} - 1} \quad (8)$$

In the case of propionic acid, for example, the product X_AP_T was greater than unity in every observation except at the most dilute concentration (mole fraction 0.0246 in the liquid phase, $X_AP_T = 0.47$). The terms containing K_2 are greater than 10 in all but the most dilute systems regardless of the constants taken. When one rearranges and expands eq. 8, there results

$$a_A = \sqrt{\frac{X_AP_T}{(2 - X_A)P_T^\circ}} \left\{ 1 + \frac{1}{8K_2} \left(\frac{1}{X_A(2 - X_A)P_T} - \frac{1}{P_T^\circ} \right) - \frac{1}{\sqrt{4K_2}} \left(\frac{1}{\sqrt{2 - X_A}X_AP_T} - \frac{1}{\sqrt{P_T^\circ}} \right) \right\} \quad (9)$$

(6) (a) F. H. MacDougall, *J. Am. Chem. Soc.*, **53**, 2585 (1936); (b) *ibid.*, **63**, 3420 (1941).

(7) R. E. Lundin, F. E. Harris and L. K. Nash, *ibid.*, **74**, 743 (1952).

(8) G. Allen and E. F. Caldin, *Quart. Rev.*, **7**, 255 (1953).

(9) M. D. Taylor and J. Bruton, *J. Am. Chem. Soc.*, **74**, 4151 (1952).

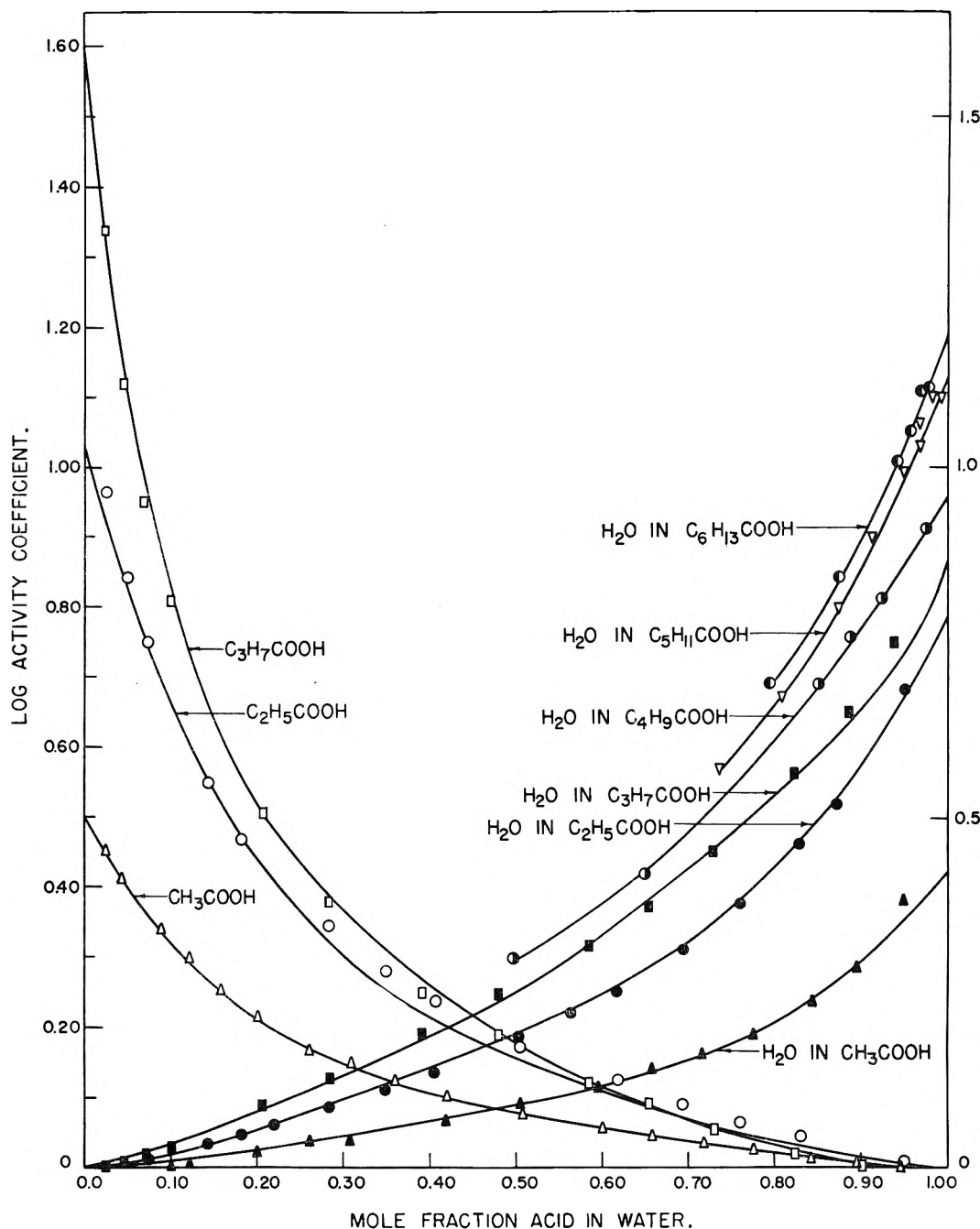


Fig. 1.—Activity coefficients as functions of concentration in the water-fatty acid systems. In the systems water-acetic acid, water-propionic acid and water-*n*-butyric acid curves are calculated from function self-consistent according to the Gibbs-Duhem equation. All points are experimental.

in which the leading term is independent of K_2 . Thus the activity coefficient of propionic acid at liquid mole fraction 0.100 was found to be 4.58 using the dimerization data of MacDougall and 4.54 using the data of Taylor and Bruton. The vapor pressure of water can be expressed in the form (considering only dimerization)

$$P_w = (1 - X_A)(P_T + P_2) \tag{10}$$

$$= (1 - X_A) \left\{ P_T + \frac{[\sqrt{4K_2(2 - X_A)X_AP_T + 1} - 1]^2}{4K_2(2 - X_A)^2} \right\} \tag{11}$$

Again, by expansion

$$P_w = (1 - X_A) \left\{ P_T + \frac{X_AP_T}{2 - X_A} + \frac{1}{4K_2(2 - X_A)^2} [1 - 4\sqrt{K_2(2 - X_A)X_AP_T}] \right\} \tag{12}$$

The third term is about 18% of the second term with the most concentrated solution studied; the indicated uncertainty in K_2 could lead to an uncertainty in P_w of about 2% at these concentrations.

Therefore, it appears that the uncertainties in dimerization constants are not an important source of uncertainties in the final activity coefficients.

Activities were obtained by dividing vapor phase fugacities (the water fugacity being assumed equal

to its partial pressure) by the fugacities of components over their pure liquids; activity coefficients were obtained by dividing activities by corresponding component mole fractions. Activity coefficient functions self consistent according to the Gibbs-Duhem equation were obtained in the manner described by Hansen and Miller.⁵

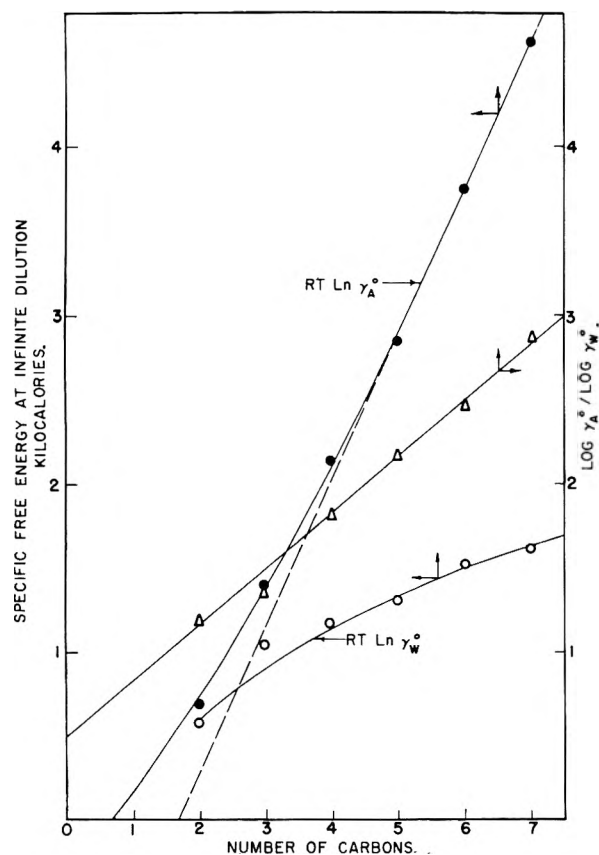


Fig. 2.—Limiting forms for specific free energy at infinite dilution in water-fatty acid systems.

Results

The experimental data for the lower three water-fatty acid systems were found to be represented by the following self-consistent activity coefficient functions: γ_A is the activity coefficient of acid; X_A , the acid mole fraction in the liquid phase; γ_w , the activity coefficient of water; logarithms are to the base 10

System water-acetic acid:

$$\log \gamma_A = (1 - X_A)^2(0.683X_A^2 + 0.080X_A^3 + 0.505e^{-2.5X_A}) \quad (13a)$$

$$\log \gamma_w = X_A^2[0.202/X_A^2 - 0.455X_A + 0.623X_A^2 + 0.080X_A^3 - e^{-2.50X_A}(0.202/X_A^2 + 0.505/X_A - 0.505)] \quad (13b)$$

System water-propionic acid:

$$\log \gamma_A = (1 - X_A)^2(0.30X_A + 0.90X_A^2 + 1.030e^{-2.8X_A}) \quad (14a)$$

$$\log \gamma_w = X_A^2 \left[\frac{0.368}{X_A^2} - 0.15 - 0.30X_A + 0.90X_A^2 - e^{-2.8X_A} \left(\frac{0.368}{X_A^2} + \frac{1.030}{X_A} - 1.03 \right) \right] \quad (14b)$$

System water-n-butyric acid

$$\log \gamma_A = (1 - X_A)^2[0.725 + 0.85e^{-11.5X_A} + 1.61e^{-23.0(1 - X_A)}] \quad (15a)$$

$$\log \gamma_w = X_A^2 \left[\frac{0.074}{X_A^2} + 0.725 - e^{-11.5X_A} \left(\frac{0.074}{X_A^2} + \frac{0.85}{X_A} - 0.85 \right) + e^{-23.0(1 - X_A)} \left(\frac{0.07}{X_A^2} - \frac{1.6}{X_A} + 1.6 \right) \right] \quad (15b)$$

These functions are compared with experimental points in Fig. 1. Experimental points for the water activities in the higher water-fatty acid systems are shown in the same figure; curves through these points, however, have not been chosen to represent particular functions. Deviations of experimental points from self-consistent functions appear to be significant only in the water-propionic acid system in the range $0.3 < X_A < 1$.

Discussion

The quantity $RT \ln \gamma_0$, where γ_0 is the limiting activity coefficient of a component as its mole fraction approaches zero, has been discussed for the aqueous alcohol systems by Butler, Thomson and MacLennan.¹⁰ It might be designated the specific free energy at infinite dilution, as it is the difference between the partial molar free energy of a component at infinite dilution and the partial molar free energy the component would have were the solution ideal. It arises largely from the difference in free energies of interaction between a molecule and an environment of molecules of its own kind on the one hand, and between a molecule and an environment of molecules of the second component in the binary solution on the other hand. To consider this difference wholly a difference in a sort of bonding free energy is not reasonable since molecules of different sizes should have a non-ideal mixing entropy from this source alone; this point has been discussed recently by Hildebrand and Scott.¹¹ Where the difference is large, most of it can be imagined due to such a difference in "bonding" free energies.

Specific free energies of the fatty acids at infinite dilution can be inferred for aqueous solutions of a number of higher fatty acids from solubility data as presented in Table I.

TABLE I

SOLUBILITIES OF FATTY ACIDS IN WATER AT 25° ACID

Acid	X_A' , mole fraction acid in water-rich phase ¹²	X_A'' , mole fraction acid in acid-rich phase
n-Valeric	0.006915	0.5028
n-Caproic	.001593	.7326
n-Heptylic	.000390	.7977

Where single primes denote water-rich phases and double primes denote acid-rich phases

$$\gamma_A' = \frac{X_A''}{X_A'} \gamma_A'' \quad (16)$$

Because of the low solubility of these acids in water the activity coefficient γ_A' is taken as γ_A^0 . The activity coefficient γ_A'' is not less than unity and the product $\gamma_A'' X_A''$ is not greater than unity. Further, the product $\gamma_A'' X_A''$ should not be less than the

(10) J. A. V. Butler, D. W. Thomson and W. H. MacLennan, *J. Chem. Soc.*, 674 (1933).

(11) J. H. Hildebrand and R. L. Scott, "The Solubility of Non-Electrolytes," 3rd Ed., Reinhold Publ. Corp., New York, N. Y., 1950, Chapter VI.

(12) R. P. Craig, Ph.D. Dissertation, Iowa State College, 1952

corresponding product for the next lower acid at the same mole fraction. The greater X_{A^n} , the smaller the range of values of the product $\gamma_{A^n} X_{A^n}$ satisfying these restrictions. The product was therefore estimated by extrapolation of corresponding products at the same concentration for the lower acids. Thus, at mole fraction 0.503 acid, the products $X_{A^n} \gamma_{A^n}$ were 0.60, 0.72, and 0.78 for acetic, propionic and *n*-butyric acid; the product $X_{A^n} \gamma_{A^n}$ for *n*-valeric acid was estimated to be 0.82 by graphical extrapolation, and this should be correct to a few per cent. The uncertainties due to this extrapolation are, of course, less for the higher homologs.

A parallel treatment of the activity coefficient of water at zero concentration in fatty acid cannot be performed with comparable accuracy because of the far greater solubilities of water in the fatty acids; for this reason, water activity coefficients in the higher fatty acids were measured in the manner described and activity coefficients at infinite dilution were evaluated by extrapolation of the functions $X_A^{-2} \log \gamma_w$ to $X_A = 1$.

Treatment of specific free energies at infinite dilution is summarized in Fig. 2, in which the quantities $RT \ln \gamma_A$, $RT \ln \gamma_w^0$, and their ratio are

plotted as functions of the number of carbons. According to Butler, Thomson and MacLennan¹⁰ the quantity $RT \ln \gamma_A^0$ should be of the form $a + bn$ for n sufficiently large, the quantity $RT \ln \gamma_w^0$ should approach a constant value for n sufficiently large, and the ratio $\ln \gamma_A^0 / \ln \gamma_w^0$ should be a linear function of n for all n . Figure 2 supports all of these conclusions. Data for $RT \ln \gamma_A^0$ could be well represented by two straight lines, one of slope 724 calories per unit increase in n from $n = 2$ to $n = 5$, and one of slope 872 calories from $n = 5$ to $n = 7$. Instead, in accordance with the arguments of Butler, Thomson and MacLennan, the latter line has been shown as an asymptote. The data cast doubt on the physical basis of their arguments in at least two respects, however. First, the change in slope of the plot of $RT \ln \gamma_A^0$ in the region of small n appears to be much too small, and the asymptote, too quickly approached. Butler, Thomson and MacLennan made a somewhat similar comment with respect to their data on the alcohols. Second, the ratio $\log \gamma_A^0 / \log \gamma_w^0$ should represent the ratio of "surface areas" of acid and water molecules; the figures 0.82 for the ratio formic acid/water (extrapolated) and 1.16 for the ratio acetic acid/water appear considerably too small.

IONIZATION CONSTANTS OF SOME ORGANOMERCURIC HYDROXIDES AND HALIDES¹

BY THOMAS D. WAUGH,² HAROLD F. WALTON AND JOHN A. LASWICK³

Contribution from Arapahoe Chemicals, Inc., and the Chemistry Department of the University of Colorado, Boulder, Colorado

Received October 18, 1954

The ionization constants of methyl-, ethyl- and phenylmercuric hydroxides and of methylmercuric chloride and bromide have been measured by potentiometric titration. All are weak electrolytes. The solubility products of methyl- and phenylmercuric halides have been found, partly potentiometrically and partly by direct solubility measurements. A convenient way of titrating alkyl mercuric hydroxides is described, and evidence is given to show that a certain method for preparing solid methyl mercuric hydroxide actually leads to the oxide.

Introduction

Methylmercuric hydroxide, CH_3HgOH , is a weak base. This fact is known from conductivity data⁴ as well as from the great degree of hydrolysis of methylmercuric nitrate, which makes it impossible to titrate this hydroxide with nitric acid. Yet statements have been made that methylmercuric hydroxide is a strong base⁵; these originated in the observation that it can be titrated easily with hydrochloric acid, using methyl red indicator.

The fact that methylmercuric hydroxide can be titrated with hydrochloric acid, but not with nitric acid, suggests that the chloride, CH_3HgCl , is weakly ionized. The conductivity studies of Maynard and Howard showed that methylmer-

curic sulfate and acetate were weakly ionized; they did not report data for the chloride, presumably because of its low solubility in water.

Our interest in the ionization of methylmercuric hydroxide and halides derives in part from our observation that the halides can be quantitatively converted to the hydroxide by ion exchange.⁶ We have found no published ionization constants for the halides, and the one published value⁴ for the hydroxide, $K_b = 3.9 \times 10^{-11}$, is based on very inadequate data. The main purpose of this investigation was, therefore, to determine ionization constants and solubility product constants of these compounds. These have been determined by potentiometric titration with glass and silver-silver halide electrodes, and confirmed, in the case of the solubility products, by non-electrical measurements. Determinations were extended to ethylmercuric hydroxide and to phenylmercuric hydroxide, chloride, bromide and iodide. A secondary aim of this study was to clarify the constitution of solid products claimed to be methylmercuric hydroxide. Widely different melting points have been

(1) Most of this work is taken from the Ph.D. thesis of Thomas D. Waugh, University of Colorado, 1954.

(2) Vice-President and Director of Research, Arapahoe Chemicals, Inc., Boulder.

(3) National Science Foundation Fellow.

(4) J. L. Maynard and H. C. Howard, *J. Chem. Soc.*, **123**, 960 (1923); I. B. Johns, W. D. Peterson and R. M. Hixon, *THIS JOURNAL*, **34**, 2218 (1930).

(5) F. C. Whitmore, "Organic Compounds of Mercury," Chemical Catalog Co., New York, N. Y., 1921, p. 88.

(6) H. F. Walton, T. D. Waugh and J. A. Laswick, forthcoming.

reported for this compound, ranging from 95 to 137°, and it was our belief that some of these compounds may have been methylmercuric oxide, rather than the hydroxide.

Experimental

Materials.—Methylmercuric hydroxide was supplied as a 17% aqueous solution by Mrs. Margareta Heineman of Panogen, Inc. It was not used in this form, except for exploratory titrations, but was converted into the chloride, bromide and iodide by adding an excess of the appropriate acid, and filtering, drying and recrystallizing the precipitated solids. Methylmercuric bromide, recrystallized from 15 times its weight of absolute ethanol and melting at 158–160° (uncor.) (lit. 161.1°⁷) was used as the source of the solid methylmercuric hydroxide and oxide preparations described below.

Ethylmercuric iodide was supplied as a yellowish crystalline solid by the Ringwood Chemical Co. It was recrystallized once from 50 times its weight of absolute ethanol; m.p. 183–185° (cor.) (lit. 186°⁷). An aqueous solution of ethylmercuric hydroxide was made from it by shaking with freshly precipitated, carbonate-free silver oxide.

Phenylmercuric hydroxide was supplied by F. W. Berk and Co. and recrystallized from dilute aqueous sodium hydroxide; m.p. 195–203° (uncor.). *Anal.* Hg, 68.3; equiv. wt., 296.5. Found: Hg, 68.1; equiv. wt., 294.7.

Analytical Methods.—Mercury was determined by a new gravimetric method which is to be published later. The organic compound is decomposed by warming under reflux with excess concentrated hydriodic acid, after which the solution is diluted and neutralized, and the mercury precipitated and weighed as the compound Cup_2HgI_4 (pn = 1, 2-propanediamine), a weighing form introduced by Spacu and Spacu.⁸ The method gives good precision, but on methylmercuric halides the results are about 1% low. Mercury analyses in this paper are reported as they were obtained, without attempting to apply a correction factor.

Halogens were determined gravimetrically as silver halides.

Oxygen was determined by Dr. E. W. D. Huffman, of Huffman Microanalytical Laboratories, Wheatridge, Colorado, using the Unterzaucher method.

Equivalent weights of oxides and hydroxides were found by adding about 2 g. of potassium bromide per 50 ml. of aqueous solution and titrating potentiometrically with standard acid. As will be seen, this method gave extremely sharp end-points.

Equipment of Potentiometric Titrations.—Two pH meters were used, a Beckman Model H (line-operated, direct reading) and a Beckman Model G. Both were calibrated with Beckman certified pH 7 buffer and with a Clark and Lubs pH 5 phthalate buffer; the two buffers checked within 0.02 pH unit.

In determining ionization constants of the halides, two series of titrations were made, one with the orthodox glass electrode–calomel electrode combination, and another in which the calomel electrode was replaced by a silver–silver halide electrode. These latter electrodes were made by plating short spirals of platinum wire with silver, then making these anodic in a solution of the appropriate hydrogen halide.

The temperature of all e.m.f. and solubility measurements was 24–25°, except for one set of titrations at 35° which will be noted. Thermostatic control at $25 \pm 0.01^\circ$ was used in a few experiments, but was not actually necessary.

Preparation of Solid Methylmercuric Oxide and Hydroxide.—Three methods were used to prepare the solid hydroxide, as follows.

(a) **Method of Slotta and Jacobi.**⁹—A mixture of 30 g. of methylmercuric bromide and 100 ml. of 40% methyl alcoholic potassium hydroxide was heated for one-half hour at 100°. The precipitated potassium bromide was filtered off and the filtrate, after adding 20 ml. of water, was evaporated to small volume at 60° under a pressure of 20 mm. The thick slurry of dark gray crystals was filtered with some difficulty on a sintered glass funnel. The solid was dis-

solved in 40 ml. of hot pyridine, and the pyridine layer separated by decantation from a little aqueous potassium hydroxide solution. On cooling, colorless crystals separated in a thick mat. These were filtered and washed with cold pyridine and anhydrous ether. After drying for several days over calcium chloride, the product melted over the range 103–129°; the yield was 16 g. (78%). Two recrystallizations from about 3 ml. of pyridine per gram of solid brought the m.p. up to 110–137°.

Anal. Calcd. for CH_3HgOH : Hg, 86.2; O, 6.88; equiv. wt., 232.6. Found: Hg, 87.6; O, 5.25; equiv. wt., 222.4. Calcd. for $(\text{CH}_3\text{Hg})_2\text{O}$: Hg, 89.7; O, 3.58; equiv. wt., 223.6.

(b) **Method of Sneed and Maynard.**¹⁰—Ten g. of methylmercuric bromide was dissolved in 300 g. of methanol and stirred for 45 minutes with the silver oxide obtained from 8.1 g. of silver nitrate and 3.3 g. of 40% sodium hydroxide. The solid was filtered off, and the solution concentrated by evaporation; by vacuum evaporation at 55° a white solid was formed, which was redissolved in a minimum amount of warm methanol, then reprecipitated by gradually adding 100 ml. of dry ether. The crystals were dried in air; yield 5.6 g. (71%); m.p. 62–68°. Other samples made similarly from methylmercuric chloride and iodide melted from 65–95°.

(c) **Ion-exchange Method.**—One-half g. of methylmercuric bromide was dissolved in 30 ml. of methanol and passed through 10 ml. of the quaternary hydroxide type anion-exchange resin Amberlite IRA-400. The effluent was evaporated to dryness under vacuum; the solid was taken up in a little methanol, and the solution decolorized with charcoal and evaporated almost to dryness. Then the solid was precipitated by adding ether; it was washed with ether and air-dried as before; yield 0.30 g. (79%); m.p. 80–100°. Neither drying for 12 hours *in vacuo* nor recrystallization from pyridine changed this melting point appreciably.

From the analysis of the product obtained by (a), we conclude that this material is probably the oxide, rather than the hydroxide, though it may be a compound of oxide and hydroxide. The wide melting range of the product suggests a solid solution or an unstable binary compound. Probably methylmercuric oxide and hydroxide form a range of solid solutions. We could also have solvates formed with the different solvents used (pyridine, methanol, ether). Until more accurate analytical methods are available, these points cannot properly be investigated. Fortunately, the exact constitution of the solid does not affect the interpretation of the titration data, since methylmercuric oxide would form the hydroxide in water. Titration of a solution prepared from the solid of procedure (a) gave very nearly the same ionization constant as a solution prepared directly from methylmercuric bromide and an aqueous carbonate-free suspension of silver oxide, which seems to exclude the possibility that this solid is a pyridine solvate.

Results

Ionization Constant of Methylmercuric Hydroxide.—This was obtained by titrating aqueous solutions of methylmercuric hydroxide with dilute nitric and perchloric acids, using the glass electrode–calomel electrode combination. At half-neutralization, if we assume that there is no association between CH_3Hg^+ and NO_3^- or ClO_4^-



Since, in our titrations $[\text{CH}_3\text{HgOH}]$ was about $100 \times [\text{H}^+]$, we can write $[\text{CH}_3\text{HgOH}] = [\text{CH}_3\text{Hg}^+]$, and $[\text{OH}^-] = K_b$.

The pH–titration curves show no sign of any inflection at equivalence, and in order to know the point of half-neutralization it was necessary to titrate portions of solution with addition of excess potassium bromide before the equivalence point. Typical titrations with and without added potassium bromide are shown in Fig. 1, curves 1a and 1b.

(10) M. C. Sneed and J. L. Maynard, *J. Am. Chem. Soc.*, **44**, 2942 (1922).

(7) E. Krause and A. von Grosse, "Die Chemie der metall-organischen Verbindungen," Borntraeger, Berlin, 1937, p. 131.

(8) G. Spacu and P. Spacu, *Z. anal. Chem.*, **89**, 187 (1932).

(9) R. H. Slotta and K. R. Jacobi, *J. prakt. Chem.*, [2] **120**, 2942 (1922).

Methylmercuric hydroxide can be titrated quite well with methyl red indicator if about 2 g. of potassium bromide is added first. A solution containing both methylmercuric hydroxide and free sodium hydroxide can be analyzed by first titrating with nitric acid to the phenolphthalein end-point, then adding potassium bromide and continuing the titration with methyl red. For accurate results by this method, carbonate must of course be absent.

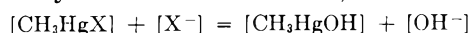
Ionization constants obtained by titrating methylmercuric hydroxide under different conditions are summarized in Table I. Since no attempt was made to correct for activities, the agreement is satisfactory. Certainly it seems justified to assume that CH_3HgNO_3 is wholly ionized in 0.005 *M* solution. Since procedure (a) probably gives the purest material, we have accepted the value found by titration of this, namely, $K_b = 3.1 \times 10^{-10}$.

TABLE I
TITRATION OF METHYLMERCURIC HYDROXIDE

Source	Temp., °C.	Acid used	Formal Hg concn.	pH at half-neut.	pK_b
Procedure (a)	25	HNO_3	5×10^{-3}	4.50	9.50
CH_3HgBr and aqueous susp. of Ag_2O	25	HNO_3	1.3×10^{-2}	4.46	9.54
	25	HClO_4	1.3×10^{-2}	4.41	9.59
	35	HClO_4	1.3×10^{-2}	4.28	9.37
"Panogen" as received	25	HNO_3	5×10^{-3}	4.58	9.42

Ethyl- and Phenylmercuric Hydroxides.—These were titrated in the same way as methylmercuric hydroxide, the first with perchloric acid, the second with nitric acid, both in 5×10^{-3} *M* solutions. The ionization constants, K_b , were 8.0×10^{-10} and 1.0×10^{-10} , respectively.

Methylmercuric Chloride and Bromide.—Two methods were used to find these ionization constants. Methylmercuric hydroxide was titrated potentiometrically with hydrochloric and hydrobromic acids, first with the conventional glass electrode-calomel electrode system, and then again with the calomel electrode of the pH meter replaced by a silver-silver chloride or silver-silver bromide electrode of the type described in the Experimental section. At the concentrations used, the methylmercuric halides remained in solution completely. At half-neutralization, therefore



and from electroneutrality

$$[\text{CH}_3\text{Hg}^+] + [\text{H}^+] = [\text{X}^-] + [\text{OH}^-]$$

where $\text{X} = \text{Cl}$ or Br . Under our conditions, $[\text{CH}_3\text{HgX}] \gg [\text{X}^-] \gg [\text{OH}^-]$. It can, therefore, be shown that

$$\log K = 2 \log K_1 + 2 \text{pOH} + \log a \quad (1)$$

where $K = [\text{CH}_3\text{Hg}^+][\text{X}^-]/[\text{CH}_3\text{HgX}]$, $K_1 = [\text{CH}_3\text{Hg}^+][\text{OH}^-]/[\text{CH}_3\text{HgOH}]$, $a = [\text{CH}_3\text{HgX}] = [\text{CH}_3\text{HgOH}]$.

With the glass electrode-Ag, AgX system, at half-neutralization

$$\log K = (E - E^\circ)/0.05915 + \text{p}K_w + \log K_1 \quad (2)$$

where E is the measured e.m.f. at 25° (taking the glass electrode as positive), E° is the standard e.m.f. of the cell with hydrochloric or hydrobromic acid

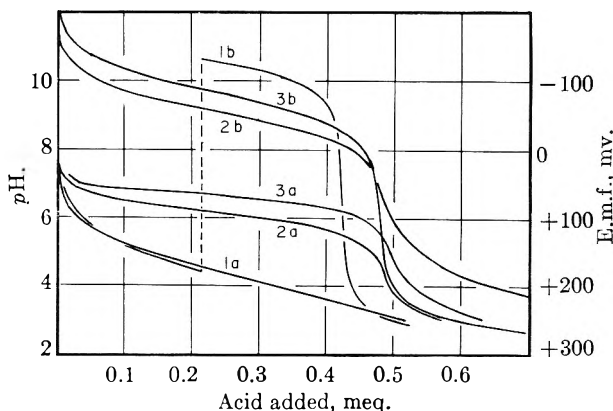


Fig. 1.—Titration of methylmercuric hydroxide: 1a and b, with HNO_3 (4 g. KBr added in b); 2a and b, with HCl ; 3a and b, with HBr ; curves 2b and 3b for glass and Ag-AgX electrodes (ordinates, e.m.f.); other curves for glass and calomel electrodes (ordinates, pH); 0.455 meq. CH_3HgOH used for 1a, different amounts for other curves; initial volumes 100 ml.; material prepared by procedure (a).

of unit activity, and K_w is the ionic product of water. Again we have assumed that $[\text{CH}_3\text{HgX}] = [\text{CH}_3\text{HgOH}]$ at half-neutralization. E° can be measured either by a separate experiment in which HX of known concentration (about 0.01 *M*) is placed between the electrodes, or by simply continuing the titrations of the mercury compounds until an appreciable excess of HX has been added. Activities, not concentrations, of HX were used in calculating E° .

Typical titration curves obtained by both methods are shown in Fig. 1. Of the two, the glass electrode-Ag, AgX data are preferred for calculating K because equation 2 is less susceptible to experimental uncertainties. Data obtained are summarized in Table II.

TABLE II
IONIZATION OF METHYLMERCURIC CHLORIDE AND BROMIDE

Compound	Source (see note)	At half-neutralization			$-\log K$	
		$a \times 10^2$	pH	$E - E^\circ$	Eq. 1	Eq. 2
Chloride	A	2.40	6.18	-0.583	6.02	5.38
	B	4.16	6.13	-0.591	5.68	5.52
	C	2.38	6.20	-0.588	6.06	5.45
Bromide	A	2.43	6.72	-0.660	7.09	6.68
	C	2.38	6.70	-0.664	7.06	6.74

NOTE: A from solid $(\text{CH}_3\text{Hg})_2\text{O}$ prepared by procedure (a); B, solution from CH_3HgBr and aqueous suspension of Ag_2O ; C, "Panogen" as received.

The accepted mean values were: CH_3HgCl , $\text{p}K = 5.45$; CH_3HgBr , $\text{p}K = 6.70$.

Phenylmercuric Chloride and Bromide.—The same two titrations which were made with methylmercuric hydroxide were made with phenylmercuric hydroxide solutions. Typical curves are shown in Fig. 2. It will immediately be noted that the pH curve with hydrobromic acid is anomalous. Instead of falling as the acid is added, the pH actually rises by about one unit before equivalence is reached.

Phenylmercuric chloride and bromide are less soluble than the methylmercuric compounds and start to precipitate soon after titration is begun. What we are measuring are, therefore, solubility product constants, $K_{s.p.}$, rather than dissociation constants. Equation 2 now takes the form

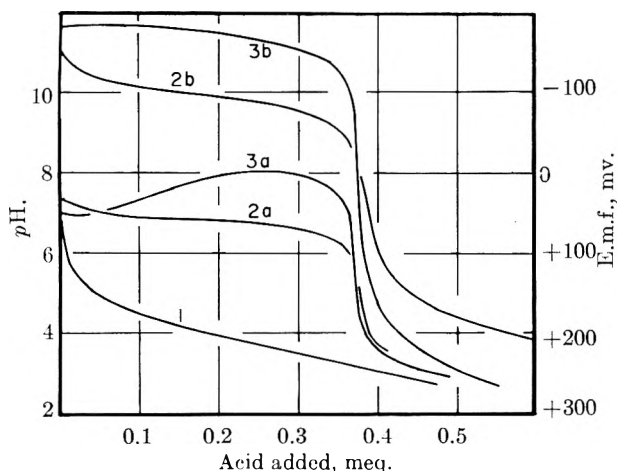
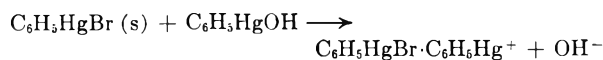


Fig. 2.—Titration of phenylmercuric hydroxide: 1, with HNO_3 ; 2a and b, with HCl ; 3a and b, with HBr ; curves 2b and 3b for glass and Ag-AgX electrodes (ordinates, e.m.f.); other curves for glass and calomel electrodes (ordinates, pH). 0.380 meq. $\text{C}_6\text{H}_5\text{HgOH}$ used for curve 1; initial volumes 100 ml.

$$\log K_{s.p.} = (E - E^\circ)/0.05915 + pK_w + \log K_1 + \log [\text{C}_6\text{H}_5\text{HgOH}] \quad (2a)$$

This is true whether or not we are at half-neutralization, since no assumption is made that $[\text{C}_6\text{H}_5\text{HgOH}] = [\text{C}_6\text{H}_5\text{HgX}]$. Equation 1 is of limited use for the chloride, since $[\text{OH}^-]$ is now commensurate with $[\text{Cl}^-]$, and it is of no use at all for the bromide. We have, therefore, used only equation 2a to calculate $K_{s.p.}$, and it is worth noting that it gives practically the same results whether we take the point of half-neutralization or other points closer to equivalence. We find: $\text{C}_6\text{H}_5\text{HgCl}$, $pK_{s.p.} = 9.30$; $\text{C}_6\text{H}_5\text{HgBr}$, $pK_{s.p.} = 11.75$.

As a tentative explanation of the anomalous pH rise in hydrobromic acid titration, we suggest that as solid phenyl mercuric bromide is formed, it absorbs $\text{C}_6\text{H}_5\text{Hg}^+$ ions



Such a process could affect the pH, since the solution is almost neutral and the ionic concentration is very low. A somewhat similar explanation has been proposed for the action of chrysoidin absorption indicators.¹¹

Methyl- and Phenylmercuric Iodides.—Instead of titrating the hydroxides with hydriodic acid, which is difficult to prepare and to keep, the hydroxide solutions were half-neutralized with nitric acid and then titrated with standard potassium iodide. The potassium iodide was standardized by potentiometric titration against silver nitrate in presence of a known concentration of nitric acid, using the glass electrode-silver, silver iodide electrode combination. This titration also served to determine E° for this cell; it was 0.799 volt, the glass electrode being positive.

Typical titration curves for the organic mercury hydroxides are given in Fig. 3. Precipitates formed as soon as potassium iodide was added. Solubility products were calculated from points in the equivalence region, using equation 2a. Where the pH

(11) E. Schulek and E. Pungor, *Anal. Chem. Acta*, **4**, 109 (1950).

was high, virtually all the mercury not precipitated as the iodides was present as RHgOH ; where the pH was below 7, the pH value was used to correct the RHgOH concentration (used in equation 2a) for the RHg^+ present. However, the calculations were insensitive to pH.

For CH_3HgI , the calculated $K_{s.p.}$ values averaged $(2.0 \pm 0.2) \times 10^{-12}$ within $\pm 20\%$ of equivalence; for $\text{C}_6\text{H}_5\text{HgI}$, the calculated $K_{s.p.}$ was very steady— 9.7×10^{-16} —once the anomalous region, shown by the dotted line in Fig. 3, had been passed. In this anomalous region the e.m.f. was affected by stirring, and we believe that some of the silver iodide of the electrode was being dissolved by the phenylmercuric nitrate



After enough potassium iodide has been added to combine with the free methylmercuric ions, the e.m.f. becomes stable and the curve becomes normal.

Direct Solubility Measurements.—The solubility products of methylmercuric chloride and bromide were determined by direct measurement, that is, by equilibrating the solids with water at 25° , and analysis of the solutions. Both halide and mercury were determined; the two analyses agreed closely. The solubility of the chloride was 2.0×10^{-2} , that of the bromide 6.5×10^{-3} mole per liter.

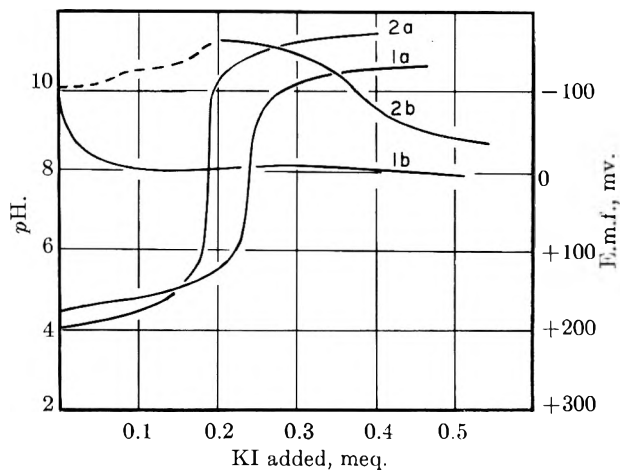


Fig. 3.—Titration of hydroxide-nitrate mixtures with KI: 1a and b, CH_3HgOH ; 2a and b, $\text{C}_6\text{H}_5\text{HgOH}$; curves 1a and 2a for glass and calomel electrodes (ordinates, pH); curves 1b and 2b for glass and Ag-AgI electrodes (ordinates, e.m.f.); initial volumes 100 ml.

To calculate the solubility product, $[\text{CH}_3\text{Hg}^+][\text{X}^-]$, from these measurements, we set up simultaneous equations for electrical neutrality, material balance and ionization constants, and, neglecting $[\text{OH}^-]$ in comparison with $[\text{H}^+]$, we obtain a fourth-power equation in $[\text{H}^+]$

$$(K_b/K_w)^2 [\text{H}^+]^4 + K_b[\text{H}^+]^3/K_w + K_2K_b[\text{H}^+]^2/K_w + K_2[\text{H}^+] - K_2a = 0$$

where K_b and K_2 are the ionization constants of CH_3HgOH and CH_3HgX , and a is the measured solubility in moles per liter. Solving for $[\text{H}^+]$ and then for the individual concentrations, we find: for the chloride, $[\text{H}^+] = [\text{CH}_3\text{HgOH}] = 8.5 \times 10^{-5}$, $[\text{CH}_3\text{Hg}^+] = 2.23 \times 10^{-4}$, $[\text{CH}_3\text{HgCl}] =$

TABLE III

Cation	IONIZATION CONSTANTS AND SOLUBILITY PRODUCTS AT 25°				
	Const.	OH	Cl	Br	I
CH ₃ Hg	K _i	3.1 × 10 ⁻¹⁰	3.5 × 10 ⁻⁶	2.0 × 10 ⁻⁷	2 × 10 ⁻⁹
	K _{s.p.}	6.9 × 10 ⁻⁸	1.2 × 10 ⁻⁹	1.9 × 10 ⁻¹²
C ₂ H ₅ Hg	K _i	8.0 × 10 ⁻¹⁰
	K _{s.p.}
C ₆ H ₅ Hg	K _i	1.0 × 10 ⁻¹⁰
	K _{s.p.}	5.0 × 10 ⁻¹⁰	1.8 × 10 ⁻¹²	1.0 × 10 ⁻¹⁵

NOTE: At 35°, K_i for CH₃HgOH is 4.3 × 10⁻¹⁰.

1.97 × 10⁻², [Cl⁻] = 3.1 × 10⁻⁴; K_{s.p.} = 6.9 × 10⁻⁸. For the bromide, [H⁺] = [CH₃HgOH] = 2.8 × 10⁻⁵, [CH₃Hg⁺] = 2.4 × 10⁻⁵, [CH₃HgBr] = 6.45 × 10⁻³, [Br⁻] = 5.2 × 10⁻⁵; K_{s.p.} = 1.25 × 10⁻⁹. Most of the dissolved halide is present as CH₃HgX. The calculated [H⁺] values were confirmed by experimental pH measurements.

The solubility of methylmercuric iodide in water is only 1.0 × 10⁻³ molar at 25°, though it rises rapidly with temperature. Without knowing the ionization constant we cannot calculate a solubility product from this figure. We, therefore, equilibrated the solid with sodium hydroxide solutions of known concentrations and determined the iodide and mercury in the resulting solutions. In 0.0699 M sodium hydroxide the molar solubility of methylmercuric iodide was 0.0186; in 0.1398 M base it was 0.0261. Subtracting from these figures the solubility of molecular CH₃HgI, we get a value

which is equal to [CH₃HgOH] and [I⁻]. The free [OH⁻], from which [CH₃Hg⁺] can be calculated, is the difference between the initial base concentration and [CH₃HgOH]. The values of K_{s.p.} obtained from these data are 1.83 × 10⁻¹² and 1.70 × 10⁻¹², respectively. These are slightly different from the potentiometric value of 2.0 × 10⁻¹², but are possibly more reliable.

Knowing the solubility of molecular CH₃HgI to be about 1.0 × 10⁻³, we can estimate the ionization constant of CH₃HgI to be about 2 × 10⁻⁹.

Summary.—The best values for the various constants are presented in Table III.

Acknowledgments.—Thanks are due to Arapahoe Chemicals, Inc., Boulder, Colorado, for the facilities generously given to one of us, and to Panogen, Inc., and the Ringwood Chemical Corporation, both of Ringwood, Illinois, for providing materials.

THE DETECTION OF HYDROPHILIC HETEROGENEITIES ON A CARBON SURFACE

By F. H. HEALEY, YUNG-FANG YU AND J. J. CHESSICK

A Contribution from the Surface Chemistry Laboratory, Lehigh University, Bethlehem, Pa.

Received October 21, 1954

The effect of increasing the amount of surface oxide on Graphon on both the water vapor adsorption isotherms and the heat of immersion in water was studied. Oxidations were carried out at 530° with both dynamic and static oxygen atmospheres for successive periods up to 20 hours total. While the volume of water adsorbed increased regularly with the time of oxidation, the shape of the isotherm up to a relative pressure of 0.6 remained unchanged; plots of surface coverage *vs.* relative pressure were identical for the original sample and for the various oxidized samples. The weight loss due to formation of volatile oxides of carbon was a linear function of time of oxidation whereas the formation of surface oxide appeared to follow a parabolic rate curve. The ratio of the apparent area available to water adsorption to the total area of Graphon determined by nitrogen adsorption was taken as a measure of the fraction of surface oxidized. After degassing for two hours at 900° the sample showed a considerable decrease in the number of hydrophilic sites due to volatilization of oxygen complexes on the surface of the original sample. The heat of immersion in water did not prove to be a linear function of the fraction of hydrophilic surface. The increasing slope of the heat of immersion *vs.* hydrophilic fraction appeared to indicate that interactions between molecules adsorbed on adjacent patches of oxide sites increased as the number of patches on the surface increased. The slope and intercept of the curve for the more hydrophobic samples was used to estimate the heat of wetting of the carbon surface and of the hydrophilic sites.

Introduction

The purpose of this investigation was to study the effect of surface heterogeneity on the adsorption of water on a hydrophobic surface. The system Graphon-water was chosen because Graphon possesses a well-defined hydrophobic and almost homogeneous surface with a very small fraction of hydrophilic heterogeneities^{1,2} which are responsible for the adsorption of water at low pressures. It appeared possible to increase the fraction of hydrophilic sites by controlled oxidation of

the Graphon and to observe the changes produced in the water adsorption isotherm and the heat of immersion in water. It was of interest to determine the relation between the heat of immersion and the fraction of surface which was hydrophilic.

The application of the BET equation to the adsorption of water on Graphon has been shown to give values consistent with the thermodynamic criteria of a complete monolayer.² Unpublished work in this Laboratory with known mixtures of a hydrophilic surface, rutile and a hydrophobic surface, Graphon, has demonstrated that the ratio of the apparent surface area determined by water adsorption to the total area determined by nitro-

(1) C. Pierce and R. N. Smith, *THIS JOURNAL*, **54**, 784 (1950).

(2) G. J. Young, J. J. Chessick, F. H. Healey and A. C. Zettlemoyer, *ibid.*, **58**, 313 (1954).

gen adsorption is a direct measure of the fraction of hydrophilic surface present in the mixture. Accordingly this ratio has been used in the present work to characterize the hydrophilic heterogeneity of the Graphon surface before and after oxidation.

Experimental

Materials and Apparatus.—The Graphon sample was from the same lot, No. 2808, as used previously² and was supplied by Godfrey L. Cabot, Inc. The area determined by nitrogen adsorption was 98 m.²/g., and the freshly prepared sample was reported to contain 0.25% ash and 0.2% volatile matter. The samples were not treated with hydrogen since it was desired to preserve any heterogeneous surface sites.

High purity nitrogen, helium, oxygen and water were used and further purified by procedures previously described.³ Nitrogen adsorption and static oxidation studies were made with a BET type adsorption apparatus; water vapor adsorption measurements and procedures using a modified Orr apparatus have been described.²

Dynamic Oxidation.—Tank oxygen at 1 atmosphere without further purification was passed slowly through the samples at 530° for various time periods (listed in Table I). The Graphon sample was then cooled to room temperature and degassed at 10⁻⁵ mm. A portion of the sample was used for adsorption measurements and the remainder subjected to further oxidation under the same conditions.

Static Oxidation.—The samples were degassed at room temperature for 12 hours before oxidation. Moist oxygen, made by mixing known volumes of water vapor and dry oxygen to obtain a relative humidity of ca. 0.5, was admitted to the sample at room temperature and the equilibrium pressure recorded. The sample was then heated to 530° within a time interval of ten minutes. The total pressure at this temperature was approximately one atmosphere. The temperature was controlled to ±5° throughout the oxidation and any changes in pressure were noted. After two hours the sample was cooled to room temperature and the final equilibrium pressure was recorded.

Adsorption Measurements.—About 0.5 g. of Graphon was used for nitrogen surface area determinations at -195°. The surface areas were calculated by the BET method using a close-packed adsorbate area of 16.2 Å.² Water vapor adsorption measurements were made at 25° with 5- to 0.5-g. samples depending on the extent of oxidation of the surface. An experimental deviation of 0.005 ml. adsorbed was observed at the lower pressures. Nitrogen adsorption-desorption isotherms carried to saturation showed no increase in capillarity after six static oxidations over that of the unoxidized material.

With sample (D) the weight change caused by successive oxidations was followed. After each oxidation water vapor was admitted to a relative pressure of 0.3, at which pressure, as determined by the volumetric measurements, the BET V_m value was reached. The amount of water adsorbed was then measured gravimetrically with a correction made for the vapor in the dead space. The results agreed with the volumetric measurements within experimental error.

Heat of Immersion Measurements.—The calorimeter and procedure have been described earlier.⁴ Heats of immersion in water were measured for Graphon after the various types of treatment given below.

Treatment of Samples.—Sample A was oxidized by the dynamic process. Sample B received the static oxidation treatment with nitrogen and water vapor adsorption determined volumetrically. A second sample treated and measured in the same way checked the results obtained with sample B. Sample C was degassed at 900° for two hours with continuous pumping to study the thermal decomposition of the heterogeneous surface sites present on the original sample. Sample D received the same oxidation treatment as sample B but weight losses on oxidation and water adsorption measurements were made gravimetrically.

When this work was initiated it was hoped that the number of surface oxide sites formed could be directly measured from the oxidation data. However the complexity of the

oxidation process⁵ and particularly when water was present⁶ prevented any direct determination of the amount and nature of the surface oxide formed. A further complication was introduced when it was found the O₂, CO and particularly CO₂ all showed some physical adsorption on Graphon at room temperature. The isotherms were linear and at 20 mm. pressure the respective volumes adsorbed were 0.0055, 0.0090 and 0.029 ml./g.

Results and Discussion

The apparent surface areas determined by application of the BET equation to the adsorption isotherms of water vapor and nitrogen on sample A after various times of dynamic oxidation are given in Table I. The apparent area available to water vapor adsorption increased, as was expected, with increasing time of oxidation. The nitrogen or "true" surface area also increased markedly, the final area of 181 m.²/g. being roughly double the original value. The ratio of the apparent water area to the nitrogen area can be considered to be a measure of the surface heterogeneity, i.e., the fraction of hydrophilic sites present on the surface. The ratio may also be considered to be a measure of hydrophobicity; the smaller the ratio, the more hydrophobic the surface. The original sample had a surface with only about 1/400 of the surface hydrophilic; after 17 hours of oxidation about 1/6 of the surface had become hydrophilic. The increase in hydrophilic sites may be caused both by an increase in oxygen complex on the surface and by the increased percentage of ash due to the appreciable decrease in the weight of the sample. The sample weight used in the last oxidation was 0.42 g. and after 17 hours this weight had been reduced to 0.09 g.

The oxidations carried out in a static, moist, oxygen atmosphere were much less drastic in their

TABLE I
DYNAMIC OXIDATION AT 530°—SAMPLE A

Total time of oxidation (hr.)	Apparent BET area (m. ² /g.) H ₂ O	N ₂	$\frac{H_2O}{N_2} \times 10^2$
0	0.26	98.0	0.27
2	1.06	110.3	0.96
3	2.05	114.2	1.80
5	3.52	135.7	2.24
10	12.45	152.0	8.20
17	22.52	180.9	12.44

effect on the sample as shown in Table II. The nitrogen surface area increased by only 5% after 12 hours of oxidation compared to an increase of

TABLE II
STATIC OXIDATION—SAMPLE B

Total time of oxidation (hr.)	BET area (m. ² /g.) ΣH ₂ O	ΣN ₂	$\frac{\Sigma H_2O}{\Sigma N_2} \times 10^2$
0	0.26	98	0.27
2	.50	101	.50
4	.64	103	.62
6	.85	102	.83
8	.96	102	.94
10	1.16	103	1.13
12	1.44	102	1.41
Sample C			
Activated, 900°, 2 hr.	0.15	100	0.15

(3) A. C. Zettlemoyer and J. J. Chessick, *THIS JOURNAL*, **58**, 242 (1954).

(4) A. C. Zettlemoyer, G. J. Young, J. J. Chessick and F. H. Healey, *ibid.*, **57**, 649 (1953).

(5) E. A. Gulbransen, *Ind. Eng. Chem.*, **44**, 1045 (1952).

(6) R. Smith, C. Pierce and C. D. Joel, *THIS JOURNAL*, **58**, 298 (1954).

over 50% after ten hours of dynamic oxidation. Further, at this point only about $1/70$ of the surface had been oxidized.

The sample activated at 900° showed only a slight increase in the nitrogen surface area and a marked decrease in the number of hydrophilic sites, presumably due to volatilization of carbon-oxygen surface complexes. About 45% of the hydrophilic sites were destroyed by activation.

To demonstrate the effect of increasing the percentage of hydrophilic heterogeneity on the adsorption of water, the isotherms at 22° after the various static oxidation treatments are shown in Fig. 1. It is evident that the successive oxidations caused a continual increase in the volume of water adsorbed at all relative pressures. The adsorption isotherm reported by Pierce and Smith⁷ for water on Graphon which had been treated with hydrogen at 1100° would lie slightly above the curve for the original (unoxidized) sample. Since their sample had a nitrogen surface area about 20% less than the present Graphon, their surface must have still contained after treatment a considerable amount of hydrophilic heterogeneities. Recently it was reported⁸ that the earlier Graphon contained considerably more sulfur than more recent samples and this may be the cause of the greater water up-take.

The number or the fraction of hydrophilic sites appeared to increase approximately linearly with time of oxidation although there was considerable scatter due in part perhaps to the uncertainty in choosing the best straight line in the BET plots used to obtain ΣH_2O . The rate of apparent surface oxidation, assuming one molecule of H_2O adsorbed per oxide site at V_m , was 0.0019 ± 0.0005 surface sites per hour. With sample D where the static oxidation was carried to 20 hours and the water pick-up determined gravimetrically the curve was shown to be actually parabolic, and, furthermore, the sample showed a considerable loss in weight. The rate of increase in the fraction of hydrophilic sites cannot, therefore be taken as a measure of the rate of total oxidation.

One of the objects of this investigation was to study the change in the nature of the water adsorption isotherm as the number of hydrophilic sites on the surface was increased. While in the preceding figure it would appear that the isotherm on the unoxidized surface was Type III and after 12 hours of oxidation the isotherm was definitely Type II, this appearance is due simply to the difference in magnitude. The two isotherms are actually identical in shape up to the highest relative pressures measured (0.5–0.6). Indeed, if the isotherms are plotted in terms of $\theta(V/V_m)$ vs. p/p_0 , all of the oxidized samples as well as the unoxidized sample fall on a single curve. The shape of the isotherm is therefore not influenced by the fraction of the surface which is hydrophobic. If, as has been postulated,^{1,2} the adsorption of water by Graphon occurs by a clustering around hydrophilic sites, it would appear that on the original sample these heterogeneities were not isolated and randomly scattered about the surface

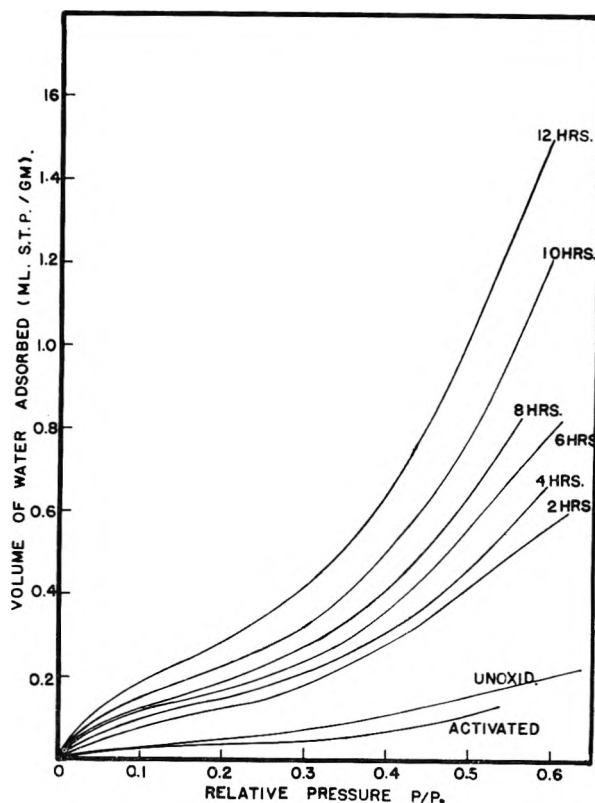


Fig. 1.

but rather were grouped together in patches perhaps at the edges of the graphitic planes. Otherwise, it would be expected that increased adsorbate interactions would show up in the isotherm as the distance between hydrophilic sites decreased. Even with sample A where $1/3$ of the surface was made hydrophilic and the maximum distance between sites could be only approximately two molecular diameters, there was no essential difference in the shape of the isotherm from that of the unoxidized sample.

The weight change of Graphon on oxidation as observed with sample D is shown graphically in Fig. 2. The figure is very similar to the curves presented by Gulbransen and Andrew⁸ for the oxidation of artificial graphite at 575°. Curve I represents the observed loss in weight of the sample with increasing time of oxidation. Curve II is the calculated gain in sample weight due to the formation of surface oxide. This curve was calculated from the water adsorption V_m values on the basis of one water molecule to each CO surface site. Curve III therefore represents the actual weight loss after correction for the gain in weight due to chemisorbed oxygen. The curves indicate that the rate of formation of volatile oxides is essentially constant over a period of 20 hours, but that the rate of stable surface oxide formation decreases with time.

Heats of immersion in water were measured for a number of the samples after the various treatments. Additional samples not shown in Tables I and II were also used in this study. These data are

(7) C. Pierce and R. N. Smith, *THIS JOURNAL*, **54**, 795 (1950).

(8) E. A. Gulbransen and K. F. Andrew, *Ind. Eng. Chem.*, **44**, 1039 (1952).

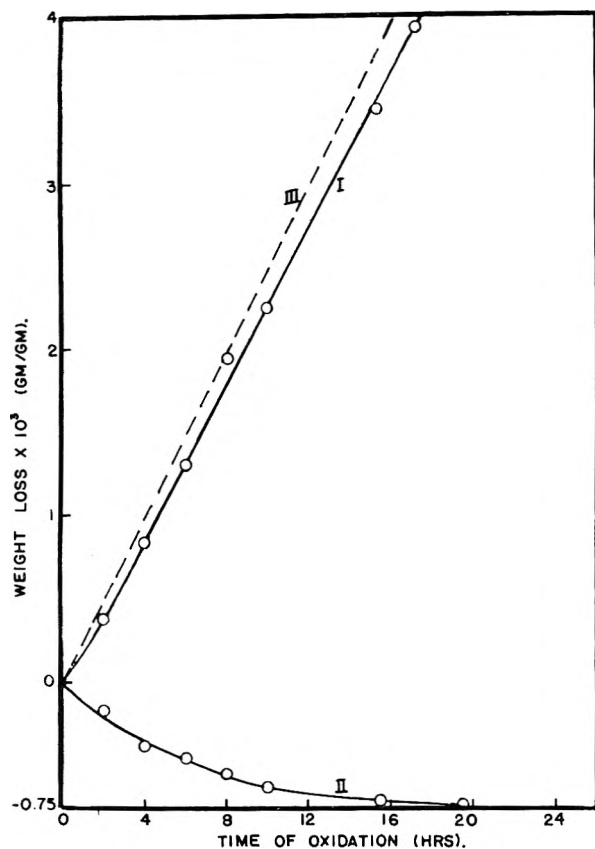


Fig. 2.—Weight change of graphon on oxidation; I, observed wt. loss; II, calcd. oxygen pickup; III, corrected wt. loss.

plotted in Fig. 3 in ergs per cm^2 of surface as measured by nitrogen adsorption against the fraction of the surface which was hydrophilic ($\Sigma \text{H}_2\text{O} / \Sigma \text{N}_2$). If the heat of wetting of the hydrophilic sites, h_0 , and the hydrophobic carbon surface, h_c , remained constant with increasing amounts of surface oxide, then a linear relation would be expected according to the equation

$$h_I = \left(\frac{\Sigma \text{H}_2\text{O}}{\Sigma \text{N}_2} \right) h_0 + \left(1 - \frac{\Sigma \text{H}_2\text{O}}{\Sigma \text{N}_2} \right) h_c$$

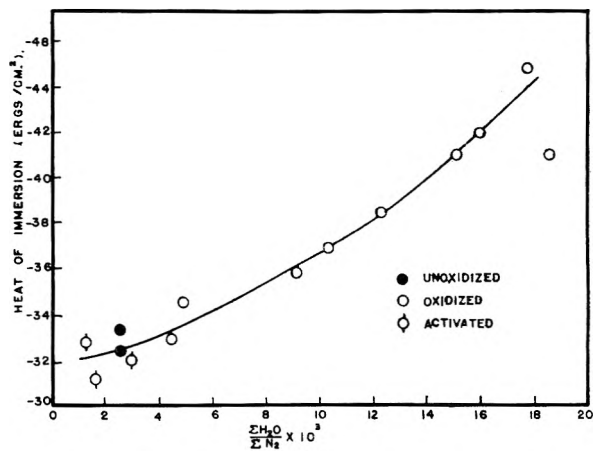


Fig. 3.

where h_I represents the observed heat of immersion. The best straight line drawn through the points would give $h_c = 31$ ergs/ cm^2 and $h_0 = 730$ ergs/ cm^2 . The latter value is not unreasonable although somewhat higher than is usually obtained with hydrophilic surfaces. Since the θ experimental curve actually increases in slope, it would appear that either h_0 increases or h_c decreases or that both occur as the percentage of hydrophilic sites increases. A decrease in h_c could be explained on the basis that the more energetic portions of the carbon surface would be most readily oxidized. However, water would interact with the carbon surface principally by non-polar van der Waals forces and this interaction would be smallest on the carbon atoms (such as edge atoms) most readily oxidized. A more reasonable explanation is that h_0 increases due to increasing adsorbate interaction between neighboring patches of hydrophilic sites. This interaction would not show up in the isotherms except at relative pressures close to saturation.

Acknowledgment.—The authors gratefully acknowledge the financial support provided by the Office of Naval Research Project NR057-186, Contract N8onr-74300.

ELECTRICAL RELAXATION DISTRIBUTION FUNCTIONS IN POLYMERS AND THEIR TEMPERATURE DEPENDENCE

BY JOHN D. FERRY, MALCOLM L. WILLIAMS¹ AND EDWIN R. FITZGERALD

Contribution from the Department of Chemistry, University of Wisconsin, Madison, Wis., and the Department of Physics, Pennsylvania State University, State College, Pa.

Received October 27, 1954

Data for dielectric constant (ϵ') and dielectric loss (ϵ'') of polyvinyl acetal (by Funt and Sutherland) and of polyvinyl acetate, polyvinyl chloroacetate and polymethyl acrylate (by Mead and Fuoss) have been treated by the method of reduced variables. The normalized variables $(\epsilon' - \epsilon_\infty)/(\epsilon_0 - \epsilon_\infty)$ and $\epsilon''/(\epsilon_0 - \epsilon_\infty)$, where ϵ_0 and ϵ_∞ are the limiting low and high frequency values of ϵ' , superpose at various frequencies and temperatures to form composite curves when the frequency scale is reduced by a temperature-dependent factor b_T . From b_T the apparent activation energy for dielectric relaxation is obtained and found to be strongly temperature dependent. From the composite reduced plots, the distribution function of electrical relaxation times is calculated over a wide range of time scale for the 4 polymers; the values from ϵ' and from ϵ'' are in good agreement. The relation of this analysis to the more customary plots of ϵ' and ϵ'' against temperature is discussed.

Introduction

In recent treatments of dynamic mechanical properties of polymers, the components of a complex modulus measured at different frequencies and temperatures are combined by using reduced variables based on the assumption of equal temperature dependence of all relaxation or retardation times.^{2,3} From the resulting composite curves, relaxation distribution functions have been calculated by methods with varying degrees of approximation.⁴⁻⁶ Similar treatments have been applied in a few cases to the components of the complex dielectric constant in polymer systems.^{3,7} The use of a relaxation distribution function⁸⁻¹⁰ and the concept of a time or frequency scale which shifts with temperature^{8,11} are of course well established in the dielectric literature; but most previous discussions have been based on functions of prescribed analytical form (*e.g.*, a Gaussian distribution for the logarithmic time dependence, and an exponential function of $1/T$ for the temperature dependence). In the more recent treatments, no *a priori* assumptions are required regarding the form of either time or temperature dependence; these functions are obtained empirically from the data.

It is of particular interest to compare the electrical relaxation spectrum with the mechanical retardation spectrum. A detailed analysis for two polyvinyl chloride compositions³ showed that these two spectra differed greatly in form but that their temperature dependences, as expressed by the temperature shift of the logarithmic time scale, were identical. Similar conclusions have been

drawn for undiluted polyvinyl acetate.¹² If the identity of the temperature dependence for mechanical and electrical relaxations can be generalized for a variety of polymer systems, this result will have considerable practical importance. Moreover, polymer viscoelasticity theory can now be applied to estimate the effective monomeric friction coefficient from the mechanical relaxation spectrum^{13,14} and an extension of the theory might provide an independent determination of this important quantity from the electrical spectrum.

Dielectric data in the literature for several other polymers have therefore been examined to determine whether the treatment of reduced variables is applicable and to provide temperature reduction factors and relaxation spectra for future comparison with dynamic mechanical data.

Reduction of Dielectric Data.—If all contributions to the dielectric constant associated with dipole orientation have magnitudes inversely proportional to absolute temperature T and directly proportional to density ρ , and if all electrical relaxation times change by the same factor b_T when the temperature changes from T_0 to T , then³ measurements at all temperatures should be reduced to T_0 by using the variables

$$\begin{aligned}\epsilon'_p &= \epsilon' [T\rho_0/T_0\rho + (\epsilon_\infty/\epsilon')(1 - T\rho_0/T_0\rho)] \\ \epsilon''_p &= \epsilon'' (T\rho_0/T_0\rho) \\ \omega_p &= \omega b_T\end{aligned}\quad (1)$$

where ϵ' and ϵ'' are the real and imaginary parts of the complex dielectric constant, ϵ_∞ is the limiting high frequency value of ϵ' , ρ_0 is the density at T_0 , and ω is the circular frequency. The value of b_T is chosen empirically at each temperature; the criteria for successful reduction are (a) the shapes of individual curves of ϵ'_p and ϵ''_p vs. $\log \omega$ must coincide with horizontal shifting; (b) the same values of b_T must superpose both ϵ'_p and ϵ''_p data. These criteria were met for the two polyvinyl chloride compositions previously treated.³ They are now found to be met also for the data on polyvinyl acetal of Funt and Sutherland,¹⁵ as shown in Fig. 1. Here data at 6 temperatures

(1) Union Carbide and Carbon Fellow in Physical Chemistry, 1952-1954.

(2) J. D. Ferry, E. R. Fitzgerald, M. F. Johnson and L. D. Grandine, Jr., *J. Appl. Phys.*, **22**, 717 (1951).

(3) J. D. Ferry and E. R. Fitzgerald, *J. Colloid Sci.*, **8**, 224 (1953).

(4) M. L. Williams and J. D. Ferry, *J. Polymer Sci.*, **11**, 169 (1953).

(5) F. Schwarzl and A. J. Staverman, *Appl. Sci. Research*, **A4**, 127 (1953).

(6) F. C. Roesler and J. R. A. Pearson, *Proc. Phys. Soc.*, **B67**, 338 (1954).

(7) P. Ehrlich and N. J. DeLollis, *J. Research Natl. Bur. Standards*, **51**, 145 (1953).

(8) K. W. Wagner, *Arch. Elektrotechnik*, **3**, 83 (1914).

(9) K. S. Cole, *J. Gen. Physiol.*, **12**, 37 (1928).

(10) R. M. Fuoss, *J. Am. Chem. Soc.*, **63**, 2401 (1941).

(11) H. Fröhlich, "Theory of Dielectrics," Oxford University Press, New York, N. Y., 1949.

(12) M. L. Williams and J. D. Ferry, *J. Colloid Sci.*, **9**, 479 (1954).

(13) P. E. Rouse, Jr., *J. Chem. Phys.*, **21**, 1272 (1953).

(14) J. D. Ferry, R. F. Landel and M. L. Williams, *J. Appl. Phys.*, in press.

(15) B. L. Funt and T. H. Sutherland, *Can. J. Chem.*, **30**, 940 (1952).

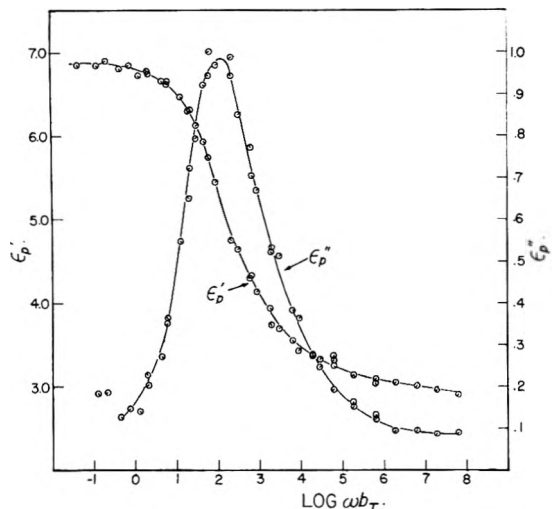


Fig. 1.—Real and imaginary parts of the complex dielectric constant of polyvinyl acetal (data of Funt and Sutherland), reduced to 80°. Pip \odot , 70°; succeeding 90° rotations of pip counterclockwise correspond to 10° increments of temperature.

and 7 frequencies have been plotted according to eq. 1, taking $\epsilon_\infty = 2.16$ and choosing $T_0 = 353^\circ\text{K}$.

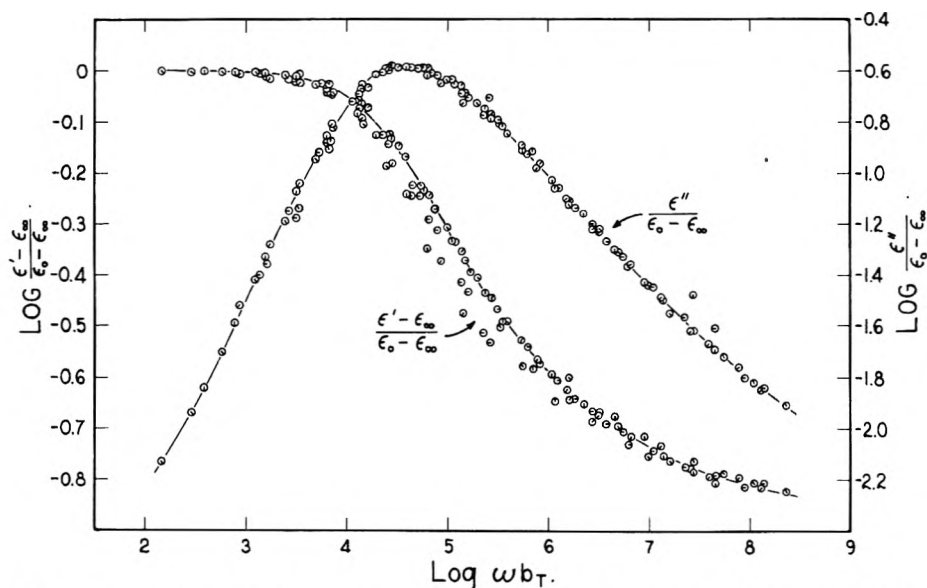


Fig. 2.—Real and imaginary parts of the complex dielectric constant of polyvinyl acetate (Gelva 15, data of Mead and Fuoss), normalized and reduced to 75°. Pip \odot , 40°; succeeding 45° rotations of pip counterclockwise correspond to 45, 48, 51, 54, 57, 60, 63, 66, 69, 71, 75 and 80°, ending with \ominus .

The same values of b_T are used for both ϵ'_p and ϵ''_p , and each component gives a single composite curve.

In other cases, eq. 1 are not so successful; the maximum values of $\epsilon' - \epsilon_\infty$ and ϵ'' decrease faster with increasing temperature than proportional to ρ/T . Thus the ϵ'_p peaks have different heights at different temperatures and cannot be superposed by horizontal shifting. (Also, earlier calculations by Mead and Fuoss yielded in such cases dipole moments which decreased substantially with increasing temperature¹⁶.) Without attempting to account for this phenomenon, it can be circumvented by normalizing the magnitudes of ϵ' and

ϵ'' , using as reduced variables $(\epsilon' - \epsilon_\infty)/(\epsilon_0 - \epsilon_\infty)$ and $\epsilon''/(\epsilon_0 - \epsilon_\infty)$, where ϵ_0 is the limiting value of ϵ' at low frequencies. These do not differ greatly from the components of the more complicated reduced polarization of Fuoss and Kirkwood.¹⁷ When they are plotted against $\log \omega b_T$, satisfactory superposition has been found¹² with data of Mead and Fuoss¹⁶ for a high molecular weight polyvinyl acetate. Similar plots are now shown in Figs. 2–4 for another sample of polyvinyl acetate,¹⁶ polyvinyl chloroacetate¹⁶ and polymethyl acrylate.¹⁸ The values of ϵ_∞ have been taken as the squares of the refractive indices,^{16,18} viz., 2.16, 2.37 and 2.19, respectively. Values of ϵ_0 have been taken from the asymptotic low frequency values of ϵ' at higher temperatures, and at lower temperatures are extrapolated therefrom by a linear relation $\epsilon_0 = A - B(T - T_0)$. For the three polymers, $A = 8.28, 27.3$ and 7.58 , respectively; $B = 0.039, 0.208$ and 0.0194 , respectively; and $T_0 = 348, 323$ and 298°K , respectively. In each case the same values of b_T have been used for both real and imaginary components, and single composite curves are obtained. (The points below the ϵ' curve in Fig. 2 are nearly all from measurements at 10,000 cycles.)

Temperature Dependence of Dielectric Relaxation.—The factor b_T , which describes the temperature dependence of all relaxation times, is plotted against temperature for the four polymers in Fig. 5. It varies over ten powers of ten. For polyvinyl acetate it has already been shown that the corresponding mechanical reduction factor a_T is identical with b_T over a considerable range of temperature overlap,¹² and recent dynamic mechanical measurements on polymethyl acrylate¹⁹ have led to

(17) R. M. Fuoss and J. G. Kirkwood, *ibid.*, **63**, 385 (1941).

(18) D. J. Mead and R. M. Fuoss, *ibid.*, **64**, 2389 (1942).

(16) D. J. Mead and R. M. Fuoss, *J. Am. Chem. Soc.*, **63**, 2832 (1941).

(19) M. L. Williams, J. D. Ferry, S. Axelrod, S. N. Chinai, J. D. Matlack and A. L. Resnick, presented at the 126th Meeting of the American Chemical Society, September 17, 1954.

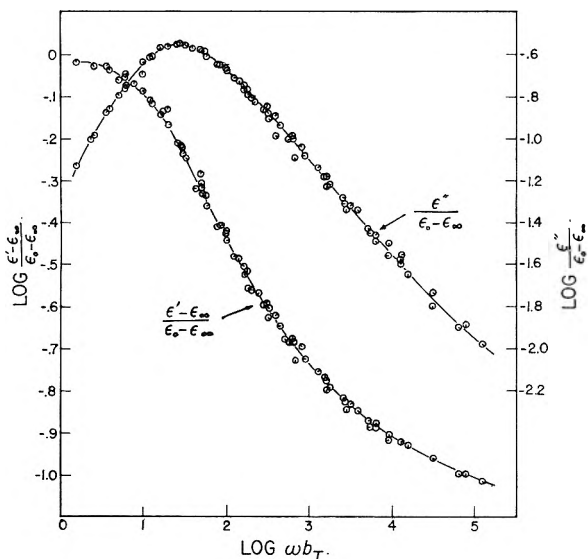


Fig. 3.—Real and imaginary parts of the complex dielectric constant of polyvinyl chloroacetate (data of Mead and Fuoss), normalized and reduced to 50°. Pip down, 42° (at highest reduced frequency); succeeding 45° rotations of pip counterclockwise correspond to 44, 46, 50, 52, 54, 56, 58, 60, 62, 64, 66, 68 and 70°, ending with ⊙ (at lowest reduced frequency).

phasized that the corresponding dielectric quantity behaves identically, although, within a limited temperature range, plots of the logarithm of relaxation time against $1/T$ appear to be straight or only slightly curved.^{7,15,22} The variation of ΔH_a with temperature is qualitatively understood to be associated with changes in free volume.^{23,24}

The identification of a_T with b_T , and the equality of the activation energies calculated from them, is restricted to the primary loss mechanisms in both mechanical and electrical dispersion, the former occurring in the transition zone (as a function of frequency) from rubber-like to glass-like behavior—the α -transition of Deutsch, Hoff and Reddish.²⁵ It is important to avoid confusion with secondary loss mechanisms which appear in both mechanical^{25,26} and dielectric^{25,27} data and are generally less temperature dependent than the primary mechanism. The correlation of ΔH_a values for different polymer samples will be discussed in a later communication.

Relaxation Distribution Functions.—The normalized electrical relaxation distribution function, $\Psi_n d \ln \tau$, is the fraction of the total orientation contribution to the dielectric constant, $\epsilon_0 - \epsilon_\infty$, associated with relaxation times lying in the logarithmic interval $d \ln \tau$. This function can be

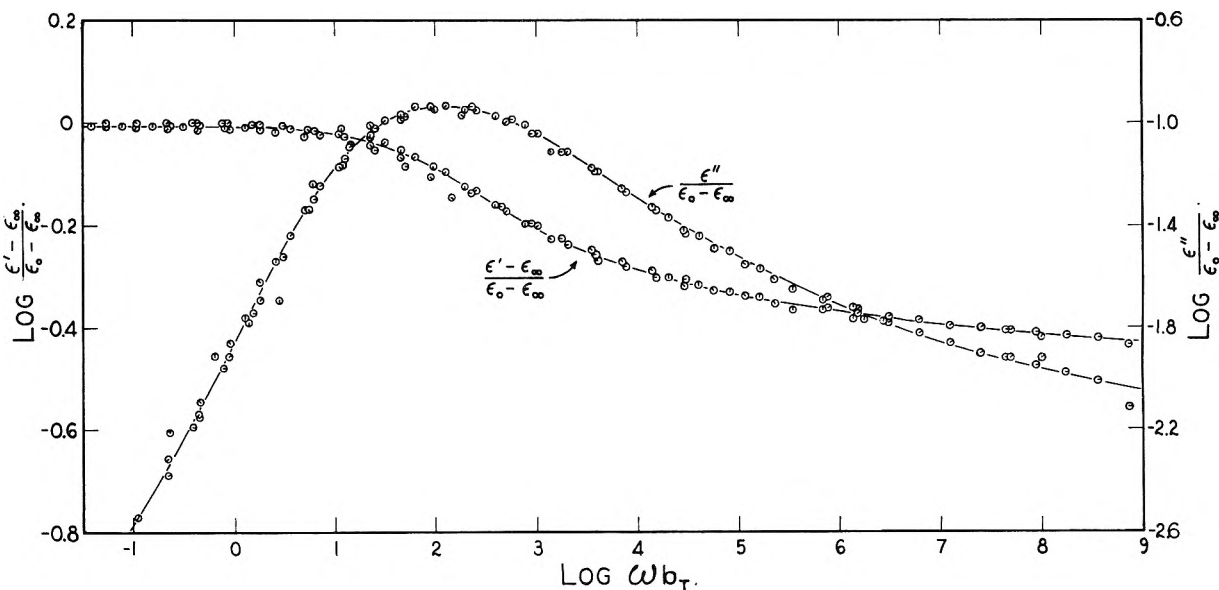


Fig. 4.—Real and imaginary parts of the complex dielectric constant of polymethyl acrylate (data of Mead and Fuoss), normalized and reduced to 25°. Pip right, 5°; succeeding 45° rotations of pip counterclockwise correspond to 10, 15, 20, 24, 30, 35, 40, 45, 50, 55, 60 and 70°, ending with ⊙.

the same conclusion for this polymer. The appropriate mechanical data for polyvinyl chloroacetate and polyvinyl acetal are not yet available.

Graphical differentiation of the curves of Fig. 5 yields the apparent activation energy for relaxation, $\Delta H_a = -RT^2 d \ln a_T/dT$. This quantity, plotted in Fig. 6, varies sharply with temperature. The apparent activation energy for mechanical relaxation is now well recognized to be strongly temperature dependent^{20,21}; it should be em-

calculated from either the real or the imaginary component of the dielectric constant by the approximation formulas of Williams and Ferry,^{4,12} noting that the function defined earlier, Ψ , is $\Psi_n(\epsilon_0 - \epsilon_\infty)$. Such calculations, from the composite curves of Figs. 1-4, are plotted against reduced time in Fig. 7. In each case the distribu-

- (22) A. Dyson, *J. Polymer Sci.*, **7**, 133 (1951).
- (23) T. G. Fox, Jr., and P. J. Flory, *J. Appl. Phys.*, **21**, 581 (1950).
- (24) F. Bueche, *J. Chem. Phys.*, **21**, 1850 (1953); *J. Applied Phys.* (to be submitted).
- (25) K. Deutsch, E. A. W. Hoff and W. Reddish, *J. Polymer Sci.*, **13**, 565 (1954).
- (26) K. Schmieder and K. Wolf, *Kolloid-Z.*, **134**, 149 (1953).
- (27) R. M. Fuoss, *J. Am. Chem. Soc.*, **63**, 369 (1941).

(20) J. D. Ferry and E. R. Fitzgerald, "Proc. 2nd Intern. Cong. Rheology, London," Butterworths, 1954, p. 140.

(21) A. V. Tobolsky and E. Catsiff, *J. Am. Chem. Soc.*, **76**, 4204 (1954).

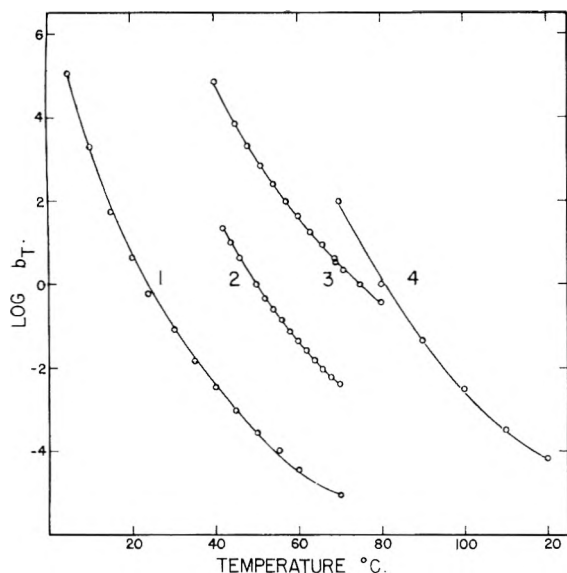


Fig. 5.—Reduction factor b_T plotted logarithmically against temperature: 1, polymethyl acrylate; 2, polyvinyl chloroacetate; 3, polyvinyl acetate; 4, polyvinyl acetal.

tions obtained from ϵ' and from ϵ'' agree very well, affording a test of internal consistency of the data which has not previously been applied.

The distributions differ considerably in sharpness. Each curve appears on this logarithmic scale to be unsymmetrical about its maximum, in contrast to most of the empirical and theoretical distribution functions previously discussed.^{8, 10, 28}

Discussion

The use of reduced variables implies that the sharpness of Ψ_n on a logarithmic time scale does not change with temperature. For all the polymers thus treated successfully here and previously,³ the maximum value of ϵ'' in frequency dispersion decreases somewhat with increasing temperature; this is believed not to be associated with a broadening of the distribution function, but rather with a decrease in magnitude of polarization, either the normal proportionality to ρ/T or an abnormally large decrease which is reflected also in the temperature dependence of ϵ_0 . This view is supported by the excellent superposition with reduced variables after normalization of both real and imaginary components with the factor $1/(\epsilon_0 - \epsilon_\infty)$, as in Figs. 2-4.

However, there are polymer systems for which the maximum value of ϵ'' in frequency dispersion increases with increasing temperature, as seen for example in polyvinyl chloride plasticized with small amounts of diphenyl²⁹ or tetrahydronaphthalene,³⁰ as well as styrene-acrylonitrile copolymers⁷. Here it must be concluded that the distribution function actually sharpens with increasing temperature, and data plotted with reduced variables at different temperatures would not superpose. The source of this effect is not understood; it may be due to structural alterations with temperature,

(28) J. G. Kirkwood and R. M. Fuoss, *J. Chem. Phys.*, **9**, 329 (1941).

(29) R. M. Fuoss, *J. Am. Chem. Soc.*, **63**, 378 (1941).

(30) R. M. Fuoss, *ibid.*, **63**, 2410 (1941).

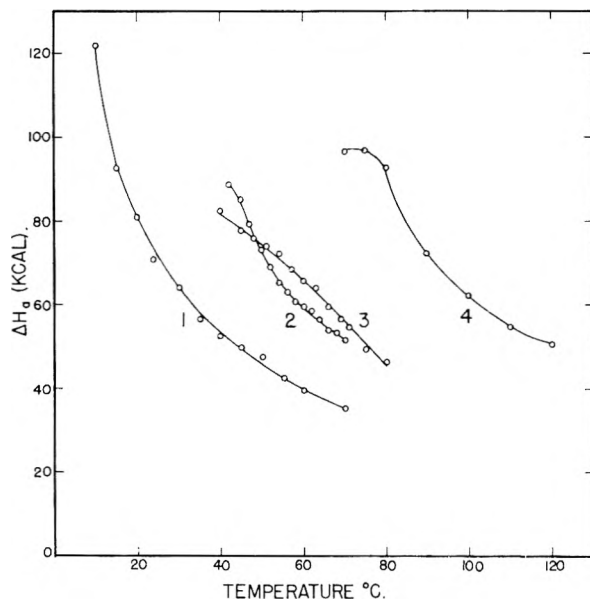


Fig. 6.—Apparent activation energy for dielectric relaxation plotted against temperature. Key same as in Fig. 5.

such as melting of crystallites or less definite changes in local ordering of molecular chains.

In earlier analyses of temperature dependence, a heat of activation often has been calculated from the temperature dependence of the frequency of maximum ϵ'' . Since the maximum may not be easy to locate exactly, and at best represents a single point, we prefer the method described here which involves matching segments of curves; each frequency shift relies on a number of experimental measurements of both ϵ' and ϵ'' .

Often, because of experimental convenience, dielectric data are plotted against temperature at constant frequency, providing so-called temperature dispersion curves. It should be emphasized that no definite conclusions can be drawn from the shapes of such curves regarding the sharpness of the relaxation distribution function and whether or not the latter is affected by temperature. The rate of change of ϵ' with temperature, and the breadth of the ϵ'' peak, depend not only on the sharpness of Ψ_n but also on the magnitude of ΔH_a . The rapid change of the latter with temperature (Fig. 6) causes the peak of ϵ'' plotted against temperature to be broad or narrow depending on where it falls on the temperature scale. For example, in polyvinyl acetal, the ϵ'' peak falls at 84° for a frequency of 0.1 kc. and at 114° for 100 kc. At the latter temperature, ΔH_a is smaller by a factor of 0.6, so the peak of ϵ'' vs. T is considerably broader at 100 kc. than at 0.1 kc. But the shape of the distribution function Ψ_n does not change with temperature. Analogous principles have been stressed for the dispersion of mechanical properties.²⁰ Thus, the rate of change of elastic modulus with temperature at constant frequency depends on both ΔH_a and the shape of the mechanical relaxation distribution function.

Acknowledgments.—This work was supported in part by a grant from Research Corporation, and in part by the Research Committee of the Graduate

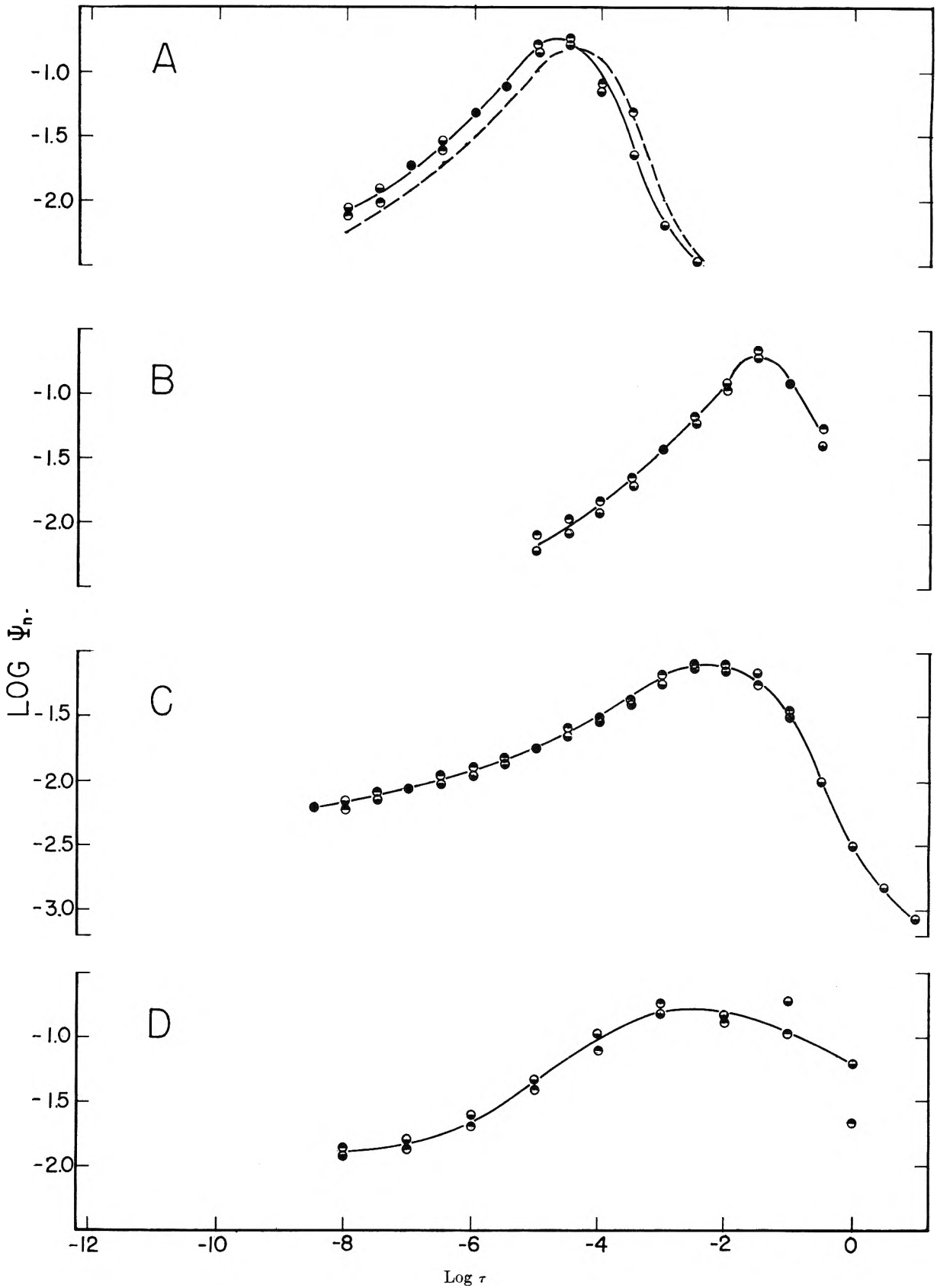


Fig. 7.—Normalized distribution function of relaxation times reduced to the following standard temperatures: A, polyvinyl acetate, 75° (solid curve Gelva 15, from Fig. 2, dashed curve Gelva 60, from reference 12); B, polyvinyl chloroacetate, 50°; C, polymethyl acrylate, 25°; D, polyvinyl acetal, 80°. Circles top black, calculated from ϵ' ; bottom black, from ϵ'' .

School of the University of Wisconsin from funds supplied by the Wisconsin Alumni Research Foundation. We are indebted to Union Carbide and

Carbon Corporation for support through its Fellowship in Physical Chemistry, and to Mrs. J. C. Alexander for assistance with calculations.

THE ADSORPTION OF CESIUM IN LOW CONCENTRATION BY PAPER¹

BY MARVIN L. GRANSTROM^{2a} AND BERND KAHN^{2b}

Oak Ridge National Laboratory, Oak Ridge, Tennessee

Received October 27, 1954

Carrier-free Cs¹³⁷ was adsorbed on Whatman #50 filter paper from aqueous solutions at a variety of pH values and cesium concentrations. The adsorption appears to take place by ion exchange and follows the Langmuir isotherm. No radio-colloidal properties were observed.

Introduction

The fact that radiocesium is extremely difficult to remove from soils stimulated the investigation of the mechanism by which the cesium is adsorbed by the soil. In very dilute solutions, adsorption is generally either radio-colloidal or by ion exchange. Formation of colloidal-type particles by many radioactive substances (hence, the term "radio-colloidal") has been observed under certain conditions, at concentrations far less than indicated by commonly accepted solubility product values, particularly in solutions in which the salt is sparingly soluble.³ Mechanical adsorption of the radio-colloid could thus be a mechanism by which radioactive substances are removed from solution onto the surfaces of solid matter. The other most likely method of removal would be ion exchange. This procedure is adequately described by the law of mass action.

The two processes can be differentiated by the behavior of the solute under varying conditions.

(1) The increase in ionic strength of a solution decreases the removal of a particular ion by the ion-exchange process whereas the increase in ionic strength enhances removal by radio-colloidal adsorption.^{3,4}

(2) The Langmuir isotherm

$$\frac{x}{m} = \frac{k_1 C}{k_2 C + 1} \quad (1)$$

in which

x = mole of solute removed
 m = wt. of adsorbant in g.
 C = equilibrium concn. of solute in mole/l.
 k_1 and k_2 = constants

describes the ion exchange process, but not necessarily colloid adsorption.⁵

At low concentrations $k_2 C$ is much less than unity, hence equation 1 can be written

$$k_1 = \frac{x/m}{C} \quad (2)$$

(1) This work was performed at the Oak Ridge National Laboratory and supported in part by the Oak Ridge Institute of Nuclear Studies of which support grateful acknowledgment is made.

(2) (a) Associate Professor of Sanitary Engineering, University of North Carolina, Chapel Hill, North Carolina. (b) Associate Chemist, Health Physics Division, Oak Ridge National Laboratory, Oak Ridge, Tennessee, Operated by Carbide and Carbon Chemicals Company.

(3) G. K. Schweitzer and W. M. Jackson, *J. Chem. Ed.*, **29**, 513 (1952).

(4) J. Schubert, *THIS JOURNAL*, **52**, 340 (1948).

(5) T. Schönfeld and E. Broda, *Mikrochem.*, **36-37**, 537 (1951).

(3) Upon subsequent passing of the solution over a new adsorbent the ion exchange process effects further solution removal of the same order of magnitude, whereas only slight additional removal is probably by colloid adsorption.^{3,4}

Since the mechanism of cesium removal was the primary objective of this investigation, filter papers rather than soils were used as the adsorbent; this eliminated any complications which might have been introduced by the non-homogeneous character of soils. The use of filter papers was suggested by previous work.⁵⁻⁷ Filter paper may be considered as cellulose with carboxyl groups, the hydrogen ion of which can be replaced by other cations.

To check the behavior of cesium by the above criteria, aqueous solutions of cesium, at various concentrations and pH values, were passed through prepared filter papers.

Procedure.—A carrier-free solution of radioactive Cs¹³⁷ in dilute HCl was obtained from the Operations Division of the Oak Ridge National Laboratory. The solution was diluted to approximately 0.1 N HCl and passed through a column of ion-exchange resin, IR-120(H⁺). The column was washed with 0.2 N HCl to remove all cations except cesium. The cesium was then removed from the resin with 0.5 N HCl, its movement being detected with a Geiger-Müller counter. After it was apparent that all of the cesium had been eluted, the elutriant was evaporated to dryness and the Cs¹³⁷ was taken up in doubly distilled water. The activity of the solution was determined in a calibrated high pressure ionization chamber,⁸ which counted the γ -activity of Ba¹³⁷ which is in secular equilibrium with 92% of the Cs¹³⁷. The concentration of the Cs¹³⁷ is then computed by the equation

$$x = \frac{dN}{dt} \left(\frac{t_{1/2}}{0.693} \right) \left(\frac{1}{6.02 \times 10^{23}} \right)$$

in which x = moles of Cs¹³⁷

$$\frac{dN}{dt} = \text{Cs}^{137} \text{ activity} = 1.1 \times \text{Ba}^{137} \text{ activity}$$

$$t_{1/2} = \text{half-life of Cs}^{137} = 33 \text{ years}$$

Filter papers were prepared by soaking them in solutions of HCl, LiCl, NaCl or KCl, then rinsing them with water, and placing in a closed vessel to keep them moist. All reagents used were C.p. grade or equivalent. The Cs¹³⁷ solution was diluted with doubly distilled water and passed through a pad of four Whatman #50 filter papers of the desired cationic form. This filter paper was used to permit comparison of results with those of other investigators. Filtration through Whatman papers nos. 1, 2, 40 and 50

(6) G. K. Schweitzer, *et al.*, *J. Am. Chem. Soc.*, **74**, 4178 (1952); **74**, 6186 (1952); **75**, 793 (1953); **75**, 4354 (1953); **75**, 6330 (1953); **76**, 3348 (1954).

(7) J. D. Kurbatov and M. H. Kurbatov, *THIS JOURNAL*, **46**, 441 (1942).

(8) J. W. Jones and R. T. Overman, *AECD-2367* (1948).

showed no important differences in the capacity of the papers.

A sketch of the filtering apparatus is shown in Fig. 1. This apparatus was soaked in cesium carrier solution and rinsed with water prior to each use. The filtrate was collected in one-milliliter volumetric flasks, and, after waiting for the Ba^{137} daughter to reach equilibrium with the parent Cs^{137} (at least 15 minutes), the Ba^{137} γ -activity in the filtrate and in aliquot portions of the original solution were counted in anthracene or NaI(Tl) scintillation counters. One milliliter portions of the filtrate were collected until the measured activity in the filtrate reached a constant value. A Cs^{137} - Ba^{137} standard was used to correct for the daily variation in counting efficiency. The samples, having counts between 300 and 30,000 counts per minute, were counted for two minutes each. All experiments were made in duplicate and the results given are averages of two determinations. The difference between duplicate results did not exceed 10%.

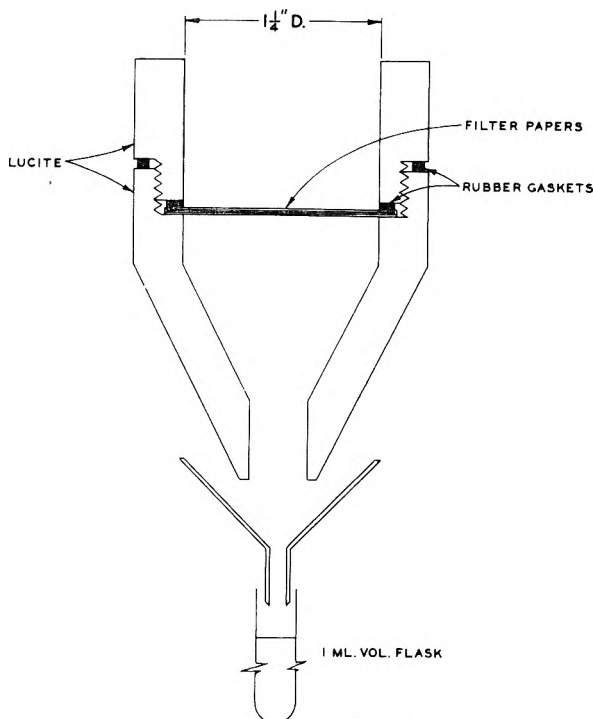


Fig. 1.—Sectional view of experimental apparatus.

Results

Cs^{137} solutions at six different concentrations and five different pH values (pH adjustment was made using HCl or LiOH) were filtered. The capacity of the paper at each pH and concentration was determined by subtracting the total activity of the filtrate, determined by measuring the area beneath the activity-volume curve, from the activity at equilibrium concentration. Typical variations in effluent activity with volume at different ranges of pH are shown in Fig. 2. The variations in the capacity of each paper in the lithium form at different concentrations with pH are shown in Fig. 3. The values of k_1 computed by equation 2 for the different experimental conditions indicated are shown in Table I.

Subsequent filtration of the effluent resulted in further removal of Cs^{137} . For example, at pH 6.0, using a single Whatman #50 filter paper (Li form), the first filtration reduced the activity from 1400 to 500 c.p.m. and the second filtration, using a second filter paper (Li form), reduced the activity from 500 to 180 c.p.m. Thus the percentage reduction

TABLE I
CAPACITY OF WHATMAN #50 FILTER PAPER, AND k_1 FOR LANGMUIR ISOTHERM

Cationic form of paper	pH	Concn. of Cs^{137} , mole l. ⁻¹ × 10 ⁶	Capacity of one paper for Cs^{137} , ^a mole × 10 ⁹	k_1 , ^b l. g. ⁻¹ × 10 ²
Li	7.0	5.17	13.6	3.43
		2.71	6.75	3.25
		1.29	3.25	3.28
		0.49	1.25	3.31
		0.074	0.215	3.78
Na	7.1	1.96	4.25	2.82
K	7.1	1.96	3.25	2.15
H	7.1	1.96	2.50	1.66

^a Each paper weighs 0.077 g. ^b From equation 2, $k_1 = (x/m)/C$.

(64%) was the same for both filtrations, this being consistent with equation 2. Increases in ionic strength of the solution at pH 6.0, by the addition

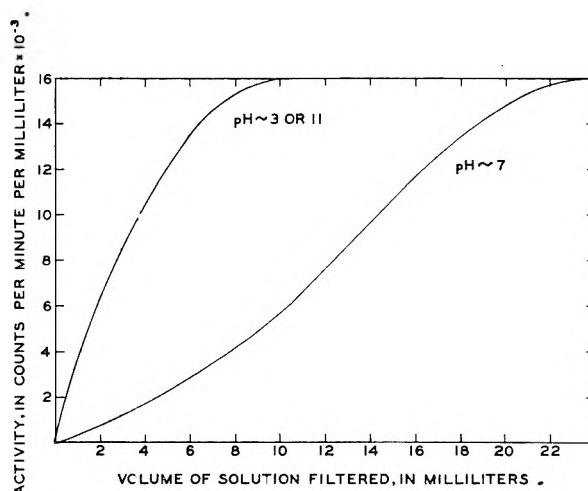


Fig. 2.—Typical activity vs. filtrate volume curve.

of NaCl, resulted in decreased removal of Cs^{137} ; in a 0.5 M NaCl solution no Cs^{137} removal was noted. The addition of silicotungstic acid or chloroplatinic acid, the cesium compounds of which are sparingly soluble, showed no increase in Cs^{137} removal.

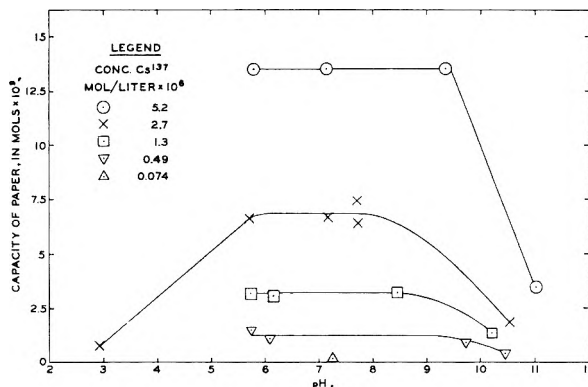


Fig. 3.—Variation of capacity of filter paper with pH for Cs^{137} Whatman #50 filter paper, L₁ form.

It was observed that Cs^{137} was readily adsorbed on glass and plastic surfaces, the phenomena occurring even after saturation of the surfaces with inac-

tive cesium in carrier concentration. This adsorption was corrected for, in part, in the calculation of Cs^{137} concentration by assuming that the Cs^{137} influent activity was the same as the equilibrium activity of the effluent; the difference was never greater than 10%. It was assumed that the differences in these activities were due to the adsorption of Cs^{137} by the glass or plastic.

Carrier-free barium is also present in solution, either as radioactive Ba^{137} , the daughter of Cs^{137} , or as inactive Ba^{137} resulting from the decay of Cs^{137} and Ba^{137m} (isomeric state). The weight of radioactive Ba^{137} is small, the ratio of Cs^{137} and Ba^{137m} (isomeric state) atoms being the ratio of their half lives, approximately $7 \times 10^6/1$. The amount of inactive Ba^{137} is dependent upon the time after chemical separation; the maximum time for this experiment being two months, the concentration of the inactive Ba^{137} was negligible. Alkalies, including inactive cesium, may be present in small amounts.

Discussion and Conclusions

Filter paper adsorbs small amounts of Cs^{137} . Its capacity increases with Cs^{137} concentration and is dependent on the cationic form of the paper, being greatest for Li and decreasing in the order Na, K and H. An increase in activity of effluent with volume up to the equilibrium value, as shown

on Fig. 2, is typical of an ion exchange phenomenon. At a given pH and for a given form of paper the values of k_1 as computed by equation 2 are essentially constant, indicating a Langmuir isotherm, which is characteristic of ion exchange. Adsorption decreases with increasing concentration of H^+ or Li^+ as shown in Fig. 2, again indicating ion exchange rather than radio-colloid formation as the removal mechanism. Subsequent passes of the filtrate through new filter paper results in continued removal of Cs^{137} ; this would be expected for ion exchange but not for colloid adsorption. Recent experiments⁹ comparing the removal of Cs^{134} at concentrations of about 10^{-7} molar and pH values between 0 and 10 by filtration through Whatman #50 paper (removal up to 17%) and by centrifugation (0–2% removal) also suggest that ion exchange rather than radio-colloid adsorption occurs. The adsorption of cesium and sodium on glass¹⁰ may be similarly explained. The evidence that ion exchange is the removal mechanism is substantiated by the lack of increase in adsorption of Cs^{137} from solutions containing silicotungstic acid or chloroplatinic acid which might best effect the formation of radio-colloids.

(9) G. K. Schweitzer and W. M. Jackson, *J. Am. Chem. Soc.*, **76**, 941 (1954).

(10) J. W. Hensley, A. O. Long and J. E. Willard, *ibid.*, **70**, 3146 (1948).

KINETICS OF THE OXIDATION OF SELENIOUS ACID BY HYDROGEN PEROXIDE¹

BY FRANCIS J. HUGHES AND DON S. MARTIN, JR.

Contribution No. 360 from the Institute for Atomic Research and Department of Chemistry, Iowa State College, Ames, Iowa

Received October 29, 1954

The oxidation of selenious acid by aqueous hydrogen peroxide in strongly acid solutions is accompanied by decomposition of the peroxide. The rate of oxidation is given by the expression $-d(\text{H}_2\text{SeO}_3)/dt = k_1(\text{H}_2\text{SeO}_3)^2(\text{H}_2\text{O}_2)/(\text{H}^+)$. The rate is not affected by the presence of iron(III) or platinum which greatly accelerate peroxide decomposition. It is also independent of selenic acid concentration. Possible mechanisms for the oxidation are discussed. The decomposition rate of hydrogen peroxide is a complex function depending upon selenious acid, selenic acid, hydrogen peroxide and hydrogen ion concentrations. Small concentrations of selenious acid inhibit the decomposition, but high concentrations accelerate it. Therefore the decomposition reaction of hydrogen peroxide probably involves a selenium-containing species entering a free radical chain. Exchange of selenium between selenite and selenate in these systems does not occur.

Introduction

The oxidation of selenious acid by hydrogen peroxide according to the reaction



serves as a very convenient preparation of pure selenic acid² since excess of the H_2O_2 can be removed easily by a vacuum distillation. This investigation was undertaken when it was noted that significant selenious acid concentrations persisted during selenic acid syntheses continued for long periods of time. The possibilities of a reverse reaction or of some unusual feature of the kinetics of the process were indicated.

Another feature of interest is the inertness of the selenite–selenate oxidation–reduction couple. Oxidation of H_2SeO_3 by chlorine or bromine requires a number of days and even weeks at room temperature. In the hydrogen peroxide oxidation the reaction is normally carried out under refluxing conditions, and the oxidation is accompanied by the decomposition of the peroxide at a comparable rate as evidenced by the evolution of oxygen and the disappearance of peroxide according to the reaction



Despite the fact that H_2SeO_4 is a thermodynamically strong oxidizing agent with an $E^0(\text{H}_2\text{SeO}_3, \text{H}_2\text{SeO}_4)$ estimated to be -1.15 v. by Latimer,³ it does not react with many reducing agents such as SO_2 , Fe^{++} and H_2S under conditions for which H_2SeO_3 with an $E^0(\text{Se}, \text{H}_2\text{SeO}_3)$ of -0.74 v. is rapidly reduced.

(1) Work was performed in the Ames Laboratory of the Atomic Energy Commission.

(2) L. I. Gilbertson and G. B. King, *J. Am. Chem. Soc.*, **58**, 180 (1936).

(3) W. M. Latimer "Oxidation Potentials," 4th Ed., Prentice-Hall, Inc., New York, N. Y., 1952, p. 83.

Edwards⁴ has pointed out that the homogeneous oxidation of each of nine different anions by hydrogen peroxide is a reaction which is first order in the anion and first order in the peroxide. He has shown that these reactions can be described as a class of general acid-catalyzed nucleophilic replacements of a hydroxide ion from hydrogen peroxide by the anion. However, other processes for such oxidations have been noted, and it is of interest to determine whether the selenious acid oxidation falls into this class.

Experimental

Materials.—Selenium was obtained as a 99.95% pure product from the A. D. Mackay Company in the form of small black pellets. Selenious acid was prepared by a nitric acid oxidation of selenium. After the element was dissolved in nitric acid, the solution was boiled to dryness to drive off the excess nitric acid. Three times additional water was added and the solution was again boiled to dryness. Finally, the selenium dioxide was sublimed onto the walls of a beaker as needle-like crystals which were dissolved in water to give the selenious acid solutions.

Hydrogen peroxide was obtained in reagent grade, free from inhibitors, and approximately 30% by weight, from the J. T. Baker Chemical Company. No further purification was attempted. Samples from different bottles gave reproducible oxidation and selenite-catalyzed decomposition rates. The water used was taken from the laboratory distilled water line and redistilled from alkaline permanganate.

Selenic acid was prepared by the hydrogen peroxide oxidation of selenious acid according to the method of Gilbertson and King.²

Iron(III) perchlorate was prepared from iron(III) nitrate by repeatedly precipitating the hydroxide with aqueous ammonia and dissolving the precipitate in perchloric acid.

Lithium perchlorate was obtained in reagent grade from the G. Frederick Smith Chemical Company. Insoluble particles were removed from this compound by the filtration of its aqueous solution.

Sheet platinum, used as a surface catalyst, was obtained from the J. Bishop and Company Platinum Works.

Radioactive selenium (Se^{76}) for the exchange experiments was obtained from the Oak Ridge National Laboratory in the form of selenious acid in a hydrochloric acid solution. It was further purified by means of precipitation of the selenium by hydrazine hydrochloride and was reconverted to selenious acid by the procedure given above.

Primary standards and other chemicals used for this work were all of reagent grade according to the A.C.S. standards.

Apparatus.—All kinetics experiments were carried out in a water-bath thermostat in which the temperature was held constant to $\pm 0.1^\circ$.

Both the Pyrex, glass-stoppered flasks and the polyethylene containers used as reaction vessels were initially steamed for several hours and were rinsed carefully with the redistilled water between experiments.

Potentiometric titrations were performed with a Beckman Model G pH meter together with a Type E high pH glass electrode and a saturated calomel reference electrode.

A Tracerlab end-window Geiger-Mueller counter Model TCG-1 was used in conjunction with a Nuclear Instrument and Chemical Corporation Model 165 scaling unit for the counting of radioactive samples.

Analyses.—Reaction mixtures were prepared from stock solutions of selenious acid, perchloric acid and hydrogen peroxide. In some solutions selenic acid was used instead of the perchloric acid; but in every case three analyses—the total acidity, the selenious acid and the hydrogen peroxide—were sufficient to determine the system.

Both the total acidity and the selenious acid concentration of a solution were determined by a complete potentiometric pH titration with standardized sodium hydroxide. Since the HSeO_3^- is such a weak acid, the difference between the first and second end-points equalled the moles of selenious acid present in the solution. Potentiometric titrations of selenious acid were of limited accuracy because of the difficulty in determining the second end-point. However,

sufficiently large samples were normally taken to give an accuracy of at least $\pm 5\%$. Titration of pure selenious acid which had been standardized by a gravimetric analysis indicated that the error due to carbonate in the standard sodium hydroxide solution was less than 2%.

Cerium(IV) in 1 M sulfuric acid solution was employed to titrate hydrogen peroxide, and the persistence of the yellow color of the cerium(IV) was taken as the end-point. Selenious acid does not interfere with this titration.⁵

Separation of selenious acid from selenic acid for the exchange experiment was accomplished by slowly adding a sulfurous acid solution to the sample. After the peroxide was consumed, the selenious acid was reduced to selenium. The precipitated element was collected on filter paper, washed, dried and mounted in a reproducible manner on cardboard for counting. Later, the sample was redissolved and the selenium determined gravimetrically.

Procedure.—Each reaction mixture was prepared by pipetting stock solution of all the reactants except the hydrogen peroxide into the reaction vessels. The mixtures were brought to the bath temperature, at which time the hydrogen peroxide was added. The reaction vessel was shaken to ensure complete mixing. The initial ionic strength was approximately 1.7 in most experiments. At low acidity the ionic strength was adjusted to this value by the addition of the calculated amount of lithium perchlorate. Two 2-ml. aliquots, taken at each sampling, were quenched to room temperature and were titrated, one for the acids present and the other for its peroxide content. For each reaction mixture the observed concentrations of H_2SeO_3 and of H_2O_2 were plotted *versus* time. The slopes, obtained graphically from smoothed curves of these plots, were taken as the rates of disappearance of the reactants. A number of the concentrations and rates taken from some of the smoothed curves have been included in Table I.

Samples from exchange experiments were analyzed for peroxide and selenious acid in the usual way. Additional aliquots were also withdrawn for the radioactive assay. The selenium present as selenious acid was separated from the selenic acid by the sulfurous acid method, and was treated as described previously. The counting of the radioactivity was done with an 80 mg./cm.² aluminum absorber between the counter and the sample. Since only the γ -rays were counted, self absorption and scattering effects were unimportant.

Results

Oxidation of Selenious Acid.—The rates of disappearance of H_2SeO_3 from a number of experiments were examined to find their dependence on the concentration variables. Figure 1 shows the variation of these rates with H_2O_2 concentration for nearly constant concentrations of H_2SeO_3 and H^+ .

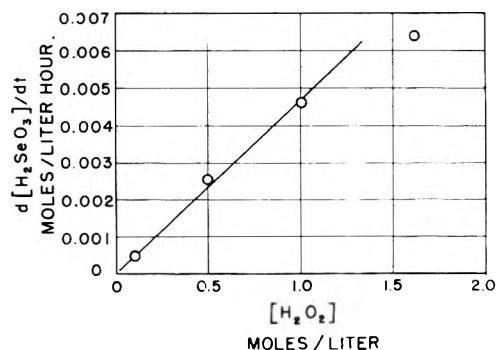


Fig. 1.—Dependence of H_2SeO_3 oxidation rate upon (H_2O_2) at 67.7° : (H_2SeO_3) = 0.5 moles/l., (H_2SeO_4) = 0, (HClO_4) = 1.9 moles/l. for (H_2O_2) = 1.6 and 1.7 moles/l. for the other points.

The straight line passing through the origin demonstrates the first-order dependence on H_2O_2 . A second-order dependence upon H_2SeO_3 is indicated

(5) H. H. Willard and P. Young, *J. Am. Chem. Soc.*, **52**, 553 (1930).

(4) J. O. Edwards, *This Journal*, **56**, 279 (1952).

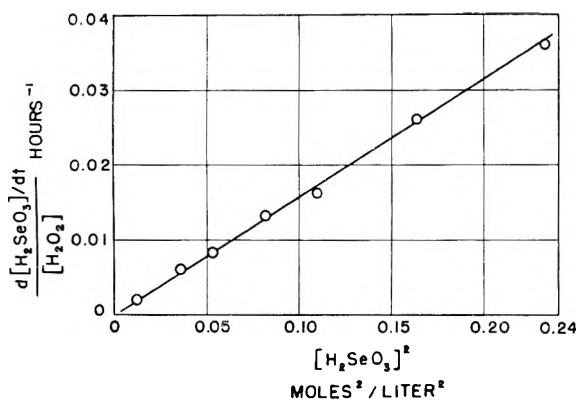


Fig. 2.—Dependence of the H_2SeO_3 oxidation rate upon (H_2SeO_3) at 67.7° : $(\text{H}_2\text{SeO}_4) = 0$, $(\text{HClO}_4) = 1.7$ moles/l., $(\text{H}_2\text{O}_2) = 2.5$ moles/l.

in Fig. 2 for the rates obtained in a series of experiments at constant H^+ concentration. Finally, the results shown in Fig. 3 show that the rate depends

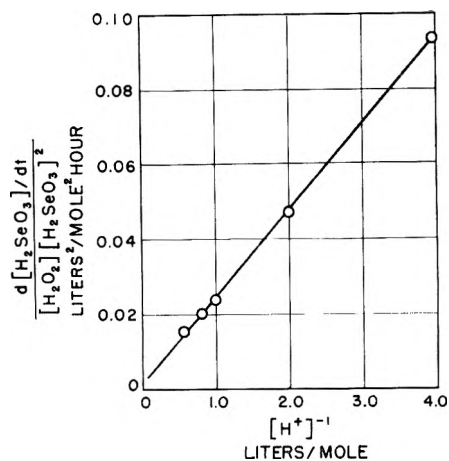


Fig. 3.—Dependence of the H_2SeO_3 oxidation rate upon (H^+) at 67.7° : $(\text{H}_2\text{SeO}_4) = 0$, $(\text{H}_2\text{SeO}_3) = 0.5$ moles/l., $(\text{H}_2\text{O}_2) = 2.5$ moles/l.

on the -1 power of the hydrogen ion concentra-

TABLE I

SELECTED CONCENTRATIONS AND SLOPES TAKEN FROM CONCENTRATION CURVES FOR GLASS REACTION FLASKS WITHOUT ADDED CATALYSTS

Re- action no.	Temp., °C.	Time, hr.	$(\text{H}_2\text{SeO}_3)^a$	(H_2O_2)	(HClO_4)	(H_2SeO_4)	(H^+)	$\frac{d(\text{H}_2\text{SeO}_3)}{dt}$ ^a	$\frac{d(\text{H}_2\text{O}_2)}{dt} - \frac{d(\text{H}_2\text{SeO}_3)}{dt}$ ^a	k_1
6	67.7	0	0.548	0.499	1.640	0	1.640	0.00254	0.00154	0.028
		30	.487	0.399	1.640	.061	1.701	.00154	.00121	.028
		60	.451	0.329	1.640	.097	1.737	.00098	.00093	.025
7	67.7	0	.487	2.47	1.233	0	1.233	.01197	.0227	.025
		20	.334	2.00	1.233	.153	1.386	.00448	.0142	.028
		40	.277	1.70	1.233	.210	1.443	.00197	.0101	.022
9	67.7	0	.503	0.099	1.717	0	1.717	.00048	.0000	.033
11	67.7	0	.493	2.46	0.992	0	0.992	.01420	.0243	.024
		30	.289	1.78	.992	.204	1.196	.00345	.0114	.028
		70	.209	1.37	.992	.284	1.276	.00131	.0061	.028
12	67.7	0	.482	2.47	1.772	0	1.772	.00890	.0203	.027
		30	.330	1.87	1.772	.152	1.924	.00304	.0108	.029
		80	.230	1.39	1.772	.252	2.024	.00117	.0057	.032
15	67.7	0	.486	2.50	0	1.717	1.717	.01033	.0511	.030
		20	.361	1.71	0	1.842	1.842	.00393	.0214	.032
		50	.284	1.17	0	1.919	1.919	.00182	.0110	.037
18	67.7	0	.533	1.62	1.968	0	1.968	.00640	.0128	.027
		30	.404	1.20	1.968	.129	2.097	.00313	.0075	.033
		60	.338	0.97	1.968	.195	2.163	.00151	.0049	.019
19	67.7	0	.485	2.47	0.253	0	0.253	.0542	.0422	.024
		15	.249	1.87	.253	.236	.489	.00615	.0161	.026
		30	.191	1.62	.253	.294	.547	.00279	.0106	.026
20	67.7	0	.486	2.48	0.501	0	0.501	.0275	.0294	.024
		15	.298	1.95	0.501	.188	0.689	.00619	.0169	.025
		50	.190	1.45	0.501	.296	0.797	.00163	.0080	.025
21	67.7	0	.550	1.005	1.727	0	1.727	.00461	.00551	.026
		30	.455	0.776	1.727	.095	1.822	.00194	.00354	.022
		60	.411	0.642	1.727	.139	1.866	.00119	.00241	.020
28	75.0	0	.540	2.44	1.704	0	1.704	.0170	.0519	.041
29	75.0	0	.496	2.43	0.558	0	0.558	.0471	.0573	.044
30	75.0	0	.578	2.48	0	1.690	1.690	.0243	.0889	.049
31	82.3	0	.552	2.43	1.681	0	1.681	.0333	.0933	.076
32	82.3	0	.495	2.44	0.551	0	0.551	.0860	.1445	.079
33	82.3	0	.597	2.46	0	1.665	1.665	.0430	.1378	.082

^a All concentrations are given in units of moles/liters and rates in units of moles/l. hr.

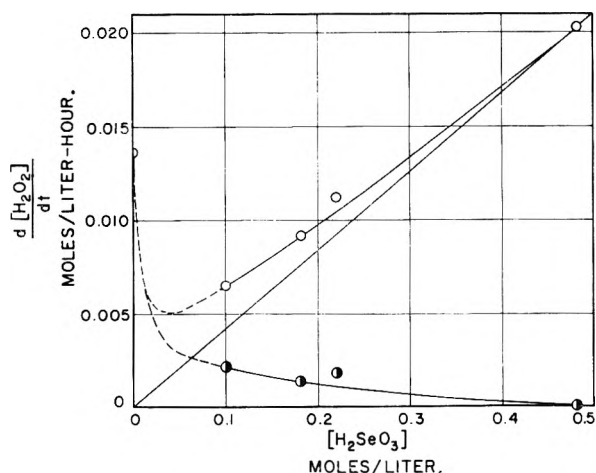


Fig. 4.—Dependence of hydrogen peroxide decomposition rate upon (H_2SeO_3) at 67.7° : $(\text{H}_2\text{O}_2) = 2.5$ moles/l., $(\text{H}_2\text{SeO}_4) = 0$, $(\text{HClO}_4) = 1.7$ moles/l.

tion. The rate law for the oxidation of H_2SeO_3 is therefore

$$-d(\text{H}_2\text{SeO}_3)/dt = k_1(\text{H}_2\text{O}_2)(\text{H}_2\text{SeO}_3)^2/(\text{H}^+) \quad (3)$$

where parentheses indicate molar concentrations. The range of validity of equation 3 is apparent from the individual values of k_1 which are given in the last column of Table I, from which it appears that $k_1 = 0.027 \pm 0.003$ l. mole $^{-1}$ hr. $^{-1}$. Since the values of k_1 were substantially unchanged over a wide range of selenic acid concentrations, it was concluded that the process was independent of selenic acid.

A number of individual experiments were performed to test the effect of various conditions. For example, when the glass surface was increased 16-fold by use of glass helices, $k_1 = 0.027$. When a polyethylene container was used, $k_1 = 0.023$. In the presence of 2 cm. 2 of bright platinum, $k_1 = 0.024$; and with a concentration of iron(III) of 5.2×10^{-4} mole/l., $k_1 = 0.021$. Within the limitations of experimental accuracy, the selenious acid oxidation rate can be considered independent of all these changes.

From additional experiments at 75.0 and 82.3° , the Arrhenius activation energy was calculated to be 16 kcal./mole.

Decomposition of Hydrogen Peroxide.—The decomposition of hydrogen peroxide during all these experiments was evident from the evolution of gas. The hydrogen peroxide decomposition rate was taken as the total peroxide disappearance rate minus the selenic disappearance rate. That the hydrogen peroxide, as used, decomposes in 1.7 molar HClO_4 at 67.7° is shown by Fig. 4. This figure also shows that the decomposition rate in the absence of selenic acid decreased one-half in the presence of 0.1 molar H_2SeO_3 . However, at higher concentrations of selenious acid, the decomposition rate approached a first order function in the selenious acid concentration.

In Fig. 4 is shown the observed decomposition rate and the rate with the first order function subtracted.

The hydrogen peroxide dependence at constant selenious acid, hydrogen ion, and zero selenic acid

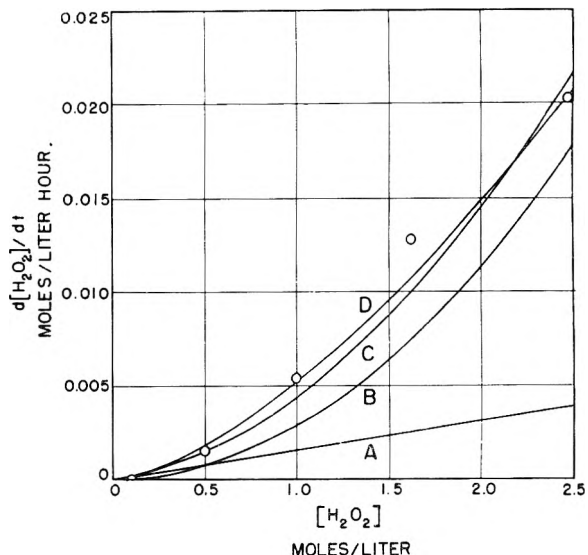


Fig. 5.—Dependence of hydrogen peroxide decomposition rate upon (H_2O_2) at 67.7° : $(\text{H}_2\text{SeO}_3) = 0.5$ mole/l., $(\text{H}_2\text{SeO}_4) = 0$, $(\text{HClO}_4) = 1.7$ moles/l. D is sum of A (first-order component) and B (second-order component). C is the fit of a $3/2$ order dependence.

is shown in Fig. 5. The points could be fitted equally well by an order of $3/2$ or by a linear combination of first and second order terms in H_2O_2 . This second alternative was selected when it was found that the two terms whose coefficients were determined by fitting the curve in Fig. 5, gave a satisfactory description of the two-term hydrogen ion dependence shown in Fig. 6. Thus, in the absence of selenic acid small concentrations of H_2SeO_3 strongly inhibited the reaction. But at higher H_2SeO_3 concentrations the rate was described by the expression

$$- [d(\text{H}_2\text{O}_2)/dt - d(\text{H}_2\text{SeO}_3)/dt] = k_2'(\text{H}_2\text{SeO}_3)(\text{H}_2\text{O}_2)/(\text{H}^+) + k_2''(\text{H}_2\text{SeO}_3)(\text{H}_2\text{O}_2)^2 \quad (4)$$

where at 67.7° $k_2' = 0.0055 \pm 0.0005$ hr. $^{-1}$ and $k_2'' = 0.0055 \pm 0.0005$ liter 2 mole $^{-2}$ hr. $^{-1}$.

When 1.7 M perchloric acid was replaced by an equal molar concentration of selenic acid, substantially the same hydrogen ion concentration was obtained. However, the rate of peroxide decomposition was increased from 0.020 to 0.050 mole/l. hr. This dependence on H_2SeO_4 required an additional term in the rate expression which is given with the coefficient k_2''' in eq. 5

$$- [d(\text{H}_2\text{O}_2)/dt - d(\text{H}_2\text{SeO}_3)/dt] = k_2'(\text{H}_2\text{SeO}_3)(\text{H}_2\text{O}_2)/(\text{H}^+) + k_2''(\text{H}_2\text{SeO}_3)(\text{H}_2\text{O}_2)^2 + k_2'''(\text{H}_2\text{SeO}_3)(\text{H}_2\text{O}_2)(\text{HSeO}_4^-)/(\text{H}^+) \quad (5)$$

where $k_2''' = 0.024 = 0.002$ liter mole $^{-1}$ hr. $^{-1}$.

The success of eq. 5 is demonstrated by a comparison of the experimental and calculated rates in Fig. 7 for an experiment in which all concentration variables changed over wide ranges.

Hydrogen peroxide decomposition rates were unchanged by the use of glass helices or by the use of a polyethylene container. The 2 cm. 2 platinum surface increased the rate by a factor of ca. 4. The same ratio in decomposition rates between 0.1 and 0.5 molar H_2SeO_3 solutions occurred in the presence or absence of platinum.

Some exploratory experiments showed that Fe(III) greatly increased the peroxide decomposition

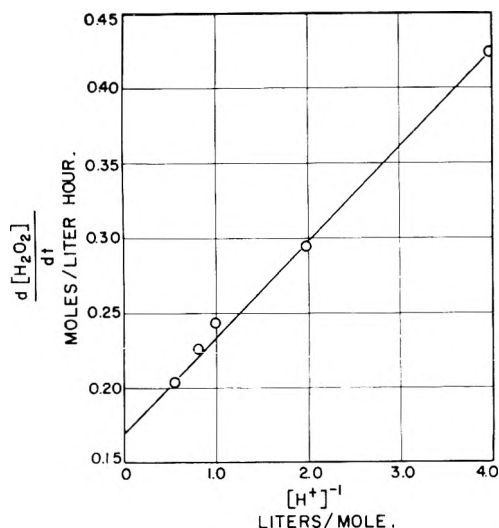


Fig. 6.—Dependence of hydrogen peroxide decomposition rate upon (H^+) at 67.7° : $(H_2SeO_3) = 0.5$ mole/l., $(H_2O_2) = 2.5$ moles/l., $(H_2SeO_4) = 0$, $(ClO_4^-) = 1.7$ moles/l., $(Li^+) = 1.7 - (H^+)$ moles/l.

rate. However, the presence of H_2SeO_3 and H_2SeO_4 inhibited the iron(III) catalyzed reaction. A 0.25 molar H_2SeO_3 solution reduced the rate of decomposition at 67.7° by a factor of nine and a 0.25 molar H_2SeO_3 and 1.7 molar H_2SeO_4 solution reduced the rate by a factor of 90.

Peroxide decomposition rates in a few experiments at 75.0 and 82.3° indicated that an expression of the form of eq. 5 was not satisfactory at 82.3° . Therefore, temperature coefficients of the rate constants are not reported.

Exchange of Selenium.—Exploratory experiments with tracer selenium had shown that less than 3% of selenium is exchanged between selenious acid and selenic acid in two days at 100° . To find whether the selenite-selenate couple could be active in the decomposition of hydrogen peroxide, H_2SeO_3 containing Se^{75} was introduced into the reaction mixture described in Table II.

TABLE II

EXTENT OF EXCHANGE OF SELENIUM IN REACTION AT 67.7°

Time, hr.	(H_2SeO_3) , moles/l.	(H_2O_2) , moles/l.	(H_2SeO_4) , moles/l.	Spec. act. of H_2SeO_3 γ -ray cts./min mg. Se
0	0.115	4.02	1.36	1.55 ± 0.03
192	.05	1.13	1.42	$1.48 \pm .03$
336	.03	0.84	1.44	$1.46 \pm .03$

The result shown in the table, that selenium could be recovered from the H_2SeO_3 without significant reduction of its specific activity, demonstrates that the decomposition of a major fraction of the hydrogen peroxide was accomplished without exchange of the selenium between the oxidation states.

Discussion

The decomposition rate of hydrogen peroxide has been shown by Rice and Reiff⁶ to depend strongly upon the presence of dust or other impurities. With extreme precautions for the elimination of colloidal materials and rigorous methods for

(6) F. O. Rice and M. O. Reiff, *THIS JOURNAL*, **31**, 1352 (1927).

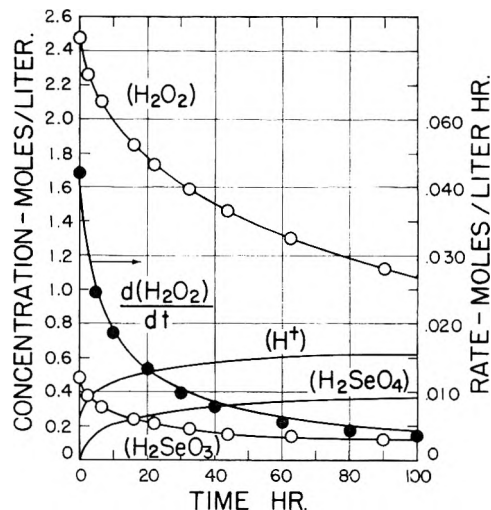


Fig. 7.—Test of eq. 5: smooth curve for $d(H_2O_2)/dt$ represents calculated rates. Points are experimental values.

the preparation of pure material, they obtained a striking reduction in the decomposition rates. The determination of quantum yields has shown that the photolytic decomposition must be a chain reaction, presumably involving free radicals. Again, impurities exert an important influence and chain lengths have not been reproducible.^{7,8} Several metals, of which platinum is one, function as very effective catalysts. Their catalytic activity was attributed by Weiss to the formation of free radicals on the metal surface.⁹ Many other substances which apparently terminate chains by the removal of the active free radicals strongly inhibit the decomposition, and some of them are used commercially for this purpose. The widely studied homogeneous catalysis of the peroxide decomposition by iron(III) has usually been discussed in terms of free radical chains; the recent investigations and proposals¹⁰⁻¹² have indicated that the system is complex and contains a number of competing processes.

Selenious Acid Oxidation.—Since the selenious acid oxidation rate was not influenced by introduction of a platinum surface or by the presence of iron(III) salts which effectively accelerated the peroxide decomposition, it has been concluded that the oxidation occurred as a homogeneous reaction which did not involve the free radicals or a chain mechanism. The observed rate law for the oxidation indicated a single process which is different from the simple nucleophilic substitution discussed by Edwards.³

Shilov and Stepanova¹³ have reported that the expression occurring in eq. 3 occurs as one term in the rate of oxidation of nitrous acid by hydrogen peroxide. In that case the existence of o_2^{\cdot} peroxy-nitrous acid has been established.¹⁴

- (7) F. O. Rice and M. L. Kilpatrick, *ibid.*, **31**, 1507 (1927).
 (8) L. J. Heidt, *J. Am. Chem. Soc.*, **54**, 2840 (1932).
 (9) S. Weiss, *Trans. Faraday Soc.*, **31**, 1547 (1935).
 (10) W. G. Barb, J. H. Baxendale, P. George and K. R. Hargrave, *ibid.*, **47**, 462, 591 (1951).
 (11) N. Uri, *Chem. Revs.*, **50**, 375 (1952).
 (12) A. E. Cahill and H. Taube, *J. Am. Chem. Soc.*, **74**, 2312 (1952).
 (13) E. A. Shilov and Z. S. Stepanova, *Zhur. Fiz. Chim.*, **24**, 820 (1950).
 (14) K. Gleu and R. Hubold, *Z. anorg. Chem.*, **223**, 305 (1935).

Although they have some striking differences, the similarities between sulfur and selenium compounds tempt the comparison of the two elements in similar compounds. For example, selenious acid and sulfurous acid have nearly the same ionization constants and the ions of both acids exchange oxygen rapidly with water.¹⁵ As with sulfite, the mechanism for this exchange with selenite is believed to be the dehydration equilibrium

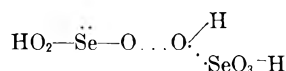


A peroxyseleous acid may form as an intermediate for the oxidation via the dehydration mechanism. Halperin and Taube¹⁶ found that in the



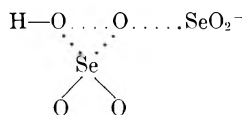
analogous sulfur system both oxygens from the peroxide appear in the sulfate. They proposed therefore that the sulfate was formed by a rearrangement of a postulated peroxysulfurous acid, HOOSO_2H . Such a simple rearrangement of the peroxyseleous acid to give selenic acid does not occur since another selenite group is required for the transition state.

Another possible mechanism involves a nucleophilic replacement of an HSeO_3^- from the peroxyseleous acid by a biselenite ion with the following transition state



In this case only one peroxide oxygen would go to the selenate which does not exchange oxygen rapidly with water,¹⁴ and the other would appear in selenite and rapidly exchange with water.

If the feature of complete oxygen transfer, that occurs in the sulfur system, also occurs in the selenite oxidation, the above mechanism is unsatisfactory. Then the attack of the peroxy-group, $\text{H}-\text{OO}-$, in a hydrogen peroxyseleous ion by SeO_2 might occur to break simultaneously the $\text{O}-\text{O}$ and the $\text{O}-\text{Se}$ bonds and to give biselenate. The transition species would have the form



Experiments with tagged oxygen in the hydrogen peroxide might permit a choice between these two mechanisms. However, results would be obscured by the fact that decomposition of hydrogen peroxide occurs simultaneously with the oxidation and that the exchange of oxygen from selenate is significantly catalyzed by hydrogen ion.

Hydrogen Peroxide Decomposition.—The decomposition of hydrogen peroxide in the presence of the selenium acids is obviously complex; however, some features of the reaction can be eluci-

dated from this investigation, although a complete description is not attempted.

Low concentrations of selenious acid significantly inhibit the thermal decomposition. This effect was apparent from the dust- and impurity-catalyzed reaction and for the homogeneous reaction in the presence of iron(III). Such inhibition can be explained by the reaction of a chain-carrying radical with H_2SeO_3 to give a selenium-containing radical if this new radical reacts rapidly with some other one to effect chain termination. However, the decomposition rate increases with higher concentrations of selenious acid and approaches a first order function of this variable. This behavior would result from the introduction into a chain process of the selenium-containing radical which can be formed by a reaction between peroxide and selenite. If the platinum metal serves primarily to accelerate the introduction of free radicals, the selenite dependence of the platinum-catalyzed reaction indicates that selenite is involved in the free radical chain.

The inhibition of the iron(III)-catalyzed reaction by selenious acid is an order of magnitude greater than the inhibition by selenic acid. Although no direct comparison was made, sulfate is reported to inhibit the iron(III) catalysis similarly and may act by complexing the iron.¹⁷

The results of the exchange experiments definitely exclude some possible mechanisms. Since there was virtually no exchange of selenium between the selenious and selenic acids while a large quantity of peroxide was consumed, it is clear that the decomposition does not involve a combined oxidation and reduction of H_2O_2 by the H_2SeO_3 - H_2SeO_4 oxidation couple. Also the decomposition of peroxide cannot occur by means of a peroxide oxidation of selenite followed by decomposition of the selenate to give oxygen and selenite. Indeed, the decomposition of selenic acid in these solutions was negligible over a period of two weeks. In addition, although one of the rate expressions contains an H_2SeO_4 concentration dependence, it must be impossible to form the same intermediate from either H_2SeO_3 or H_2SeO_4 which then returns to the selenite form in a subsequent reaction.

From the complexity of the rate expression for the peroxide decomposition the reaction appears to occur by several paths. Since the decomposition of hydrogen peroxide is considered to involve a number of high energy intermediates whose behavior is affected by both selenite and selenate, it seems surprising that the oxidation of the selenite remains so completely indifferent to the peroxide decomposition rate. The relatively rapid decomposition of peroxide in the presence of selenite and selenate together with the high order of the selenious acid oxidation appear to explain the effect noted originally that significant concentrations of H_2SeO_3 persist during the synthesis of H_2SeO_4 for exceptionally long periods of time.

(15) N. F. Hall and O. R. Alexander, *J. Am. Chem. Soc.*, **62**, 3455 (1940).

(16) J. Halperin and H. Taube, *ibid.*, **74**, 380 (1952).

(17) V. L. Bohnson, *THIS JOURNAL*, **25**, 19 (1921).

A MOLECULAR DYNAMIC THEORY OF CHROMATOGRAPHY¹

BY J. CALVIN GIDDINGS AND HENRY EYRING

Department of Chemistry, University of Utah, Salt Lake City, Utah

Received November 1, 1964

The molecular dynamic problem of passage of substances through a chromatographic column is investigated for the linear range of the adsorption isotherm. It is found, assuming uniform adsorption sites of only one type, that a reasonable concentration distribution of molecules in the effluent of a column can be obtained. Equations are also derived for the case in which there are two and more different type sites. The sorption rate constants of a typical chromatographic process are experimentally determined.

Introduction

The general problem of chromatography is, in a practical sense, not solvable. For ordinary column chromatography unknowable variables exist involving everything from the nature of the complex multi-site surface to the details of the method of packing the column. Assumptions can be, and have been made that allow for an approximate solution to the theoretical problem. The approximate results have been shown to check experience to a fair degree.

The principal problem of chromatography is the separation of substances. In a typical procedure the material of interest is started from a band near the top of the column and is washed down the column with pure solvent. As the washing proceeds, there is a separation of the original band into component substances. The value of the method is enhanced by any factor that can further the separation of the component bands, and that can minimize each band's dispersion. If there is extensive dispersion, the bands of two neighboring components may considerably overlap. The theory developed in this paper sheds some light upon the dispersion of bands of separable solutes.

It has been found elsewhere, and is true here, that reasonable solutions to the chromatography problem can be obtained only if the adsorption isotherm is linear.² For cases in which it is not linear, dispersion may still be important, and it should be affected in roughly the same way as in the linear case.

If the isotherm is linear, each molecule behaves independently of the others. The problem of dispersion of these molecules is analogous to the random walk problem. The number of steps may qualitatively be considered as the number of reactions to the surface. It is a well-known result that any factor increasing the number of steps, and correspondingly decreasing their length, decreases the dispersion. Thus, in going between two points in the chromatographic column, we might guess that we can decrease dispersion if we can find ways of increasing the number of combinations with the surface. For one thing, this is simply done by decreasing the rate of solvent flow. And, as our theory verifies, the dispersion is proportional to the square root of flow rate.

In actual cases, there are two other causes of dispersion. Channeling, for one thing, smears individual bands. This dispersion will not de-

pend strongly upon the flow rate—it is minimized by careful packing of the column. Diffusion also causes dispersion. The dispersion due to diffusion is inversely proportional to the square root of flow rate. Thus, flow rate affects oppositely dispersion due to diffusion and dispersion due to "random walk." In practice, one should be able to find the optimum flow rate for minimum dispersion. Unless the rate of adsorption is very high, or the rate of flow very low, the "random walk" dispersion will be the more important of the two.

The majority of papers written on chromatography have started with the partial differential equations expressing the conservation of solute molecules.²⁻⁷ Thomas² has solved these equations for several interesting cases with a finite rate of adsorption and desorption explicitly included. He has thereby obtained the values of adsorption and desorption constants from experimental data. When the adsorption isotherm is not linear, the equations can be solved only by assuming instantaneous equilibrium between solute and surface. These solutions are of great practical interest, but will not be considered here. Papers^{8,9} also have been written which compare chromatographic separation with distillation. The results are useful in demonstrating the efficiency of column separation as compared to distillation, but the theory is not based on considerations of actual molecular processes.

Single Site Adsorption

The problem we first wish to consider is that in which a narrow band of solute is started at the top of the column and then washed through with pure solvent. Experimentally, the same velocity of flow, w , must be maintained in the column throughout the course of the experiment. We define t° by the equality $wt^\circ = L$, where L is the length of the column. t° , then, is the time it takes the solvent to flow completely through the column. The theory here presented is based on the following assumptions.

1. There is negligible net diffusion of any given solute molecule within the solvent in the direction of the column.

(3) (a) J. N. Wilson, *J. Am. Chem. Soc.*, **62**, 1583 (1940); (b) D. DeVault, *ibid.*, **65**, 532 (1943).

(4) J. Weiss, *J. Chem. Soc.*, 297 (1943).

(5) H. C. Thomas, *J. Am. Chem. Soc.*, **66**, 1664 (1944).

(6) J. E. Walter, *J. Chem. Phys.*, **13**, 229 (1945).

(7) E. Glueckauf, *Proc. Roy. Soc. (London)*, **A186**, 35 (1946); *J. Chem. Soc.*, 1302 (1947).

(8) A. J. P. Martin and R. L. M. Synge, *Biochemical J.*, **35**, 1358 (1941).

(9) S. W. Mayer and E. R. Tompkins, *J. Am. Chem. Soc.*, **69**, 2866 (1947).

(1) The authors wish to thank the National Science Foundation for a grant in support of this work.

(2) H. C. Thomas, *Ann. N. Y. Acad. Sci.*, **49**, 161 (1948).

2. When a molecule is in the liquid phase there is a definite, non-varying constant k_1 representing the probability per unit time that the molecule will adsorb on the surface. Also, when the molecule is on the surface, there is a definite probability per unit time of desorption which we call k_1' . k_1' is simply the unimolecular rate constant for dissociation of the surface and the solute molecule. k_1 is a rate constant for adsorption multiplied by the concentration of sites.

Assumption (2) implies several things. For one thing, it is a sufficient (but not necessary) condition for the existence of a linear adsorption isotherm. It further ensures that there is only one type of non-interacting site available to adsorb on. Since assumption (2) must hold at all times, it implies also that diffusion is not the rate-controlling step for adsorption (otherwise there would be a greater probability for adsorption of a molecule immediately following its desorption, since it would then be near the surface, but we have assumed that the probability of adsorption is a constant). Even for the most carefully packed column, assumption (2) is not realizable simply because of the fact that k_1 will be larger when the molecule is passing between two closely adjacent surfaces than when the two surfaces are farther apart. However, an average k_1 is satisfactory provided that k_1 for a molecule goes through its range of fluctuations many times between successive adsorptions.

Because of assumption (1) we may say that a given solute molecule spends exactly a time t° in the liquid phase while it is in the chromatographic column. The molecule will then spend time t adsorbed on the surface. By the application of probability theory we wish to find a distribution function in t representing the chance that in unit time the solute molecule will be eluted from the bottom of the column. Let us say to begin with that the particular molecule under study is in the liquid phase at the top of the column. In the course of its descent through the column it will adsorb on the surface, in general, r times. Assumption (2) assures us that the probability of reacting exactly r times is given by Poisson's probability law

$$\gamma_r = \frac{(k_1 t^\circ)^r}{r!} e^{-k_1 t^\circ} \quad (1)$$

Since the molecule must be in the liquid phase to pass through the bottom of the column, the molecule must also desorb exactly r times. The chance that this r th desorption occurs between the time t and $t + dt$ is the chance that just $r - 1$ desorptions occur in time t , multiplied by the chance that the r th desorption occurs between t and $t + dt$. The probability differential is

$$dP_r = P_r dt = \frac{(k_1' t)^{r-1}}{(r-1)!} e^{-k_1' t} k_1' dt \quad (2)$$

The quantity we want, of course, is the total probability differential, which is the sum over r of dP_r , weighted by the chance of exactly r reactions.

$$dP = \sum_{r=1}^{\infty} \gamma_r dP_r = P dt \quad (3)$$

Substituting (1) and (2) into (3) we arrive at the equation

$$P = e^{-k_1' t - k_1 t^\circ} \left(\frac{k_1 k_1' t^\circ}{t} \right)^{1/2} \sum_{r'=0}^{\infty} \frac{\left(\frac{\sqrt{4k_1 k_1' t^\circ}}{2} \right)^{2r'+1}}{r'!(r'+1)!} \quad (4)$$

where $r' = r - 1$. This is also equal to

$$P = e^{-k_1' t - k_1 t^\circ} \left(\frac{k_1 k_1' t^\circ}{t} \right)^{1/2} I_1(\sqrt{4k_1 k_1' t^\circ} t) \quad (5)$$

It will be noticed that the argument, x , of the Bessel function, $I_1(x)$, is twice the geometrical mean of the expected number of adsorptions to the surface in time t° , and the expected number of desorptions in time t . For most cases of interest, and for most values of t this will be a large number. To a good degree of approximation we may use the first term of the asymptotic expansion of $I_1(x)$, obtaining the result

$$P = \frac{(k_1' k_1 t^\circ)^{1/4}}{2\sqrt{\pi}} \frac{e^{-(\sqrt{k_1' t} - \sqrt{k_1 t^\circ})^2}}{t^{3/4}} \quad (6)$$

It is to be noted that in equation 3 we allowed for any number of reactions from one to infinity. We did not allow for zero number of reactions, which event has a definite probability. If no reactions to the surface occur, then the molecule will be eluted from the column in exactly the time $t = 0$ (throughout the paper we use as the origin of the t axis the time t° after the beginning of the experiment). The probability that there is no adsorption in passing through the column is $e^{-k_1 t^\circ}$. This will be negligibly small under the same conditions which allow us to make the asymptotic expansion leading to (6).

To derive equation 6 we have assumed that the molecule started in the liquid phase. However, the molecule might initially be found attached to the surface. This leads to a slightly different distribution $P(t)$. As a matter of practice we can usually state the fraction of molecules of this thin band that are adsorbed on the surface. If the band is introduced rapidly into the column and the experiment started at once, nearly all molecules will start in the liquid phase. If the band is allowed to stay at the top of the column for a time, then equilibrium with the surface will be reached, and the fraction $k_1/k_1' + k_1$ of total molecules will start from the surface.

Centering our attention on a particular molecule initially adsorbed on the surface, the chance that it will adsorb exactly r times before reaching the bottom of the column is given, as before, by (1). However, r adsorptions are now associated with $r + 1$ desorptions, and the probability distribution function in t is given by

$$P_r = \frac{(k_1' t)^r}{r!} e^{-k_1' t} k_1' \quad (7)$$

Unlike the previous case, we can find the total distribution P by summing from zero to infinity

$$P = \sum_{r=0}^{\infty} \gamma_r P_r \quad (8)$$

Upon substitution we find that

$$P = e^{-k_1 t^\circ - k_1' t} k_1' I_0(\sqrt{4k_1 k_1' t^\circ} t) \quad (9)$$

The asymptotic expansion of the Bessel function,

$I_0(x)$, is allowable under the same conditions as before, and leads to

$$P = \frac{k_1'}{2\sqrt{\pi}(k_1 k_1' t^0)^{1/4}} \frac{e^{-(\sqrt{k_1' t} - \sqrt{k_1 t^0})^2}}{t^{1/4}} \quad (10)$$

Equations 6 and 10, weighted by the probability of the initial state of the molecule, should approximately yield the distribution curve for elution.

Multiple-site Adsorption

The surfaces encountered in adsorption work will always contain many different types of sites, each with different constants of adsorption and desorption. A more general treatment of chromatography would include the effect of n different types of sites with adsorption constants k_1, k_2, \dots, k_n , and desorption constants k'_1, k'_2, \dots, k'_n . The expressions found for such a general treatment are very cumbersome. Instead of giving a general solution of the n -site system we will solve the 2-site system. This may be of practical interest for certain surfaces—but many more quantitative measurements must be made to establish the extent of its value.

Just as we did for the single-site system, we will neglect diffusion along the column. We also state that the constants $k_1, k_2, \dots, k'_1, k'_2, \dots$, represent probabilities of reaction per unit time, and that they are constants independent of time, distance along the column, presence of other molecules, etc. These assumptions, as before, guarantee the existence of a linear adsorption isotherm, and assure us that diffusion is not the rate-controlling step for adsorption.

In the 2-site problem the molecule may initially be found in one of three places: in the liquid phase, on site 1, or on site 2. This is treated just as before.

To begin with, we will find the function P for a molecule that begins in the liquid phase. In the time t^0 , the independent probabilities that the molecule will adsorb r times on site 1 and s times on site 2 are given by equations 1 and 11, respectively.

$$\gamma_s = \frac{(k_2 t^0)^s}{s!} e^{-k_2 t^0} \quad (11)$$

Having reacted in this manner, the respective probabilities per unit time of remaining with sites of type 1 for time t_1 , and sites of type 2 for time t_2 , are given by equations 12a and 12b.

$$P_r = \frac{(k_1' t_1)^{r-1}}{(r-1)!} e^{-k_1' t_1} k_1' \quad (12a)$$

$$P_s = \frac{(k_2' t_2)^{s-1}}{(s-1)!} e^{-k_2' t_2} k_2' \quad (12b)$$

We are not interested in the unobservables t_1 and t_2 , but only in their sum $t_1 + t_2 = t$, since this is the measure of the elution time. To obtain the distribution function in t , we combine these independent probabilities in the standard manner, and obtain

$$P_{rs}(t) = \int_0^t P_r(t_1) P_s(t - t_1) dt_1 \quad (13)$$

$$= \frac{k_1' k_2'^s}{(r-1)!(s-1)!} e^{-k_2' t} t^{(r+s-1)} \int_0^1 x^{r-1} (1-x)^{s-1} e^{k_1' t x} dx$$

where we have made use of the substitution $t_1 =$

tx and $k = k'_2 - k'_1$. If we use the series expansion of $e^{k_1' t x}$, we obtain

$$P_{rs} = \frac{k_1' k_2'^s}{(r-1)!} e^{-k_2' t} t^{(r+s-1)} \sum_{m=0}^{\infty} \frac{(k_1' t)^m}{m!} \frac{(r+m-1)!}{(r+m+s-1)!} \quad (14)$$

For the total probability expression, we must allow properly for all values of the subscript r and s . Following the example of 1-site theory, we can write

$$P = \sum_{r=1}^{\infty} \sum_{s=1}^{\infty} P_{rs} \gamma_r \gamma_s + e^{-k_1' t^0} \sum_{s=1}^{\infty} \gamma_s P_s(t) + e^{-k_2' t^0} \sum_{r=1}^{\infty} \gamma_r P_r(t) \quad (15)$$

There is also the probability $e^{-(k_1 + k_2)t^0}$ that the molecule will be eluted at exactly $t = 0$.

The last two terms of equation 15 allow for the distribution in time if there are no reactions to site 1 and if there are no reactions to site 2, respectively. The reason that these terms (and also the term $e^{-(k_1 + k_2)t^0}$) cannot be included in the first term merely by summing from zero, instead of one, is that P_r and P_s of equation 12 are without meaning for $r = 0$ and $s = 0$. In general, a site of a given type will affect the distribution very little unless a molecule adsorbs on this type site very many times on the average. A molecule's probability, then, of adsorbing zero times is negligible, unless the site is of no importance and can be neglected from the treatment altogether. A possible exception to this rule, which neglects the probability of zero reactions, would result from a site that would hold molecules very tightly, making k'_1 a very small number. Neglecting the probability of zero reactions we can write

$$P = \sum_{r=1}^{\infty} \sum_{s=1}^{\infty} P_{rs} \gamma_r \gamma_s = [e^{-k_2' t} - (k_1 + k_2)t^0] X \quad (16)$$

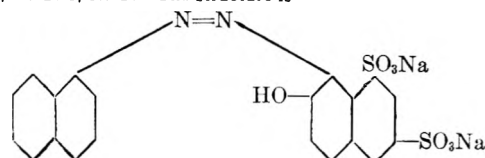
$$\left[\sum_{m=0}^{\infty} \sum_{r=1}^{\infty} \sum_{s=1}^{\infty} \frac{(k_1' t)^r (k_2' t)^s k_1^m t^{2r+s+m+s-1} (r+m-1)!}{(r-1)!(r+m+s-1)! m! r! s!} \right]$$

It is hoped that in future work this expression can be reduced to a more usable form.

Experimental

Exploratory experiments were run to determine the approximate rate of adsorption and desorption for a typical chromatographic process. A five cm. wide chromatographic column was filled with a 2.5:1 mixture, by volume, of commercial grade Magnesol and Celite. The solvent used was water. The column was kept under a continuous vacuum of approximately 60 cm. from before the solute was introduced to the end of the experiment. 0.001737 gram of brilliant scarlet 3R¹⁰ dissolved in 15 ml. of water was introduced into the top of the column. A narrow band with original approximate width of 0.5 cm. was then washed on

(10) Information on this dye has kindly been provided by Allied Chemical and Dye Corporation, National Aniline Division, 40 Rector Street, N. Y. 8, N. Y. The structure is



through the 20 cm. long column. Despite the wide column used, the dispersion due to channeling was kept down to about 0.5 cm. (as estimated visually), a small value compared to the total dispersion. The temperature was kept within a few degrees of 24°. When quantities of solute much greater than that mentioned above were run through the column, they passed through much faster, indicating that many sites were taken up and that the isotherm was not linear. The above quantity of solute is that at which the center of the band moves no faster upon further dilution. Samples were collected every 25 ml. The concentration of each sample was determined by a Beckman quartz spectrophotometer set at a wave length of 500 m μ .

Figure 1 shows the experimentally determined effluent curve, and that predicted from one-site theory with $k_1' = 0.01 \text{ sec.}^{-1}$ and $k_1 = 0.0176 \text{ sec.}^{-1}$. Plotted along the abscissa is the reduced volume, $V/V^0 = X$ where V_0 is the total volume of solvent within the column, and V is a measure of input volume. For consistency with the equations derived in the last section, we let $V + V^0$ be the measure of input volume from the beginning of the experiment. The ordinate is a measure of the concentration in arbitrary units.

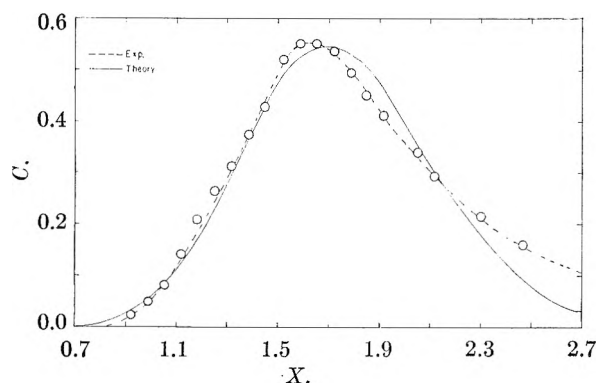


Fig. 1.

Equation 6 was used in plotting the theoretical curve since the solute molecules were introduced into the column directly from the liquid phase, and there was not a time lag which would allow unaccounted for equilibration. If equation 6 is written in terms of our new variable, X , we have

$$P = \frac{Ae^{-t^0(\sqrt{k_1'X} - \sqrt{k_1})^2}}{X^{3/4}} \quad (17)$$

where A is a normalization constant. t^0 may also be written as V^0/\dot{V} . \dot{V} is the rate of input flow measured in $\text{cm.}^3 \text{ sec.}^{-1}$. Written in terms of \dot{V} , the dependence of the dispersion upon flow rate is easily appreciated.

t^0 , in our particular experiment, was equal to 2480 sec. V^0 and \dot{V} were 300 cm.^3 and 0.121 $\text{cm.}^3 \text{ sec.}^{-1}$, respectively. The expected number of reactions to the surface of a molecule during its course of descent down the column, $k_1 t^0$, was 43.7.

The measured value of concentration fits equation 17 quite well for the front boundary, but the back boundary is significantly different, and so is the curvature near the maximum. It is probable that with the use of meticulously prepared adsorbents, a better fit could be made. It is possible that the observed discrepancy is due to a second type site which, because of its scarcity, does not adsorb molecules very often, but holds solute molecules very strongly when it does adsorb them (k_1' very small). This could well increase the concentration for large value of X , and leave it unaffected for the front boundary. No attempt has been made, however, to fit the data to the more difficult two-site theory.

Harris and Tompkins¹¹ have collected data on the effluent curves of rare earth ions. In their experiments, the band was eluted with a complexing agent. Assumption two should hold provided the rate constant of complexing is fast. Otherwise, the rare earth ions would be more prone to return to the surface immediately after they had left it.

(11) O. H. Harris and E. R. Tompkins, *J. Am. Chem. Soc.*, **69**, 2792 (1947).

The fact that some of the reactions are bimolecular is of no significance providing the other reactant (complexing agent, and ions of a given type on the surface) is at constant concentration.

Figure 2 shows the experimental points for praseodymium from Table IV of their paper, and the theoretical curve plotted with $k_1 = 0.02174$ and $k_1' = 0.0001890 \text{ sec.}^{-1}$. Equation 10 was used in this case, since it is assumed that nearly all molecules were on the surface when the complexing agent was added. (Equations 6 and 10, however, yield nearly identical curves.) In their experiment, t^0 was 17,420 seconds and the expected number of combinations of a given ion, with the surface, is 378.7. The fit is seen to be quite satisfactory.

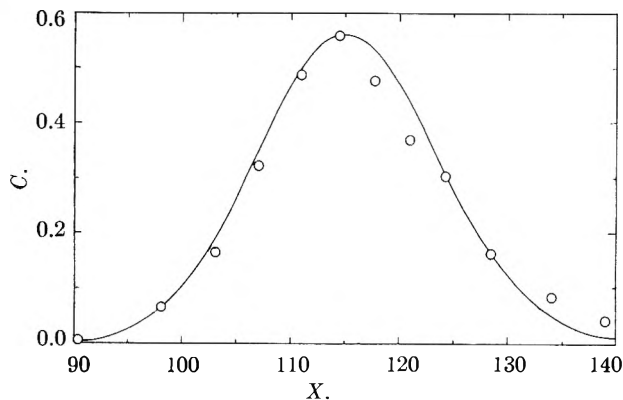


Fig. 2.

We will now show that the dispersion is nearly proportional to one over the square root of t^0 . To do this, we assume that $X_{1/2}$ is a slowly varying function of X as compared to the exponential. Equation 17, then, goes over into

$$P \sim e^{-t^0(\sqrt{k_1'X} - \sqrt{k_1})^2} \quad (18)$$

For our purposes, $X_{1/2} - X_m$ is a sufficiently good measure of dispersion. $X_{1/2}$ is the value of the coordinate X for which the concentration has dropped to half of its highest value. X_m is the value of X for which the concentration is a maximum. The above distribution yields

$$X_m = k_1/k_1' \quad (19)$$

$$X_{1/2} - X_m = (\ln 2)^{1/2}(k_1/k_1') \left(\frac{(\ln 2)^{1/2}}{E} + \frac{2}{E^{1/2}} \right)$$

where $E = k_1 t^0$ is the expected number of reactions to the surface. $1/E$ is ordinarily small compared to $1/E^{1/2}$, so that we can write

$$X_{1/2} - X_m \cong \pm 2 \left(\frac{\ln 2}{E} \right)^{1/2} \left(\frac{k_1}{k_1'} \right) \quad (20)$$

Since E is proportional to t^0 (and inversely proportional to \dot{V}), our assumption is true. It is not surprising that any factor altering the rate constant can strongly affect the separability of compounds when we notice the way in which dispersion depends upon rate constants. Factors such as pH, ionic strength, and especially temperature, are significant, and could be studied for individual cases.

It is interesting that the distribution curves predicted from theory are not symmetric, and thus not of the same form as the Gaussian function. As demonstrated in Fig. 1, these distributions are characterized by a positive skew.

A More General Case

In previous sections of this paper various cases in which the solute molecules were originally found within the confines of a narrow band were considered. There are, however, many other initial conditions of importance. Some of these will be treated in the following general discussion. It is unfortunate that simple expressions do not result in a majority of cases.

The expressions that we derive will be more useful if we let V (volume) instead of t (time) be the independent variable. In this case, $V = \dot{V}t$ and $V^\circ = \dot{V}t^\circ$. With this transformation equations 4 and 9, respectively, go over into (21) and (22), respectively.

$$P(V) = \frac{1}{\dot{V}} e^{-\frac{1}{\dot{V}}(k_1 V^\circ + k_1' V)} \left(\frac{k_1 k_1' V^\circ}{\dot{V}} \right)^{1/2} \times I_1 \left(\frac{1}{\dot{V}} \sqrt{4k_1 k_1' V^\circ V} \right) \quad (21)$$

$$P(V) = \frac{k_1'}{\dot{V}} \exp \left[\frac{1}{\dot{V}}(k_1 V^\circ + k_1' V) \right] \times I_0 \left(\frac{1}{\dot{V}} \sqrt{4k_1 k_1' V^\circ V} \right) \quad (22)$$

It will be useful to review the significance of the above equations. If N molecules all start from a single narrow band at the beginning of the experiment ($t = -t^\circ$, $V = -V^\circ$), $P(V) dV$ represents the chance that any given molecule will be eluted between volume V and $V + dV$. The probable number of molecules eluted between V and $V + dV$ will then be $NP(V) dV$. $NP(V)$ is the number of molecules per unit volume and thus is the concentration, C .

Suppose now that the molecules are not all originally contained within the small band at the top of the column. Instead, let the first small volume element, dV' , and every small volume element thereafter contain a number of molecules equal to $C_0(V') dV'$. (We have introduced V' as representing the volume introduced into the top of the column. At $V' = 0$ the first solute molecule enters the top layer of adsorbent. Eventually, we will want to write $C(V) dV$, the number of molecules in the volume between V and $V + dV$, as a function of V . The sum of the molecules eluted between V and $V + dV$ will be the sum of the molecules contributed to this particular band by all of the small volume elements, dV' . Since many small volume elements, dV' , contribute to one measured concentration, $C(V)$, we will have to integrate over V' . It is well to remember that $C_0(V')$ is an initial, but not necessarily constant, concentration.) Since all molecules will be in the liquid phase upon first entering the column, equation 20 must be used. The concentration of solute molecules in the column efflux is

$$C(V) = \int_{V'=0}^V C_0(V') P(V - V') dV' \quad (23)$$

The upper integration limit is V since molecules arriving at the top of the column after $V' = V$ do not contribute at all to $C(V)$. In rare cases those molecules that adsorb on the surface zero times must be considered. In those cases we add the term $[e^{-(k_1 V^\circ / \dot{V})}] C_0(V)$ to the right-hand side of (23). The value of this term for the experiment considered in the last section is approximately $10^{-18} C_0(V)$.

If a band of considerable width is introduced into the column, $C_0(V')$ may be of the following form

$$\begin{aligned} C_0(V') &= C_0 \quad 0 < V' < V'' \quad (24) \\ C_0(V') &= 0 \quad V' > V'' \end{aligned}$$

If we may approximate a given finite band by the expression

$$C_0(V') = N\delta(V') \quad (25)$$

where $\delta(V')$ is the Dirac delta function, we obtain from (23)

$$C(V) = NP(V) \quad (26)$$

As has been pointed out, this is the concentration obtained by assuming a very thin band. We have used this equation throughout the paper.

As a second general case, suppose that the solute molecules are somehow initially distributed in the column, and then be washed through with pure solvent. It will be convenient to introduce a new independent variable, $v = V + v'$, where V is the measure of volume used previously, and v' is equivalent to V° for any given band of solute within the column. v is the volume of liquid passed through the column after the initial conditions have been specified.

The concentration of molecules in the liquid phase is given by $C_1(v')$, and if all the molecules in the surface phase were suddenly desorbed, their concentration would be $C_s(v')$. The concentration in the effluent is the sum of several terms. One term is contributed by original liquid phase molecules, and another by surface phase molecules. For the concentration of molecules originally in the liquid phase, $C^1(v)$, we can write

$$C^1(v) = \int_{v'=0}^v C_1(v') P(v - v') dv' \quad (27)$$

$P(v - v')$ is given by equation 21, providing $v' = V^\circ$.

Molecules beginning in the surface phase contribute the following to the concentration

$$C^s(v) = \int_{v'=0}^v C(v') P(V - v') dv' \quad (28)$$

$P(v - v')$ is now given by (22). If there are molecules near the lower end of the column at the beginning of the experiment, the probability of zero reactions may well be important. This case will contribute a term

$$C^o(v) = [e^{-k_1 v' / \dot{V}}] C_1(v) \quad (29)$$

The final concentration, $C(v)$, is given exactly by

$$C(v) = C^1(v) + C^s(v) + C^o(v) \quad (30)$$

Appendix

1. **Normalization.**—To assure us that the equations for effluent distribution are *bona fide* probability functions, we will show that they are normalized. Equation 21 can be written as

$$P(V) = e^{-\left(\frac{k_1 V^\circ}{\dot{V}} + \frac{k_1' V}{\dot{V}}\right)} \sum_{r=1}^{\infty} \frac{\left(\frac{k_1 k_1' V^\circ}{\dot{V}^2}\right)^r V^{r-1}}{(r-1)! r!} \quad (31)$$

The integral of $P(V) dV$ from zero to infinity should give the total probability that there are one or more adsorptions on the surface.

$$\int_0^{\infty} P(V) dV = 1 - e^{-\left(\frac{k_1 V^\circ}{\dot{V}}\right)} \quad (32)$$

We have mentioned that the probability of zero adsorptions is $e^{-k_1 V^\circ / \dot{V}}$. Adding this term to (32), we arrive at the value unity. Equation 22 can likewise be shown to be normalized.

2. **Expectation Values.**—Equation 4 can be written

$$P(t) = e^{-E - k_1 t} \sum_{r=1}^{\infty} \frac{(k_1' E)^r t^{r-1}}{r! (r-1)!} \quad (33)$$

where $E = k_1 t^0$. The expectation value of the N th power of t is

$$Ex(t^n) = \int_0^{\infty} P(t) t^n dt = \frac{E e^{-E}}{(k_1')^n} \sum_{r=0}^{\infty} \frac{E^r (r+n)!}{r! (r+1)!} \quad (34)$$

We can approximately evaluate (34) by assuming that $E^r/r!$ is a rapidly varying function of r as compared to the other terms. $E^r/r!$ is near its maximum when $r = E$. If we factor the other terms out with r equal to this value, we obtain

$$\begin{aligned} Ex(t^n) &\cong \frac{(E+n)!}{(E+1)!} \times \frac{E}{(k_1')^n} \\ Ex(t) &= \frac{E}{k_1'} = \frac{k_1 t^0}{k_1'} \\ Ex(t^2) &\cong \frac{(E+2)E}{k_1'^2} \end{aligned} \quad (35)$$

3. **Position of Mode.**—The single-site distribution can be written

$$P \sim \exp \frac{[-t^0(\sqrt{k_1' X} - \sqrt{k_1})^2]}{X^n} \quad (36)$$

where $n^{3/4}$ or $1/4$. By setting the derivative of P with respect to X equal to zero, we can solve for X (max.), the maximum point of the distribution. This is

$$X(\text{max.}) = \frac{k_1}{k_1'} \left(1 - \frac{2n}{E}\right) \quad (37)$$

provided that $X \gg n$.

4. **Reduction of Two-site Theory for Identical Sites.**—If $k_1' = k_2' = k'$ in equation 13, P_{rs} reduces to

$$P_{rs} = \frac{(k')^{r+s} e^{-k't} t^{r+s-1}}{(r+s-1)!} \quad (38)$$

Let $r + s = n$.

$$P_n = \frac{(k_1' t)^{n-1}}{(n-1)!} k_1' \quad (39)$$

This is the equation derived for one site theory.

THE VAPOR PRESSURES OF LITHIUM AND SODIUM OXIDES¹

BY LEO BREWER AND JOHN MARGRAVE²

Department of Chemistry and Chemical Engineering and the Radiation Laboratory, University of California, Berkeley, California

Received November 11, 1954

Theoretical calculations of the stability of alkali oxide gaseous molecules have been checked experimentally for Li_2O and Na_2O . The results indicate that Li_2O vapor under neutral conditions may contain gaseous molecules in concentrations comparable to the gaseous elements. It is possible that both Li_2O and LiO gaseous molecules may be important, especially under oxidizing conditions. Na_2O vapor consists predominately of Na atoms and O_2 molecules with any oxide molecules being less important than the elements under neutral conditions. Thus Na gas and O_2 gas do not react with one another unless they are at high enough pressures to deposit solid or liquid Na_2O . No experimental data are available for the heavier alkali oxides but the calculations indicate that gaseous MO molecules might be of importance even under neutral conditions. The M_2O gaseous molecules are expected to be less important than the MO or elemental molecules. In a hydrogen-oxygen system all of the alkali metals react to form stable gaseous hydroxides.

Theoretical

Brewer and Mastick³ have calculated the vapor pressures of the alkali oxides using the Born-Haber cycle with an ionic model to calculate the heats of formation of the gaseous molecules. In this work their calculations have been extended and the vapor pressures of Li_2O and Na_2O have been experimentally determined to check these calculations.

The calculations of Brewer and Mastick indicated that none of the M_2O gaseous molecules should be of chemical importance except possibly for the Li_2O molecule. The calculations of Rittner⁴ for the gaseous alkali halide molecules and those of Klemperer and Margrave⁵ indicate that it might be possible to extend these calculations to consider in detail the polarization and repulsive contributions to the stability of the molecules. Use of the gaseous ionic radii given by Rittner would indicate that the interatomic distances should be larger and therefore the M_2O molecules less stable than calculated by Brewer and Mastick. However the Li_2O calculations indi-

cate that it still might be of chemical importance in oxidizing systems and possibly even in neutral systems.

The stabilities of the MO gaseous molecules were calculated by considering that the O^- ion would be intermediate in size between F^- and Cl^- . The heats of formation of the gaseous alkali halide molecules from the gaseous ions as given by Rittner do not differ by more than 20 kcal. Thus the corresponding values for the MO gaseous alkali oxide molecules were taken as the mean of the fluoride and chloride values with a maximum uncertainty of 10 kcal. These values combined with the ionization potentials of the alkali metals and the electron affinity of 53.8 kcal. for oxygen yielded the following heats of dissociation of the MO gaseous molecules to the gaseous atoms or D_0 values going from Li to Cs: 97, 71, 81, 79 and 80 kcal. By combining these values with the heats of sublimation of the metals and the heat of dissociation of O_2 , one obtains for the ΔH of formation of gaseous MO molecules from the elements in the standard states going from Li to Cs: 0, +14, 0, +1 and -2 kcal. with an uncertainty of 10 kcal.

Free energy functions were estimated for the MO gaseous oxides and the above heats used to calcu-

(1) Presented at the 121st Meeting of the American Chemical Society, Buffalo, New York, March, 1952.

(2) Atomic Energy Commission Postdoctoral Fellow, 1951-1952.

(3) L. Brewer and D. Mastick, *J. Am. Chem. Soc.*, **73**, 2045 (1951).

(4) E. Rittner, *J. Chem. Phys.*, **19**, 1030 (1951).

(5) W. Klemperer and J. Margrave, *ibid.*, **20**, 527 (1952).

late the equilibrium constants for the reaction $M_2O(s) = M(g) + Mo(g)$. The $-\log K$ values at $1000^\circ K.$, going from Li to Cs are: 23.9, 15.1, 9.4, 7.6 and 5.9. Comparison with the partial pressures to be expected due to the reaction $M_2O(s) = 2M(g) + \frac{1}{2} O_2(g)$ as given by Brewer and Mastick indicate that the MO molecule should not be of importance under neutral conditions for the Na system, but it is possible that the MO molecule might be comparable in concentration with the elemental species for the K, Cs and Rb systems even under neutral conditions.

The only direct check on the stability of an alkali MO molecule is given by the work of Bawn and Evans⁶ who have studied the reaction of sodium vapor with oxygen and various oxides at low temperature and pressures. Under their conditions, they conclude that a molecule NaO is formed from atomic sodium and atomic oxygen with a heat of formation of approximately 72 kcal. They also conclude that a molecule NaO_2 is formed from atomic sodium and molecular O_2 with a heat of formation of 40 kcal. One can readily show that molecules with such stabilities will be of no chemical importance in the vaporization of sodium oxide. The partial pressures of the elemental species will be greater than partial pressures of these oxide molecules. $D(Na_2O)$ would have to be >145 kcal. or $D(NaO)$ would have to be >82 kcal. to make either of them comparable to the elements under neutral conditions. Our calculation of the heat of formation of NaO from the atomic elements yields a value of 71 kcal. Our calculations also show that gaseous Na_2O can be of no chemical importance. Thus sodium and oxygen are stable in contact with each other in the gaseous phase at high temperatures. If they are present together at sufficiently high pressure, they can react to form solid or liquid oxides but no gaseous oxide molecules can be expected to be of any chemical importance under equilibrium conditions. Under the conditions of the experiments of Bawn and Evans, the presence of diluting nitrogen and low concentration of reactants prevented the condensation of sodium oxide in the time of duration of the experiments. Thus it was possible to produce the gaseous molecules NaO and NaO_2 . However the data show them to be thermodynamically unstable with respect to solid Na_2O .

In order to check the theoretical calculations, the vapor pressures of lithium and sodium oxides were determined experimentally. There have been no previous quantitative measurements of the vapor pressures of the alkali oxides. Lebeau⁷ reported that lithium oxide vaporized completely at 1000° in one hour. DeForcrand⁸ noted no weight loss on heating lithium oxide for several hours at $780-800^\circ$.

Mott⁹ fixed the order of volatility of the oxides as $K_2O > Na_2O > Li_2O$. Preston and Turner¹⁰ have studied the vaporization from metal oxide-silica

systems but there is some doubt as to whether or not they attained equilibrium in their measurements and any vapor pressures calculated from their work are subject to doubt. The volatilities of these silicate systems should be much smaller than those of the pure oxides, but in every system studied by Preston and Turner, including the PbO-SiO₂ system, the calculated vapor pressures are much higher than observed by other experimenters for the pure metal oxides. Bunzel and Kohlmeier¹¹ recently determined the melting point of Na_2O and stated that the vaporization of Na_2O was just observable at 1350° .

Experimental

The compounds studied in this work, Li_2O and Na_2O , are extremely hygroscopic, react with CO_2 and consequently were difficult to handle. It was necessary to prepare such samples often and handle them in a dry, CO_2 -free atmosphere at all times. The loading of samples and transfer of materials were accomplished in a dry-box with an atmosphere of argon and in the presence of molten sodium which acts both as a desiccator and a getter for oxygen and CO_2 .

The lithium oxide was prepared by heating lithium carbonate to about 1000° for 20 to 30 minutes and pumping off the CO_2 . A platinum crucible was used as a container and X-ray studies of the product formed indicated that lithium oxide was the main phase with no major impurities. The lattice constant agreed with the literature value. Base titration indicated greater than 96% lithium oxide in every sample. The melting point was found to be $1700 \pm 15^\circ K.$ This is lower than the value of approximately 1700° reported by van Klooster and Jaeger.¹²

Four different methods were used for the preparation of Na_2O : (1) heating sodium nitrate with sodium azide, (2) heating sodium peroxide, (3) reducing sodium peroxide with sodium, and (4) reducing sodium superoxide with sodium. Samples used for the vapor pressure studies were prepared by the reduction of sodium peroxide and superoxide by sodium metal. A MgO crucible was used for the preparation. Excess sodium was added and distilled off after heating to 500° . The excess sodium was necessary to remove NaOH by formation of Na_2O and hydrogen. X-Ray powder patterns of a material containing excess sodium showed no apparent change in lattice constant indicating that at least at room temperature the solid solution of Na in Na_2O has a narrow homogeneity range. Analyses by titration showed greater than 95% Na_2O with some NaOH impurity indicated by X-ray analysis. It was expected that the NaOH impurity which is introduced by handling of the oxides would be removed by the preliminary heating before the vapor pressure runs were carried out as the NaOH should be more volatile than the sodium oxide. Analyses of samples remaining after vapor pressure runs indicate purities as high as 97% Na_2O . Visual examination of Na_2O samples which had been heated to different temperatures indicated a melting point of $1190 \pm 10^\circ K.$ in good agreement with the value of $1193^\circ K.$ reported by Bunzel and Kohlmeier.¹¹

The apparatus used for the effusion studies was essentially the same as that described previously by Brewer and Mastick¹³ and Brewer and Searcy.¹⁴ For some of the sodium oxide runs at lower temperatures, it was found convenient to use a quartz apparatus heated in a resistance furnace; all other samples were heated inductively. Platinum crucibles were used for the lithium oxide runs and MgO crucibles for the sodium oxide runs. Spectroscopic analyses of samples heated for long periods over wide temperature ranges failed to show more than traces of the container materials. Lids containing different size holes were used for the crucibles with the edges shaped to give as near a knife-edge as possible. Except for some runs in which the lithium oxide was collected on a water cooled platinum disc the amount of material which had effused out during the run was determined by the weight loss of the crucible.

(6) C. E. H. Bawn and A. G. Evans, *Trans. Faraday Soc.*, **33**, 1571 (1937).

(7) P. Lebeau, *Compt. rend.*, **136**, 1256 (1903).

(8) R. DeForcrand, *ibid.*, **144**, 1403 (1907).

(9) W. Mott, *Trans. Am. Electrochem. Soc.*, **34**, 255 (1918).

(10) E. Preston and W. Turner, *J. Soc. Glass Tech.*, **16**, 331 (1932); **17**, 122 (1933); **18**, 143 (1934); **19**, 311 (1935).

(11) E. Bunzel and E. Kohlmeier, *Z. anorg. Chem.*, **254**, 1 (1947).

(12) H. van Klooster and F. Jaeger, *Proc. Roy. Acad. Sci. Amsterdam*, **16**, 857 (1914).

(13) L. Brewer and D. Mastick, *J. Chem. Phys.*, **19**, 534 (1951).

(14) L. Brewer and A. Searcy, *J. Am. Chem. Soc.*, **73**, 5308 (1951).

The vaporization data for lithium oxide and sodium oxide are given in Tables I and II. The temperatures were determined by a calibrated optical pyrometer and corrected for absorption by the Pyrex window. The results were calculated assuming that the vaporization proceeded to the gaseous metal atom and the O₂ molecule. Since these compounds have homogeneity ranges one cannot be sure what the ratio of alkali atoms to oxygen molecules will be but the homogeneity range should be small for these oxides and therefore the effusing vapor should contain approximately four alkali atoms for every O₂ molecule when the constant boiling composition has been reached. However, when low vapor pressures are being measured and only small amounts of material are vaporized, one may find widely varying ratios of metal to oxygen depending upon whether the starting material was near the metal-rich or oxygen-rich edge of the homogeneity range. Thus it was found that the Li/O₂ ratio varied considerably when only a few milligrams of Li₂O were vaporized due to slight variations in the composition of the starting material. As larger amounts of sodium oxide were vaporized, it was assumed that the sample quickly reached a constant boiling composition near Na₂O and that the Na/O₂ ratio in the effusing vapor was 4.

TABLE I
VAPORIZATION DATA ON Li₂O

T, °K.	Wt. effusate collected, mg.	Li/O Effusate ^a	Total wt. loss, mg.	Time, sec.	Hole area, cm. ²
1532	1.3	4.0	..	7,200	0.07550
1541	2.7	1.7	55.7	5,400	.07550
1573	2.8	3.0	..	14,400	.07550
1579	2.7	1.3	..	7,200	.02836
1590	0.7	3.8	..	3,600	.07550
1596	2.5	0.97	..	5,400	.07550
1618	2.6	(2)	65.0	5,820	.02836
1643	3.8	0.97	..	6,000	.02836
1669	..	(2)	57.8	1,080	.0804

^a Bracketted figures indicate estimated values.

TABLE II
VAPORIZATION DATA ON Na₂O^a

T, °K.	Total wt. loss, mg.	Time, sec.	Hole area, cm. ²
918	6.2	11,640	0.1156
943	7.8	64,980	.0314
998	22.7	59,820	.0314
1006	21.3	73,260	.0314
1241	21.7	1,500	.0855
1260	134.4	1,320	.0855
1467	641.1	600	.0804

^a Na/O ratio was not determined and was assumed to be 2/1 in all calculations on Na₂O.

For the reaction M₂O(s) = 2M(g) + 1/2O₂(g), the equilibrium constant was calculated as

$$K = \frac{Z_M^{3/2} M_M M_{O_2}^{1/4} T^{3/4}}{n^{1/2} (44.331at)^{3/2}}$$

where Z_M is moles of metal effusing through effusion hole of area, *a*, in cm.², *t* is time in sec., *n* is the ratio of moles of metal to moles of O₂ effusing, M_M is the atomic weight of the metal, M_{O₂} is the molecular weight of O₂, and *T* is the absolute temperature.

To check the assumption that the vapors consisted primarily of the elements, it is necessary to calculate the decomposition vapor pressure from the heats of formation of the oxides. If there are any important oxide species, the observed volatility should be higher than the calculated volatility. If the decomposition assumption is correct, one should obtain agreement between calculated and observed equilibrium constants.

To calculate the equilibrium constants, one needs the heats of formations of the oxides from the gaseous elements and the free energy functions. The heats of formation of the oxides, the entropies of formation, and the free energy

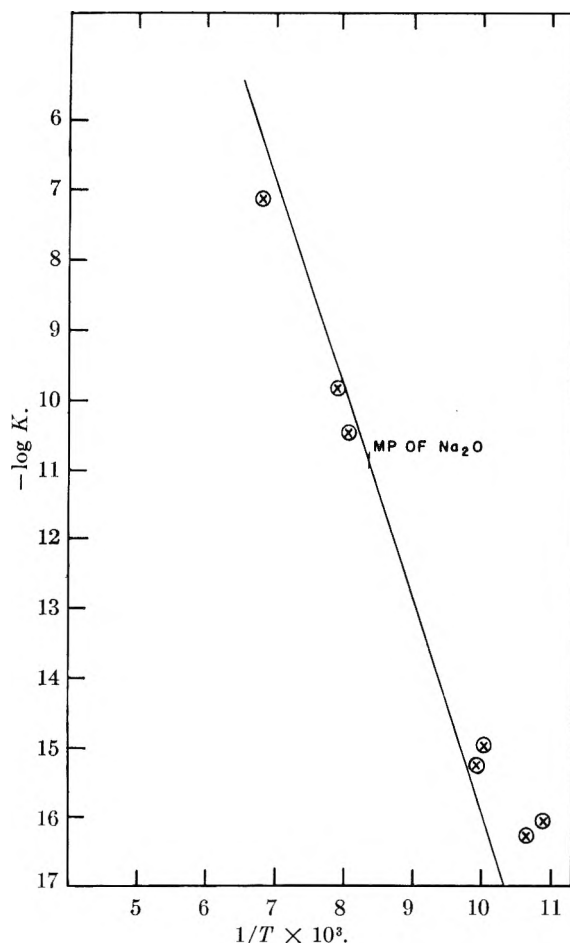


Fig. 1.—Log *K* vs. 1/*T* for the reactions Na₂O(s) = 2Na(g) + 1/2O₂(g) and Na₂O(l) = 2Na(g) + 1/2O₂(g); ⊗, log *K* calcd. from total weight loss data; —, calcd. curve from thermodynamic data.

functions of the elements are given by Brewer.^{15,16} The heats of sublimation of Na and Li at 298°K. were obtained from the Series III Tables of the National Bureau of Standards.¹⁷ The only additional data needed are high temperature heat contents for the oxides. Naylor¹⁸ has estimated the high temperature heat capacity of Na₂O(s), but no data are available for the liquid. At 920°, the melting point of Na₂O, we have estimated a heat of fusion of 10 kcal./mole and an entropy of fusion of 8.4 e.u. We have taken the heat capacity of Na₂O(l) as 24 cal./mole/deg. For the vaporization process to the elements

$$\frac{\Delta F - \Delta H_{298}}{T} = -76.0 \text{ e.u. at } 1000^\circ\text{K.}$$

The heat capacity of Li₂O has been measured by Shomate and Cohen¹⁹ to 1045°K. At 1600°K., for the vaporization of Li₂O to the elements

$$\frac{\Delta F - \Delta H_{298}}{T} = -77.35 \text{ e.u.}$$

In Fig. 1 are shown the experimentally determined equilibrium constants for the vaporization of Na₂O together with the calculated curve assuming no important gaseous

(15) L. Brewer, "The Thermodynamics and Physical Properties of the Elements," NNEs, Vol. 19b, Papers 3 and 5, McGraw-Hill Co., New York, N. Y., 1950.

(16) L. Brewer, *Chem. Revs.*, **52**, 1 (1953).

(17) "Selected Values of Chemical Thermodynamic Properties," Series III, March 1, 1954, U. S. National Bureau of Standards.

(18) B. Naylor (as cited by K. K. Kelley, Bur. of Min. Bull. 476 (1949)).

(19) C. H. Shomate and A. J. Cohen, Tech. Memorandum 982, U. S. Naval Ordnance Test Station, Inyokern, February, 1953.

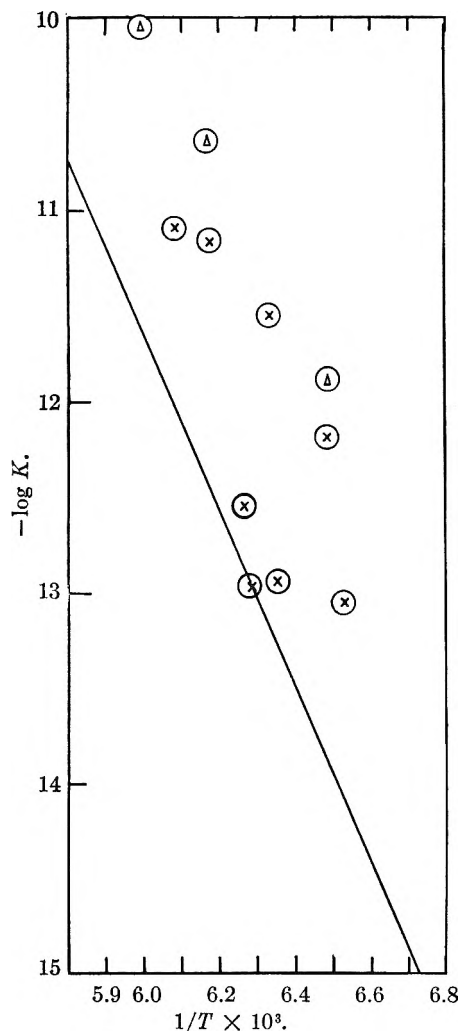


Fig. 2.—Log K vs. $1/T$ for the reaction $\text{LiO}(s) = 2\text{Li}(g) + \frac{1}{2}\text{O}_2(g)$: \otimes , log K calcd. from collected effusate weight; \ominus , log K calculated from total weight loss data.

oxide molecules. The general range of agreement between the calculated and experimental points is within the experimental error of the data. Thus the experimental data confirm the theoretical calculations which indicate that Na_2O should vaporize by decomposition to the gaseous elements with no important contribution by any oxide molecules.

It is of interest to consider the vaporization behavior of the NaOH impurity present in the sodium hydroxide. James and Sugden²⁰ and Smith and Sugden²¹ have demonstrated the importance of alkali hydroxides in flames although NaOH was found to be the least stable. Millman and Kusch²² have also shown that NaOH and KOH vapors consist of about one-third molecules and two-thirds atoms.

Von Wartenberg and Albrecht²³ have determined the vapor pressures of NaOH and KOH. Jackson and Morgan²⁴ have determined the vapor pressure of KOH. These data may also be used to confirm the stability of the gaseous hydroxides. Using the heats of formation of the hydroxides from the National Bureau of Standards²⁵ together with necessary thermodynamic data from Kelley²⁶ and Brewer¹⁶

and the entropy of sodium hydroxide determined by Kelley and Snyder,²⁷ one can calculate that at 1000°K. the partial pressure of atomic sodium in equilibrium with NaOH should be about 10^{-6} atm. compared to the observed total pressure in equilibrium with NaOH liquid of about 10^{-3} atm. The larger proportion of atomic species reported by Millman and Kusch indicates some reduction by their container. The calculations are less exact for KOH but they indicate about 10^{-6} atm. atomic potassium at 1000°K. in equilibrium with liquid KOH compared to observed total pressures of 10^{-3} to 10^{-2} atm. Taking the calculated partial pressures of alkali atoms and OH molecules in equilibrium with the liquid hydroxide together with the partial pressure of hydroxide molecule from the total pressure measurements, one calculates $K = (M)(\text{H}_2\text{O})^{1/2}(\text{O}_2)^{1/4}/(\text{MOH}) = 10^{-7}$ at 1000°K. for both NaOH and KOH within a factor of ten. For comparison with the data of Smith and Sugden, $K = (K)(\text{OH})/(\text{KOH}) = 10^{-13}$ at 1000°K. compared with 10^{-12} obtained by extrapolations of Smith and Sugden's data at higher temperatures. Comparison of these results with the volatility of the oxides shows that the gaseous hydroxide molecules must be quite important chemically and that hydroxide impurities should vaporize at a much greater rate than the oxide. Thus most of the hydroxide should be removed in the preliminary heating, but the slightly high vapor pressures observed for Na_2O might be due to small amounts of NaOH remaining in solid solution.

In Fig. 2 are shown the experimentally determined equilibrium constants for the vaporization of Li_2O together with the calculated curve, assuming no important oxide molecules. The experimental points are mostly above the calculated curve. To check the importance of Li_2O and LiO , preliminary experiments were carried out in which argon, oxygen, and argon-oxygen mixtures were passed over lithium oxide solid. If no gaseous oxide molecules were important, one would expect oxygen to decrease the volatility of lithium oxide. No effect would be observed if Li_2O were the main species and an increase in volatility would be expected if LiO were the main species.

Erratic results were obtained which can most likely be explained on the basis of small amounts of water in the flow gases which would result in vaporization of lithium hydroxide. A single run was made with gases passed over calcium chloride and some enhancement of the vaporization of lithium oxide in oxygen was observed at 1500–1600°K. In view of the difficulty of demonstrating the absence of water in the gas flow experiments and the absence of lithium hydroxide dissolved in the solid lithium oxide, it does not appear possible to definitely conclude the existence of a lithium oxide molecule.²⁸ One can definitely state that no oxide molecule could be of chemical importance under reducing conditions. In view of the somewhat high experimental results as well as the theoretical calculations of the stabilities of Li_2O and LiO , it seems quite possible that at least one of these molecules might be comparable to the elements under neutral conditions. At least one or both molecules should be important under oxidizing conditions.

To calculate an upper limit to the stabilities of these gaseous oxide molecules, one can assume that the observed volatilities are due entirely to either Li_2O or LiO . $-(\Delta F - \Delta H_0)/T = 28.8$ e.u. was estimated for $\text{Li}_2\text{O}(s) = \text{Li}_2\text{O}(g)$ at 1550°K. For the corresponding sodium reaction, 35.6 e.u. was estimated at 1000°K. A similar calculation was made on the basis of the sodium oxide data. One obtains the following limits to the values for ΔH_f , the heats of formation at 298°K., and D_0 , the dissociation energies to the gaseous atoms at 0°K.

Gaseous molecule	Li_2O	LiO	Na_2O	NaO
ΔH_f (kcal./mole)	≥ -64	$\geq +4$	≥ -35	$\geq +2$
D_0 (kcal./mole)	≤ 198	≤ 93	≤ 144	≤ 84

One finds that mixtures of alkali metal gases and oxygen can be quite stable. Thus at 1350°K. a mixture of sodium and oxygen gases at 1 mm. pressure is calculated to be thermo-

(20) C. G. James and T. M. Sugden, *Nature*, **171**, 428 (1953).

(21) H. Smith and T. M. Sugden, *Proc. Roy. Soc. (London)*, **A211**, 58 (1952).

(22) S. Millman and F. Kusch, *Phys. Rev.*, **60**, 91 (1941).

(23) H. Von Wartenberg and P. Albrecht, *Z. Elektrochem.*, **27**, 162 (1921).

(24) M. D. Jackson and I. D. Morgan, *J. Ind. Eng. Chem.*, **13**, 110 (1921).

(25) "Selected Values of Chemical Thermodynamic Properties," Circular of the National Bureau of Standards 500, Feb. 1, 1952.

(26) K. K. Kelley, U. S. Bureau of Mines Bulletin 476 (1949).

(27) John C. R. Kelley and P. E. Snyder, *J. Am. Chem. Soc.*, **73**, 4114 (1951).

(28) NOTE ADDED IN PROOF.—Recent work of Van Arkel, Spitsbergen and Heyding, *Can. J. Chem.*, **33**, 446 (1955), also indicates an enhanced evaporation rate of Li_2O in an atmosphere containing $\text{H}_2\text{O}(g)$, and further supports the possible importance of $\text{LiOH}(g)$.

dynamically stable while a mixture of sodium and oxygen gases at 1 atm. pressure is stable above 2100°K. and should not undergo reaction.

The authors wish to express their thanks to Mr. James Kane who made several preparations of Li₂O and Na₂O and

also carried out some of the flow studies of Li₂O vaporization. Mrs. Carol H. Dauben and Mrs. Helena Ruben are to be thanked for making the necessary X-ray powder patterns of many samples. This work was supported by the Atomic Energy Commission.

THE THEORETICAL ENERGIES OF MIXING FOR FLUOROCARBON-HYDROCARBON MIXTURES

BY T. M. REED, III

Fluorine Research Center, University of Florida, Gainesville, Florida

Received November 11, 1954

Hydrocarbons and fluorocarbons have two properties which differ to such an extent that the usual equations, found in the Hildebrand regular solution theory, for calculating energies of mixing are rendered inaccurate for mixtures containing both of these kinds of molecules. These properties are the molal volume and the molecule ionization potential. The latter enters into the potential energy function for non-polar molecules as given by the London formula for the dispersion effect. A more accurate equation for calculating energies of mixing which includes the effects of these properties is obtained from theory. It is found that the ratio 1.55 of the ionization potential of *n*-C₅F₁₂ to that of *n*-C₅H₁₂ is sufficient to account for about 25% of the calculated partial molal energies of mixing in liquid solutions of these two compounds. These calculated energies, as well as those for the system *n*-C₄F₁₀:*n*-C₄H₁₀, agree very well with experimental partial molal heats of mixing reported in the literature.

In the Hildebrand-Scatchard theory¹ of solutions, equation 1 is given for the energy of mixing

$$\Delta E^M = (x_1 V_1 + x_2 V_2)(c_{11} + c_{22} - 2c_{12})\varphi_1\varphi_2 \quad (1)$$

ΔE^M per mole of mixture in a two component system, in terms of the mole fractions *x* of the components, the molar volumes *V* of the pure components, the volume fractions φ , and the so-called "cohesive energy densities," *c*₁₁ and *c*₂₂ for the pure components and *c*₁₂ for the mixture. *c*₁₁ and *c*₂₂ are identified with $\Delta E_1^v/V_1$ and $\Delta E_2^v/V_2$, respectively, where ΔE^v is the energy of vaporization of the pure liquids 1 and 2. To obtain a useful relationship *c*₁₂ is usually assumed to be the geometric mean of *c*₁₁ and *c*₂₂. With these values for the *c*'s equation 1 becomes

$$\Delta E^M = (x_1 V_1 + x_2 V_2) \left[\left(\frac{\Delta E_1^v}{V_1} \right)^{1/2} - \left(\frac{\Delta E_2^v}{V_2} \right)^{1/2} \right]^2 \varphi_1 \varphi_2 \quad (2)$$

The partial molal energies of mixing $\overline{\Delta E}^M$ are obtained from equation 3 as

$$\begin{cases} \overline{\Delta E}_1^M = V_1 \varphi_2^2 (\delta_1 - \delta_2)^2 \\ \overline{\Delta E}_2^M = V_2 \varphi_1^2 (\delta_1 - \delta_2)^2, \quad \delta = (\Delta E^v/V)^{1/2} \end{cases} \quad (2a)$$

Equations 2 and 2a adequately represent experimental data when (a) the partial molal volumes in the mixture are essentially the molal volumes of the pure liquids, and (b) *c*₁₂ is essentially the geometric mean of *c*₁₁ and *c*₂₂.

Refinements for Volume Change in Mixing.—

In most systems to which equation 2 has been applied these assumptions give satisfactory comparison with observed energies of mixing. Recently, however, the vapor-liquid phase equilibria of mixtures containing a fluorocarbon and a hydrocarbon have been studied.^{2,3} The difference between the partial molal volumes and the molal volumes of the pure liquids in these mixtures invalidates assumption (a) above. This situation has been recog-

nized.² Equation 2 in a more exact form derived from a model without assumption (a), but retaining assumption (b), is

$$\begin{aligned} \Delta E^M = (x_1 \bar{V}_1 + x_2 \bar{V}_2) \varphi_1 \varphi_2 \left[\left(\frac{\Delta E_1^v V_1}{\bar{V}_1^2} \right)^{1/2} - \left(\frac{\Delta E_2^v V_2}{\bar{V}_2^2} \right)^{1/2} \right]^2 \\ + \Delta E_1^v (1 - V_1/\bar{V}_1) x_1 + \Delta E_2^v (1 - V_2/\bar{V}_2) x_2 \end{aligned} \quad (3)$$

in terms of the partial molal volumes \bar{V} and the volume fractions φ calculated from the partial molal volumes. The partial molal energies of mixing according to equation 3 are

$$\overline{\Delta E}_1^M = \bar{V}_1 \varphi_2^2 (\delta_1 - \delta_2)^2 + \Delta E_1^v (1 - V_1/\bar{V}_1) \quad (3a)$$

and similarly for component 2 with subscripts interchanged. $\delta = (\Delta E^v V/\bar{V}^2)^{1/2}$.

Refinements in *c*₁₂.—Hydrocarbons and fluorocarbons are both non-polar liquids. As such, according to present-day theory, the only attractive forces which come into play between these molecules are London forces, the so-called dispersion forces. The mutual energy ϵ_{12} of a pair of molecules may be presented by

$$\epsilon_{12} = -k_{12}/r^6 + j_{12}/r^n \quad (4)$$

where $-k_{12}/r^6$ represents the contribution of attraction to the potential, j_{12}/r^n the contribution of repulsion to the potential, and *r* is the distance between molecule centers. It may be shown further that

$$j_{12} = \frac{6}{n} (d_{12}^0)^n - 6k_{12} \quad (5)$$

where d_{12}^0 is the distance between the centers of molecules 1 and 2 when ϵ_{12} is minimum. Considering the attraction as arising only from the dispersion effects

$$-k_{12} = \frac{-3}{2} \alpha_1 \alpha_2 \frac{I_1 I_2}{I_1 + I_2} \quad (6)$$

where α_1 is the polarizability of a molecule of liquid 1, α_2 that of liquid 2, *I*₁ and *I*₂ the ionization potentials of molecules of liquid 1 and 2.

(1) J. H. Hildebrand and R. L. Scott, "Solubility of Nonelectrolytes," 3rd Ed., Reinhold Publ. Corp., New York, N. Y., p. 124.

(2) J. H. Simons and R. D. Dunlap, *J. Chem. Phys.*, **18**, 335 (1950).

(3) J. H. Simons and J. W. Mausteller, *ibid.*, **20**, 1516 (1952).

For 1-1 pairs and 2-2 pairs, equation 6 becomes

$$\begin{cases} k_{11} = \frac{3}{4} \alpha_1^2 \times I_1 \\ k_{22} = \frac{3}{4} \alpha_2^2 \times I_2 \end{cases} \quad (7)$$

Then from 6 and 7

$$k_{12} = \frac{2(I_1 I_2)^{1/2}}{I_1 + I_2} \times k_{11}^{1/2} \times k_{22}^{1/2} \quad (8)$$

Using equations 4 and 5, Hildebrand has shown⁴ that the cohesive energy densities c_{11} , c_{22} and c_{12} of equation 1 may be related to the attraction coefficients k_{11} , k_{22} and k_{12} . By methods paralleling the derivation of Hildebrand but not assuming constant volume mixing, these relationships are obtained as

$$c_{11}(V_1/\bar{V}_1)^2 = \frac{2\pi N^2 k_{11}}{\bar{V}_1^2 (d_{11}^0)^3} \left[\int \right] \quad (9)$$

$$c_{22}(V_2/\bar{V}_2)^2 = \frac{2\pi N^2 k_{22}}{\bar{V}_2^2 (d_{22}^0)^3} \left[\int \right] \quad (10)$$

$$c_{12} = \frac{2\pi N^2 k_{12}}{\bar{V}_1 \bar{V}_2 \left(\frac{d_{11}^0 + d_{22}^0}{2} \right)} \left[\int \right] \quad (11)$$

In these equations $[\int]$ stands for

$$\left[\int \frac{\rho(y) dy}{y^4} - \frac{6}{n} \int \frac{\rho(y) dy}{y^{n-2}} \right]$$

y is r/d^0 where d^0 is the distance from the center of a molecule to the first maximum in the density distribution $\rho(y)$ of other molecule centers located around the first molecule. Based on the experimental evidence that $\rho(y)$ vs. y is essentially the same for various substances, the integrals in brackets are taken to be identical in each of the above equations.

Using k_{12} from equation 8, c_{12} becomes

$$c_{12} = \frac{2\pi N^2 k_{11}^{1/2} k_{22}^{1/2}}{\bar{V}_1 \bar{V}_2 \left(\frac{d_{11}^0 + d_{22}^0}{2} \right)^3} \times \frac{2(I_1 I_2)^{1/2}}{I_1 + I_2} \times \left[\int \right] \quad (12)$$

Dividing c_{12} by $\sqrt{c_{11}(V_1/\bar{V}_1)^2 c_{22}(V_2/\bar{V}_2)^2}$ from equations 9 and 10 gives

$$c_{12} = (c_{11} c_{22})^{1/2} (V_1/\bar{V}_1)(V_2/\bar{V}_2) \left[2 \frac{(d_{11}^0 d_{22}^0)^{1/2}}{d_{11}^0 + d_{22}^0} \right]^3 \left[\frac{2(I_1 I_2)^{1/2}}{I_1 + I_2} \right] \quad (13)$$

Thus c_{12} is equal to the geometric mean of c_{11} and c_{22} when the product of the bracketed terms in 13 is unity, and $V = \bar{V}$ for each component. Letting $I_2/I_1 = q$ and $d_{22}^0/d_{11}^0 = s$, f_1 and f_d may be defined by

$$\frac{2(I_1 I_2)^{1/2}}{I_1 + I_2} = \frac{2q^{1/2}}{1+q} = f_1 \quad (14)$$

$$\left[\frac{2(d_{11}^0 d_{22}^0)^{1/2}}{d_{11}^0 + d_{22}^0} \right]^3 = \left(\frac{2s^{1/2}}{1+s} \right)^3 = f_d \quad (15)$$

Equation 13 becomes

$$c_{12} = f_1 f_d (V_1/\bar{V}_1)(V_2/\bar{V}_2) \sqrt{c_{11} c_{22}} \quad (16)$$

Substituting this expression for c_{12} in equation 1

(4) Reference (1), p. 127 ff.

and using partial molal volumes throughout as in equation 3, the energy of mixing is

$$\begin{aligned} \Delta E^M = & (x_1 \bar{V}_1 + x_2 \bar{V}_2) \varphi_1 \varphi_2 \left[c_{11} \left(\frac{V_1}{\bar{V}_1} \right)^2 + c_{22} \left(\frac{V_2}{\bar{V}_2} \right)^2 \right. \\ & \left. - 2 f_1 f_d \left(\frac{V_1}{\bar{V}_1} \right) \left(\frac{V_2}{\bar{V}_2} \right) \sqrt{c_{11} c_{22}} \right] + \Delta E_1^v (1 - V_1/\bar{V}_1) x_1 \\ & + \Delta E_2^v (1 - V_2/\bar{V}_2) x_2 \end{aligned} \quad (17)$$

Substituting $\Delta E^v/V$ for c , letting $\bar{\delta} = (\Delta E^v \times V/\bar{V}^2)^{1/2}$, and rearranging for comparison with equation 3 gives

$$\begin{aligned} \bar{\Delta E}^M = & (x \bar{V}_1 + x_2 \bar{V}_2) \varphi_1 \varphi_2 [(\bar{\delta}_1 - \bar{\delta}_2)^2 + 2\bar{\delta}_1 \bar{\delta}_2 (1 - f_1 f_d)] \\ & + \Delta E_1^v (1 - V_1/\bar{V}_1) x_1 + \Delta E_2^v (1 - V_2/\bar{V}_2) x_2 \end{aligned} \quad (18)$$

The partial molal energies are

$$\Delta E_1^M = \bar{V}_1 \varphi_2^2 [(\bar{\delta}_1 - \bar{\delta}_2)^2 + 2\bar{\delta}_1 \bar{\delta}_2 (1 - f_1 f_d)] + \Delta E_1^v (1 - V_1/\bar{V}_1) \quad (18a)$$

and, with subscripts interchanged, similarly for component 2. This equation does not take into account the change in $\bar{\delta}$ with composition.

Application of Equation 18 to Fluorocarbon-Hydrocarbon Mixtures.—Values of f_1 and f_d are given below for various values of q and s , respectively.

q or s	f_1	f_d	q or s	f_1	f_d
1.0	1.0000	1.0000	1.4	0.9860	0.9586
1.1	0.9989	0.9966	1.5	.9798	.9405
1.2	.9958	.9875	1.6	.9730	.9212
1.3	.9915	.9747			

For mixtures composed only of hydrocarbons of approximately the same boiling point, q is no greater than about 1.2, and s is no greater than about 1.1 so that c_{12} is usually within about 1% of $\sqrt{c_{11} c_{22}}$. For mixtures containing a fluorocarbon and a hydrocarbon q has a value greater than 1.3. Heats of mixing have been obtained from experimental data for the system $n\text{-C}_6\text{F}_{12} : n\text{-C}_6\text{H}_{12}$ ² and for the system $n\text{-C}_4\text{F}_{10} : n\text{-C}_4\text{H}_{10}$.³ These data provide a test for equation 18. The values of q and f_1 for these mixtures may be obtained as shown in Table I.

TABLE I

IONIZATION POTENTIALS OF C₄ AND C₆ HYDROCARBONS AND FLUOROCARBONS

Component		I, e.v.		q	f_1
1	2	1	2		
$n\text{-C}_6\text{F}_{12}$	$n\text{-C}_6\text{H}_{12}$	16.3 ^a	10.55 ^c	1.55	0.9760
$n\text{-C}_4\text{F}_{10}$	$n\text{-C}_4\text{H}_{10}$	17.4 ^b	10.34 ^d	1.69	0.9666

^a Calculated by method of reference 5 using a polarizability of $n\text{-C}_6\text{F}_{12}$ equal to 13.1×10^{-24} cm.³ taken from reference 6. ^b Calculated by method of reference 5 using a polarizability of $n\text{-C}_4\text{F}_{10}$ equal to 10.2×10^{-24} cm.³ taken from reference 6. ^c R. E. Honig, *J. Chem. Phys.*, **16**, 105 (1948). ^d W. C. Price, *Chem. Revs.*, **41**, 257 (1947).

The magnitude of f_d may be approximated from the molal volume V , or from the polarizability α of the pure liquids, or from the van der Waals radii of the molecules. For mixtures of $n\text{-C}_6\text{F}_{12}$ and $n\text{-C}_6\text{H}_{12}$ the following values of f_d may be calculated

(5) T. M. Reed III, *This Journal*, **59**, 428 (1955).

(6) J. H. Simons and J. B. Hickman, *ibid.*, **56**, 420 (1952)

TABLE II
VALUES OF THE TERMS IN BRACKETS OF EQUATION 18 FOR THE TWO-COMPONENT SYSTEMS
 $n\text{-C}_5\text{F}_{12}:n\text{-C}_5\text{H}_{12}$ AND $n\text{-C}_4\text{F}_{10}:n\text{-C}_4\text{H}_{10}$

Mole fract. fluorocarbon	$\bar{\delta}_1, (\text{cal./cc.})^{1/2}$		$\bar{\delta}_2, (\text{cal./cc.})^{1/2}$		$(\bar{\delta}_1 - \bar{\delta}_2)^2, \text{cal./cc.}$		$2\bar{\delta}_1\bar{\delta}_2(1 - f_1f_d), \text{cal./cc.}$	
	C_5 Mixture	C_4 Mixture	C_5 Mixture	C_4 Mixture	C_5 Mixture	C_4 Mixture	C_5 Mixture	C_4 Mixture
0.1	5.32	5.56	7.08	7.38	3.10	3.31	2.18	3.20
.2	5.40	5.66	7.02	7.29	2.62	2.66	2.20	3.22
.3	5.51	5.81	7.02	7.21	2.28	1.96	2.25	3.27
.4	5.60	5.97	6.90	7.06	1.69	1.19	2.25	3.30
.5	5.66	6.03	6.79	6.94	1.28	0.83	2.24	3.26
.6	5.72	6.10	6.68	6.74	0.92	.41	2.22	3.20
.7	5.75	6.15	6.55	6.66	.64	.26	2.18	3.20
.8	5.80	6.15	6.39	6.60	.35	.20	2.15	3.19
.9	5.80	6.19	6.17	6.49	.14	.09	2.08	3.13

TABLE III
COMPARISON OF EXPERIMENTAL HEATS OF MIXING WITH CALCULATED ENERGIES OF MIXING FOR MIXTURES OF
 $n\text{-C}_5\text{F}_{12}$ AND $n\text{-C}_5\text{H}_{12}$

x_1 mole fract. $n\text{-C}_5\text{F}_{12}$	$\overline{\Delta H}_1^M$, exptl., cal./mole	$\overline{\Delta E}_1^M$ by eqn.		x_2 mole fract. C_5H_{12}	$\overline{\Delta H}_2^M$, exptl., cal./mole	$\overline{\Delta E}_2^M$ by eqn.			
		(2a)	(3a)			(2a)	(3a)		
0.1	1425	220	940	1230	0.9	140	4	50	50
.2	925	155	650	880	.8	205	15	75	135
.3	655	110	450	600	.7	275	30	130	175
.4	490	80	265	380	.6	355	50	240	300
.5	320	45	175	240	.5	415	75	280	430
.6	250	30	65	130	.4	535	95	440	555
.7	150	15	25	70	.3	735	120	560	705
.82	870	145	670	850
.91	985	170	775	1030

TABLE IV
COMPARISON OF EXPERIMENTAL HEATS OF MIXING WITH CALCULATED ENERGIES OF MIXING FOR MIXTURES OF
 $n\text{-C}_4\text{F}_{10}$ AND $n\text{-C}_4\text{H}_{10}$

x_1 mole fract. $n\text{-C}_4\text{F}_{10}$	$\overline{\Delta H}_1^M$, cal./mole	$\overline{\Delta E}_1^M$ by eqn.		x_2 mole fract. $n\text{-C}_4\text{H}_{10}$	$\overline{\Delta H}_2^M$, cal./mole	$\overline{\Delta E}_2^M$ by eqn.			
		(2a)	(3a)			(2a)	(3a)		
0.1	1455	171	825	1275	0.9	49	3	56	65
.2	1062	123	610	920	.8	69	12	120	150
.3	786	86	410	590	.7	222	24	185	240
.4	638	57	225	340	.6	403	39	300	370
.5	513	37	165	235	.5	495	56	405	505
.6	386	21	75	115	.4	574	75	550	675
.7	138	11	30	50	.3	696	94	605	760
.8	0	5	25	35	.2	992	114	650	845
.9	0	1	-14	-12	.1	1185	133	745	975

	s	f_d
From α	1.10	0.9966
From V at 20°	1.17	.9917
From v.d. Waals radii ²	1.13	.9944

Using the value of s from the van der Waals radii, since $d^0/2$ may be identified approximately with this radius, $f_d = 0.9944$. These same values of s and f_d based on van der Waals radii apply to $n\text{-C}_4\text{F}_{10}:n\text{-C}_4\text{H}_{10}$ mixtures. For the C_5 system $f_1f_d = (0.9760)(0.9944) = 0.971$ and for the C_4 system $f_1f_d = (0.9666)(0.9944) = 0.961$. The value of s in these systems is of less importance than q . c_{12} deviates considerably from $\sqrt{c_{11}c_{22}}$ in both of these two component systems.

The calculated values of the separate terms in brackets in equation 18 are listed in Table II as calories/cc. to show the magnitude of the correction arising from the ratio of ionization potentials. The term $2\bar{\delta}_1\bar{\delta}_2(1 - f_1f_d)$ is seen to be a large fraction of the total in these two systems.

The partial molal energies of mixing for $n\text{-C}_5\text{F}_{12}:n\text{-C}_5\text{H}_{12}$ mixtures at 20° calculated according to equation 18a are compared in Table III and Fig. 1 with the experimental heats of mixing $\overline{\Delta H}^M$ and in Table III with the values calculated by equations 2a and 3a. The same comparisons are made in Table IV and Fig. 1 for the systems $n\text{-C}_4\text{F}_{10}:n\text{-C}_4\text{H}_{10}$ at -13.2° . Equation 18a produces very good agreement with the experimental values for the hydrocarbon components in both systems. The fluorocarbon components are not as satisfactory particularly in the case of $n\text{-C}_4\text{F}_{10}$. This discrepancy in the case of the fluorocarbon component probably arises from inaccurate vapor pressure-temperature measurements on the pure fluorocarbon compounds. Such an inaccuracy produces incorrect values for the activity as a function of temperature which in turn gives incorrect values for the partial molal heats of mixing obtained from the experimental data. The vapor pressure-temperature

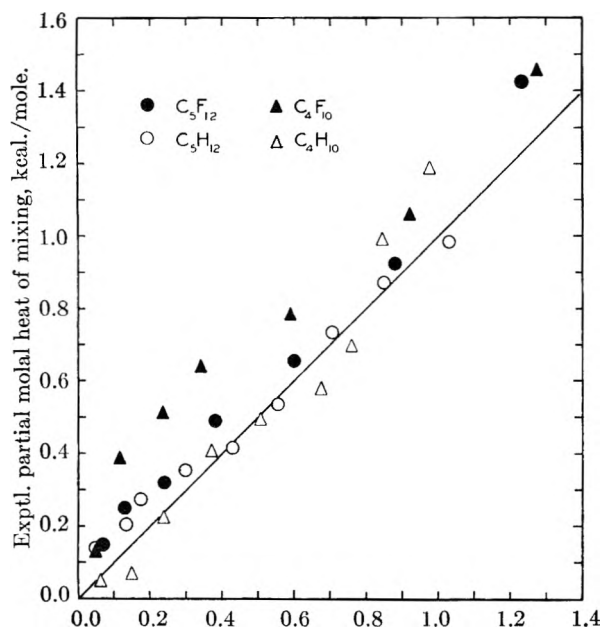


Fig. 1.—Partial molal energy of mixing, kcal./mole (calcd. by eq. 18a).

functions for the pure hydrocarbons were not measured by Simons, *et al.*, but were taken from other sources in the literature. In view of the agreement shown for the hydrocarbons in Fig. 1, it is probable that the vapor pressures used for the hydrocarbons are accurate while those measured for the fluorocarbons are not.

Conclusions

The heats of mixing paraffin hydrocarbons with fluorocarbons of the same carbon atom skeleton in liquid solution may be calculated by the Hildebrand-Scatchard theories when the interaction between unlike pairs of molecules in solution is properly evaluated. Insofar as the heats of mixing are concerned this interaction may be evaluated on the basis of London's dispersion forces, but the relatively large ratio of ionization potentials of hydrocarbons and fluorocarbons, heretofore neglected, must be taken into account as they appear in the London treatment. The correction to the calculated partial molal heats of mixing arising from the ratio of ionization potentials in the two systems $n\text{-C}_3\text{F}_{12} : n\text{-C}_3\text{H}_{12}$ and $n\text{-C}_4\text{F}_{10} : n\text{-C}_4\text{H}_{10}$ amounts to about 25% of the total calculated values.

THE IONIZATION POTENTIAL AND THE POLARIZABILITY OF MOLECULES

BY T. M. REED, III

Fluorine Research Center, University of Florida, Gainesville, Fla.

Received November 11, 1954

For molecules composed of an atom or a group of atoms completely surrounded by a single species of atoms, i , connected by single bonds to the central group, a correlation between the molecule ionization potential I , the molecule polarizability α and the number p_i of the peripheral atoms in the molecule is found to be $I\alpha = Ap_i$. A is a constant characteristic of both the kind of peripheral atom and the central group. For $i = \text{H}$, A has the same value for the hydrogen in the paraffin hydrocarbons, NH_3 and the methylamines. When the peripheral atoms are of two or more kinds, a relationship of the same form applies if a hypothetical polarizability is used in place of α . This hypothetical polarizability is arbitrarily assumed to be that for the part of the molecule which is directly concerned in the ionization process. A basis from quantum theory is postulated for the correlation found.

It is shown in this paper that in many cases there is a simple correlation between the ionization potential and the polarizability of a molecule. The ionization potential considered is that required to remove one electron from a molecule.

In the case of molecules composed of an atom or group of atoms essentially completely surrounded by a single species of atoms (peripheral atoms) connected by single bonds to the central group, the relationship between the ionization potential I of the molecule and the polarizability α of the whole molecule is given by

$$I\alpha = Ap_i \quad (1)$$

A is a constant characteristic of the type of peripheral atom, and p_i is the number of peripheral atoms of kind i per molecule. Series of substances for which A is a constant value are, for example, the paraffin hydrocarbons, or NH_3 and the alkyl amines.

When the type of molecules under consideration is composed of two or more species of peripheral atoms connected to a central group, it is found that an equation of the same form as (1) holds when the

polarizability α is replaced by a hypothetical polarizability α' postulated to be that for the part of the molecule apparently directly concerned in the ionization process. Since it is impossible to measure the polarizability of an atom in a molecule or of a connection between atoms in a molecule, the term "polarizability of a part of a molecule" must be hypothetical. The hypothetical polarizability α' of those parts of the molecule apparently directly concerned in the ionization process is obtained as the difference between the measured polarizability α of the molecule and the hypothetical polarizability of the extraneous portion of the molecule, *i.e.* of the atoms or groups of atoms arbitrarily selected as those apparently not directly concerned in the ionization process. In the specific instances with which this paper is concerned, the hypothetical polarizability of the extraneous portion is obtained as follows.

1. For extraneous parts containing C to H bonds and C to C bonds, the hypothetical polarizability of the CH bond is taken as one-fourth the measured polarizability of CH_4 ($\alpha_{\text{CH}} = 1/4 \alpha_{\text{CH}_4} = 0.645 \times$

10^{-24} cm.³), and the hypothetical polarizability of the CC bond is taken as the measured polarizability of C₂H₆ minus $6\alpha_{\text{CH}}$ ($\alpha_{\text{CC}} = \alpha_{\text{C}_2\text{H}_6} - 6\alpha_{\text{CH}} = 0.58 \times 10^{-24}$ cm.³). The hypothetical polarizability of an alkyl group which may apparently not be directly concerned in the ionization is the sum of these hypothetical bond polarizabilities for the alkyl group.

2. If the oxygen portion of molecules of alcohols and ethers is arbitrarily selected as the extraneous part, the extraneous hypothetical polarizability is taken as the measured polarizability of water.

Hydrogen and Paraffin Hydrocarbons.—Values¹ of $I\alpha$ taken from Table I are plotted in Fig. 1 vs. p_{H} , the number of H atoms per molecule for the paraffins. These points lie on a straight line through the origin. The value of $I\alpha$ for the H atom falls on this line at $p_{\text{H}} = 1$, but $I\alpha$ for the H₂ molecule is below the line at $p_{\text{H}} = 2$. The values of $I\alpha/p_{\text{H}}$ for each molecule are given in Table I. This ratio is practically constant for H and the paraffins. The mean value of $I\alpha/p_{\text{H}}$ (excluding H₂) for these molecules is 8.8×10^{-24} e.v. \times cm.³ per atom of H per molecule.

TABLE I
 $I\alpha/p_{\text{H}}$ FOR THE PARAFFIN HYDROCARBONS

Molecule	p_{H}	I , e.v.	α , cm. ³ $\times 10^{-24}$	$I\alpha$, e.v. \times cm. ³ $\times 10^{-24}$	$I\alpha/p_{\text{H}}$, e.v. \times cm. ³ $\times 10^{-24}$ molecule ⁻¹ \times H atom ⁻¹
H	1	13.595	0.66	9.0	9.0
H ₂	2	15.43 ²	0.81	12.42	6.21
		16.4		13.3	6.65
CH ₄	4	13.1 ²	2.58	33.8	8.45
		13.16 ³		34.0	8.50
		14.5		37.4	9.35
C ₂ H ₆	6	11.6 ²	4.47	51.9	8.65
			4.44	51.5	8.58
C ₃ H ₈	8	11.3 ²	6.31	71.3	8.91
		11.21 ⁴		70.7	8.84
<i>n</i> -C ₄ H ₁₀	10	10.34 ²	8.30	85.8	8.58
		10.8 ⁴		89.6	8.96
<i>i</i> -C ₄ H ₁₀	10	10.80	8.27	89.4	8.94
<i>n</i> -C ₅ H ₁₂	12	10.55 ⁴	10.00	105.5	8.79
<i>n</i> -C ₆ H ₁₄	14	10.43 ⁴	11.81	123.2	8.80
<i>n</i> -C ₇ H ₁₆	16	10.35 ⁴	13.69	141.7	8.86
<i>n</i> -C ₈ H ₁₈	18	10.24 ⁴	15.50	158.7	8.82
<i>n</i> -C ₉ H ₂₀	20	10.21 ⁴	17.38	177.4	8.87
<i>n</i> -C ₁₀ H ₂₂	22	10.19 ⁴	19.10	194.6	8.85

Ammonia and Alkyl Amines.—The values of $I\alpha/p_{\text{H}}$ for NH₃ and the methylamines are given in Table II. In Fig. 1, $I\alpha$ vs. p_{H} for these compounds fall on the line for the normal hydrocarbons and the hydrogen atom. The mean value of $I\alpha/p_{\text{H}}$ for ammonia and these amines, exclusive of CH₃NH₂ for which the value of α is apparently in error, is 8.7×10^{-24} e.v. \times cm.³ per atom of H per molecule.

According to Price² the first ionization potential of the amines is that for a non-bonding electron on the nitrogen. The apparent correlation of the ionization potential with the total polarizability and

(1) The values of I and of α are taken from the Landolt-Börnstein Tables, except where otherwise noted.

(2) W. C. Price, *Chem. Revs.*, **41**, 257 (1947).

(3) J. D. Morrison and A. J. C. Nicholson, *J. Chem. Phys.*, **20**, 1021 (1952).

(4) R. E. Honig, *ibid.*, **16**, 105 (1948).

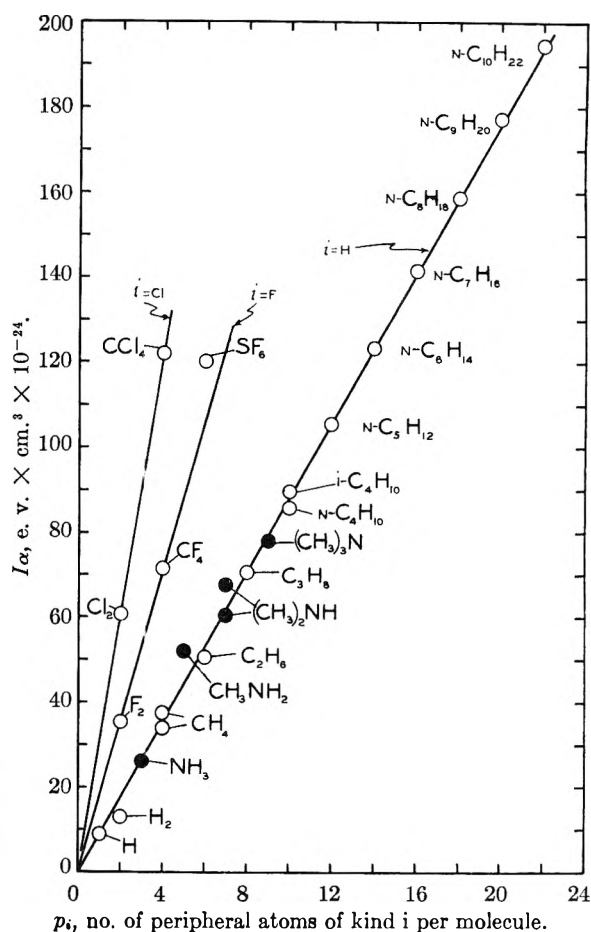


Fig. 1.

number of peripheral hydrogen atoms in ammonia and the amines seems to contradict such an assignment.

TABLE II
 $I\alpha/p_{\text{H}}$ FOR NH₃ AND SOME AMINES

Molecule	p_{H}	I , e.v.	α , cm. ³ $\times 10^{-24}$	$I\alpha$	$I\alpha/p_{\text{H}}$, e.v. \times cm. ³ $\times 10^{-24}$ molecule ⁻¹ \times H atom ⁻¹
N ₂	..	15.51, 16.8	1.74	27.0, 29.2	...
NH ₃	3	10.8 ⁶	2.46	26.6	8.87
		10.52 ³		25.9	8.63
CH ₃ NH ₂	5	9.8	5.31	52.0	10.40
		9.41 ³			
(CH ₃) ₂ NH	7	9.6	6.26	60.1	8.59
			7.05	67.7	9.67
(CH ₃) ₃ N	9	9.4	8.29	77.9	8.66

Water, Alcohols and Ethers.—For compounds containing oxygen linked covalently to hydrogen and alkyl radicals the values of $I\alpha$ and $I\alpha/p_{\text{H}}$ are given in Table III. $I\alpha/p_{\text{H}}$ for H₂O is 9.4×10^{-24} e.v. \times cm.³ per H atom per molecule. The alcohols and the ether show $I\alpha/p_{\text{H}}$ values of approximately 10×10^{-24} e.v. \times cm.³ per H atom per molecule. $I\alpha$ vs. p_{H} for these oxygen-containing molecules give points close to a straight line through the origin on Fig. 2.

(5) W. C. Price and W. T. Tutte, *Proc. Roy. Soc. (London)*, **A174**, 207 (1940).

TABLE III
 $I\alpha/p_H$ AND $I\alpha'/p_{HC}$ FOR H_2O , ALCOHOLS AND AN ETHER

Molecule	p_H	I , e.v.	α , $cm.^3 \times 10^{-24}$	$I\alpha$	$I\alpha/p_H$	p_{HC}	α' $= \alpha - \alpha_{H_2O}$, $cm.^3 \times 10^{-24}$	$I\alpha'$	$I\alpha'/p_{HC}$
O_2	..	12.2	1.57	19.2
H_2O	2	12.56	1.49	18.7	9.35
		12.61 ^b		18.8	9.4
CH_3OH	4	10.8	3.76	40.6	10.15	3	2.27	24.5	8.16
			4.00	43.2	10.8		2.51	27.1	9.03
C_2H_5OH	6	10.7	5.62	60.1	10.0	5	4.13	44.2	8.85
$n-C_3H_7OH$	8	10.7	7.32	78.4	9.8	7	5.83	62.4	8.91
$(C_2H_5)_2O$	10	10.2	10.01	102	10.2	10	8.52	86.9	8.69

An alternate treatment of the data for the oxygen-containing molecules is possible. By considering the alkyl radicals as the parts directly concerned in the ionization, the hypothetical polarizability of these parts, obtained as $\alpha' = \alpha - \alpha_{H_2O}$, multiplied by the molecule ionization potential give the figures

compounds, shown in Fig. 3, gives points on the $I\alpha$ vs. p_H line for the hydrocarbons. This correlation again seems to contradict the assignment² of the first ionization potential of the alcohols to a non-bonding electron of the oxygen atom.

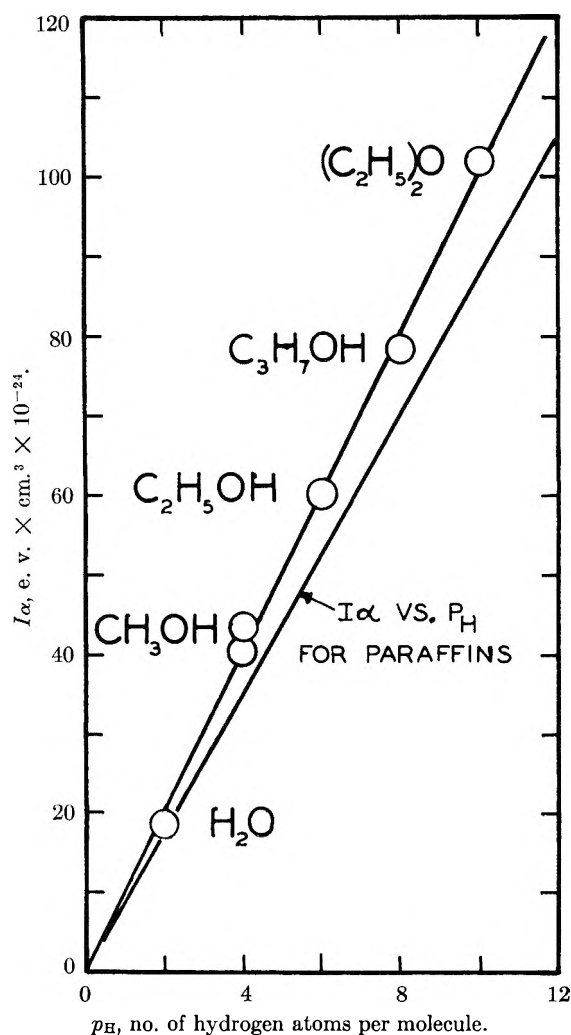


Fig. 2.

for $I\alpha'$ shown in column 9 of Table III. $I\alpha'/p_{HC}$, where p_{HC} is the number of H atoms attached directly to carbon per molecule, appears to be fairly constant. The average is 8.7×10^{-24} e.v. \times $cm.^3$ per H atom per molecule. This is essentially the value of A obtained for the hydrocarbons and the amines. A plot of $I\alpha'$ vs. p_{HC} for these oxygen

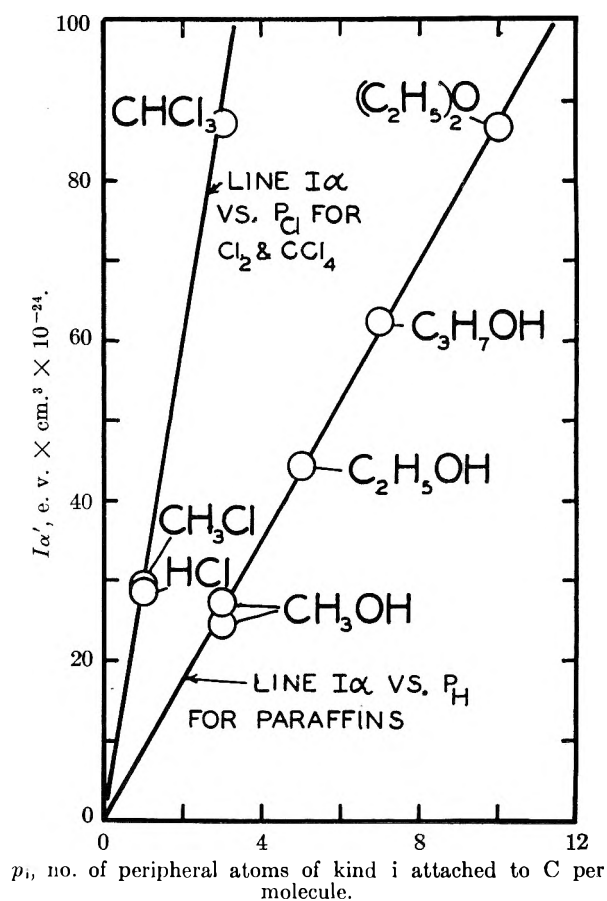


Fig. 3.

Fluorine Compounds.—The values available for compounds consisting of fluorine attached to multi-valent atoms is given in Table IV. The values of $I\alpha$ vs. p_F , the number of F atoms per molecule, for F_2 and CF_4 lie on a straight line through the origin in Fig. 1. The slope of this line is 17.8×10^{-24} e.v. \times $cm.^3$ per F atom per molecule. $I\alpha/p_F$ for SiF_4 , SF_6 , and UF_6 are not equal to this value, although SF_6 is not far off. The high value for the polarizability of UF_6 gives the high $I\alpha/p_F$ figure for this molecule.

Chlorine Compounds.—Table V gives data available for compounds containing chlorine. Values of

TABLE IV
 $I\alpha/p_F$ FOR SOME FLUORINE COMPOUNDS

Molecule	p_F	I , e.v.	α , $\text{cm.}^3 \times 10^{-24}$	$I\alpha$	$I\alpha/p_F$, e.v. $\times \text{cm.}^3$ $\times 10^{-24}$ molecule ⁻¹ $\times F \text{ atom}^{-1}$
F	..	17.43
F ₂	2	17.8 ⁹	1.98 ¹⁰	35.2	17.6
CF ₄	4	17.8 ⁶	4.02 ¹¹	71.5	17.9
SiF ₄	4	16.9 ⁷	5.48	92.6	23.2
SF ₆	6	19.3	6.21	120	20.0
			6.55 ¹¹	126	21.0
UF ₆	6	15.5	10.8 ¹²	167	27.8

$I\alpha$ vs. p_{Cl} for Cl₂ and CCl₄ lie on a straight line which passes through the origin, and has a slope of 30.3×10^{-24} e.v. $\times \text{cm.}^3$ per Cl atom per molecule. The values of BCl₃ and SiCl₄ are greater than this, indicating that the effects of the central atoms in these molecules are different from those of C and N, as was seen above for SiF₄, SF₆ and UF₆.

 TABLE V
 $I\alpha/p_{Cl}$ FOR SOME CHLORINE COMPOUNDS

Molecule	p_{Cl}	I , e.v.	α , $\text{cm.}^3 \times 10^{-24}$	$I\alpha$	$I\alpha/p_{Cl}$, e.v. $\times \text{cm.}^3$ $\times 10^{-24}$ molecule ⁻¹ $\times Cl \text{ atom}^{-1}$
Cl ₂	2	13.2	4.60	60.7	30.3
CCl ₄	4	11.0	11.11 ¹³	122	30.5
BCl ₃	3	12.0	9.60 ¹³	115	38.4
SiCl ₄	4	11.6	13.38 ¹³	155	38.8

The compounds given in Table VI contain both H and Cl. If the ionization potentials of these

 TABLE VI
 $I\alpha'/p_{Cl}$ FOR SOME COMPOUNDS CONTAINING H AND Cl

Molecule	I , e.v.	α , $\text{cm.}^3 \times 10^{-24}$	$p_{H\alpha H}$, $\text{cm.}^3 \times 10^{-24}$	$\alpha' =$ $\alpha - p_{H\alpha H}$	$I\alpha'$	$I\alpha'/p_{Cl}$, e.v. $\times \text{cm.}^3$ $\times 10^{-24}$ Cl atom ⁻¹ \times molecule ⁻¹
HCl	12.84	2.63	0.40 ^a	2.23	28.6	28.6
	12.78					
CH ₃ Cl	11.17	4.56	1.94 ^b	2.62	29.3	29.3
CHCl ₃	11.5	8.23	0.645 ^b	7.58	87.1	29.1

^a $\alpha_H = 1/2 \alpha_{CH_2}$. ^b $\alpha_H = \alpha$ for CH bond in paraffin hydrocarbons, e.g., $1/4 \alpha_{CH_4}$.

molecules are attributed to chlorine in carbonaceous substances, the polarizability α of the whole mole-

(6) The ionization potential given for CF₄ has been questioned. The value of 17.8 e.v. appears too high when compared with the appearance potential of 15.9 e.v. observed⁷ for CF₃⁺ in the mass spectrum of CF₄. However, it is found⁷ in the mass spectrum of SiF₄ that the appearance potential of SiF₄⁺ (16.9 ± 0.5 e.v.) is significantly greater than that of SiF₃⁺ (16.1 ± 0.2 e.v.). Furthermore, in the mass spectra of CF₄ and other fluorocarbons⁸ the molecule ions occur in negligible quantities. These results indicate⁷ that the CF₃⁺ and SiF₃⁺ ions are formed directly from CF₄ and SiF₄, respectively, by the loss of F⁻. It is also observed⁷ that none of the positive ion fragments in the mass spectrum of CF₄ appear at potentials below the appearance potential of CF₃⁺. Under these circumstances the ionization potential CF₄ to CF₄⁺ cannot be less than the appearance potential of CF₃⁺ and may be greater, as in the case of SiF₄⁺ compared to SiF₃⁺.

(7) V. H. Dibeler and F. L. Mohler, *J. Research Natl. Bur. Standards*, **40**, 25 (1948).

(8) F. L. Mohler, *et al.*, *J. Am. Chem. Soc.*, **71**, 337 (1949).

(9) "Handbook of Chemistry and Physics," Chemical Rubber Co.

(10) E. Kanda, *Bul. Chem. Soc., Japan*, **12**, 469 (1937).

(11) H. E. Watson, K. L. Ramaswamy and G. P. Kane, *Proc. Roy. Soc. (London)*, **A156**, 130 (1936).

(12) J. H. Simons and J. B. Hickman, *This Journal*, **56**, 420 (1952).

(13) R. J. W. LeFevre and D. A. A. S. Narayana Rao, *Australian J. Chem.*, **7**, 135 (1954).

cule must be reduced by the hypothetical polarizabilities of the H atoms to give the hypothetical polarizabilities corresponding to the observed ionization potentials of the molecule.

Taking a value for the hypothetical polarizability equal to 0.40×10^{-24} cm.³ (from one-half α of H₂) for H in HCl, and equal to 0.645×10^{-24} cm.³ for H in CHCl₃ and CH₃Cl, the values of $\alpha' = \alpha - p_{H\alpha H}$ shown in Table VI are obtained. $I\alpha'/p_{Cl}$ calculated in this manner for these three compounds is about 29×10^{-24} e.v. $\times \text{cm.}^3$ per Cl atom per molecule. $I\alpha'$ vs. p_{Cl} on Fig. 3 give points close to the line of $I\alpha$ vs. p_{Cl} for Cl₂ and CCl₄.

Sulfur Compounds.—The first ionization potentials of the mercaptans and the thioethers given in Table VII seem to be characteristic of the S group. Consequently, as in the case of CHCl₃ and CH₃Cl, there is no correlation of the $I\alpha$ values on the basis of the number of peripheral hydrogen atoms per molecule. The polarizability of these molecules must be reduced by the terms $\Sigma\alpha_{R}$, arising from the alkyl radicals, before the product of ionization potential and hypothetical polarizability α' will be constant.

 TABLE VII
 $I\alpha'$ FOR S IN H₂S, C₂H₅SH AND (C₂H₅)₂S

Molecule	I , e.v.	α , $\text{cm.}^3 \times 10^{-24}$	$\Sigma\alpha_{R}$, $\text{cm.}^3 \times 10^{-24}$	α' , $\text{cm.}^3 \times 10^{-24}$	$I\alpha'$, e.v. $\times \text{cm.}^3$ $\times 10^{-24}$ S atom ¹ \times molecule ⁻¹
S	10.36
S ₂	10.7
H ₂ S	10.42	3.61	0	3.61	37.6
	10.47				
C ₂ H ₅ SH	9.70	7.56	3.80	3.76	36.5
(C ₂ H ₅) ₂ S	9.30	11.18	7.60	3.58	33.4
		(11.51)		(3.91)	(36.4)

The hypothetical polarizability of the ethyl radical was obtained as the sum of the polarizabilities of 5CH bonds and one CC bond as defined above. $I\alpha'$, where $\alpha' = \alpha - \Sigma\alpha_{R}$, for H₂S and C₂H₅SH are about 37×10^{-24} e.v. $\times \text{cm.}^3$ per S atom per molecule. The value of $I\alpha'$ for (C₂H₅)₂S obtained using the experimental α of 11.18×10^{-24} cm.³ is 33.4×10^{-24} e.v. $\times \text{cm.}^3$. Using a calculated α of 11.51×10^{-24} cm.³ (in parentheses in Table VII), obtained from the sum of the hypothetical polarizabilities of the bonds derived from H₂S, C₂H₅SH, and the paraffins, $I\alpha'$ for (C₂H₅)₂S is 36.4×10^{-24} e.v. $\times \text{cm.}^3$ per S atom per molecule, in line with this product for the other sulfur-containing molecules.

It is well known that α alone in the paraffin hydrocarbons is a linear function of p_{H} , and that H₂ lies on this line. This line, however, does not pass through the origin. By multiplying α by I , a non-linear function of p_{H} , a linear relationship between $I\alpha$ and p_{H} is obtained for the paraffins which passes through the origin but does not include H₂.

Discussion

Equation 1 seems to be a fairly accurate relationship between ionization potentials of molecules and polarizabilities. It is evident from the increase in values for $I\alpha/p_F$ for CF₄, SF₆, SiF₄ and UF₆ in this sequence that the nature of the central atom (or

group of atoms in general) has an effect on the value of A for a given species of peripheral atom.

The essential identity of the A values for the hydrocarbon series and for the amine series when the peripheral atoms are all H indicates that a central group composed of C and N atoms is equivalent to a central group composed entirely of C atoms. A central group composed of C and O is apparently not quite equivalent to one composed of C alone, since A for the entire molecule of alcohols and ether is larger than A for the hydrocarbons.

The A values increase in order of increasing atomic numbers for the peripheral atoms

Atom in a molecule	A -value, e.v. \times cm. ³ $\times 10^{-24}$
H	8.8
F	17.8
Cl	30.3

The value of $I\alpha' = 37 \times 10^{-24}$ e.v. \times cm.³ per S atom is out of order. A -value for oxygen, obtained as $I\alpha$ for H₂O, is 18.8×10^{-24} e.v. \times cm.³. This is also above but close to the A -value of the neighboring atom, F, in the periodic table.

These correlations allow the calculation of ionization potentials of fluorocarbons for which, other than CF₄, there are no measured values. The ratio of ionization potentials of fluorocarbons to those of hydrocarbons of the same carbon skeleton is in the range 1.3 to 1.6. A contrast of this magnitude in the ionization potential of non-polar substances can account¹⁴ for a significant part of the non-ideal behavior of solutions containing both a fluorocarbon and a hydrocarbon.

(14) T. M. Reed, *THIS JOURNAL*, **58**, 425 (1955).

Postulations.—A theoretical basis may be given equation 1. In the quantum theory of dispersion it is shown that the polarizability α of an atom in a stationary electric field is given by

$$\alpha = 2 \sum_m \frac{(\text{ex})_m^2}{h\nu_m} \quad (2)$$

where $(\text{ex})_m$ and ν_m are the electric moment and the characteristic frequency associated with the transition from the ground state to state m . As a postulate for the situation in molecules the polarizability α might similarly be the sum of such terms.

Consider the case of a molecule composed of a central group of atoms essentially completely surrounded by a single species of atoms. As a second postulate it is assumed that there is a series of values of ν for the molecule which are p_i degenerate when p_i is the number of peripheral atoms of kind i per molecule. Assuming further that the main contribution to this series of ν values may be approximated by a single transition and that $h\nu$ for this transition is approximately the first ionization potential of the molecule, equation 2 for these special molecules becomes

$$\alpha = 2p_i(\text{ex})_m^2/I \quad (3)$$

I is the first ionization potential of the molecule, and $(\text{ex})_m$ is the magnitude of the dipole associated with the postulated single transition. If $(\text{ex})_m$ is a constant for various molecules having the same kind of peripheral atoms, $I\alpha$ vs. p_i should be a straight line through the origin of slope $2(\text{ex})_m^2 = I\alpha/p_i$. Thus A in equation 1 becomes $2(\text{ex})_m^2$.

Acknowledgment.—The author benefited from discussions of this work with Dr. J. H. Simons.

THE CRITICAL MICELLE CONCENTRATIONS IN AQUEOUS SOLUTIONS OF POTASSIUM ALKYL MALONATES

By Kōzō SHINODA

Department of Physical Chemistry, Faculty of Engineering, Yokohama National University, Minamiku, Yokohama, Japan

Received November 12, 1954

The critical micelle concentrations (CMC) in aqueous solutions of homologous surfactants which possess two carboxyl radicals at one end of their hydrocarbon chain have been determined by the visual color change of dye, absorption spectrum of dye, solubilization and surface tension. Relation between the logarithm of the CMC of aqueous potassium alkyl malonates and the number of carbon atoms in hydrocarbon chain, m , is linear and the slope of the line is 0.51. Relation between the logarithm of the CMC versus m under the condition of definite concentration of counterions is also linear, and the slope of this line is 1.07. This value is nearly equal to the slope (1.08) between \log CMC versus m in the case of fatty acid soaps. Accordingly the environmental energy change at the micelle formation per methylene radical is given as about $1.08kT$. The effect of added univalent salts on the CMC has also been measured. Relations between the logarithm of CMC and the logarithm of the total concentration of counterions, $\log C_s$, in all alkyl malonates investigated are linear, and the slopes of these lines are 1.12 within experimental error. This slope is just twice the mean slope 0.56 in the case of fatty acid soaps. This may result from the fact that the alkyl malonic acid ion is a bivalent anion, while the fatty acid ion is univalent.

Introduction

On the micelle of colloidal electrolytes, there have been done many investigations during the past forty years.¹⁻⁴ It has become clear that

(1) G. S. Hartley, "Aqueous Solutions of Paraffin-Chain Salts," Hermann et Cie., Paris, 1936.

(2) J. W. McBain, "Colloid Science," Reinhold Publ. Corp., New York, N. Y., 1950.

(3) W. D. Harkins, "The Physical Chemistry of Surface Films," Reinhold Publ. Corp., New York, N. Y., 1952.

(4) Per Ekwall, *J. Colloid Sci.*, Supplement, **1**, 66 (1954).

colloidal electrolytes show all the phenomena of colloids and exhibit a remarkably varied behavior which, however, has been shown to be subject to quantitative control and to be perfectly reproducible. These experimental results impress that the micelle formation is a thermodynamically reversible process and the micellar solution obeys the phase rule for heterogeneous equilibrium.⁵ Especially in

(5) J. W. McBain, R. D. Vold and M. J. Vold, *J. Am. Chem. Soc.*, **60**, 1866 (1938).

recent years the mechanism for the formation of micelle, association number and shapes of micelle have become clear by the investigations on the critical micelle concentration (CMC) of various colloidal electrolytes under various conditions,⁶⁻¹⁴ X-ray small angle scattering¹⁶⁻¹⁹ and light scattering,²⁰⁻²⁴ etc. After all, it is to be expected that scores of surfactants aggregate into a micelle directing their hydrocarbon chains end-to-end and side-by-side and their polar groups toward the water, forming oblate spheroidal double layer. On the other hand a theoretical equation of the CMC,²⁵ which is derived from equating the chemical potentials of long-chain electrolytes in the micelle and that in the solution, has explained many experimental results coherently. It is apparent from this equation that the charges on the polar group play an important role on the properties of surfactants. In order to comment the anticipations derived from the theoretical equation of the CMC, the following experiments are needed: the systematic investigation of (1) the effect of added salts on the CMC,^{8,9} (2) the effect of added alcohols on the CMC,^{10,11} (3) the CMC of soap mixtures,¹²⁻¹⁴ etc. These investigations had already been carried out, showing good agreement with the theory, but they were restricted to substances which possess one polar radical at one end of the hydrocarbon chains.

Consequently it has become important and interesting to investigate the substances which possess two or three polar-ionic radicals at one end of the hydrocarbon chains, to obtain the new knowledge on the micelle. In this purpose, the experiments of the alkyl malonic acids, which are considered the most convenient compounds for the theoretical treatment, are eagerly demanded.

The present investigation has been undertaken to measure the CMC of aqueous solutions of a series of potassium alkyl malonates, $R_nCH(COOK)_2$: especially the relation of log CMC *versus* the number of carbon atoms in the hydrocarbon chain of alkyl malonates in case no salts added and under the condition of definite concentration of counterions, and the effect of added salts on the CMC of the respective potassium alkyl malonate.

- (6) H. B. Klevens, *J. Am. Oil Chemist's Soc.*, **30**, 74 (1953).
- (7) H. B. Klevens, *THIS JOURNAL*, **52**, 130 (1948).
- (8) M. L. Corrin and W. D. Harkins, *J. Am. Chem. Soc.*, **69**, 683 (1947).
- (9) H. Lange, *Kolloid-Z.*, **121**, 66 (1951).
- (10) S. H. Herzfeld, M. L. Corrin and W. D. Harkins, *THIS JOURNAL*, **54**, 271 (1950).
- (11) K. Shinoda, *ibid.*, **58**, 1136 (1954).
- (12) H. B. Klevens, *J. Chem. Phys.*, **14**, 742 (1946).
- (13) H. Lange, *Kolloid-Z.*, **131**, 96 (1953).
- (14) K. Shinoda, *THIS JOURNAL*, **58**, 541 (1954).
- (15) K. Hess and H. Kiessig, *Ber.*, **81**, 327 (1948).
- (16) J. Stauff, *Kolloid-Z.*, **89**, 224 (1939); **96**, 244 (1941).
- (17) R. W. Mattoon, R. S. Stearns and W. D. Harkins, *J. Chem. Phys.*, **15**, 209 (1947); **16**, 644 (1948).
- (18) W. D. Harkins and R. Mittelmann, *J. Colloid Sci.*, **4**, 367 (1949).
- (19) E. W. Hughes, W. M. Sawyer and J. R. Vinograd, *J. Chem. Phys.*, **13**, 131 (1945).
- (20) P. Debye and E. W. Anacker, *THIS JOURNAL*, **55**, 644 (1951).
- (21) E. W. Anacker, *J. Colloid Sci.*, **8**, 402 (1953).
- (22) J. J. Hermans, *Rec. trav. chim.*, **68**, 859 (1949).
- (23) T. M. Doscher and K. J. Mysels, *J. Chem. Phys.*, **19**, 254 (1951).
- (24) E. Hutchinson, *J. Colloid Sci.*, **9**, 191 (1954).
- (25) K. Shinoda, *Bull. Chem. Soc. Japan*, **26**, 101 (1953).

Materials

Alkyl bromides have been prepared by the bromination of aliphatic alcohols with sodium bromide and concentrated sulfuric acid. Alkyl malonic acid diethyl esters have been synthesized by the addition of malonic acid diethyl ester to the alkyl bromides under the existence of sodium alcoholate. Alkyl malonic acid diethyl esters have been saponified with alkali in alcohol and then acidified to alkyl malonic acids. These acids have been recrystallized two times in benzene. Solution of potassium alkyl malonate has been prepared by the similar procedures as in the case of fatty acid soap. Aliphatic alcohols, alkyl bromides and alkyl malonic acid diethyl esters have been purified by fractional distillation through a 50-cm. glass packed column. The melting points or boiling points of alkyl malonic acids and related compounds are shown in Table I. 2-Nitrodi-phenylamine is a product of Daiichi Pure Chemicals Co., Ltd.

TABLE I

Alkyl radical	Malonic acid diethyl ester B.p., °C.	at Mm.	Malonic acid m.p., °C.
Octyl	130~134	3	111
Dodecyl	165~170	2	121~121.5
Tetradecyl	196~200	4.5	122~123
Hexadecyl	174~184	0.15	112.5~113
Octadecyl	185~200	0.2	119~121

Experimental Results

The determination of the CMC has been performed by the change in color and spectrum of pinacyanole and the break in surface tension-concentration and solubilization-concentration curves.

(1) **The Effect of Chain Lengths on the CMC.**—The values for the CMC of the potassium alkyl malonates from the octyl malonate to the octadecyl malonate as determined by the change in color are shown in column 2 of Table II.

TABLE II

THE CMC OF POTASSIUM ALKYL MALONATES (MOLES/L.)

Mol. formula	Methods of the determination of CMC	
	Visual color change, 25°	Surface tension, 20°
$R_8CH(COOK)_2$	0.35	0.30
$R_{10}CH(COOK)_2$.13 ^a	...
$R_{12}CH(COOK)_2$.048	.048
$R_{14}CH(COOK)_2$.017	.019
$R_{16}CH(COOK)_2$.006	.009
$R_{18}CH(COOK)_2$.0023	...

^a This value is obtained from the intersection in Fig. 1.

Experimental procedures are described in the preceding reports.^{11,14} It has been found that the logarithm of the CMC of the homologous alkyl malonates as obtained by the visual method at 25° fits the equation

$$\log \text{CMC} = -K_1 m + \text{const.} \quad (1)$$

where m is the number of carbon atoms in the hydrocarbon chain (number of carbon atoms in the alkyl radical plus one), and K_1 is the experimental constant given as 0.51.

A similar relation of log CMC *versus* m had been noted previously for several homologous series of long-chain electrolytes,²⁶⁻²⁹ and the slope was about

- (26) J. Stauff, *Z. physik. Chem.*, **A183**, 55 (1939).
- (27) G. S. Hartley, *Kolloid-Z.*, **88**, 22 (1939).
- (28) K. Hess, W. Philippoff and H. Kiessig, *ibid.*, **88**, 40 (1939).
- (29) A. B. Scott and H. V. Tartar, *J. Am. Chem. Soc.*, **66**, 692 (1943).

0.69 in the case of fatty acid soap.³⁰ These relationships are shown in Fig. 1.

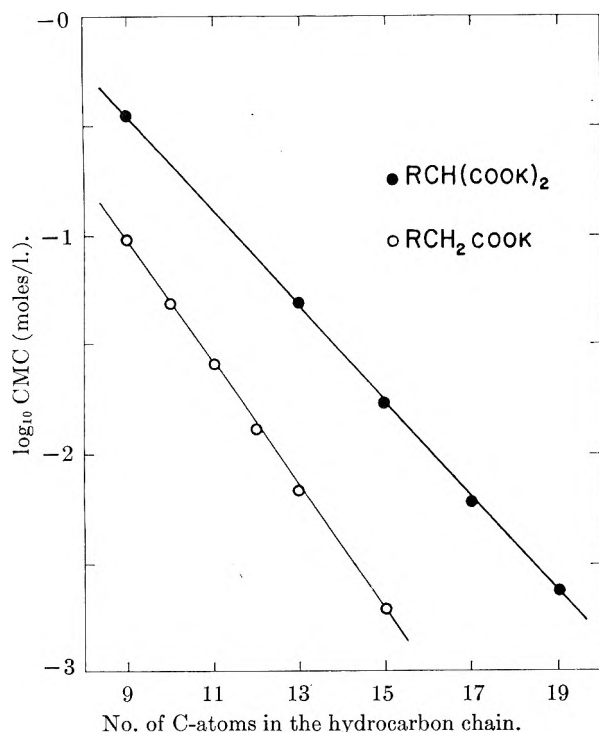


Fig. 1.—The relation between the logarithm of the CMC and the number of carbon atoms in the hydrocarbon chain.

The absorption spectrum of pinacyanole iodide at varying concentrations of potassium dodecyl malonate is measured spectrophotometrically at 20°. The optical densities for pinacyanole iodide at average wave lengths of respective band maxima are shown in Fig. 2.

The spectrophotometrical value of the CMC is 0.048 mole/l. in the case of potassium dodecyl malonate, showing good agreement with the value obtained by visual method. But the agreement between visual and spectral methods may not always be satisfactory.³⁰

The surface tensions of aqueous solutions of potassium alkyl malonates at varying concentrations are measured by a drop weight method at 20°. The diameter of the stalagmometer is 5.96 mm. The values of the CMC obtained from the break point of the surface tension-concentration curves are shown in column 3 in Table II. These values are essentially in agreement with the values obtained from the other methods.

For the solubilization measurements made with solid colored compound, 2-nitrodiphenylamine, the procedure is to shake the soap solution with an excess of the solid until equilibrium is reached in the air thermostat at $25 \pm 1^\circ$, and then to measure the amount of solubilization by measuring the depth of color of the solution by colorimetric methods. The depth of color of saturated 2-nitrodiphenylamine in varying concentrations of surfactants remains constant until the CMC is passed after which there is a remarkable increase due to solubilization in micelles. The values of CMC determined

(30) S. H. Herzfeld, *THIS JOURNAL*, **56**, 953 (1952).

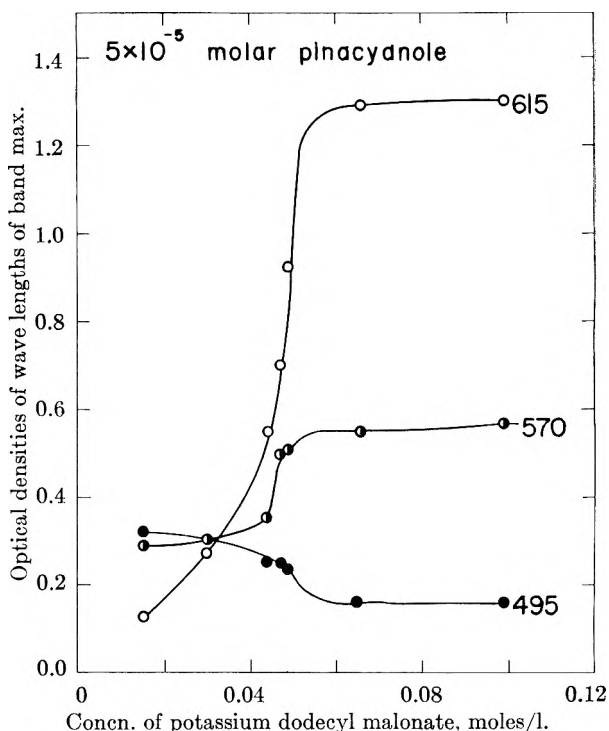


Fig. 2.—Intensities of absorption by pinacyanole iodide at average wave lengths ($m\mu$) of band maxima as functions of concentration of potassium dodecyl malonate at 20°.

by the solubilization method are given as 0.050 mole/l. for potassium dodecyl malonate and 0.018 mole/l. for potassium tetradecyl malonate.

(2) **The Effect of Added Salts on the CMC.**—The values of the CMC of a series of potassium alkyl malonates in the presence of added univalent salts are determined by the change in color of pinacyanole. The logarithm of the CMC *versus* the logarithm of the total concentrations of counterions, $\log C_s$, is linear in each homologous alkyl malonate, and the logarithm of the CMC *versus* the number of carbon atoms in hydrocarbon chain, m , is also linear under the condition of definite concentration of counterions. Observed data fit the following equation

$$\log \text{CMC} = -K_2 \log C_s - K_3 m + \text{const.} \quad (2)$$

where K_2 and K_3 are the experimental constants given as $K_2 = 1.12$ and $K_3 = 1.07$. These relations are shown in Fig. 3.

It is interesting that the constant K_2 in the case of alkyl malonate (dicarboxylate) is just twice as much as in the case of fatty acid soaps^{8,31} (monocarboxylate).

Discussion

The CMC value of respective potassium alkyl malonate is larger than the CMC value of corresponding fatty acid salt. This may result from the fact that alkyl malonate has two dissociable groups at one end of the hydrocarbon chain while the fatty acid possesses one.

The relation between the logarithm of the CMC *versus* the number of carbon atoms in potassium alkyl malonates has been linear. This linearity between $\log \text{CMC}$ *versus* m had been noted previously

(31) S. H. Herzfeld, *ibid.*, **56**, 959 (1952).

for several homologous series of long-chain electrolytes.²⁶⁻²⁹ It has been believed that the slopes of the plot of $\log \text{CMC}$ versus m for all long-chain electrolytes are constant within experimental error.^{6,7} However, homologous series of potassium alkyl malonates which possess two dissociable groups at one end of their hydrocarbon chain offer the evidence that this is not to be the case. It has become clear that the slope of $\log \text{CMC}$ versus m rather varies with the number and kinds of polar groups concerned.

The plot of $\log \text{CMC}$ versus m of homologous series of potassium alkyl malonates under the condition of definite concentration of counterions has been also linear, but in this condition the slope is equal to that of fatty acid salts. This fact agrees with the following view; in a homologous group of long-chain electrolytes, the work done against the coulomb forces can be taken as independent of chain length under the condition of the definite concentration of counterions. The work performed by a number of chains in the transition from a free to an aggregated state, however, clearly increases linearly with the number of methylene groups in each chain. This work is a logarithmic function of CMC and it follows that m should be a linear function of $\log \text{CMC}$. Accordingly the coefficient of m under the condition of definite concentration of counterions expresses the energy change per methylene group divided by kT .

On the other hand, the coefficient of m in case no salts added is affected by the change of electrical energy at the micelle formation, *i.e.*, by the change of the concentration of counterions. The electrical energy change at the micelle formation and the concentration of counterions are the function of the number and the kinds of polar groups concerned. Thus, the coefficient of m in case no salts added varies by the number and kind of polar groups of long-chain electrolytes.

From the experiments of added uni-univalent

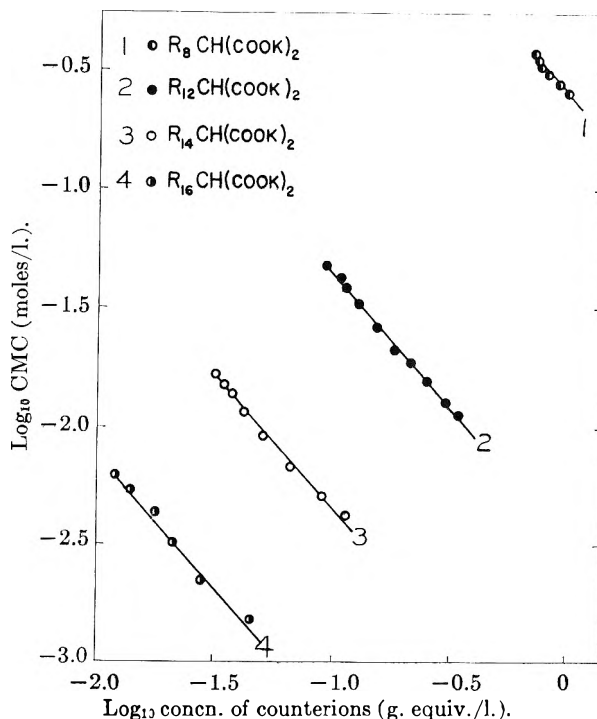


Fig. 3.—Variation of the logarithm of the CMC as functions of the logarithm of the concentration of counterions at 25°.

salts on the CMC it has been found that the plot of $\log \text{CMC}$ versus $\log C_s$ is linear in all potassium alkyl malonates and their slopes are twice as much in the case of fatty acid salts. This seemingly indicates that the micelle surfaces are quite similar in regard to spacing and charge density.³²

Acknowledgment.—The author is greatly indebted to Mr. K. Houji of Daiichi Pharmaceutical Co. Ltd. for the synthesis of a series of alkyl malonic acids.

(32) M. L. Corrin, private communication.

THE POLYMERIZATION OF SILICIC ACID

BY SIDNEY A. GREENBERG AND DAVID SINCLAIR

Johns-Manville Research Center, Manville, N. J.

Received November 20, 1954

This paper describes a light scattering study of the formation of polysilicic acid in basic media prepared by mixing very clean solutions of ammonium acetate and sodium metasilicate. The growth of the colloidal silica sols was observed by turbidity, dissymmetry and depolarization measurements. The rate of polymerization of silicic acid was followed in equivolume mixtures of 3% ammonium acetate and sodium metasilicate solutions whose concentrations varied from 0.1 to 10%. It was found that the rate increased with silicate concentration up to 1%. Above this concentration the rates were lower. Similarly, equivolume mixtures of 1% sodium silicate and 1, 3, 5 and 10% solutions of ammonium acetate showed an increase in rate with ammonium acetate concentration. Measurements of the pH of the solutions show that the reaction does not proceed above the pH of 11 and increases in rate as the pH is lowered to 8.6. Depolarization and dissymmetry measurements indicate that the particles are large isotropic spheres. Mechanisms of polymerization and aggregation are discussed.

Introduction

When acids or some salts are added to a sodium silicate solution the pH is lowered and the viscosity of the mixture increases until a gel is formed.¹

(1) For complete reviews see W. Eitel, "The Physical Chemistry of the Silicate Systems," University of Chicago Press, Chicago, Ill., 1954; J. G. Vail, "Soluble Silicates," Reinhold Publ. Corp., New York, N. Y., 1952.

During this transformation colloidal and chemical changes are occurring: (1) any monomeric silicic acid present polymerizes² to form polysilicic acid particles, (2) the colloidal polysilicic acid in the reaction mixture adds monomeric silicic acid by condensation on the surface and these polymeric particles aggregate by physical bonds and cross-

(2) C. B. Hurd, *Chem. Revs.*, **22**, 403 (1938).

linking reactions, (3) finally the colloidal sol is transformed into a gel.

In some of the earlier work³ it was not clear whether colloidal silica was present in the original solutions. More recently Alexander⁴ has studied the kinetics of the polymerization of monomeric silicic acid by freezing point depression measurements, and Richardson and Waddam⁵ have reported a study in which the amount of silicic acid remaining in the reaction mixture after a set period of time was determined by the silicomolybdate method.

In the present study the polymerization of silicic acid in dilute solutions of ammonium acetate and sodium metasilicate was followed by light scattering measurements. Sodium metasilicate was used because it has been shown^{6,7} to form molecular-ionic solutions if reasonable care is taken in the preparation. The light scattering technique offers several advantages: (1) the system can be examined *in situ*, (2) information about the size, structure and shape of the polysilicic acid particles can be obtained simultaneously from depolarization measurements and from the angular distribution of scattering, and (3) frequent measurements can be made conveniently during the course of the reaction.

Experimental

Light Scattering Measurements.—Debye⁸ derived the expression for the turbidity of dilute solutions and expressed it in this form

$$\tau = \frac{32\pi^3 \mu_0^2 (\mu - \mu_0)^2}{3\lambda^4 n} \quad (1)$$

where λ is the wave length of the incident light, μ_0 and μ are the indices of refraction of the solvent and solution, respectively, and n is the number of particles per cc.

For convenience, this equation can also be written

$$\tau = \frac{32\pi^3}{3\lambda^4} \mu_0^2 \frac{(\mu - \mu_0)^2}{\varphi} V \quad (2)$$

where V is the volume of each solute particle and $\varphi = nV$ is the volume of solute per cc. of solution. It will be shown that the equation is useful when written in this way.

When solutions of monomers polymerize, the volume of a polymer particle increases as the number of particles decreases. Therefore, the turbidity increases as the diameter or the volume of the polymer particles increases, depending upon the changes in μ and φ .

Although μ and φ may not change for some polymerizing systems,⁹ they would be expected to change during the polymerization of silicic acid. Heymann¹⁰ has reported that during the formation of a hydrogel from solutions of sodium silicate ($\text{SiO}_2/\text{Na}_2\text{O}$, 1.0/0.85) and hydrochloric acid, the volume of the system increased. This volume increase was attributed to the formation of water by condensation of Si-OH groups, and to the decrease in solvation of the silicic acid and its polymers as the Si-OH groups reacted and the surface decreased. It was, of course, assumed by Heymann that the "free" water occupied a larger volume than that water associated with the solute particles. Because of this increase in volume of the system, it would be ex-

pected that φ and μ would both decrease. Similarly, the increase of the relative volume of "free" water of refractive index lower than that of the particles causes a decrease of the refractive index μ .

Therefore, as polymerization proceeds in this system, the turbidity would be assumed to increase because of an increase in the volume of each particle and a decrease in φ , but to decrease with the lowering of μ .

The equation derived by Debye applies to small isotropic spheres whose diameter is less than $1/10$ the wave length of the incident light. For larger particles,¹¹ it is necessary to correct the measured turbidity for dissymmetry in order to obtain a corrected turbidity (τ_c) which fits this equation. The corrected turbidity may then be written

$$\tau_c \propto \frac{(\mu - \mu_0)^2}{\varphi} V \quad (3)$$

To describe completely an ideal polymerizing system, turbidity, dissymmetry and refractive index difference measurements would be necessary. With this information φ could be calculated.

In the present study, the formation of the polysilicic particles was followed by turbidity and dissymmetry¹¹ (I_{45}/I_{135}) measurements which were taken periodically. By means of the dissymmetry measurements it was possible to determine the volume (V) and diameter (D) of the particles after the shape of the sol particles had been determined from the angular distribution of scattering.¹¹ In addition, depolarization measurements were made because they have been found useful^{12,13} for determining the structure and size of colloidal sol particles.

The depolarization measurements were made using unpolarized, horizontally polarized and vertically polarized incident light. In each case both the horizontal and vertical components of the scattered light were measured. Three terms are thus obtained.

$$\rho_v = H_v/V_v \quad (1)$$

$$\rho_h = V_h/H_h \quad (2)$$

$$\rho_u = (H_v + H_h)/(V_v + V_h) = H_u/V_u \quad (3)$$

where ρ is the depolarization, H and V refer to the intensity of the horizontal component and vertical component of the scattered light, respectively, and u , v and h refer to unpolarized, vertically polarized and horizontally polarized incident light, respectively.

Solutions.—The solutions were prepared from Baker analyzed reagent, sodium metasilicate and Mallinckrodt analyzed reagent, ammonium acetate. The distilled water used in these experiments showed turbidities as low as 4×10^{-5} cm.⁻¹. Solutions were stored in polyethylene bottles.

Equipment.—Light scattering measurements were made with a Brice-Phoenix Photometer.¹⁴ This equipment was calibrated in several ways. The turbidities of a standard polystyrene (obtained from B. Zimm, General Electric Laboratories) in toluene were determined with blue (4358 Å.) and with green (5461 Å.) light and were found to be 0.00356 and 0.00143 which compares very well with the values reported in the literature.¹⁴ In addition a turbidity 0.00369 for blue light was obtained on the solution with a Beckman DU spectrophotometer^{15,16} (without special slits). Turbidity, depolarization and dissymmetry measurements of du Pont Ludox compared very well with those of Mommaerts.¹⁵ The cylindrical cell used for angular distribution studies was calibrated with the sodium salt of fluorescein after the procedure of Witnauer and Scherr.¹⁷ Blue light was used for all measurements except the depolarization determinations. For depolarization measurements green light was employed. This was done because the Polaroids transmitted 1% of the blue light which should have been absorbed.

(3) M. Prasad and S. Guruswamy, *Proc. Ind. Acad. Sci.*, **19A**, 77 (1944).

(4) G. B. Alexander, *J. Am. Chem. Soc.*, **76**, 2094 (1954); **75**, 2887 (1953).

(5) R. Richardson and J. A. Waddam, *Research*, **7**, S42 (1954).

(6) P. Debye and P. V. Nauman, *J. Chem. Phys.*, **17**, 664 (1949); *THIS JOURNAL*, **55**, 1 (1951).

(7) R. W. Harman, *ibid.*, **31**, 355 (1927); **32**, 44 (1928).

(8) P. Debye, *J. Appl. Phys.*, **15**, 338 (1944); *THIS JOURNAL*, **51**, 18 (1947).

(9) G. Oster, *J. Colloid Sci.*, **2**, 291 (1947).

(10) E. Heymann, *Trans. Faraday Soc.*, **32**, 462 (1936).

(11) P. Debye and E. W. Anacker, *THIS JOURNAL*, **55**, 644 (1951).

(12) B. H. Zimm, R. S. Stein and P. Doty, *Polymer Bull.*, **1**, 40 (1945).

(13) G. H. Jonker, "Colloid Science," Vol. I, edited by H. R. Kruyt, Elsevier Publ. Co., New York, N. Y., 1952.

(14) B. A. Brice, M. Halwer and R. J. Speiser, *J. Opt. Soc. Am.*, **40**, 268 (1950).

(15) W. F. H. M. Mommaerts, *J. Colloid Sci.*, **7**, 71 (1952).

(16) P. Doty and R. F. Steiner, *J. Chem. Phys.*, **18**, 1211 (1950).

(17) L. P. Witnauer and H. J. Scherr, *Rev. Sci. Instruments*, **23**, 1 (1952).

Approximate refractive indices were determined with a Bausch and Lomb Abbé refractometer. The pH measurements of the solutions were made with a Beckman model H-2 meter. A constant-temperature bath regulated by a Thermocap (Niagara Electron Laboratories, Andover, N. Y.) was used for the experiments carried out above 27°. Control was good to about $\pm 0.05^\circ$. The cells were removed from the bath periodically to make the light scattering measurements. Other measurements were made in a room in which the temperature was controlled at approximately 27°.

Various filters were used to clean the solutions. A Millipore filter (Lovell Chemical Company, Watertown, Mass.) was found most useful for filtering dilute basic solutions and distilled water, and a fritted-disc, Pyrex glass, ultrafine filter was convenient for cleaning acid solutions.

Electrical conductivity measurements on sodium metasilicate solutions were made at 30° with an Industrial Instruments RCB bridge. The constant of the dip type conductivity cell was 0.840.

Results

Sodium Metasilicate Solutions.—In order to establish that these solutions contained essentially no colloidal polysilicic acid, electrical conductivity and turbidity measurements were made on each of them.

The values of molar conductance ($\text{ohms}^{-1} \text{cm.}^2$) were plotted as a function of the square root of concentration (moles/l.) and a method of averages curve intercepted the conductance axis (infinite dilution) at 242. This conductivity corresponds to that of four equivalents of small ions.¹⁰

The low turbidity of the solutions and a rough calculation of the molecular weight of the solute according to the procedure of Debye and Nauman⁶ indicated that very little, if any, colloidal silica was present.

Dependence of Rate on Silicate Concentration.—Equivolumes of 0.1, 0.25, 0.5, 1, 3, 5 and 10% sodium metasilicate and 3% ammonium acetate solutions were mixed and the increase in turbidity with time was measured at approximately 27°. (The increase in pH of these solutions with silicate concentration is shown in curve 3, Fig. 4.) It may be noted in Fig. 1 that the rate of polymerization,

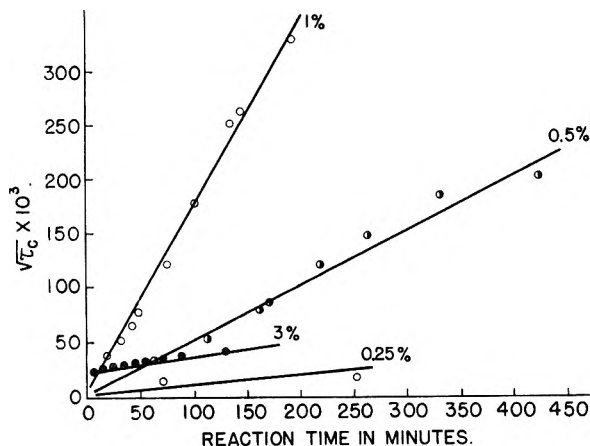


Fig. 1.—Effect of silicate concentration on reaction rate as shown by the increase in corrected turbidity (τ_c) with reaction time in equivolume mixtures of 3% ammonium acetate solutions and solutions of sodium metasilicate (% indicated on the curve).

as shown by the increase in the square root of corrected turbidity with time, increased with concentration from 0.25 to 1%, but that the mixture with

the 3% silicate solution polymerized at a slower rate. The turbidities of the mixtures with the 5 and 10% solutions of silicate did not change. At a concentration of 3% sodium silicate, the mixture shows an initial pH of 10.7. Above this concentration the pH rises in the manner shown in Fig. 4.

It should be noted that the erratic values of the turbidity obtained in the early stages of the reaction were probably influenced by dust.

Plots of the square root of corrected turbidity versus time were made because this function was approximately linear. With close temperature control during the reaction the points fell more precisely on a straight line (Fig. 3).

Dependence of Rate on Ammonium Acetate Concentration (pH).—Equivolumes of 1, 3, 5 and 10% ammonium acetate and 1% sodium metasilicate solutions at approximately 27° were mixed and turbidity measurements were made periodically. With a constant concentration of sodium metasilicate an increase in the concentration of acetate solutions decreases the pH from approximately 10.5 at 1% to 8.6 at 10% as is shown in curve 4, Fig. 4. It may be seen in Fig. 2 that the rate of polymerization increases with ammonium acetate concentration. The solution (pH 8.6) with the 10% acetate addition gelled too rapidly for turbidity measurements to be made. No experimental information was obtained on the effect of the increase in electrolyte concentration in the present study.

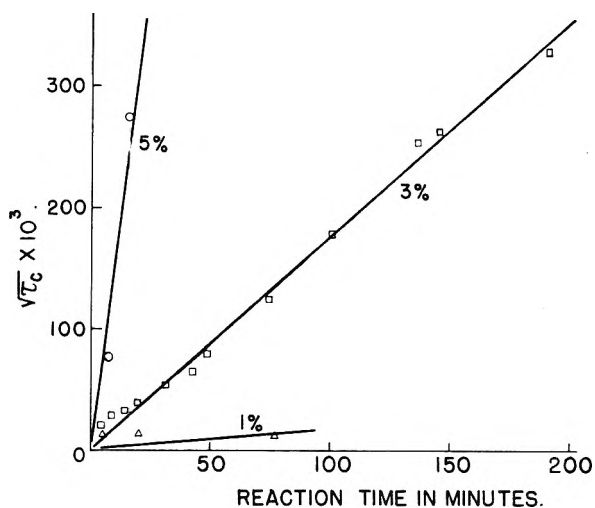


Fig. 2.—Effect of ammonium acetate concentration on reaction rate as shown by the increase in corrected turbidity (τ_c) with reaction time in equivolume mixtures of 1% sodium metasilicate and solution of ammonium acetate (% indicated on curves).

Dependence of Rate on Temperature.—The rate of turbidity change of equivolume mixtures of 1% sodium metasilicate and 3% ammonium acetate solutions was measured at 27, 30, 40 and 65°. It may be noted in Fig. 3 that the rate increases with temperature very rapidly. The points of the 30, 40 and 65° runs fell on a straight line much more closely than those of the 27° run, probably because of the closer control at the higher temperatures.

pH of the Solutions.—The pH measurements were made on various solutions in order to deter-

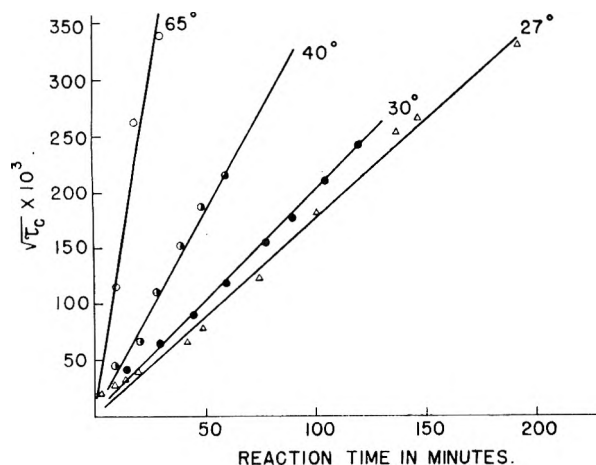


Fig. 3.—The increase in rate of polymerization with temperature as shown by the increase in corrected turbidity (τ_c) with reaction time.

mine the dependence of rate of polymerization on hydrogen ion concentration. Figure 4 shows pH as a function of the concentration of solutions of: (1) sodium metasilicate, (2) ammonium acetate, (3) mixtures of $X\%$ sodium metasilicate and 3% ammonium acetate taken initially and after polymerization had gone to completion, and (4) mixtures of $X\%$ ammonium acetate and 1% sodium metasilicate. X increases as shown on the abscissa of Fig. 4. Curves 3 show that the pH of the sodium metasilicate-ammonium acetate solutions does not change markedly during the course of the reaction.

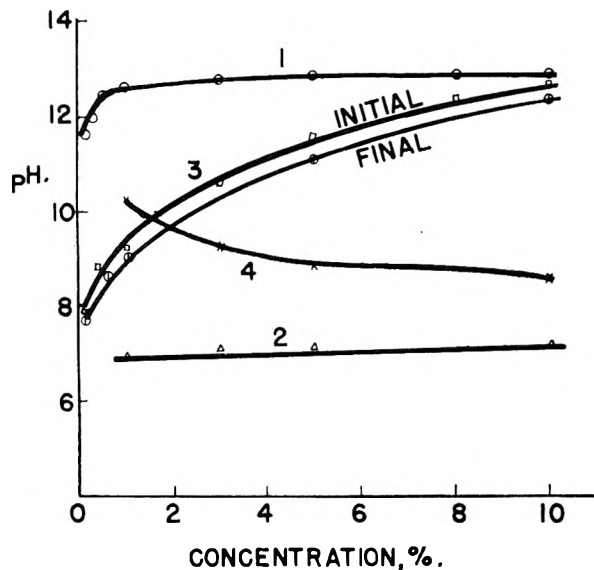


Fig. 4.—The variation of pH with concentration of solutions: 1, sodium metasilicate; 2, ammonium acetate; 3, equivolume mixtures of 3% ammonium acetate and $X\%$ sodium silicate (X increases as shown on abscissa), initial and final refer to the stages of the reaction; 4, equivolume mixtures of 1% sodium metasilicate and $X\%$ ammonium acetate.

Structure of Polysilicic Acid Sol Particles.—Both dissymmetry and depolarization measurements were used to study the structure and size of the polysilicic acid polymers.

To establish that the sol particles were spherical,

complete dissymmetry measurements were made on several suspensions. Sols formed from a mixture of 1% sodium metasilicate and 3% ammonium acetate (curve I, Fig. 5) and a mixture of 3% sodium metasilicate and 3% ammonium acetate (curve II, Fig. 5) show dissymmetry values in close agreement with those of theoretical spheres.¹¹

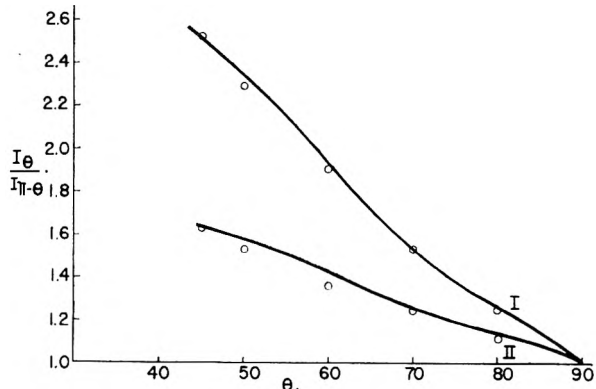


Fig. 5.—Relationship of dissymmetry ($I_\theta/I_{\pi-\theta}$) and angle θ for two sols. Circles are experimental values and curves are theoretical for spheres. Curve I, sol was prepared from an equivolume mixture of 3% ammonium acetate and 1% sodium metasilicate; curve II, sol was prepared from an equivolume mixture of 3% ammonium acetate and 3% sodium metasilicate.

In order to corroborate the conclusion that the sol particles were large isotropic spheres, the depolarization of several sols was examined just before flocculation occurred when the particle diameters were approximately 1500 \AA . Theoretically,¹² for large isotropic spheres $\rho_u = H_u/V_u$ should be greater than zero, and $\rho_h = V_h/H_h$, and $\rho_v = H_v/V_v$ should be zero. A sol prepared from 0.1% sodium metasilicate and 3% ammonium acetate which contains 0.048% silica was examined and the results were compared with those made on a 0.03% silica sol (Ludox) which contains isotropic particles approximately 200 \AA in diameter ($I_{45}/I_{135} = 1.02$). In Table I, it may be seen that the value of ρ_u is larger for the silica sol prepared from sodium metasilicate than for the Ludox sol, as would be expected because of the larger size of the particles.

TABLE I
DEPOLARIZATION OF SILICA SOLS

	0.1% Sodium metasilicate- 3% ammonium acetate (0.048% silica)	Ludox (0.03% silica)
ρ_u	0.026	0.0098
ρ_v	0	0
ρ_h	0	0

The values of ρ_u for a sol prepared from 1% sodium metasilicate and 3% ammonium acetate at 27° were determined periodically during polymerization. It was found that initially the values were relatively high (0.045) because of the influence of dust at low turbidities, but as the degree of polymerization increased, ρ_u decreased to 0.028 ($\tau_c = 0.00880$). When the size of the particle and the turbidity increased to 1500 \AA . and 0.02500, respectively, the value of ρ_u rose to 0.040.

An attempt was made to obtain dissymmetry measurements just before flocculation or gelation occurred. It may be seen in Table II that the dissymmetry of most of the sols made from equivalent volumes of solutions of ammonium acetate and sodium metasilicate in the percentages listed, was between 3.92 and 4.56, which indicates particle diameters between 1500 and 1580 Å. In the case of the 0.1% sodium metasilicate-3% ammonium acetate solution (0.048% silica) a sol was formed that had a dissymmetry of 6.77 which corresponds to a particle diameter of 1740 Å. However, because of the low turbidity (0.00070) of this solution, dust may have been a factor contributing to this large dissymmetry.

TABLE II

DISSYMMETRY BEFORE FLOCCULATION			
Sodium silicate, % (3% ammonium acetate)	τ_{max} $\times 10^{-4}$	I_{45}/I_{135}	Diam., Å.
0.10	70	6.77	1740
0.25	840	4.41	1580
0.50	2380	4.26	1540
1.0	4550	3.93	1500
3.0	5400	3.92	1500
(5% ammonium acetate)			
1.0	12800	4.56	1560

Thus both dissymmetry and depolarization measurements corroborate the conclusion that the sol particles are large isotropic spheres.

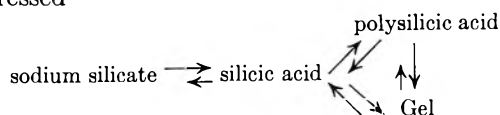
Change in Diameter of Particles with Time.—

In each of the polymerization experiments in which turbidity measurements were made, dissymmetry (I_{45}/I_{135}) values were simultaneously obtained and diameters were calculated from them. A few examples are given in Fig. 6 in which mixtures of 1% sodium metasilicate-3% ammonium acetate solutions were polymerized at 27, 30 and 40°. It may be seen that the growth of diameter with time is essentially linear during most of the reaction. Dissymmetry measurements could not be made until polymerization had progressed sufficiently for the turbidity of the polysilicic acid sol to be greater than that of the dust in the solution. If the curves are extrapolated to zero time, they would intercept the ordinate at a diameter of approximately 200 Å.

Diameter vs. Turbidity.—Plots of the log of corrected turbidity (τ_c) versus log diameter showed a relationship $\tau_c \propto D^2$ during most of the reaction and $\tau_c \propto D^3$ during the final stages. These relationships would be expected from the $\sqrt{\tau_c}$ -time and diameter-time curves shown in Figs. 1, 2, 3 and 6.

Discussion

The reactions occurring during the formation of a silica gel and the equilibria established can be expressed



Thus sodium metasilicate solutions are in equilibrium with silicic acid and its ions. The silicic acid under the proper pH conditions polymerizes to form polysilicic acid. In turn the polysilicic acid

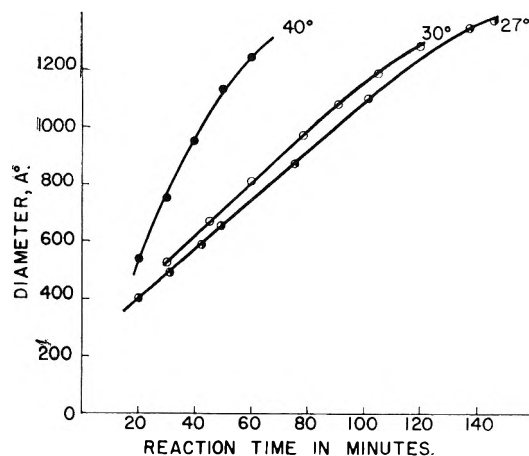
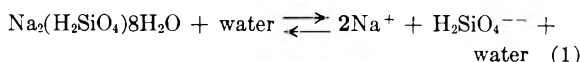


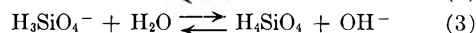
Fig. 6.—The time rate of change of the diameters of silica sol particles formed from equivalent mixtures of 1% sodium metasilicate and 3% ammonium acetate at three different temperatures.

sol transforms into a gel. It may be noted that there are equilibria between silicic acid, polysilicic acid and the gel.

Sodium Metasilicate Solutions.—It is now fairly well established that hydrated sodium metasilicate should be written $\text{Na}_2(\text{H}_2\text{SiO}_4) \cdot 8\text{H}_2\text{O}$ ^{7,18,19} and it dissociates in this way



Because of the low ionization constants of silicic acid ($K_1 = 10^{-9.8}$, $K_2 = 10^{-12.4}$)¹⁸ most of the $(\text{H}_2\text{SiO}_4)^{--}$ ions in dilute, basic (pH 8-9) solutions will hydrolyze in two steps



and the concentration of each ionic species will depend upon the pH. Calculations were made on the basis of the reported¹⁸ ionization constants of the ratios of singly ionized to un-ionized silicic acid, $(\text{H}_3\text{SiO}_4)^- / (\text{H}_2\text{SiO}_4)$. At pH 10.5 the ratio is 5/1; at pH 9.5, 1/1; at pH 9, 1.6/10; and at pH 8, 1.6/100. Obviously between pH 8 and 10.5 there is a reasonable concentration of both ions and molecules of silicic acid.

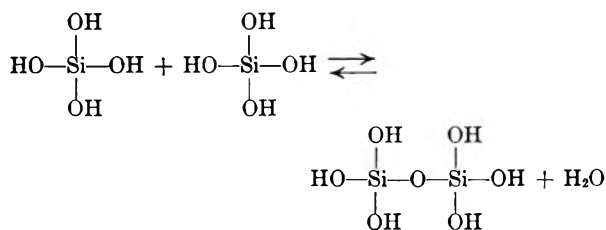
The molar conductance of 242 obtained for the sodium metasilicate solutions shows clearly that four equivalents of small ions carry the current. The four equivalents would largely consist of two Na^+ ions, and two from a mixture of H_3SiO_4^- and OH^- ions whose concentrations depend on the pH. A negligible concentration of $\text{H}_2\text{SiO}_4^{--}$ ions would be expected.

If sodium metasilicate hydrate crystals are exposed to carbon dioxide, solutions made from this material contain colloidal silicic acid.^{6,19} However, freshly opened bottles of the silicate formed clear solutions.

Polymerization of Silicic Acid.—The polymerization of silicic acid has been referred to frequently as a condensation reaction² which would proceed in this way

(18) P. S. Roller and G. Erwin, *J. Am. Chem. Soc.*, **62**, 461 (1940).

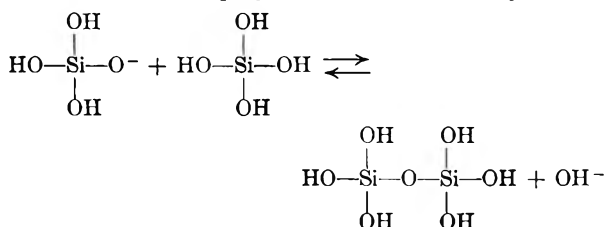
(19) E. Thilo and W. Miedreich, *Z. anorg. allgem. Chem.*, **267**, 76 (1951).



Therefore, an increase in silicate concentration would be expected to increase the rate of reaction, and this result was found in the present study and that of Richardson and Waddam.⁵ The increase in rate with temperature (Fig. 3) could also have been expected, and Hurd, *et al.*,²⁰ have reported an activation energy of 9–11 kcal./mole in acid solution and 24 kcal./mole in basic solution.

On the other hand, the effect of the *pH* on the rate of polymerization has several aspects. First, it is well known^{2,4,5} that the rate is slow in high and low *pH* solutions. Second, Richardson and Waddam⁵ found that in the *pH* range 4–10, polymerization was most rapid between *pH* 8–9. Merrill and Spencer²¹ obtained similar results for gelation reactions. In the present study the rate was a maximum at *pH* 8.6 (the lowest *pH* studied).

On the basis of the foregoing, it appears that the polymerization of silicic acid proceeds by the reaction of singly ionized silicic acid and un-ionized silicic and polysilicic acid in this way



a mechanism previously proposed by Ashley and Innes.²² This mechanism is consistent with the information known concerning the reaction.

1. No reaction takes place at high *pH* where the solutions consist mainly of silicic acid ions which would tend to repel each other and any polysilicic acid formed would be expected to depolymerize.

2. Reaction takes place slowly,⁵ if at all, at low *pH* where the concentration of un-ionized silicic acid is high. At very low *pH* the reaction may go by a different mechanism.⁴

3. The reaction does go at its maximum rate in the *pH* 8–9 range. In this range the concentration of silicic acid and the singly ionized form are both reasonably high ($(\text{H}_3\text{SiO}_4)^-/(\text{H}_4\text{SiO}_4)$ at *pH* 9 is 1.6/10, at 8 is 1.6/100).

It should also be pointed out that Grubb²³ has proposed a similar mechanism for the condensation of trimethylsilanol in basic solutions.

Interpretation of the Relationships $\tau_c \propto D^2$ or D^3 .—It was previously shown that during most of

the polymerization reaction τ_c is proportional to D^2 and during the final stages is proportional to D^3 (where D is the diameter of the sol particle). These results can be interpreted on the basis of Debye's equation ($\tau_c \propto (\mu - \mu_0)^2 V / \varphi$), and Heymann's work¹⁰ in which it was found that the volume of a polymerizing silicic acid system increases during the reaction. This increase has previously been attributed to desolvation and the formation of water by the condensation of Si-OH groups.

The relationship $\tau_c \propto D^3$ (or the volume V of the particle) can be explained easily by assuming that aggregation is occurring during the final stages of the reaction. During aggregation it would be expected that the cross-linking condensation reactions taking place and the physical attraction of the particles would cause only small changes in μ the index of refraction of the solution and φ the volume of solute per cc.^{9,24} Therefore, τ_c would be proportional to D^3 or V .

On the other hand, during most of the reaction when the volume of the system is increasing, the index of refraction of the solution will decrease²⁵ and φ will decrease. Because the experimental relationship is $\tau_c \propto D^2$ which is less than D^3 , it can be assumed that the quantity $(\mu - \mu_0)^2$ decreases faster than φ in such a manner that $(\mu - \mu_0)^2 / \varphi$ is proportional to D^{-1} .

Structure of the Polysilicic Acid Sol Particles.—

Because silicic acid is a tetrafunctional monomer, it is not readily evident why it has been reported^{1,2} previously that fibrils or fibers have been seen during the formation of silica gels. In the present study no evidence was found that particles other than spheres were formed at any time in the reaction. The evidence showed that the polysilicic acid sol particles were spherical, isotropic and amorphous.

Summary of Colloidal and Chemical Changes.—

From the experimental evidence of this study, it is concluded that when sodium metasilicate and ammonium acetate solutions in the proper proportions are mixed the following changes occur. (1) Polymerization of monomeric silicic acid occurs and goes most rapidly at *pH* 8–9, at higher temperatures and at high concentrations of silicic acid. (2) Soon after polymerization begins, particles form of approximately 200 Å. diameter in a *highly solvated state*. This is based on the finding that diameter *versus* time curves (Fig. 6) when extrapolated to zero time intercept the ordinate at approximately 200 Å. It is interesting to note that *dried* silica gel and aerogel consist of spherical particles of from 30–60 Å. in diameter.²⁶ (3) During most of the reaction, polymerization and aggregation are occurring simultaneously. (4) Finally aggregation alone predominates until a gel is formed.

Acknowledgment.—The authors wish to thank Mr. Walter Gulick for making many of the light scattering measurements and for keeping the photometer in good working order.

(20) C. B. Hurd, R. C. Pomatti, J. H. Spittle and F. J. Alois, *J. Am. Chem. Soc.*, **66**, 388 (1944).

(21) R. C. Merrill and R. W. Spencer, *This Journal*, **54**, 806 (1950).

(22) K. D. Ashley and W. B. Innes, *Ind. Eng. Chem.*, **44**, 2857 (1952).

(23) W. T. Grubb, *J. Am. Chem. Soc.*, **76**, 3408 (1954).

(24) S. A. Troelstra, Thesis, Utrecht, 1941; S. A. Troelstra and H. R. Kruyt, *Kolloid-Beihfte*, **54**, 225 (1943).

(25) G. Oster, *Chem. Revs.*, **43**, 319 (1948).

(26) I. Shapiro and I. M. Kolthoff, *J. Am. Chem. Soc.*, **72**, 776 (1950).

THE VAPOR PRESSURE OF MONOFLUOROACETIC ACID

BY JOSEPH J. JASPER AND GEORGE B. MILLER

Department of Chemistry, Wayne University, Detroit, Michigan

Received November 30, 1964

The vapor pressure of monofluoroacetic acid was studied as a function of the temperature over the range 20 to 170°. The method employed was an isotensimetric one with the use of a modified version of the Smith-Menzies apparatus in conjunction with an electronic mutual-inductance micrometer adapted for manometric use. The vapor pressures were measured in an all-glass system with the electronic manometer operating as a null-point detector. A diagram of the tensimeter is given together with two tables, one comparing the experimental and literature values of the test compound *n*-butyric acid, and the other a table of vapor pressures of monofluoroacetic acid.

In a systematic study of the effects of electronegative groups on the surface energy, when substituted on either or both ends of the acetic acid molecule, monofluoroacetic acid was chosen as the starting compound. Search of the literature, however, brought to light but little reliable information concerning this compound, therefore, it became necessary to prepare it in a pure form, and to determine from experiments as many of its properties as were required for the proposed study. The capillary-rise method was chosen as most suitable for the surface energy measurements, and since the effective density appears in the equation as an explicit variable it was necessary to determine this accurately over a considerable temperature range. The primary purpose of this investigation, therefore, was to obtain vapor pressure data of monofluoroacetic acid and to use these data to calculate the vapor densities.

Experimental

Preparation and Purification of the Compound.—The starting compound, sodium monofluoroacetate, was obtained from the Monsanto Chemical Company and purified according to instructions received from them. The monofluoroacetic acid was prepared as follows: 300 g. of the sodium salt was added to 800 ml. of water in a 3-liter erlenmeyer flask. To this was added slowly and with constant stirring, a solution containing 294 g. of sulfuric acid dissolved in 800 ml. of water. The resulting mixture was filtered and the filtrate extracted four times with 50-ml. portions of ether. The combined ether extracts were dried with anhydrous sodium sulfate and the supernatant solution decanted. The ether was distilled off leaving a transparent crystalline solid which was purified by repeated fractionations, first under partial vacuum and finally under high vacuum. The final product selected for the vapor pressure measurements solidified into colorless transparent needles of m.p. 35.3°. Swarts¹ reported a m.p. of 35.2°. The melting point was determined from a time-temperature curve with a 150-g. sample, and the observed freezing time was greater than 50% of the total cooling time. Since the monofluoroacetic acid was extremely hygroscopic, this operation, as well as all subsequent ones except the vapor pressure measurements, was carried out in an atmosphere of dry nitrogen.

Description and Operation of the Apparatus.—The static isotensimetric method was employed to measure the equilibrium vapor pressures. The isotenscope, though identical in principle to that of Smith and Menzies² was modified in a number of ways to meet the requirements of experimental convenience and high precision. The tensimeter is shown in Fig. 1. The sample flask is connected to the trap by means of a mercury cup-seal. It was necessary that the flask be removable since the tensimeter, once installed in the bath, had to be leveled and secured to the bath floor. Thus, samples of the compound could be introduced or removed without the necessity of disturbing the rest of the apparatus. The tensimeter trap consisted of two arms 44 mm. in diameter connected through a capillary tube, the latter of which served both to dampen oscillations caused

by mercury surging from one arm to the other, and as a means of communication to the mercury reservoir. Each arm had sealed into it a glass probe tube with an open top and a flat-sealed bottom. Within each of these tubes there was inserted an induction coil, the secondary of which was sensitive to the distance between it and the mercury surface in the tensimeter arms below it. The direction of mercury flow in the arms was determined by the pressure differential between the tensimeter and the space above the mercury surface in the reservoir. The pressure in the reservoir was controlled by a valve which opened either to the atmosphere or to the vacuum pump.

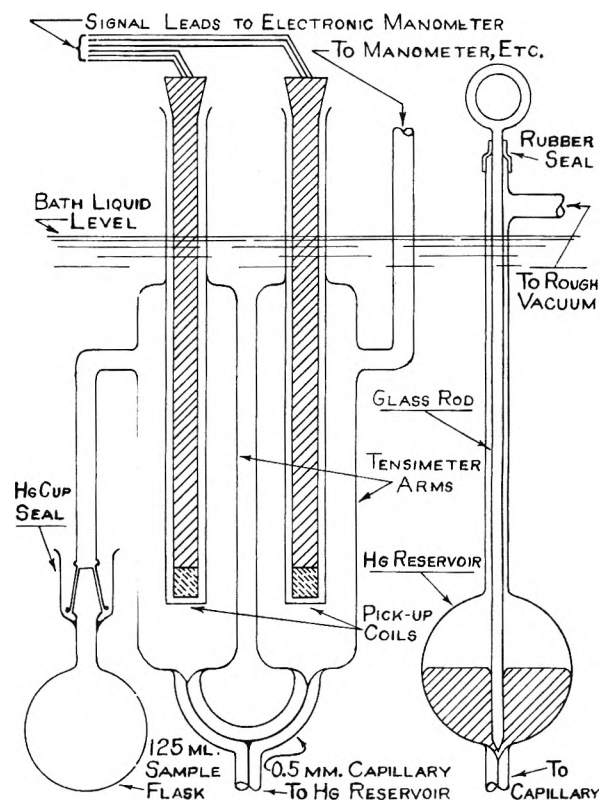


Fig. 1.—The tensimeter.

In this investigation the temperature range employed necessitated the use of a mineral oil as a bath medium. In order to obtain close temperature control a large volume (30 gallons) of oil was used. Temperature measurements were made with a NBS certified Leeds and Northrup resistance thermometer used in conjunction with a NBS certified Leeds and Northrup G-2 Mueller bridge. The galvanometer used in the bridge circuit was a HS ballistic type with shielded leads.

The method of detection involved a modification of the mutual-inductance micrometer originally employed in pressure measurements at the National Bureau of Standards.³

(3) W. E. Williams, Jr., *J. Research Natl. Bur. Standards*, **48**, 54 (1952). The authors acknowledge with gratitude the helpful advice of Dr. Williams, who, in several private communications, volunteered much information concerning construction and operation of the electronic manometer.

(1) F. Swarts, *J. chim. phys.*, **17**, 23 (1919).(2) A. Smith and A. W. C. Menzies, *J. Am. Chem. Soc.*, **32**, 1412 (1910).

With this electronic manometer it was possible to measure the column-height differentials in the tensimeter arms with great precision. The induction coils inserted in the probe tubes of the tensimeter arms served to determine the balance point. This was accomplished from the fact that the output of the secondary coil is not only a function of the input to the primary but also a function of the proximity of any closed loop or conducting surface. The output of the secondary is in direct proportion to the distance between it and the conducting surface at constant primary input. Furthermore, the secondary output is independent of the dielectric constant of any medium between the coil face and the conducting surface. Thus, if two matched coils are used, one in each arm of the tensimeter, and if the input to both primaries is equal, it follows that the mercury surfaces will be at equal distances from their respective secondary-coil faces when the outputs of the secondaries are equal. The most accurate method for determining the equality of such outputs is to oppose them so that they will just cancel each other out. The null-point was indicated by the galvanometer. The electronic manometer, therefore, operated as a null device. When the temperature of the system became constant the balancing pressure was adjusted until the galvanometer indicated zero pressure differential between the two arms of the tensimeter. The balancing pressure was then measured on a closed-end mercury manometer with a long-scale cathetometer. Although the sensitivity of the manometer was very great, the final accuracy of the measurements was dependent upon the readings made with the cathetometer.

Procedure.—The initial procedure was to test the apparatus and *n*-butyric acid was chosen as the test compound since it boils at a temperature very close to that of monofluoroacetic acid. The test samples were obtained by repeated vacuum fractionations of the purest acid obtainable from the Eastman Kodak Company. The final product had a refractive index of 1.3954 at 24.8°. Dreisbach and Martin⁴ report the value of 1.3959 at this temperature. The difference between these values was believed to be due to traces of water. The apparatus test procedure was carried out in exactly the same manner as the subsequent vapor pressure measurements of monofluoroacetic acid. A 50-ml. sample of the compound was transferred in an atmosphere of dry nitrogen to the sample flask of the tensimeter. The flask and contents were attached to the tensimeter and the entire system evacuated for eight hours to about 0.2 μ . After the evacuation, the line was isolated from the pumps and mercury introduced into the tensimeter arms from the reservoir. When thermal equilibrium was reached the electronic manometer was put into operation. The mercury was adjusted to a predetermined level and the pressure of the balancing line adjusted to zero galvanometer reading. The temperature of the bath was then determined and the balancing pressure measured on the line manometer with the cathetometer. The individual readings were taken on each arm four times, giving a total of eight sets of ten readings of the mercury heights. The average difference was recorded as the observed pressure.

Results

Treatment of the data from the test compound involved three corrections, namely, (a) zero correc-

tion of the mercury column of the line manometer, (b) correction for the vapor pressure of the mercury, and (c) correction for the traces of water in the test sample. The correction for the latter was calculated on the assumption that the extremely dilute solution of water in the *n*-butyric acid deviated but slightly from Raoult's law. The literature values⁵ and those obtained by us are given from 20 to 150° in Table I. The close agreement indicates that a high degree of confidence can be placed in the apparatus and method, and also in the vapor pressures of the monofluoroacetic acid which involved no corrections for moisture. The most probable values of the vapor pressure of monofluoroacetic acid are shown in Table II.

TABLE I
COMPARISON OF CALCULATED AND LITERATURE VAPOR PRESSURES OF *n*-BUTYRIC ACID

Temp., °C.	Vapor pressure, mm.		Temp., °C.	Vapor pressure, mm.	
	Calcd.	Lit.		Calcd.	Lit.
20	0.77	0.76	90	45.30	46.60
30	1.60	1.50	100	73.80	73.80
40	3.00	3.00	110	112.40	114.00
50	5.50	5.40	120	166.70	171.30
60	9.80	9.80	130	247.00	251.60
70	16.80	17.00	140	357.20	361.40
80	28.00	28.60	150	509.10	508.50

TABLE II
MOST PROBABLE VALUES OF THE VAPOR PRESSURES OF MONOFLUOROACETIC ACID

Temp., °C.	Vapor pressure, mm.	Temp., °C.	Vapor pressure, mm.
20	4.00	100	55.68
25	4.10	105	69.60
30	4.20	110	86.51
35	4.30	115	106.9
40	4.39	120	131.5
45	4.49	125	160.8
50	4.59	130	195.7
55	5.49	135	237.1
60	7.32	140	285.7
65	9.69	145	343.1
70	12.71	150	409.8
75	16.55	155	487.7
80	21.38	160	587.2
85	27.44	165	682.5
90	34.96	168.29	760.0
95	44.26	170	903.1

(4) In J. Timmermanns, "Physico-Chemical Constants of Pure Organic Compounds," Elsevier Publications, New York, N. Y., 1950.

(5) "International Critical Tables," Vol. III, McGraw-Hill Book Co., New York, N. Y., 1926, p. 219.

THERMAL DIFFUSION AND MOLECULAR MOTION IN LIQUIDS¹

BY E. L. DOUGHERTY, JR., AND H. G. DRICKAMER

*Department of Chemistry and Chemical Engineering, University of Illinois, Urbana, Illinois**Received December 2, 1954*

A theory for thermal diffusion in liquids has been developed which permits the prediction of the separation using only molecular weights, molar volumes, activation energies for viscous flow, and excess thermodynamic properties. Measurements have been made on a series of binary mixtures of isomers with CS₂ at atmospheric pressure. These results and previously published results at high pressure are compared with the theory. There is excellent qualitative agreement, and in many cases the agreement is essentially quantitative.

In a series of recent publications²⁻⁶ we have presented data on liquid phase thermal diffusion both at atmospheric pressure and under pressures to 10,000 atmospheres, and outlined a fairly satisfactory theory qualitatively consistent with our results. In this paper we present a revised theory, utilizing a sounder basis, which gives considerably more accurate results and which permits prediction of thermal diffusion separations from viscosity data and thermodynamic data on the solutions. The theory is compared with our earlier results and with new results obtained for a series of binary mixtures of isomeric compounds with carbon disulfide.

For a binary mixture the thermal diffusion ratio α is defined by the equation

$$\vec{J}_1 = -\rho D [\text{grad} X_1 + \alpha X_1(1 - X_1) \frac{1}{T} \text{grad} T] \quad (1)$$

where

- J_1 = flux of component 1
 D = diffusion coefficient
 ρ = density
 X_1 = mole fraction of component 1
 T = absolute temperature

The solution of equation 1 for the steady state is

$$\ln \left(\frac{X_1}{1 - X_1} \right)_H \left(\frac{1 - X_1}{X_1} \right)_C = \alpha \ln \frac{T_H}{T_C} \quad (2)$$

where the subscripts H and C refer to hot and cold chambers of a single stage cell. One can see that the sign of α is arbitrary. The convention used in this work is discussed below.

The starting point for the revised theory, as for our earlier work, is the thermodynamics of irreversible processes^{7,8} which gives for the thermal diffusion ratio

$$\alpha = \frac{M_1 Q_2^* - M_2 Q_1^*}{\bar{M} X_1 \frac{\partial \mu_1}{\partial X_1}} \quad (3)$$

where

- M_i = molecular weight of component i
 $\bar{M} = M_1 X_1 + M_2 X_2$

(1) This work was supported in part by the A.E.C.

(2) (a) W. M. Rutherford and H. G. Drickamer, *J. Chem. Phys.*, **22**, 1157 (1954); (b) R. L. Saxton, E. L. Dougherty, Jr., and H. G. Drickamer, *ibid.*, **22**, 1166 (1954).

(3) W. M. Rutherford and H. G. Drickamer, *ibid.*, **22**, 1284 (1954).

(4) R. L. Saxton and H. G. Drickamer, *ibid.*, **22**, 1287 (1954).

(5) W. M. Rutherford, E. L. Dougherty, Jr., and H. G. Drickamer, *ibid.*, **22**, 1289 (1954).

(6) E. L. Dougherty, Jr., and H. G. Drickamer, *ibid.*, accepted for publication.

(7) J. Prigogine, "Etude Thermo. de Processes Irrev.," Dumond, Paris, 1947.

(8) S. R. deGroot, "Thermodynamics of Irreversible Processes," Interscience Publishers, New York, N. Y., 1950.

- μ_i = chemical potential of component i
 Q_i = the heat of transport of component i , the net heat crossing a boundary with one mole of component i in the absence of a temperature gradient

In our earlier work we used an equation, used also by other authors,^{9,10} of the form

$$\alpha = \frac{Q_2^* - Q_1^*}{X_1 \frac{\partial \mu_1}{\partial X_1}} \quad (3')$$

This latter equation is derived under the assumption that the center of mass of the system is stationary. Since, in the actual experiments, the velocity of the center of mass is very small, the numerical difference between the results obtained from (3') and (3) is negligible. Nevertheless (3) will be used in this work as it is more nearly correct. This fundamental point was first made by Prigogine.⁷

Our initial formulation for the heat of transport will be similar, but not identical with our previous work^{2,6} and that of Denbigh.¹¹

Consider a large volume of the mixture and in particular consider a region within the mixture with fixed bounding surfaces (these are mathematical, not physical). Assume that the entire volume is in equilibrium with a thermostat thereby assuring the absence of a temperature difference between the region and the remainder of the fluid. Assume that a molecule of component 1 diffuses out of the region.

Let W_{H_1} be the energy which must be supplied to move one mole of component one across a boundary in a liquid. W_{H_1} is the energy transported when a molecule moves from one equilibrium position to the next. In general the hole left by the molecule of type 1 will be filled from across the boundary of the region. If the molecules are distributed randomly, it will be filled by either a type one or type two molecule with the relative probability X_1/X_2 . The energy transported in this process will be

$$W_L = X_1 W_{H_1} + X_2 W_{H_2} \quad (4)$$

The net energy transported will be

$$W_{H_1} - W_L = (1 - X_1)(W_{H_1} - W_{H_2}) \quad (5)$$

provided there is a one for one exchange, *i.e.*, if all molecules are the same size. However, in the process described above there has been a net transport out of the region of only $(1 - X_1)$ moles of component one. The heat of transport for com-

(9) K. G. Denbigh, "Thermodynamics of the Steady State," John Wiley and Sons, New York, N. Y., 1951.

(10) S. R. deGroot, "L'Effet Soret," North Holland Publishing Co., Amsterdam, Netherlands, 1945.

(11) K. G. Denbigh, *Trans. Faraday Soc.*, **48**, 1 (1952).

ponent one, which involves the net transport of one mole of this component will then be

$$Q_1^* = \frac{W_{H_1} - W_L}{1 - X_1} = W_{H_1} - W_{H_2} \quad (6)$$

Similarly

$$Q_2^* = W_{H_2} - W_{H_1} \quad (7)$$

Equation 3 then gives for α

$$\alpha = \frac{M_1 + M_2 (W_{H_2} - W_{H_1})}{\bar{M} X_1 \frac{\partial \mu_1}{\partial X_1}} \quad (8)$$

Now if molecules of type one and type two are not the same size, on the average ψ_1 molecules will enter a hole left by a type one molecule and ψ_2 molecules will enter a hole left by a type two molecule. Then

$$Q_1^* = \frac{W_{H_1} - \psi_1 W_L}{1 - \psi_1 X_1} \quad (9)$$

$$Q_2^* = \frac{W_{H_2} - \psi_2 W_L}{1 - \psi_2 X_2} \quad (10)$$

Now, assuming the volume of the considered region to remain constant, it follows (equating volume of leaving and entering molecules) that

$$\psi_1 = \frac{\bar{V}_1}{X_1 \bar{V}_1 + X_2 \bar{V}_2}$$

where V_i is the partial molal volume of component i . Then equations 9 and 10 become

$$Q_1^* = W_{H_1} - \frac{\bar{V}_1}{\bar{V}_2} W_{H_2} \quad (11)$$

$$Q_2^* = W_{H_2} - \frac{\bar{V}_2}{\bar{V}_1} W_{H_1} \quad (12)$$

and the expression for α becomes

$$\alpha = \frac{M_2 \bar{V}_1 + M_1 \bar{V}_2}{\bar{M} X_1} \left[\frac{\partial M_1}{\partial X_1} \left(\frac{W_{H_2}}{\bar{V}_2} - \frac{W_{H_1}}{\bar{V}_1} \right) \right] \quad (13)$$

It remains then to obtain a satisfactory expression for W_{H_i} in terms of measurable molecular properties. In previous work we considered it to be a fraction of the "cohesive energy" of the liquid, and evaluated this latter quantity from the energy of vaporization.

Further consideration, however, indicates that it should be much more closely related to the energy of activation for molecular motion. The energy of activation is the energy supplied to move the molecule from an equilibrium position to the activated state. No further energy need be supplied for the molecule to move to the next equilibrium position.

For the systems under study here the activation energy for motion can most conveniently be evaluated from viscosity measurements. According to Eyring¹²

$$\eta = \frac{Nh}{V} \exp \left[\frac{\Delta F^\ddagger}{RT} \right] \quad (11)$$

Then

$$R \left[\frac{\partial \ln(\eta V)}{\partial \frac{1}{T}} \right]_p = \Delta H^\ddagger = \Delta V^\ddagger + p\Delta V^\ddagger \quad (12)$$

(12) S. Glasstone, K. J. Laidler and H. Eyring, "Theory of Rate Processes," McGraw-Hill Book Co., New York, N. Y., 1941.

where

$$\left(\frac{\partial \ln(\eta V)}{\partial p} \right)_T = \frac{\Delta V^\ddagger}{RT} \quad (13)$$

At atmospheric pressure $p\Delta V^\ddagger$ is negligible and $\Delta H^\ddagger \cong \Delta U^\ddagger$. This is not true at high pressure. At present it is not possible to analyze the activation energy in terms of fundamental molecular properties, or to say unequivocally what portion must be supplied to the molecule and what portion to the surroundings. Nevertheless certain facts can be pointed out. Bondi¹³ made important contributions in this field, and much of the following discussion is based on his work.

It is not difficult to show that

$$\left(\frac{\partial \ln \eta}{\partial 1/T} \right)_v = \Delta H_i^\ddagger = \Delta H^\ddagger - T \left(\frac{\partial p}{\partial T} \right)_v \Delta V^\ddagger \quad (14)$$

$$= \Delta U^\ddagger - \left(\frac{\partial E}{\partial V} \right)_T \Delta V^\ddagger \quad (14')$$

The term $[T(\partial p/\partial T)_v \Delta V^\ddagger]$ is ΔH_h^\ddagger in Bondi's nomenclature. This is clearly the work to create the volume ΔV^\ddagger against the thermal pressure of the liquid. Bondi has shown that for many liquids

$$\frac{\Delta H_h^\ddagger}{\Delta E^v} = \frac{\Delta V^\ddagger}{V} \quad (15)$$

ΔE^v = energy of vaporization

The range of validity of this relationship can be shown as follows. For a van der Waals liquid

$$\frac{\partial E}{\partial V} = \frac{a}{V^2} \quad (16)$$

$$E = -a/V \quad (17)$$

Hildebrand¹⁴ has proposed as a generalization of this expression for liquids, $E = -a/V^n$. Then, at atmospheric pressure

$$T \left(\frac{\partial p}{\partial T} \right)_v \cong \frac{na}{V^{n+1}} = \frac{-nE}{V} \cong n \frac{\Delta E^v}{V} \quad (18)$$

Then

$$\Delta H_h^\ddagger = T \left(\frac{\partial p}{\partial T} \right)_v \Delta V^\ddagger = n \frac{\Delta E^v}{V} \Delta V^\ddagger \quad (19)$$

Then equation 15 follows whenever $n = 1$, *i.e.*, for van der Waals liquids. Hildebrand has shown that $n \cong 1$ for many simple non-hydrogen bonding liquids.

It is not so clear whether this energy is supplied uniformly around the moving molecule or at a particular point to create a hole. Bondi showed that it was approximately the change in potential energy (calculated from a Lennard-Jones potential) between a molecule and its neighbors when the intermolecular distance is increased from $V^{1/3}$ to $(V + \Delta V^\ddagger)^{1/3}$. This would indicate it is supplied around the moving molecule more or less uniformly. The activation volume is not the volume of an equilibrium site as it is only $1/5$ to $1/10$ of the molar volume. At low pressures the internal pressure is 3000–5000 atmospheres and ΔH_h^\ddagger amounts to 80–90% of ΔU^\ddagger . Thus at atmospheric pressure ΔH_i^\ddagger amounts to only 10–20% of ΔU^\ddagger . $\partial E/\partial V$ decreases with increasing pressure and becomes negative for many organic liquids at

(13) A. Bondi, *J. Chem. Phys.*, **14**, 590 (1946).

(14) J. H. Hildebrand and R. L. Scott, "Solubility of Non-Electrolytes," Reinhold Publ. Corp., New York, N. Y., p. 97.

7000–9000 atmospheres. Thus at high pressure ΔH_j^\ddagger is equal to or larger than ΔU^\ddagger . Values of ΔH_j^\ddagger evaluated from Bridgman's¹⁵ data for several compounds are plotted as a function of pressure in Fig. 1. It can be seen that ΔH_j^\ddagger increases by an order of magnitude in 10,000 atmospheres. It is unlikely then that it is merely the energy to break cohesive bonds. It is probably associated in part with the necessity for assuming a favorable configuration for motion by rotation or otherwise, and its large increase with pressure is probably caused by a decrease in free volume making the realization of any given configuration more difficult. This viewpoint is quite similar to that adopted by Bondi.

A precise understanding of the nature of the activation energy is most important. Experiments are being undertaken in this Laboratory which, we hope, will help clarify our understanding. In the absence of a detailed picture we shall assume that one-half the activation energy is removed by the molecule and one-half is dissipated among the molecules at the old equilibrium site. This gives good agreement with our experiments and is as justifiable as any other assumption at present. Then

$$W_{B_1} = \frac{1}{2} \Delta \bar{U}_1^\ddagger \quad (20)$$

In principle $\Delta \bar{U}_1^\ddagger$ is the partial molal activation energy where

$$\Delta \bar{U}^\ddagger_{\text{mixture}} = X_1 \Delta \bar{U}_1^\ddagger + X_2 \Delta \bar{U}_2^\ddagger \quad (21)$$

Since viscosity data were not available for the mixtures we assume here that

$$\Delta \bar{U}_i^\ddagger = (\Delta U^\ddagger_{\text{pure component } i}) \quad (22)$$

Then equation 13 becomes

$$\alpha = \frac{M_1 \bar{V}_2 + M_2 \bar{V}_1}{2M} \left[\frac{\Delta U_2^\ddagger}{V_2} - \frac{\Delta U_1^\ddagger}{V_1} \right] \frac{1}{X_1 \frac{\partial \mu_1}{\partial X_1}} \quad (23)$$

indicating the "activation energy density" to be the controlling quantity in thermal diffusion.¹⁶

Now

$$X_1 \frac{\partial \mu_1}{\partial X_1} = RT + X_1 \frac{\partial U_{el}}{\partial X_1} + X_1 p \frac{\partial \bar{V}_{el}}{\partial X_1} - X_1 T \frac{\partial S_{el}}{\partial X_1} \quad (24)$$

Unfortunately, the excess thermodynamic properties are not known for the mixtures studied here and present methods for predicting them are scarcely quantitative, and totally unsatisfactory for the derivatives.

In this work we shall take $X_1(\partial \mu_1 / \partial X_1) = RT$, its ideal solution value. This should be fairly satisfactory for the mixtures considered here. It would fail totally near the critical solution temperature where $X(\partial \mu / \partial X)$ approaches zero.

(15) P. W. Bridgman, *Proc. Am. Acad. Arts Sci.*, **49**, 1 (1913): 61, 57 (1926); **66**, 185 (1931).

(16) A development leading to rather similar results can be given from a purely kinetic viewpoint^{17,18} but it appears to us that the treatment of molecules of different size and shape arises less naturally in the kinetic picture than it does above.

(17) K. Wirtz and J. W. Hiby, *Physik. Z.*, **44**, 221, 369 (1943).

(18) I. Prigogine, R. Amand and L. deBrookere, *Physica*, **16**, 577, 851 (1950).

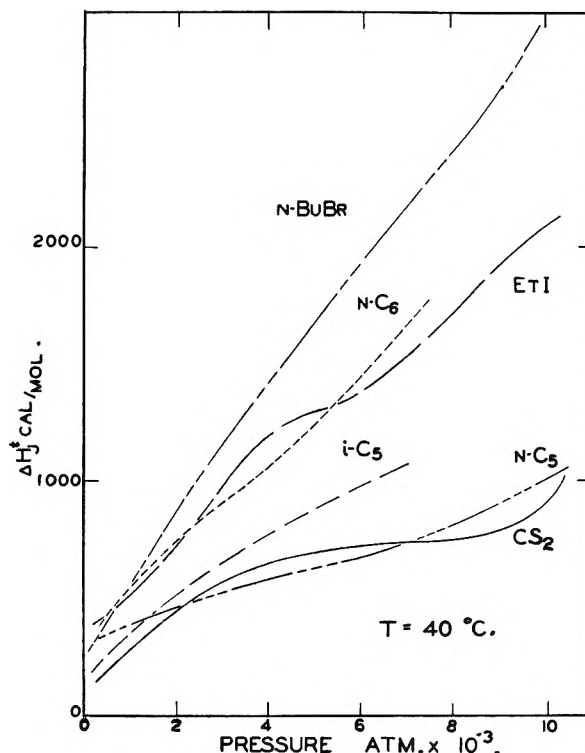


Fig. 1.—The energy of motion, ΔH_j^\ddagger , vs. pressure for some normal liquids.

An investigation of thermal diffusion in binary mixtures where the excess thermodynamics quantities are known is being undertaken along with viscosity measurements on both pure components and mixtures. This will provide a still more quantitative test of the theory.

The new experiments reported (Table I) here were performed on cells very nearly identical to those described previously.^{2b} Each point was run several times and on two or more cells as before. The calibrating mixture used was 50 mole per cent. *n*-heptane–50 mole per cent. *n*-propyl iodide. Considerable further work in a variety of two chamber cells as well as an open column apparatus indicate that the most reliable value of α for this system lies in the range 2.25–2.40. The value of 2.30 was used here rather than the value 2.00 utilized in previous work. All data reported here for the first time and also all previously published data discussed in this paper are corrected to this figure.

Parenthetically, it should be pointed out here that a limitation on the usefulness of these cells has been discovered. As the viscosity of the liquid mixture increases beyond two centipoises the two chambered cell of our design tends to give low results. Above about 4 centipoises the values from the two chamber cell may be 50% or more below values obtained on an open column of liquid.

In comparing theory with experiment, it should be kept in mind that three approximations have been made which are not inherent in the theory but are necessitated by the lack of various thermodynamic and viscosity data.

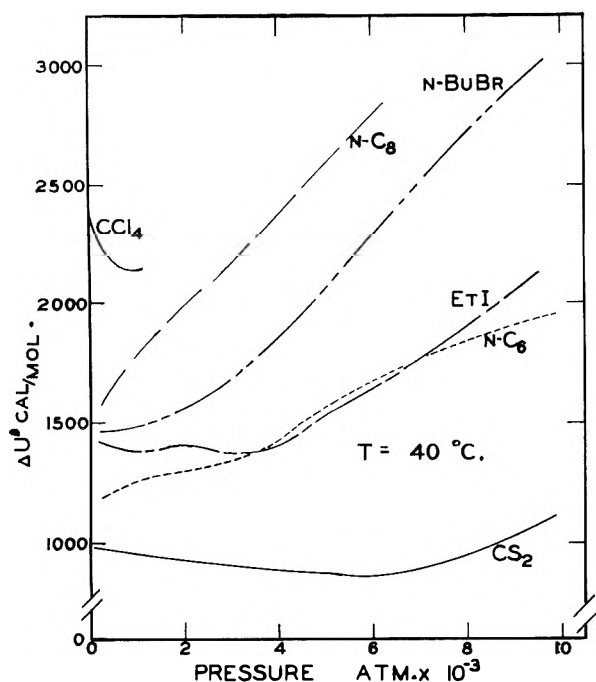


Fig. 2.—Effect of pressure on the energy of activation.

(1) The volumes of the pure components have been used instead of partial molar volumes. The effect of this is not large (see Fig. 10).

TABLE I

EXPERIMENTAL AND CALCULATED RESULTS FOR ISOMERIC SYSTEMS

Isomer	X_{CS_2}	Temp., °C.	$\alpha_{exp.}$	$\alpha_{calc.}$
<i>o</i> -Xylene	0.2	7	0.0	-0.32
	.5	8.5	-.19	-.35
	.8	8	-.38	-.39
<i>m</i> -Xylene	.2	9	.0	+.17
	.5	6	+.14	+.19
	.8	8	-.06	+.21
<i>p</i> -Xylene	.35	7	+.14	+.16
	.5	7.5	+.16	+.17
	.8	6	+.21	+.19
Ethylbenzene	.2	9	+.12	+.11
	.5	9.5	+.12	+.12
	.8	8.5	+.08	+.13
<i>cis</i> -Dichloroethylene	.2	8	-.51	-.29
	.5	8	-.41	-.31
	.8	7	-.31	-.33
<i>trans</i> -Dichloroethylene	.2	8	-.26	-.22
	.5	7	-.15	-.24
	.8	8.5	-.18	-.26
1,1-Dichloroethane	.2	7	-.75	-.33
	.5	6	-.84	-.36
	.8	5.5	-.66	-.39
1,2-Dichloroethane	.2	6	-1.35	-1.30
	.5	6	-1.75	-1.40
	.8	6	-0.96	-1.52
<i>n</i> -Hexane	.5	5	+1.13	+1.07
	.8	6	+1.16	+1.10
2-Methylpentane	.5	6	+0.90	+1.10
	.8	7	+1.09	+1.15
3-Methylpentane	.5	6	+.82	+1.03
	.8	6	+.87	+1.07
2,3-Dimethylbutane	.5	6	+.49	+0.80
	.8	6	+.48	+.83

2,2-Dimethylbutane	.5	6	+.34	+.62
	.8	6	+.21	+.65
<i>n</i> -Butyl chloride	.2	9	+.07	+.24
	.5	6	+.11	+.25
	.8	8	+.20	.27
<i>sec</i> -Butyl chloride	.2	6.5	+.00	+.17
	.5	6	+.02	+.18
	.8	9.5	+.11	+.20
Isobutyl chloride	.2	8	-.13	+.10
	.5	7.5	-.13	+.11
	.8	8	-.14	+.12
<i>t</i> -Butyl chloride	.2	7	-.58	-.40
	.5	6.5	-.60	-.42
	.8	9	-.96	-.45
<i>n</i> -Butyl alcohol	.5	7	.0	-4.24
<i>sec</i> -Butyl alcohol	.5	7	-1.11	-7.04
Isobutyl alcohol	.5	9	-0.83	-5.83

(2) $X(\partial\mu/\partial X)$ has been assumed equal to RT . The molar volumes of the pairs are seldom equal and for many systems a significant heat of mixing would be predicted by the Scatchard-Hildebrand theory. In general, for the systems studied here the effect should not be larger than 20-30%. The use of the Scatchard-Hildebrand theory to predict $X(\partial\mu/\partial X)$, as was done in previous papers, was considered. However, the theory, although reasonably satisfactory for μ gives values for $X(\partial\mu/\partial X)$ which deviate widely from experiment and it was thought best to test the denominator of eq. 23 in a later paper with measured values of the thermodynamic parameters.

(3) The activation energies of the pure components were used, rather than activation energies for the components in the solution. It is not at present possible to estimate the error of this approximation.

High Pressure Data.—The activation energies as evaluated from Bridgman's data are shown in Fig. 2. The theory and experiment are compared in Figs. 3-7. The experimental results were previously presented.² In all cases, the systems consisted of binary mixtures with CS_2 , and the con-

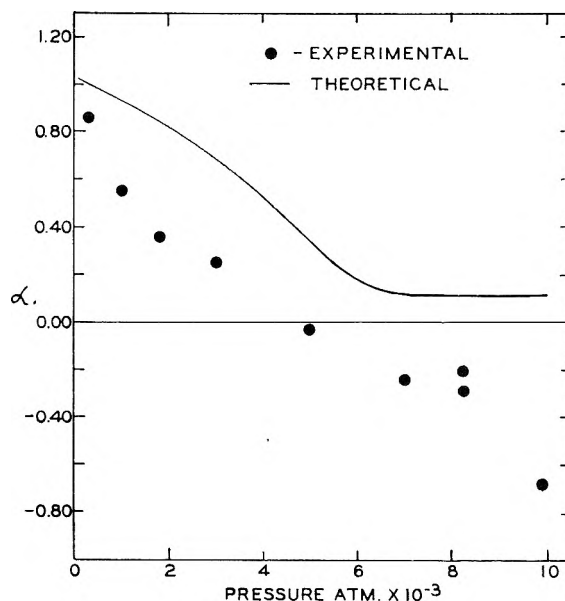


Fig. 3.— α vs. P for $n-C_6H_{14}-CS_2$ (80% CS_2 , 40°).

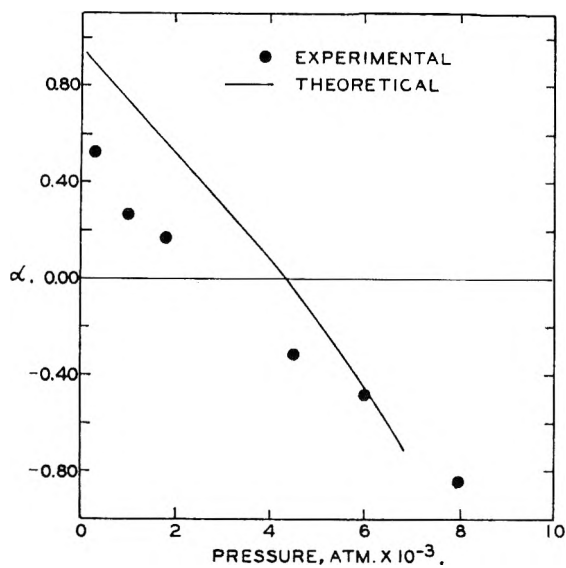


Fig. 4.— α vs. P for $n\text{-C}_8\text{H}_{18}\text{-CS}_2$ (80% CS_2 , 40°).

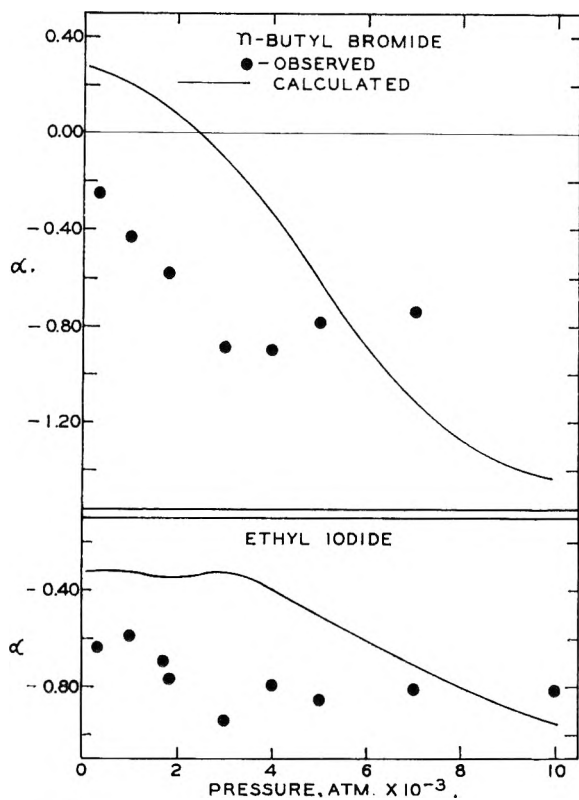


Fig. 5.— α vs. P for n -butyl bromide and ethyl iodide in CS_2 (50% CS_2 , 40°).

vention used was that a positive α denotes that CS_2 went to the cold wall. In general the trends are predicted correctly. It is felt that the high pressure thermal diffusion data for CS_2 - n -butyl bromide may be in error, possibly due to the high viscosity. Besides the general agreement, the following items are worthy of note: (1) a sign change is predicted and observed for the system n -octane- CS_2 at intermediate pressures (Fig. 4); (2) a small pressure effect is predicted and observed for the system ethyl iodide- CS_2 (Fig. 5); (3) theory gives a very nearly quantitative estimate

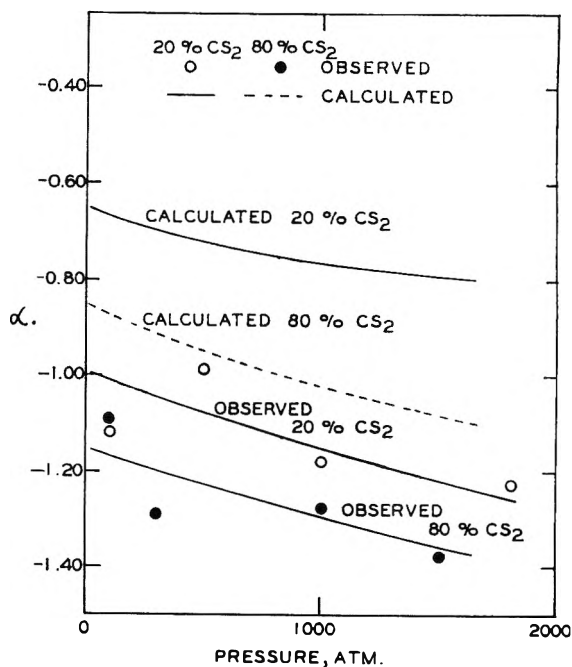


Fig. 6.—Effect of concentration on α for $\text{CS}_2\text{-CCl}_4$ (40°).

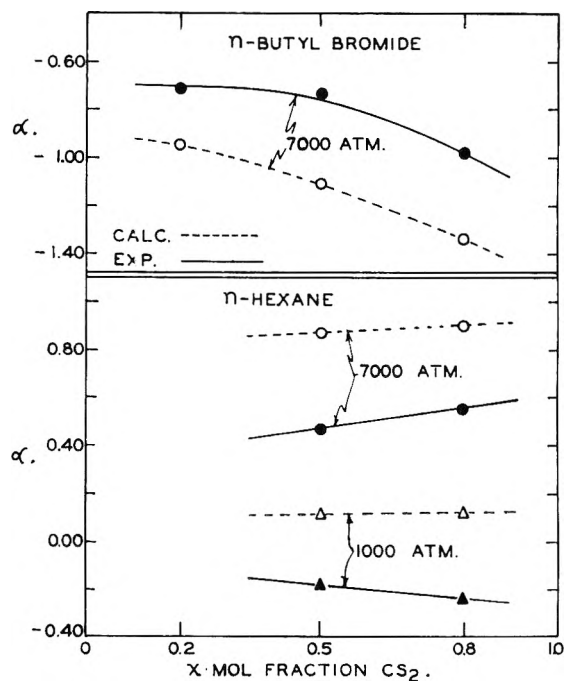


Fig. 7.—Effect of concentration on α for n -butyl bromide and n -hexane in CS_2 (40°).

of the effect of both composition and pressure on α for $\text{CCl}_4\text{-CS}_2$ (Fig. 6); (4) the theory gives an excellent prediction of the effect of concentration for n -butyl bromide- CS_2 and a satisfactory prediction for n -hexane- CS_2 (Fig. 7).

Isomeric Data.—These studies consisted of a series of isomeric sets measured against CS_2 . The activation energies and molar volumes used are shown in Table II, together with the sources of viscosity data. Where data were not available for a complete isomeric set, they were run in this Laboratory, using a Cannon-Fenske viscometer,

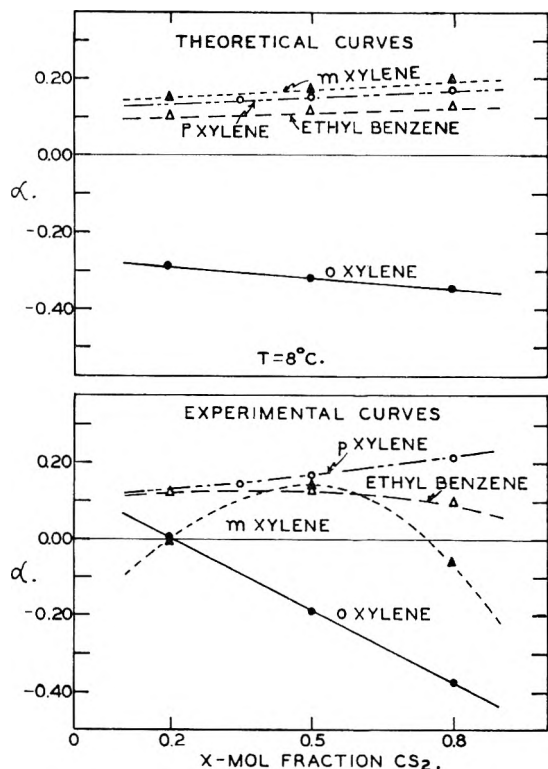


Fig. 8.—Comparison of theoretical and experimental values of α : xylene isomers.

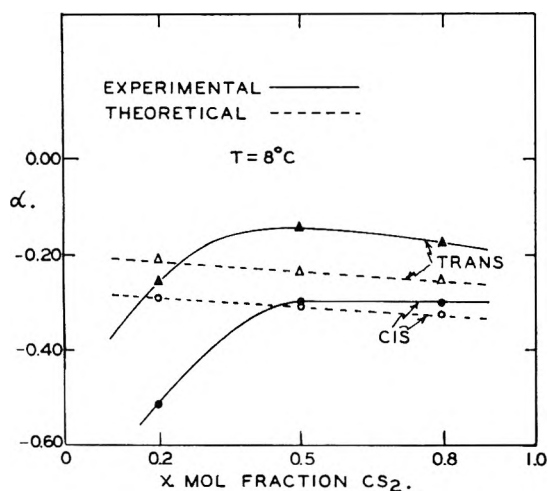


Fig. 9.—Comparison of theoretical and experimental values of α : dichloroethylene isomers.

and a bath controlled to 0.01° . All points were repeated 4–6 times. The deviations were never larger than one in the third place, and were usually less. In the case of the hexane isomers values were available for four isomers.²¹ The activation energies obtained from Geist and Cannon's data were about 80 calories less than ours. The average values obtained from the two sets were used.

The comparisons between theory and experiments appear in Figs. 8–12 and Table I. The sign convention is the same as for the high pressure data. In general, the correct magnitude and relative order of separation among the isomers is predicted. The only exceptions are *m*-xylene and 2-methylpentane which are slightly out of order.

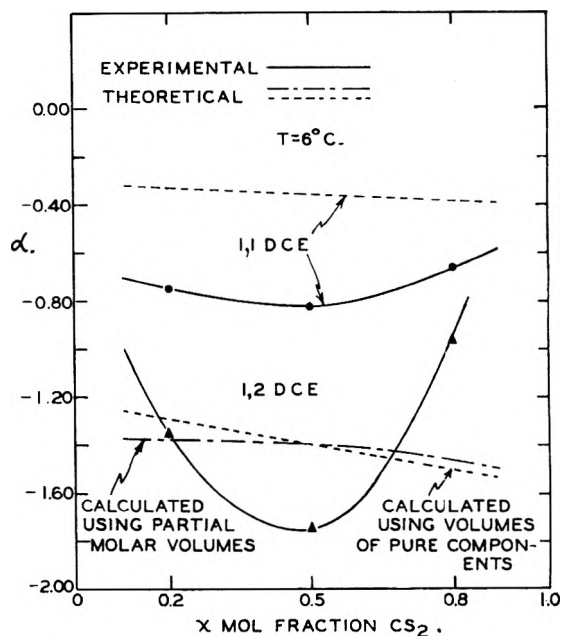


Fig. 10.—Comparison of theoretical and experimental values of α : dichloroethane isomers.

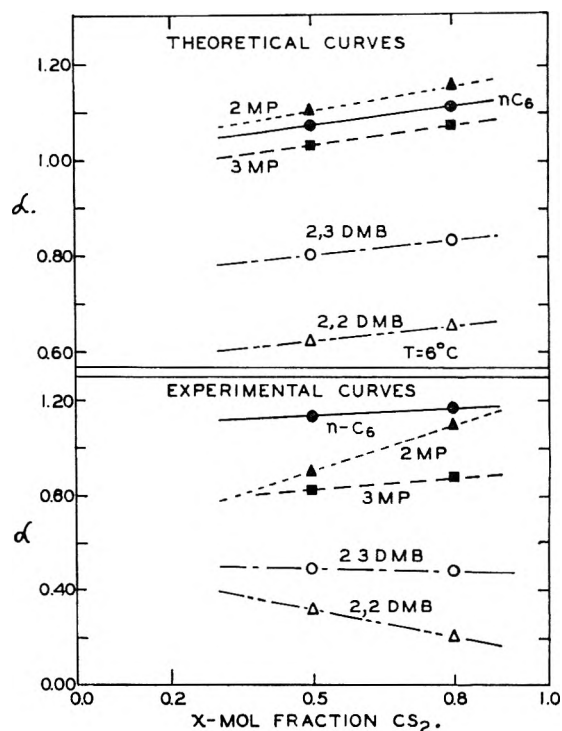


Fig. 11.—Comparison of theoretical and experimental values of α : hexane isomers.

A change of 1–2% in the activation energies for these compounds would correct this effect, and such a change is well within the experimental error for activation energies. In general the concentration effect is not well predicted. This is most probably due to approximations two and three discussed above.

Points to be particularly noted include the following.

(1) It is predicted and found that *o*-xylene behaves much differently than the other xylene

TABLE II
ACTIVATION ENERGIES AND MOLAR VOLUMES²³

Compound	ΔU^\ddagger , cal./mole	V/mole (cc.)	Ref. for viscosity
CS ₂	1045	59.4	19
<i>o</i> -Xylene	2351	119.3	20
<i>m</i> -Xylene	2007	121.4	20
<i>p</i> -Xylene	2024	121.8	20
Ethylbenzene	2043	120.9	19
<i>n</i> -Hexane	1420	128.6	21, 22
2-Methylpentane	1400	129.0	21, 22
3-Methylpentane	1450	128.0	21, 22
2,3-Dimethylbutane	1620	128.0	21, 22
2,2-Dimethylbutane	1850	132.9	22
<i>cis</i> -Dichloroethylene	1500	74.4	22
<i>trans</i> -Dichloroethylene	1490	76.0	22
1,1-Dichloroethane	1690	82.6	19
1,2-Dichloroethane	2230	76.5	19
<i>n</i> -Butyl chloride	1620	102.9	22
<i>sec</i> -Butyl chloride	1700	104.4	22
Isobutyl chloride	1740	103.9	22
<i>t</i> -Butyl chloride	2220	108.2	22
<i>n</i> -Butyl alcohol	4440	90.5	22
<i>sec</i> -Butyl alcohol	6340	90.8	22
Isobutyl alcohol	5550	91.4	22

isomers. It goes to the cold wall strongly, whereas the others go to the hot wall with CS₂ (Fig. 8).

(2) The *cis* isomer goes more strongly to the cold wall than the *trans* isomer as predicted (Fig. 9).

(3) 1,2-Dichloroethane goes much more strongly to the cold wall than the 1,1-isomer (Fig. 10). The large concentration effect for 1,2-dichloroethane is probably due to the non-ideality of the system. (CS₂ and 1,2-dichloroethane separate into two layers at about -20°.) Such non-ideality would predict the type of concentration dependence obtained.

(4) While exceptions may be found to any generalization, it appears that among isomers, the more "streamlined" the isomer, the greater the extent to which it tends to go to the hot wall (*i.e.*, the lower its activation energy). The more "ball like" the isomer, the more strongly it tends to go to the cold wall.

Experimental results and theoretical predictions are shown for three isomers of butyl alcohol in 50 mole % mixture with CS₂ in Table I. It can be seen that the order is correctly predicted but the

(19) "International Critical Tables," McGraw-Hill Book Co., Inc., New York, N. Y., 1927.

(20) API Research Project 44.

(21) J. Geist and M. Cannon, *Ind. Eng. Chem., Anal. Ed.*, **18**, 611 (1946).

(22) This Laboratory, unpublished data.

(23) M. Ketelaar, S. deVries, J. von Velden and P. Koez, *Rec. trav. chim.*, **66**, 733 (1945).

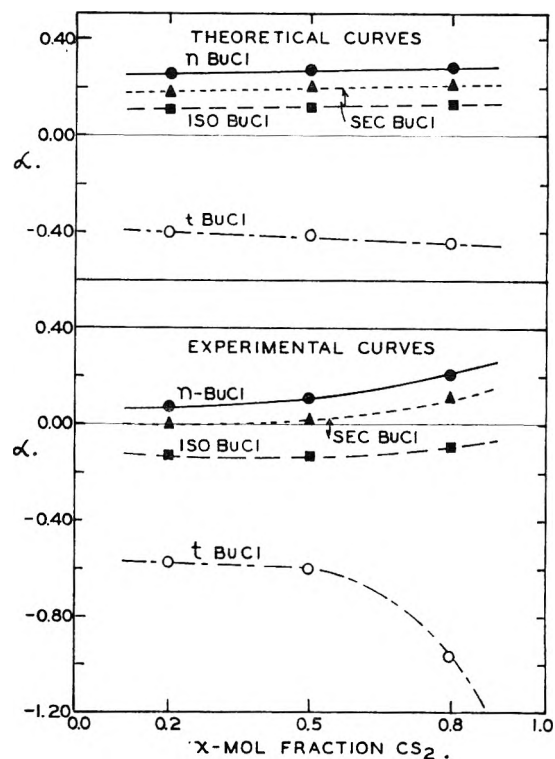


Fig. 12.—Comparison of theoretical and experimental values of α : butyl chloride isomers.

magnitude of separation is not. If one assumes a degree of association a_1 for type one molecules (*i.e.*, the moving unit of type one molecules contains a_1 molecules and the activation energy for motion of such a unit), one obtains for the thermal diffusion ratio

$$\alpha = \frac{M_1 V_2 + M_2 V_1}{2MRT} \left[\frac{\Delta U_2^\ddagger}{V_2} - \frac{\Delta U_1^\ddagger}{a_1 V_1} \right]$$

The values of a_1 obtained are shown in Table III. Within experimental error they are remarkably consistent, especially considering the 40% variation in activation energy, but seem rather too large to be true values for the moving unit. A thorough investigation of associated mixtures is being undertaken.

TABLE III

ASSOCIATION OF THE BUTYL ALCOHOLS (50 MOLE %)

Isomer	a_1
<i>n</i> -Butyl alcohol	2.79
<i>sec</i> -Butyl alcohol	2.69
Isobutyl alcohol	2.48

E.L.D. would like to acknowledge assistance from the Pan American Refining Corporation.

THE SPECTROPHOTOMETRIC DETERMINATION OF DISSOCIATION CONSTANTS OF DIBASIC ACIDS. METHODS USING A MINIMUM AMOUNT OF DATA¹

BY BURTON J. THAMER

University of California, Los Alamos Scientific Laboratory, Los Alamos, New Mexico

Received December 8, 1964

Two spectrophotometric methods are given for determining dissociation constants of dibasic acids. Each method is applicable for any degree of overlapping of the dissociation constants. Neither method requires a direct measurement of the extinction coefficient of any of the individual species that are in equilibrium with each other. A minimum amount of data is required in either method. The equations are expressed in a form that readily allows the use of differential spectrophotometry the use of which should give better experimental accuracy. The one method features the direct calculation of the dissociation constants without the need for any approximations. The other method uses rapidly converging successive approximations to give the same results. The two methods are thought to be of comparable usefulness. Their use is illustrated with an example.

The ionization equilibria of a light-absorbing acid frequently may be investigated by measurements of the optical density *versus* pH at a wave length such that the different ionic forms of the acid have markedly different absorption coefficients. The concentration of the acid under investigation and the length of the absorption cell are kept constant for this purpose. If, in addition, the temperature and ionic strength are maintained constant the equilibria of a dibasic acid H₂A may be represented by the equations

$$k_1 = \frac{a[\text{HA}]}{[\text{H}_2\text{A}]} \text{ and } k_2 = \frac{a[\text{A}]}{[\text{HA}]} \quad (1)$$

where a represents the measured hydrogen ion activity and brackets indicate concentrations.² The thermodynamic dissociation constants can be estimated from the measured dissociation constants k_1 and k_2 if the value of the ionic strength is fairly low. As previously indicated the optical density D after correction for absorption by the solvent and any buffer that may be present may be represented by

$$D = \frac{Lc[E_1 + \frac{k_1}{a}E_2 + \frac{k_1k_2}{a^2}E_3]}{1 + \frac{k_1}{a} + \frac{k_1k_2}{a^2}} \quad (2)$$

where L is the length of the absorption cell, c is the total concentration of the acid in all its forms, and E_1 , E_2 and E_3 are the molar extinction coefficients of the forms H₂A, HA and A, respectively.³

If k_1 and k_2 are greatly different in magnitude they can be determined separately⁴ since then only one stage of ionization is appreciably operative at a given pH. If the dissociation constants do not overlap too much, for example if k_1/k_2 is greater than 50, they could be determined separately without serious error by the method of "indirect colorim-

etry," which, however, requires equipment not ordinarily available in the laboratory.⁵ The separate determination of k_1 and k_2 can be accomplished by a new spectrophotometric method by Rosenblatt but the method is subject to some inaccuracy if k_1 and k_2 are strongly overlapping.⁶ A method by Thamer and Voigt is designed specifically for the case in which the dissociation constants do overlap and k_1/k_2 is less than 1000.³ Their treatment requires that a plot of optical density *versus* pH have a maximum or a minimum in the region of the curve where the intermediate species HA predominates. The latter requirement can frequently be met, but one must devote at least a few points to the determination of the optical density at the maximum (or minimum) of the curve. It is assumed in their method that the optical densities $D_1 = LcE_1$ and $D_3 = LcE_3$ can be measured directly by obtaining the pure forms H₂A and A, respectively. This may not be possible and D_1 or D_3 may have to be estimated from the available data at the lowest or highest pH, respectively.

Equation 2 is valid for each solution that is measured at the given wave length and under the experimental conditions mentioned in the first paragraph. Making the substitutions $LcE_1 = D_1$ and $LcE_3 = D_3$, and rearranging terms, equation 2 can be brought into the following form for each i -th designated solution of a series of solutions

$$a_i D_1(k_1) + D_1(k_1 k_2) - (D_3 k_1 k_2) - \frac{a_i(LcE_2 k_1) - a_i^2(D_1)}{a_i^2} = -a_i^2 D_1 \quad (3)$$

In the general case of a dibasic acid each of the five quantities enclosed in parentheses in equation 3 is an unknown constant and all quantities outside of parentheses are measurable. As has been suggested by Rosenblatt the five unknowns could be determined by the simultaneous solution of five equations of the type of equation 3 thus requiring measurements at only five different values of pH.⁷ Two methods of implementing this attack on the problem will be derived. Each of these methods (1) will be rigorously applicable for any value of k_1/k_2 that may be encountered, (2) will not require direct measurement of $D_1 = LcE_1$ for pure H₂A or $D_3 = LcE_3$ for pure A, and (3) will not require that a plot of optical density against pH have a maximum

(1) Work done under the auspices of the Atomic Energy Commission.

(2) Charges are not attached to the symbols H₂A, HA and A in the equilibria



and



because the "dibasic acid" H₂A might be a conjugate acid of an ampholyte, for example.

(3) B. J. Thamer and A. F. Voigt, *THIS JOURNAL*, **56**, 225 (1952).

(4) D. H. Rosenblatt, *ibid.*, **58**, 40, equation (c) (1954).

(5) L. Sacconi, *ibid.*, **54**, 829 (1950).

(6) D. H. Rosenblatt, *ibid.*, **58**, 41, equation e (1954).

(7) D. H. Rosenblatt, *ibid.*, **58**, 42 (1954).

or a minimum corresponding to the intermediate species HA. Furthermore a minimum amount of data will be required.

In either method the hydrogen ion activity a_i and a measure of the optical density D_i must be known for each of five solutions. The five measured solutions will be referred to as α , β , γ , δ and ϵ . The individual significance of each solution can best be described by reference to Fig. 1 which contains data previously reported by Thamer and Voigt for isophthalic acid.³ (The fact that there is a maximum in the curve is immaterial for the present discussion.) The labeled solid points have been chosen for solutions α , β , γ , δ and ϵ . Solution α , in effect, serves for a determination of $D_1 = LcE_1$ in equation 3 and, as such, should have as low a pH as possible in order to have a high concentration of H_2A .⁸ Solution γ should be located at a pH near which a maximum concentration of the intermediate species HA exists in order for it to best fulfill its function of allowing an evaluation of the quantity LcE_2 in equation 3. Solution ϵ corresponds to the determination of D_3 and it should have as much as possible of the species A present, *i.e.*, be at a high pH. Solution β , in conjunction with points α and γ , is the most important point in the evaluation of k_1 . For best accuracy its optical density should lie about midway between the optical densities of α and γ . Similarly solution δ , in conjunction with γ and ϵ , is the important point in evaluating k_2 . Its optical density preferably should lie midway between the optical densities of γ and ϵ .

The first method of handling the problem might be referred to as a "complete" solution because it allows the direct calculation of k_1 and k_2 without making any simplifying assumptions regarding the values of D_1 , LcE_2 or D_3 . In the derivation advantage may be taken of the fact that only differences in optical densities need to be employed. Thus the basic equation, equation 2, may be written in the form

$$D_i - D_\alpha = \frac{(D_1 - D_\alpha) + \frac{k_1}{a_i}(LcE_2 - D_\alpha) + \frac{k_1 k_2}{a_i^2}(D_3 - D_\alpha)}{1 + \frac{k_1}{a_i} + \frac{k_1 k_2}{a_i^2}} \quad (4)$$

or

$$a_i(D_i - D_\alpha)[k_1] + (D_i - D_\alpha)[k_1 k_2] - [k_1 k_2(D_3 - D_\alpha)] - a_i[k_1(LcE_2 - D_\alpha)] - a_i^2[D_1 - D_\alpha] = -a_i^2(D_i - D_\alpha) \quad (5)$$

where $D_1 = LcE_1$, $D_3 = LcE_3$ and i represents the i -th solution. When i denotes solution α , *i.e.*, $i = \alpha$, the latter equation reduces to

$$-[k_1 k_2(D_3 - D_\alpha)] - a_\alpha[k_1(LcE_2 - D_\alpha)] - a_\alpha^2[D_1 - D_\alpha] = 0 \quad (6)$$

Upon combining the latter two equations one obtains

$$a_i(D_i - D_\alpha)[k_1] + (D_i - D_\alpha)[k_1 k_2] + (a_\alpha - a_i)[k_1(LcE_2 - D_\alpha)] + (a_\alpha^2 - a_i^2)[D_1 - D_\alpha] = -a_i^2(D_i - D_\alpha) \quad (7)$$

The four unknown quantities enclosed in brackets in equation 7 may be determined by the simultane-

(8) In the example given, a pH of approximately 1.6 was the lowest obtainable in order not to exceed an ionic strength of 0.030 that was maintained for each solution.

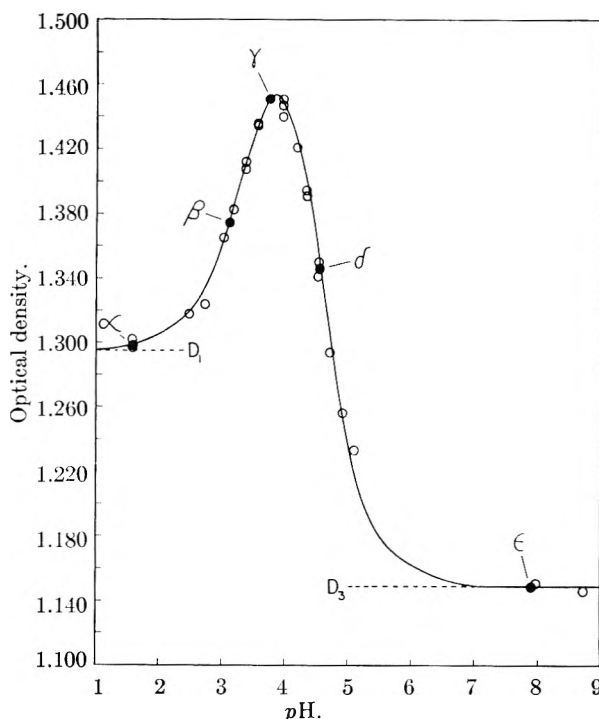


Fig. 1.—Spectrophotometric data on isophthalic acid at 2460.0 Å.: solid circles, experimental points used in the calculations of this paper; open circles, other experimental points; solid curve, calculated from eq. 2 using the results of Table II.

ous solution of the four equations resulting when i equals successively β , γ , δ and ϵ . Solving for the first two unknown quantities one obtains

$$k_1 = \Delta_1 / \Delta \quad (8)$$

and

$$k_1 k_2 = \Delta_2 / \Delta \quad (9)$$

giving

$$k_2 = \Delta_2 / \Delta_1 \quad (10)$$

where

$$\Delta = \begin{vmatrix} a_\beta(D_\beta - D_\alpha) & (D_\beta - D_\alpha) & (a_\alpha - a_\beta) & (a_\alpha^2 - a_\beta^2) \\ a_\gamma(D_\gamma - D_\alpha) & (D_\gamma - D_\alpha) & (a_\alpha - a_\gamma) & (a_\alpha^2 - a_\gamma^2) \\ a_\delta(D_\delta - D_\alpha) & (D_\delta - D_\alpha) & (a_\alpha - a_\delta) & (a_\alpha^2 - a_\delta^2) \\ a_\epsilon(D_\epsilon - D_\alpha) & (D_\epsilon - D_\alpha) & (a_\alpha - a_\epsilon) & (a_\alpha^2 - a_\epsilon^2) \end{vmatrix} \quad (11)$$

$$\Delta_1 = \begin{vmatrix} -a_\beta^2(D_\beta - D_\alpha) & (D_\beta - D_\alpha) & (a_\alpha - a_\beta) & (a_\alpha^2 - a_\beta^2) \\ -a_\gamma^2(D_\gamma - D_\alpha) & (D_\gamma - D_\alpha) & (a_\alpha - a_\gamma) & (a_\alpha^2 - a_\gamma^2) \\ -a_\delta^2(D_\delta - D_\alpha) & (D_\delta - D_\alpha) & (a_\alpha - a_\delta) & (a_\alpha^2 - a_\delta^2) \\ -a_\epsilon^2(D_\epsilon - D_\alpha) & (D_\epsilon - D_\alpha) & (a_\alpha - a_\epsilon) & (a_\alpha^2 - a_\epsilon^2) \end{vmatrix} \quad (12)$$

$$\Delta_2 = \begin{vmatrix} a_\beta(D_\beta - D_\alpha) & -a_\beta^2(D_\beta - D_\alpha) & (a_\alpha - a_\beta) & (a_\alpha^2 - a_\beta^2) \\ a_\gamma(D_\gamma - D_\alpha) & -a_\gamma^2(D_\gamma - D_\alpha) & (a_\alpha - a_\gamma) & (a_\alpha^2 - a_\gamma^2) \\ a_\delta(D_\delta - D_\alpha) & -a_\delta^2(D_\delta - D_\alpha) & (a_\alpha - a_\delta) & (a_\alpha^2 - a_\delta^2) \\ a_\epsilon(D_\epsilon - D_\alpha) & -a_\epsilon^2(D_\epsilon - D_\alpha) & (a_\alpha - a_\epsilon) & (a_\alpha^2 - a_\epsilon^2) \end{vmatrix} \quad (13)$$

Upon simplification⁹ these equations given solutions for k_1 and k_2 in the form

(9) Discussions of the properties of determinants and means of simplifying them may be found in such texts as: J. W. Mellor, "Higher Mathematics for Students of Chemistry and Physics," Dover Publications, New York, N. Y., 1946, p. 587; H. Margenau and G. M. Murphy, "The Mathematics of Physics and Chemistry," D. Van Nostrand Co., Inc., New York, N. Y., 1947, p. 288; H. W. Kuhn and J. H. Weaver, "Elementary College Algebra," The Macmillan Co., New York, N. Y., 1947, p. 284; E. J. Wilczynski and H. E. Slaight, "College Algebra with Applications," Allyn and Bacon, New York, N. Y., 1916, p. 380.

$$k_1 = \frac{[-\lambda_1(a\beta + a_\gamma) + \lambda_2(a\beta + a_\delta) - \lambda_3(a\beta + a_\epsilon) - \lambda_4(a_\gamma + a_\delta) + \lambda_5(a_\gamma + a_\epsilon) - \lambda_6(a_\delta + a_\epsilon)]}{[\lambda_1 - \lambda_2 + \lambda_3 + \lambda_4 - \lambda_5 + \lambda_6]} \quad (14)$$

and

$$k_2 = \frac{[\lambda_1 a_\beta a_\gamma - \lambda_2 a_\beta a_\delta + \lambda_3 a_\beta a_\epsilon + \lambda_4 a_\gamma a_\delta - \lambda_5 a_\gamma a_\epsilon + \lambda_6 a_\delta a_\epsilon]}{[-\lambda_1(a\beta + a_\gamma) + \lambda_2(a\beta + a_\delta) - \lambda_3(a\beta + a_\epsilon) - \lambda_4(a_\gamma + a_\delta) + \lambda_5(a_\gamma + a_\epsilon) - \lambda_6(a_\delta + a_\epsilon)]} \quad (15)$$

where

$$\lambda_1 = (D_\beta - D_\alpha)(D_\gamma - D_\alpha)(a_\alpha - a_\delta)(a_\alpha - a_\epsilon)(a_\beta - a_\gamma)(a_\delta - a_\epsilon) \quad (16)$$

$$\lambda_2 = (D_\beta - D_\alpha)(D_\delta - D_\alpha)(a_\alpha - a_\gamma)(a_\alpha - a_\epsilon)(a_\beta - a_\delta)(a_\gamma - a_\epsilon) \quad (17)$$

$$\lambda_3 = (D_\beta - D_\alpha)(D_\epsilon - D_\alpha)(a_\alpha - a_\gamma)(a_\alpha - a_\delta)(a_\beta - a_\epsilon)(a_\gamma - a_\delta) \quad (18)$$

$$\lambda_4 = (D_\gamma - D_\alpha)(D_\delta - D_\alpha)(a_\alpha - a_\beta)(a_\alpha - a_\epsilon)(a_\gamma - a_\delta)(a_\beta - a_\epsilon) \quad (19)$$

$$\lambda_5 = (D_\gamma - D_\alpha)(D_\epsilon - D_\alpha)(a_\alpha - a_\beta)(a_\alpha - a_\delta)(a_\gamma - a_\epsilon)(a_\beta - a_\delta) \quad (20)$$

$$\lambda_6 = (D_\delta - D_\alpha)(D_\epsilon - D_\alpha)(a_\alpha - a_\beta)(a_\alpha - a_\gamma)(a_\delta - a_\epsilon)(a_\beta - a_\gamma) \quad (21)$$

$$k_1 = \begin{vmatrix} a_\beta(D_1 - D_\beta) & \frac{1}{a_\beta}(D_\beta - D_3) & -1 \\ a_\gamma(D_1 - D_\gamma) & \frac{1}{a_\gamma}(D_\gamma - D_3) & -1 \\ a_\delta(D_1 - D_\delta) & \frac{1}{a_\delta}(D_\delta - D_3) & -1 \\ D_\beta & \frac{1}{a_\beta}(D_\beta - D_3) & -1 \\ D_\gamma & \frac{1}{a_\gamma}(D_\gamma - D_3) & -1 \\ D_\delta & \frac{1}{a_\delta}(D_\delta - D_3) & -1 \end{vmatrix} \quad (22)$$

$$k_1 = \frac{[a_\beta(D_\beta - D_1) - a_\gamma(D_\gamma - D_1)] \left[\frac{1}{a_\delta}(D_\delta - D_3) - \frac{1}{a_\beta}(D_\beta - D_3) \right] - [a_\beta(D_\beta - D_1) - a_\delta(D_\delta - D_1)] \left[\frac{1}{a_\gamma}(D_\gamma - D_3) - \frac{1}{a_\beta}(D_\beta - D_3) \right]}{(D_\gamma - D_\beta) \left[\frac{1}{a_\delta}(D_\delta - D_3) - \frac{1}{a_\beta}(D_\beta - D_3) \right] - (D_\delta - D_\beta) \left[\frac{1}{a_\gamma}(D_\gamma - D_3) - \frac{1}{a_\beta}(D_\beta - D_3) \right]} \quad (23)$$

The points referred to in Fig. 1 have been collected in Table I. The values of k_1 and k_2 calculated from equations 14 and 15 are $k_1 = 2.51 \times 10^{-4}$ and $k_2 = 3.96 \times 10^{-5}$. These figures agree with $k_1 = (2.67 \pm 0.28) \times 10^{-4}$ and $k_2 = (4.00 \pm 0.42) \times 10^{-5}$ previously calculated by Thamer and Voigt from all of the data of Fig. 1.³

The second method involves successive approximations which converge rapidly to the final solu-

$$k_2 = \begin{vmatrix} D_\beta & a_\beta(D_1 - D_\beta) & -1 \\ D_\gamma & a_\gamma(D_1 - D_\gamma) & -1 \\ D_\delta & a_\delta(D_1 - D_\delta) & -1 \\ a_\beta(D_1 - D_\beta) & \frac{1}{a_\beta}(D_\beta - D_3) & -1 \\ a_\gamma(D_1 - D_\gamma) & \frac{1}{a_\gamma}(D_\gamma - D_3) & -1 \\ a_\delta(D_1 - D_\delta) & \frac{1}{a_\delta}(D_\delta - D_3) & -1 \end{vmatrix} \quad (24)$$

$$k_2 = \frac{(D_\gamma - D_\beta)[a_\beta(D_\beta - D_1) - a_\delta(D_\delta - D_1)] - (D_\delta - D_\beta)[a_\beta(D_\beta - D_1) - a_\gamma(D_\gamma - D_1)]}{\left[\frac{1}{a_\delta}(D_\delta - D_3) - \frac{1}{a_\beta}(D_\beta - D_3) \right] [a_\beta(D_\beta - D_1) - a_\gamma(D_\gamma - D_1)] - \left[\frac{1}{a_\gamma}(D_\gamma - D_3) - \frac{1}{a_\beta}(D_\beta - D_3) \right] [a_\beta(D_\beta - D_1) - a_\delta(D_\delta - D_1)]} \quad (25)$$

tion. In this method, as will be shown shortly, successive approximations are made of the value of $D_1 = LcE_1$ from the point α and of the value of $D_3 = LcE_3$ from the point ϵ . In each cycle of the suc-

Values of k_1 and k_2 are calculated from equations 23 and 25. These values are used in the following equations (26, 27 and 28) which are rearranged forms of equation 2. A value for LcE_2 is calculated from point γ and the equation

$$LcE_2 = D_\gamma + \frac{a_\gamma}{k_1}(D_\gamma - D_1) + \frac{k_2}{a_\gamma}(D_\gamma - D_3) \quad (26)$$

The values obtained thus far are then used in the following two equations to obtain better approximations to D_1 and D_3 . Point α is used for a recalculation of the value of D_1

$$D_1 = D_\alpha - \frac{k_1}{a_\alpha}(LcE_2 - D_\alpha) + \frac{k_1 k_2}{a_\alpha^2}(D_\alpha - D_3) \quad (27)$$

Point ϵ is used for the recalculation of the value of D_3

$$D_3 = D_\epsilon - \frac{a_\epsilon}{k_2}(LcE_2 - D_\epsilon) + \frac{a_\epsilon^2}{k_1 k_2}(D_\epsilon - D_1) \quad (28)$$

The new values of D_1 and D_3 are then used in the next cycle of calculations using equations 23, 25, 26, 27 and 28 in succession. The calculations would be continued until the new values for D_1 and D_3 agreed within the limits of experimental error with their respective preceding values. For the very first cycle of calculation it might be assumed that $D_1 \approx$

TABLE I

SPECTROPHOTOMETRIC DATA FOR ISOPHTHALIC ACID AT 2460.0 Å.³

i	(pH)i	a_i	D_i	$D_i - D_\alpha$
α	1.58	2.63×10^{-2}	1.298	0.000
β	3.12	7.59×10^{-4}	1.375	.077
γ	3.75	1.78×10^{-4}	1.451	.153
δ	4.55	2.82×10^{-6}	1.346	.048
ϵ	7.90	1.26×10^{-8}	1.149	-.149

cessive approximations k_1 and k_2 are calculated as if the approximations to D_1 and D_3 were the actual values of D_1 and D_3 . A rearrangement of equation 3 with D_1 and D_3 assumed to be known gives the equation

$$D_1 k_1 + \frac{1}{a_1}(D_1 - D_3) k_1 k_2 - LcE_2 k_1 = a_1(D_1 - D_1) \quad (3')$$

where k_1 , k_2 and LcE_2 are unknown quantities. Points β , γ and δ provide the necessary three equations of the form of equation 3'. The solution of the three equations gives

D_α and $D_\beta \approx D_\epsilon$. The application of this method to the data of Table I is summarized in Table II.

TABLE II

THE CALCULATION BY SUCCESSIVE APPROXIMATIONS OF k_1 AND k_2 FOR ISOPHTHALIC ACID FROM THE DATA OF TABLE I

	First Cycle	Second Cycle
Assumed value of D_1	1.298	1.295
Assumed value of D_2	1.149	1.149
Calcd. value of k_1	2.34790×10^{-4}	2.50441×10^{-4}
Calcd. value of k_2	4.06920×10^{-5}	3.97290×10^{-5}
Calcd. value of LcE_2	1.636,032	1.629,281
Calcd. value of $D_1 (= LcE_1)$	$1.294,984 \approx 1.295$	$1.294,848 \approx 1.295$
Calcd. value of $D_2 (= LcE_2)$	$1.148,849 \approx 1.149$	$1.148,848 \approx 1.149$

Since the respective calculated values of D_1 and D_2 in the first two cycles agree with each other within experimental error (± 0.001 optical density units at best), the values of k_1 and k_2 calculated in the second cycle can be taken as final values. These values of $k_1 = 2.50 \times 10^{-4}$ and $k_2 = 3.97 \times 10^{-5}$ differ by only one in the third place from the values obtained by the "complete" solution. The difference is probably due to the rounding of the assumed values of D_1 and D_2 in Table II and, in any event, the difference is negligible compared with the actual experimental error. The values of the second cycle in Table II have been used in equation 2 to calculate the solid curve plotted in Fig. 1. The agreement between the plotted curve and the experimental points provides some experimental support for the validity and usefulness of the two methods presented here.

Although the two methods required about the same amount of calculating in the example that was given, the "complete" method sometimes will be quicker because the points D_α and/or D_ϵ may not lie so close to the respective values of D_1 and/or D_2 and more than two cycles then might be required in the above method of successive approximations. Disadvantages of the "complete" method are the slightly greater complexity of the terms involved in it and the fact that arithmetical errors might be harder to detect than they would be in the method of successive approximations. In the interests of accuracy it would be desirable in either method to determine each of the five points at least in duplicate. Also the measurement of a few trial points

might be helpful in finding a favorable pH at which to measure solution γ . Only optical density differences such as $D_i - D_\alpha$ need to be measured. Consequently only four spectrophotometric quantities, e.g., $D_\beta - D_\alpha$, $D_\gamma - D_\alpha$, $D_\delta - D_\alpha$ and $D_\epsilon - D_\alpha$, require measurement and in measuring them increased accuracy could be obtained by using the technique of differential spectrophotometry.¹⁰

Each of the above methods provides a solution to the problems posed by overlapping values of k_1 and k_2 as does also the method of Thamer and Voigt.³ A possible disadvantage of the methods presented here is the fact that the amount of data employed does not itself permit a verification that equations 1 and footnote 2 represent the actual equilibria of the system. Agreement between the plotted curve and additional points as in Fig. 1 would be necessary to show that such were the equilibria over the whole pH range. The advantage of the present methods lies in the fact that they would require little experimental work and little calculating. In the event that the optical densities were measured for each solution at more than one wave length they could be combined for calculating purposes into a composite C by means of the relation

$$C = \sum_j g_j D_j \quad (29)$$

where j represents each wave length at which measurements were made and each g_j is an arbitrarily chosen weighting factor.³ Each resulting C -value could be used in place of the D value at the same pH in each of the foregoing equations. The weighting factors would be chosen to give maximum values for

$$\frac{|C_\alpha - C_\gamma|}{\sum_j |g_j|} \text{ and } \frac{|C_\gamma - C_\epsilon|}{\sum_j |g_j|} \quad (30)$$

Instead of making the calculation at each wave length at which data were available and averaging the results, one could by this means utilize all of the data in a less time-consuming manner by making one calculation with composite values.

(10) See, for example, R. Bastian, R. Weberling and F. Palilla, *Anal. Chem.*, **22**, 160 (1950).

THE EFFECT OF PRESSURE ON THE SOLUBILITY OF SOLIDS IN NON-POLAR LIQUIDS*

BY E. P. DOANE AND H. G. DRICKAMER

Department of Chemistry and Chemical Engineering, University of Illinois, Urbana, Illinois

Received December 10, 1954

Solubility measurements under pressures to 10,000 atmospheres have been made in the following systems: phenanthrene in CS₂, *n*-hexane, *n*-heptane, *n*-octane; SnI₄ in CS₂, *n*-hexane, *n*-heptane, *n*-octane; C₂Cl₆ in CS₂, *n*-hexane, *n*-heptane, *n*-octane, 2-methylpentane, 3-methylpentane, 2,3-dimethylbutane, 2,2-dimethylbutane; anthracene in CS₂. The results are analyzed in terms of Scatchard-Hildebrand theory. In general, the effects of molecular structure assume greater importance at the higher pressures, especially for *n*-heptane.

While the measurement of solubility is one of the older fields of physical chemistry, there have been very few attempts to study the effect of an extended range of pressure on the solubility of simple molecular solids in non-polar organic liquids. This paper presents the results of such a study made at 25° with a maximum pressure of 10,000 atmospheres. The systems studied and the maximum pressure for each are listed in the Tables I-IV.

Experimental Procedure

A. Chemicals and Purification.—The hydrocarbons were all Phillips Petroleum Co. "Pure Grade," the carbon disulfide was J. T. Baker C.P. grade. The solvents were dried over P₂O₅ and distilled slowly in a two-foot packed column using only a center cut amounting to 50-60% of the charge. The boiling range of the product was never over 0.5°. Actually tests run with phenanthrene and SnI₄ indicated that the drying procedure had very little effect on solubility.

The SnI₄ was obtained as reagent crystals from Herstein Laboratories. Its melting range was 145.7-147.9° compared with the literature value of 143.5°. Since its atmospheric solubilities in CS₂ and heptane checked very closely the values given by Dorfman and Hildebrand,¹ it was used without further purification.

The phenanthrene, anthracene and hexachloroethane were Eastman Kodak Co. purest grade. The phenanthrene melted 100-101.1° and the anthracene melted 216.7-218.2°. These were used without further purification. A few experiments on recrystallized phenanthrene gave no significant deviation from the other results.

The C₂Cl₆ melted 187.7-188.9°. It was resublimed and recrystallized from ether and ethanol, and carefully dried. The final product melted 188.5-189.2°.

B. Analytical Procedure.—Analyses were performed either by weight or by refractive index. The weighing procedure was used for all phenanthrene systems, for anthracene-CS₂ for SnI₄-CS₂ and for C₂Cl₆-CS₂. Weighings were made on an Ainsworth type DLB chainomatic balance. For the hydrocarbons, standard weighing bottles were used, while special weighing pipets were constructed for the CS₂ systems. Considerable care was necessary, and many tests on known solutions were performed, but the methods were fairly standard except for C₂Cl₆-CS₂. In this case the relatively high vapor pressure of C₂Cl₆ made it impossible to evaporate to dryness without losing C₂Cl₆, so a special procedure was adopted.²

The analyses by refractive index were performed on a Bausch and Lomb Precision Refractometer. The light source was a sodium vapor lamp. The systems analyzed in this manner included all of the SnI₄ and C₂Cl₆ data, except for the CS₂ runs in both cases.

The percentage error for the highest pressure runs may be 10%, at atmospheric pressure the error was certainly less than 0.3%.

C. Measurement of Solubility.—The technique used to determine solubilities at one atmosphere was essentially that of Hildebrand, Ellefson and Beebe.³

The high pressure equipment consisted of an intensifier, a bomb and a solubility cell. The method of obtaining and measuring the pressure was identical to that described previously.⁴ The solubility cell consisted of a stainless steel tube 1/2" in diameter and 1 5/8" long which screwed into a cup filled with mercury. The mercury served to separate the pressure transmitting fluid from the solution. The cell was separated into two sections by a layer of filter paper supported on either side by two pieces of 200 mesh stainless steel screening. These rested on a shelf about 5/8" from the top. The edges were sealed by a Teflon gasket held in place by a steel sleeve. Each chamber contained an iron ring. Attached to the upper plug and surrounding the cell was a solenoid through which was sent a pulsed d.c. current. This activated the iron stirrers and caused mixing in each chamber. The top cup contained a hole for a 2-56 screw and two No. 70 holes for thermocouple wires. The wires were coated with collodion and the whole top of the cell was painted with collodion after assembling.

The lower chamber contained the solid and solution, the upper chamber just solution. The solid was either placed on the mercury or separated from it by a polyethylene disk. Since the solubility dropped very rapidly with increasing pressure it was necessary to prevent supersaturation at one atmosphere. For this purpose the solid was carefully covered by a piece of tin foil amalgamated with mercury. A third small stirrer was enclosed with the solid. After loading and applying pressure the coil was started and the stirrer tore open the weakened foil.

At the end of a run the system was depressured, the top plug and pressure transmitting fluid removed, and the liquid sampled through one of the No. 70 thermocouple wire holes.

For the case of phenanthrene in CS₂ the procedure had to be modified. In the first place, phenanthrene is very soluble, and secondly it is less dense than CS₂ and floats. The solid was fused into a lump in order to get enough in, and a piece of medium porosity fritted glass one mm. thick replaced the filter paper. This was successful only because of the small pressure coefficient of viscosity of CS₂.

The bomb was immersed in a bath which was controlled to ±0.1°. With the large mass of steel it is doubtful if even these fluctuations got through to the cell. Since the stirrer coil also supplied heat, the bath was maintained at 22.4°. The thermocouple measured the temperature in the upper chamber of the cell.

In order to guarantee equilibrium, runs were made with various initial concentrations of solution, since this was more convenient than varying the time of the run. (The runs were generally 20-24 hours). Various other tests were applied to insure the validity of the method.

Results

The experimental results are shown in Table I-IV. The reproducibility is ±1-2% at atmospheric pressure, and ±10% at the highest pressures. The larger deviation at high pressure is due primarily to difficulties in analysis.

Figure 1 is a plot of relative solubility *versus* relative volume of solvent for different solutes in CS₂. On the same graph are shown the atmospheric pressure results obtained for SnI₄ in CS₂ at

(* This work was supported in part by the A.E.C.

(1) M. E. Dorfman and J. H. Hildebrand, *J. Am. Chem. Soc.*, **49**, 729 (1927).

(2) E. P. Doane, Ph.D. Thesis, Univ. of Illinois, Urbana, Illinois.

(3) J. H. Hildebrand, E. T. Ellefson and C. W. Beebe, *J. Am. Chem. Soc.*, **39**, 2301 (1917).

(4) R. C. Koeller and H. G. Drickamer, *J. Chem. Phys.*, **21**, 267 (1953).

TABLE I

SOLUBILITY OF PHENANTHRENE, 25°

The pressure in atmospheres is followed by the solubility in mole percentage in parentheses.

<i>n</i> -Hexane	1 (3.26), 500 (2.72), 1000 (2.26), 2000 (1.80), 4300 (1.04), 7150 (0.50), 8750 (0.36)
<i>n</i> -Heptane	1 (4.01), 500 (3.21), 900 (2.92), 1000 (2.72), 2000 (1.84), 3430 (1.11), 5000 (0.84), 7000 (0.52)
<i>n</i> -Octane	1 (4.64), 490 (3.81), 1000 (2.84), 1960 (1.97), 3850 (1.20), 5200 (0.88)
CS ₂	1 (23.5), 500 (16.2), 1000 (12.5), 2000 (7.3), 4000 (4.5), 6000 (2.9), 7000 (2.2)

TABLE II

SOLUBILITY OF SnI₄

The pressure is given in atmospheres followed by the solubility in mole percentage in parentheses.

<i>n</i> -Hexane	1 (0.470), 10 (0.443), 480 (0.315), 1000 (0.199), 2000 (0.099), 3100 (0.057), 5100 (0.047), 7200 (0.033), 9100 (0.019)
<i>n</i> -Heptane	1 (0.553), 470 (0.383), 980 (0.163), 2000 (0.048), 3000 (0.031), 4600 (0.019), 7200 (0.018)
<i>n</i> -Octane	1 (0.621), 500 (0.429), 1000 (0.245), 1500 (0.148), 2000 (0.115)
CS ₂	1 (14.61), 1000 (7.99), 2000 (5.64), 3600 (3.45), 5000 (1.96), 7000 (0.77), 10,000 (0.11)

TABLE III

SOLUBILITY OF C₂Cl₆

The pressure in atmospheres is followed by the solubility in mole percentage in parentheses.

<i>n</i> -Hexane	1 (13.92), 400 (9.84), 1000 (6.36), 2000 (3.40), 3300 (1.72), 5000 (0.64), 5830 (0.29), 6750 (0.26)
<i>n</i> -Heptane	1 (15.18), 410 (10.48), 1000 (6.79), 2000 (2.30), 2970 (1.63), 4000 (0.83), 5000 (0.40)
<i>n</i> -Octane	1 (15.72), 400 (10.35), 1000 (6.33), 2000 (3.44)
CS ₂	1 (19.5), 500 (12.0), 1000 (8.0), 1970 (4.1), 3400 (2.3), 5000 (1.3), 7000 (0.31)
2-Methylpentane	1 (13.02), 400 (9.15), 1000 (5.76), 1950 (3.14), 3350 (1.43), 5000 (0.52), 6900 (0.22)
3-Methylpentane	1 (13.52), 400 (9.56), 1000 (6.21), 2000 (3.15), 3500 (1.19), 5000 (0.61), 7000 (0.18)
2,3-Dimethylbutane	1 (13.15), 400 (9.19), 990 (5.74), 1970 (2.83), 3500 (1.15), 4950 (0.51), 6800 (0.14)

2,2-Dimethylbutane

1 (12.02), 400 (8.48), 990 (5.41), 2000 (2.72), 3500 (0.98), 4500 (0.45)

TABLE IV

SOLUBILITY OF ANTHRACENE

The pressure in atmospheres is followed by the solubility in mole percentage in parentheses.

CS ₂	1 (0.84), 240 (0.70), 500 (0.59), 1000 (0.41), 2000 (0.27), 4000 (0.13)
-----------------	---

various temperatures by Dorfman and Hildebrand.¹ The density coefficient of solubility varies considerably more rapidly at constant pressure than at constant temperature. A similar result was found for SnI₄ in *n*-heptane.

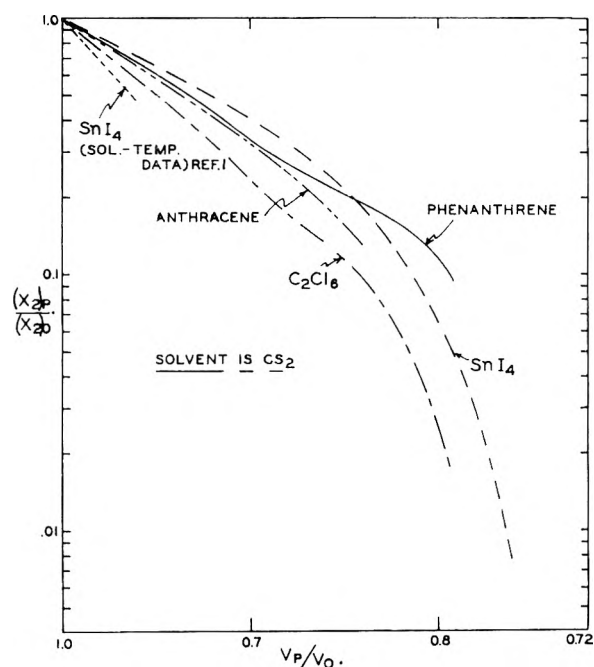


Fig. 1.—Relative solubility vs. relative molar volume of solvent.

It is useful to compare our atmospheric pressure data with values in the literature. In Table V

TABLE V

COMPARISON OF SOLUBILITIES OBTAINED IN THIS WORK WITH PUBLISHED SOLUBILITY VALUES OF SnI₄ (MOLE %)

Solvent	Dorfman and Hildebrand ¹	This work
Heptane	0.533	0.552
CS ₂	14.64	14.61

Solubility of phenanthrene (mole %)

Solvent	Hildebrand Ellefson and Beebe ¹	This work Eastman	Recrystallized
CS ₂	25.5	23.5	21.6
<i>n</i> -Hexane	4.2	3.26	3.09

Solubility of anthracene (mole %)

Solvent	Ref. 2	This work
CS ₂	1.09	0.84

we see such a comparison. We find excellent agreement for the solubility of SnI₄ in CS₂ and in heptane, but no agreement for the solubility of

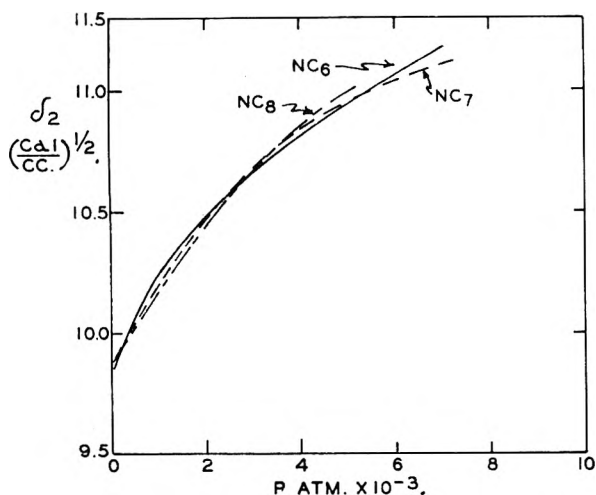


Fig. 2.—Solubility parameter vs. pressure for phenanthrene.

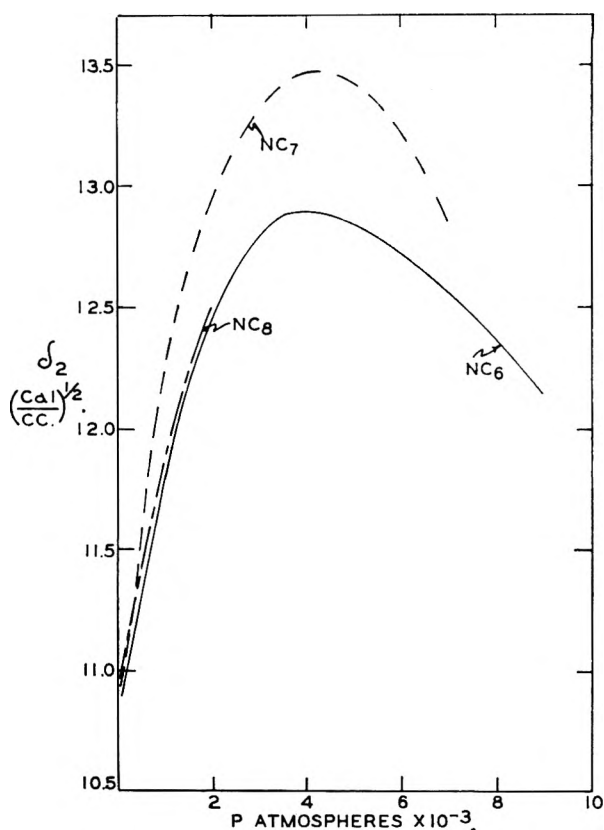


Fig. 3.—Solubility parameters vs. pressure for SnI₄.

phenanthrene and anthracene in heptane. We have no good explanation of this. We tried two different batches of Eastman phenanthrene, and recrystallized one batch several times. We never obtained any variation from batch to batch greater than 10%, and the more highly purified batches deviated most widely from Hildebrand's values.

Comparison of Theory and Results.—By far the most widely used theory of solutions is that developed by Scatchard and Hildebrand. Recently theories with a sounder basis in statistical mechanics have been developed by Guggenheim,⁵

(5) E. A. Guggenheim, "Mixtures," Oxford Univ. Press, New York, N. Y., 1952.

Kirkwood⁶ and Prigogine and co-workers.⁷ These, however, are not readily applied to a discussion of solubility under pressure.

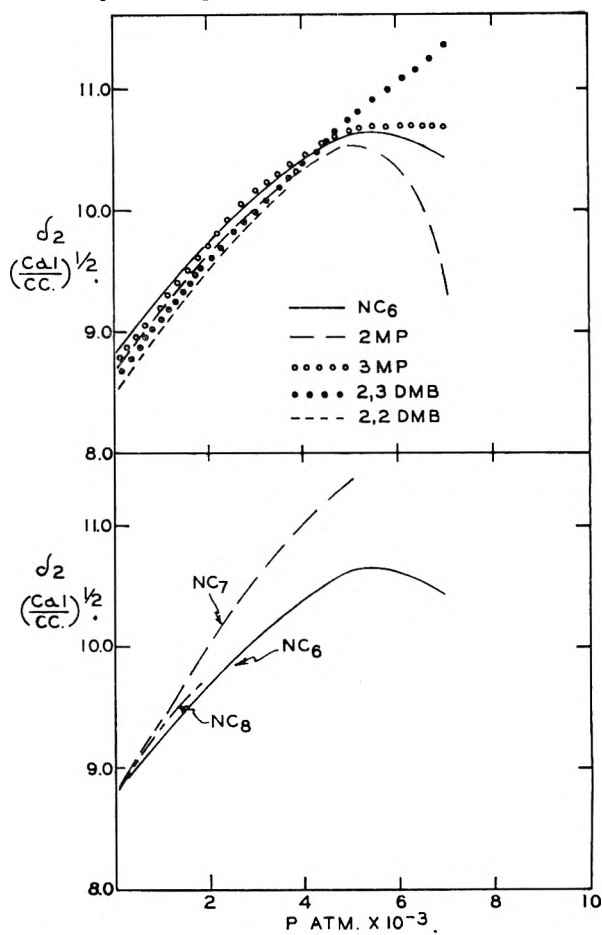


Fig. 4.—Solubility parameter vs. pressure for C_2Cl_6 .

To discuss our results we shall use the S-H theory. This theory gives⁸ for the partial molal free energy of the solute

$$\Delta \bar{F}_2 = V_2 \varphi_1^2 (\delta_2 - \delta_1)^2 + RT \ln X_2 \quad (1)$$

if the entropy of mixing is ideal, or

$$\left[\Delta \bar{F}_2 = V_2 \varphi_1^2 (\delta_2 - \delta_1)^2 + RT \ln \varphi_2 + \varphi_1 \left(1 - \frac{V_2}{V_1} \right) \right] \quad (2)$$

if the Flory-Huggins entropy is used. Here

V_i = molal vol. of i (of the supercooled liquid for the solute)

X_2 = mole fraction of solute (measured)

φ_1 = vol. fraction of i

δ_i = solubility parameter of i

$$= \left(\frac{-E}{V} \right)^{1/2}$$

where $-E$ = cohesive energy, at one atmosphere, the energy of vaporization into a perfect gas.

It is not hard to show⁸ that

$$\Delta \bar{F}_2 = RT \ln X_2^i \quad (3)$$

(6) Z. Salzberg and J. H. Kirkwood, *J. Chem. Phys.*, **20**, 1538 (1952); **21**, 2169 (1953).

(7) I. Prigogine and V. Mathot, *ibid.*, **20**, 49 (1952); I. Prigogine and A. Bellemans, *Disc. Faraday Soc.*, No. 15, 80 (1953); I. Prigogine, N. Trappeniers and V. Mathot, *ibid.*, No. 15, 93 (1953). See also other articles referred to in these papers.

(8) J. H. Hildebrand and R. L. Scott, "The Solubility on Non-electrolytes," 3rd Ed., Reinhold Publ. Corp., New York, N. Y., 1950.

where X_{2i} is the "ideal solubility" of the solid.

To evaluate solubility parameters under pressure the relationship

$$\left(\frac{\partial E}{\partial p}\right)_T = -T \left(\frac{\partial \bar{V}}{\partial T}\right)_p - P \left(\frac{\partial \bar{V}}{\partial p}\right)_T \quad (4)$$

is used. Then

$$E_P = E^\circ + \int_1^P \left(\frac{\partial E}{\partial p}\right)_T \partial P \quad (5)$$

The p - v - t data of Bridgman⁹ were used. The volumes of the supercooled liquids were estimated from Bridgman's data on compressibility of organic solids and volume changes or melting under pressure. It can be shown that no reasonable change in these values would change our calculations materially.

In these equations X_{2i} and δ_2 are not known under pressure. The solutions were considered in pairs; one solvent in each pair was CS₂. It was then possible to solve for δ_2 , the solubility parameter of the solute, using either the Flory-Huggins entropy (eq. 2) or the ideal entropy (eq. 7). Both calculations were made. In Figs. 2-4 are shown the calculated values of δ_2 using the Flory-Huggins entropy. There were no significant differences in the trends obtained using eq. 1 or 2.

(9) P. W. Bridgman, *Proc. Amer. Acad.*, **49**, 1 (1913); **66**, 1 (1931); **76**, 9 (1945).

The measure of the applicability of the S-H theory is the consistency of the solubility parameter of the solute δ_2 calculated from different solvent pairs. From Fig. 2, it can be seen that the theory describes phenanthrene solutions quite well. From Fig. 3 and 4 we note that the theory gives consistent results for SnI₄ and C₂Cl₆, in hexane and octane, but that solubility parameters for these almost spherical solutes in heptane are high, particularly at the higher pressures. It is known that the odd-numbered normal paraffin chains pack differently than those with an even number of links. Their freezing points are displaced to a lower temperature indicating there are fewer ways of packing them in a lattice. It would seem that the deviation of heptane is due to an entropy effect not accounted for in eq. 2.

In Fig. 4 are shown the solubility parameters for C₂Cl₆ calculated for solutions in the isomers of hexane. The agreement is good to 5000 atmospheres, but beyond this point there is a spread in solubility parameters far outside experimental error. Apparently there are different packing effects for different isomers, and these become important at high densities.

E. P. Doane would like to acknowledge the Visking Corporation Fellowship which he held for two years.

SOLUBILITY CHARACTERISTICS OF SEVERAL LONG-CHAIN METHYL ALKYL KETONES IN COMMON ORGANIC SOLVENTS^{1,2}

BY C. W. HOERR, R. A. RECK, GERALDINE B. CORCORAN AND H. J. HARWOOD

Research Division, Armour and Company, Chicago, Illinois

Received December 11, 1964

Solubilities are given for 2-nonanone, 2-tridecanone and 2-nonadecanone in *n*-hexane, benzene, cyclohexane, toluene, carbon tetrachloride, chloroform, ethyl acetate, methanol, 95% ethanol, 2-propanol, acetone, *p*-dioxane and acetonitrile. The marked correlation between internal pressures of the solvents and solubility of the unsymmetrical ketones is discussed with reference to the mole fraction plots of the 2-tridecanone solubilities. The apparent polymorphism of these ketones in the presence of certain solvents is discussed. Comparison of the behavior of 2-nonadecanone with that of its symmetrical homolog on a mole fraction basis suggests that the solubility characteristics of the methyl alkyl ketones are influenced by their relatively greater hydrogen-bonding propensities.

Although the unsymmetrical dialkyl ketones have not been studied so extensively as their symmetrical isomers, many of the methyl alkyl ketones have been prepared and described.³ Knowledge of the physical properties of these compounds is very limited. The literature contains no reference to the quantitative solubilities of the methyl alkyl ketones in organic solvents. This paper presents the solubilities of 2-nonanone, 2-tridecanone and 2-nonadecanone in *n*-hexane, benzene, cyclohexane, toluene, carbon tetrachloride, chloroform, ethyl acetate, methanol, 95% ethanol, 2-propanol, acetone,

p-dioxane and acetonitrile. Comparison of the behavior of 2-nonadecanone on an equimolecular basis with that of the previously published 10-nonadecanone⁴ suggests that the behavior of the former appears to be influenced by hydrogen bonding to a somewhat greater extent than that of the latter. Although the symmetrical isomers do not exhibit polymorphism, the methyl alkyl ketones precipitate from certain solvents in an unstable crystalline modification which transforms relatively rapidly to a stable form.

Experimental

The purified ketones used in this investigation were obtained by carefully fractionating pilot-plant lots in a Podbielniak Hypercal. The compounds were characterized by means of infrared spectra,⁵ such as that of 2-tridecanone shown in Fig. 1.

(4) F. M. Garland, C. W. Hoerr, W. O. Pool and A. W. Ralston, *J. Org. Chem.*, **8**, 344 (1943).

(5) The infrared analyses and interpretations were made by A. E. Brake, Research Division, Armour and Company, using a Baird Associates Infrared Recording Spectrophotometer.

(1) Presented in part at the 126th Meeting of the American Chemical Society in New York, New York, September 17, 1954.

(2) Material supplementary to this paper has been deposited as Document number 4461 with the ADI Auxiliary Publications Project, Photoduplication Service, Library of Congress, Washington 25, D. C. A copy may be secured by citing the Document number and by remitting \$1.25 for photoprints, or \$1.25 for 35 mm. microfilm, in advance by check or money order payable to: Chief, Photoduplication Service, Library of Congress.

(3) A. W. Ralston, "Fatty Acids and Their Derivatives," John Wiley and Sons, Inc., New York, N. Y., 1948, p. 841.

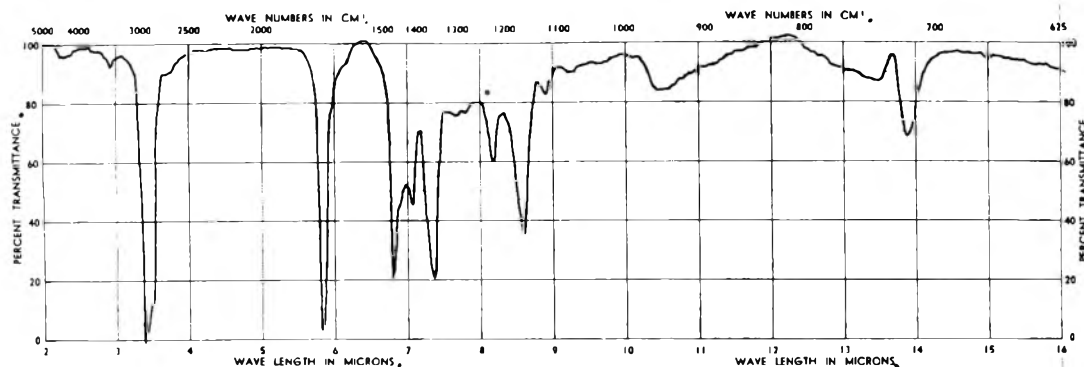


Fig. 1.—Infrared absorption spectrum of 2-tridecanone; 10% ketone in carbon tetrachloride in 0.10 mm. cell.

As this spectrum shows, the usual carbon-hydrogen bands occur at 3.4 and 6.8 μ , the carbonyl-stretching band at 5.83 μ and a non-symmetrical carbon-carbon stretching band at 8.60 μ . These bands are typical of the spectra of aliphatic ketones, but the enhanced intensity of the carbon-hydrogen deformation band at 7.35 μ , which indicates a greater carbon-hydrogen bond dipole moment, may be used to distinguish the methyl alkyl ketones.

The fractions of distilled ketone possessing the highest freezing points were retained for the solubility determinations. The freezing points of these samples are listed in Table I with the respective boiling points.

TABLE I

BOILING AND FREEZING POINTS OF THE METHYL ALKYL KETONES

Ketone	B.p., °C.	B.p. mm.	F.p., °C.	
			This investigation	Lit.
2-Nonanone	194	760	-7.46	-8.20 ⁶
2-Tridecanone	145	10	27.46	27.5 (m.p.) ⁷
2-Nonadecanone	165	2	54.59	55 (m.p.) ⁷

It will be noted that the freezing point of 2-nonanone is appreciably higher than that of the reference sample. The freezing points of the other two ketones are substantially the same as the recorded melting points.

The freezing points of the methyl alkyl ketones were determined by means of cooling curves such as that of 2-tridecanone shown in Fig. 2. These curves were obtained

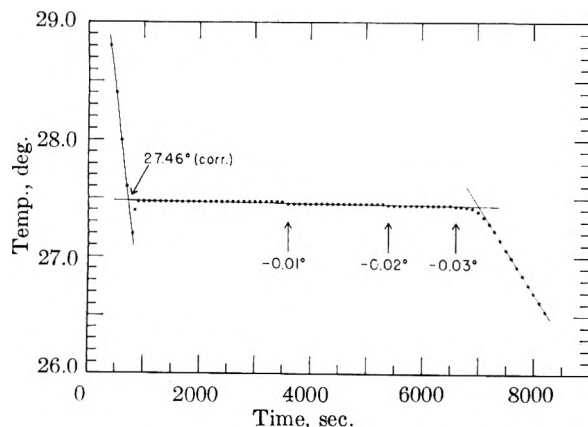


Fig. 2.—Cooling curve of 2-tridecanone. The curve dropped 0.01, 0.02 and 0.03° in 46, 78 and 98 min., respectively, after freezing began. The total freezing period was 105 min.

by cooling 15-g. samples in jacketed Pyrex tubes immersed in acetone or water-baths maintained 20° below the freezing temperatures. The samples were agitated by means of a motor-driven Nichrome wire stirrer until freezing was well

(6) L. Deffet, *Bull. soc. chim. Belg.*, **40**, 385 (1931).

(7) G. T. Morgan and E. Holmes, *J. Chem. Soc. Ind.*, **44**, 108T (1925).

under way. Temperatures were measured by mercury thermometers whose bulbs were immersed. These were total-immersion thermometers graduated in 0.1° intervals, which had been calibrated by the National Bureau of Standards. Appropriate emergent-stem corrections were added to the readings. The freezing points are considered accurate within 0.01°.

The solubilities of the methyl alkyl ketones were determined in the manner used for the earlier studies of symmetrical ketone solubilities.⁴ For solution temperatures above about 0°, known amounts of ketone and solvent were sealed in small glass tubes which were rotated in a water bath while the bath temperature was raised gradually. The temperature at which the last visible crystal dissolved was recorded. For solubilities from room temperature to about -40°, more rapid determinations were made by observations on known mixtures of ketone and solvent as they were alternately cooled and heated in jacketed Pyrex test-tubes equipped with a Nichrome wire stirrer and calibrated thermometer. These measurements agreed within 0.1° with those made by the sealed-tube method.

The ketones generally precipitated upon cooling and redissolved on heating well within a 0.1° range. In certain solvents two solution temperatures were observed which differed by about 2-5°. In such cases the more soluble form was obtained by chilling sharply a portion of the tube. The solution temperature of this form was then obtained by rapid reheating in baths of predetermined temperatures. By repetition of this process, the solution temperature of the unstable modification could be determined reproducibly within 0.1°. When a mixture was held at or below the solution temperature of the more soluble form for only a short time, visible transformation to the less soluble, stable form occurred spontaneously. Transformation to the stable form was so rapid in the higher concentration range as to preclude direct observation of the solution temperatures of the more soluble form. Solution temperatures of the stable modification were reproducible within 0.1° and are considered accurate within about 0.2°. Solution temperatures of the unstable form are probably accurate within 0.5°.

The solvents employed were of the best grade available, freshly distilled before use. The aqueous ethanol was commercial "absolute" diluted to 95.0% by weight with conductivity water, the ethanol content being determined by density.

Results and Discussion

The solubilities of 2-nonanone, 2-tridecanone and 2-nonadecanone are listed in Tables II, III and IV, respectively. These data were obtained by drawing curves from the observed solution temperatures² on large scale cross-section paper and tabulating the solubilities at certain selected temperatures.

The solubility curves of these three representative methyl alkyl ketones are shown graphically in Fig. 3. The diagrams in this figure show that these ketones form simple eutectics with the higher melting solvents. Although measurements were not carried below -40°, the general configuration of the curves indicates that the ketones also form eutec-

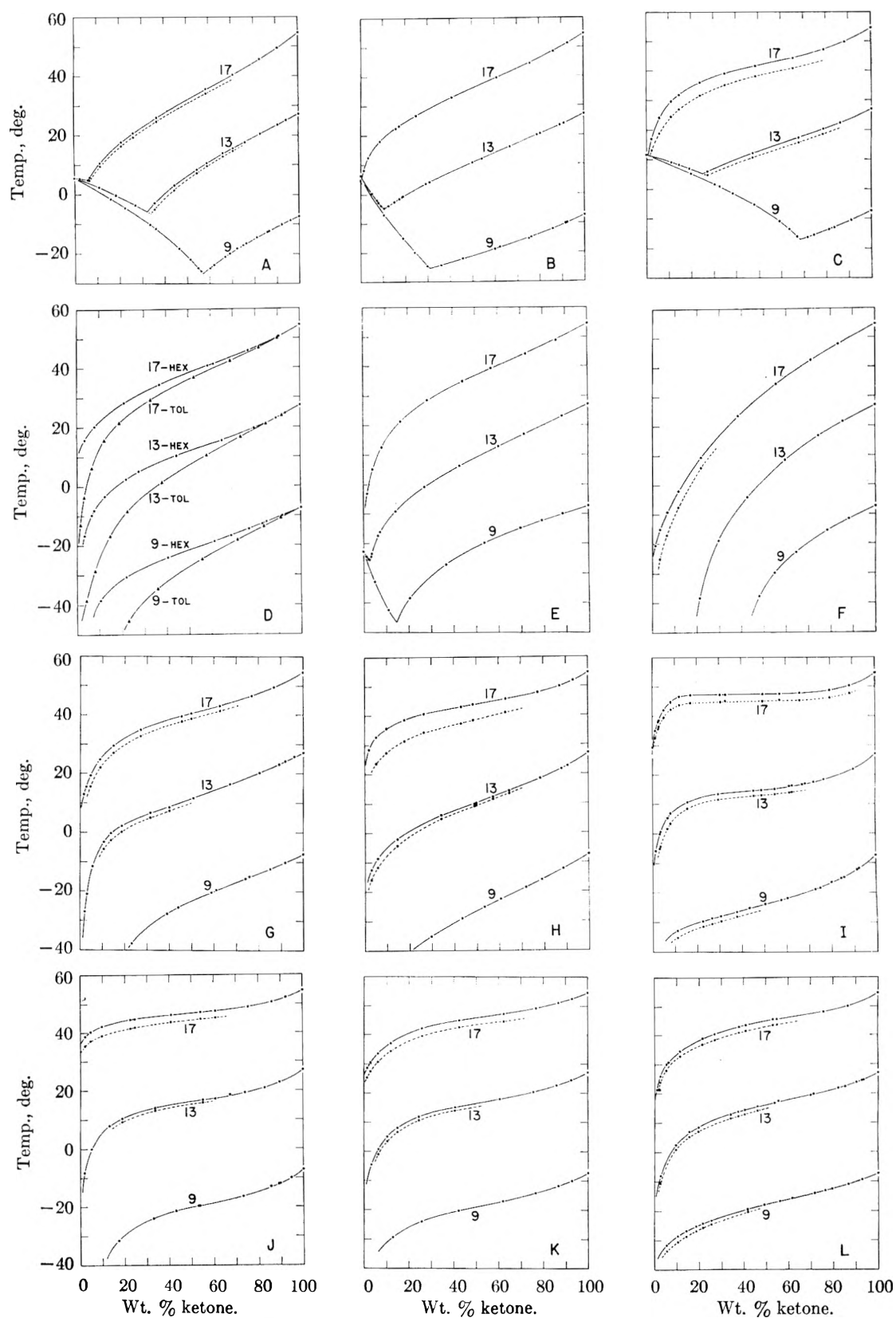


Fig. 3.—Solubilities of the methyl alkyl ketones in organic solvents: A, benzene; B, cyclohexane; C, *p*-dioxane; D, hexane and toluene; E, carbon tetrachloride; F, chloroform; G, ethyl acetate; H, acetone; I, acetonitrile; J, methanol; K, 95% ethanol; L, 2-propanol. The broken lines represent the solubilities of unstable crystal modifications. The numbers on the curves refer to the total number of carbon atoms in the compounds.

influences of different solvents, suggests that the observed phenomena do not represent true polymorphism. Ordinarily, definite changes in the angle of tilt of the molecules in the crystal lattices of

long-chain compounds characterize polymorphic transformations. Such alterations in crystalline structure result in consistent differences in physical properties which are generally not influenced by changes in environment, such as variation in the nature of the solvent.

The observed behavior of the ketones with respect to the solvent environment indicates that the unstable forms possess crystal lattices which are only slightly different from those of the stable forms. It is possible that the lattices of the respective forms differ only in degree of magnitude in one or more of their dimensions. This difference may be occasioned by a transition similar to that observed⁹ in the higher hydrocarbons, wherein a slight alteration in the lateral arrangement of the molecules permits some degree of rotation of the paraffin chains about their long axes. Thus, in the case of the unsymmetrical ketones, the more polar solvents may effect precipitation of relatively loosely packed crystals of the unstable form, which, by virtue of their lower free surface energy, would dissolve at temperatures below those of the corresponding more densely packed crystals of the stable form. Such a difference in degree of packing would account for the apparent dependence of the solubilities of the respective forms upon the specific properties of the solvents. Thus, the environmental conditions imposed upon the solute molecules by solvents of different polarities may induce varying degrees of lattice transformation and, consequently, solution temperatures of the unstable form would depend upon the energy requirements of the system. This hypothesis also could explain the observed irreversibility of the transition, for once the lattice has condensed to the more dense structure, it is not thermodynamically possible that it could reversibly "unpack."

Mole Fraction Solubilities.—Consideration of the solubilities of the stable crystal modifications on a mole fraction basis is illustrated by the 2-tridecanone systems shown in Fig. 4. These curves are typical of systems in which there is a substantial disparity between the molecular volumes of the solvent and solute. Such curves are generally characterized by abrupt deviation from linearity at relatively high concentrations of solute, relatively long transitional segments, and relatively gradual approximation to linearity at low concentrations of solute.

In the absence of thermodynamic data for the unsymmetrical ketones, the ideal solubility curve for 2-tridecanone was drawn empirically as shown in Fig. 4. The heat of fusion of this compound, calculated from the probable ideal solubility by means of the Hildebrand equation,¹⁰ was found to be 7.1 ± 0.1 kcal./mole. This value agrees favorably with 7.6 ± 0.5 kcal./mole for the heat of fusion of methyl laurate, which differs from 2-tridecanone only in possessing an additional oxygen atom (ester C-O linkage) in its molecular structure. The latter value was estimated by graphical ex-

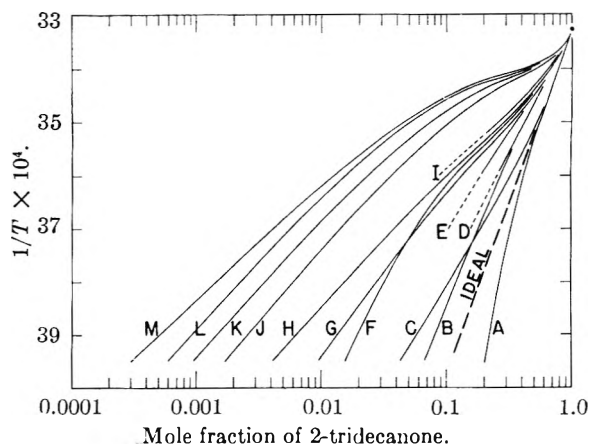


Fig. 4.—Mole fraction solubilities of 2-tridecanone in organic solvents: A, chloroform; B, toluene; C, carbon tetrachloride; D, benzene; E, cyclohexane; F, ethyl acetate; G, hexane; H, acetone; I, *p*-dioxane; J, 2-propanol; K, 95% ethanol; L, methanol; M, acetonitrile.

trapolation of the heats of fusion of methyl esters containing 14–22 carbon atoms in the acid chain.¹¹

The order of deviations from ideal solubility in Fig. 4 can be correlated directly with the relative magnitude of the internal pressures of the solvents,¹⁰ which are, in turn, partially dependent upon the respective polarities of the solvents. Thus, the solubility of 2-tridecanone is limited in such highly polar solvents as the alcohols and acetonitrile. Acetone because of its high internal pressure is a poor solvent for 2-tridecanone, whose internal pressure is considerably less because of its long paraffin chain. The relatively limited solubility of 2-tridecanone in *n*-hexane indicates, on the other hand, that the internal pressure of the solute is considerably higher than that of this simple aliphatic hydrocarbon. The internal pressure of 2-tridecanone apparently approximates those of carbon tetrachloride and toluene. The marked positive deviation of the chloroform solubility from ideal behavior is attributable to the highly active hydrogen-bonding characteristics of this halogenated hydrocarbon.

The solubilities of the other methyl alkyl ketones exhibit a pattern of deviations similar to those of 2-tridecanone, but differing in magnitude.

Further insight into the behavior of aliphatic ketones is obtained by comparing the mole fraction solubilities of symmetrical and unsymmetrical ketones of the same total chain length. Figure 5 shows the mole fraction solubilities of 2-nonadecanone together with those calculated from the previously published solubilities of 10-nonadecanone.⁴

Calculation of the heats of fusion from the initial slope¹⁰ of the chloroform solubility curves yields a value of 15.0 ± 0.2 kcal./mole for 2-nonadecanone and 15.4 ± 0.2 kcal./mole for 10-nonadecanone. These values agree favorably with that of a compound with similar molecular structure, 15.40 kcal./mole for methyl stearate.¹¹ The slight difference in the heats of fusion of the symmetrical and unsymmetrical ketones is probably attributable to

(9) J. D. Hoffman and B. F. Decker, *THIS JOURNAL*, **57**, 520 (1953).

(10) J. H. Hildebrand and R. L. Scott, "The Solubility of Nonelectrolytes," 3rd Edition, Reinhold Publ. Corp., New York, N. Y., 1950.

(11) A. M. King and W. E. Garner, *J. Chem. Soc.*, 1372 (1936).

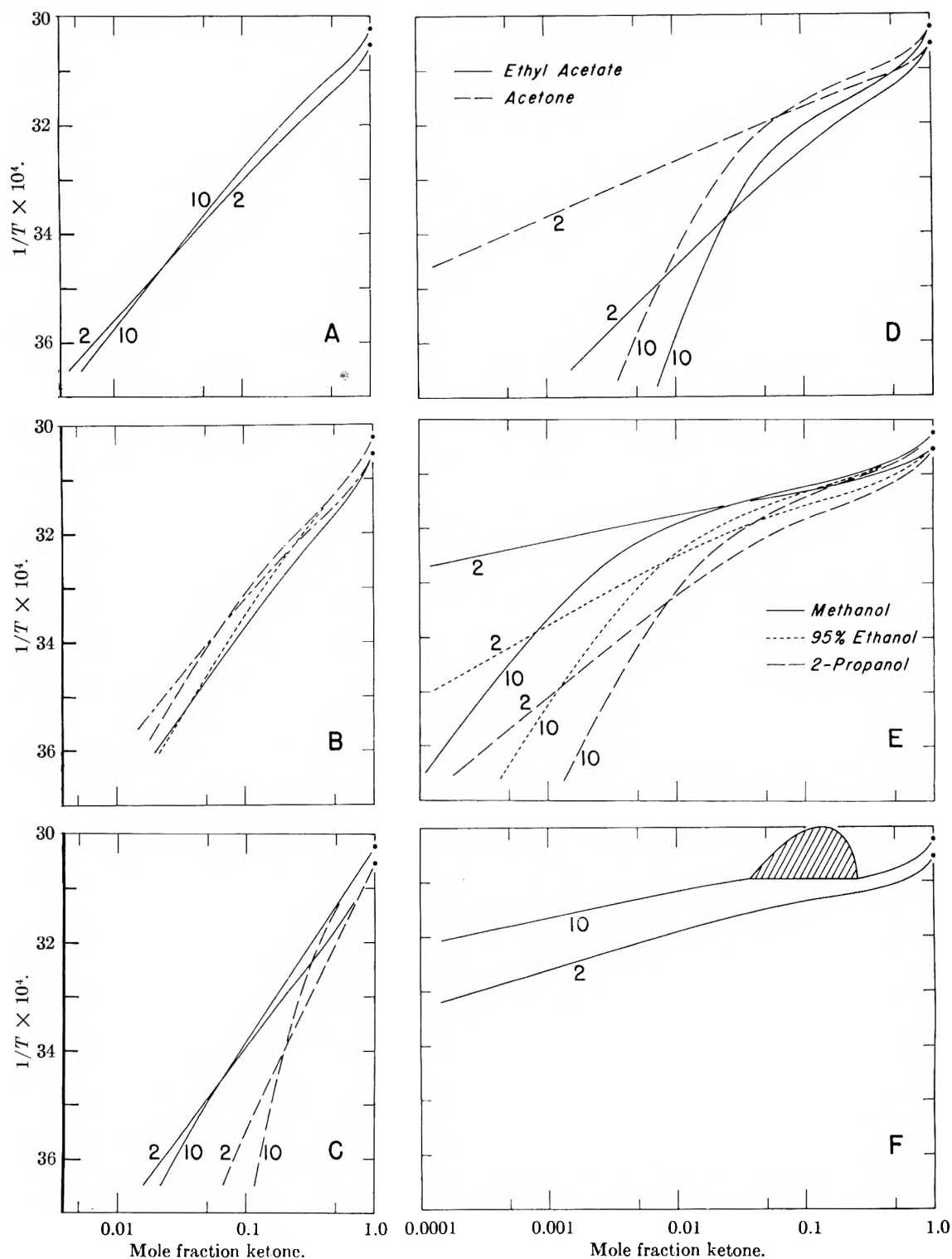


Fig. 5.—Mole fraction solubilities of 2-nonadecanone and 10-nonadecanone in organic solvents: A, hexane; B, benzene (—, ---, for 2-nonadecanone) and cyclohexane (---, ---, for 10-nonadecanone); C, carbon tetrachloride (—) and chloroform (---); D, ethyl acetate and acetone; E, methanol, 95% ethanol, and 2-propanol; and F, acetonitrile. The numbers on the curves refer to the respective isomer.

variation in the activation energy of melting which is supplied by a torsional oscillation of the paraffin chains about the carbonyl group.¹²

The estimated heats of fusion of 2-tridecanone and 2-nonadecanone can be used in evaluating

(12) J. W. H. Oldham and A. R. Ubbelohde, *Trans. Faraday Soc.*, **35**, 328 (1939).

their degree of purity by the method developed by Rossini and his associates for estimating the purity of certain hydrocarbons.^{13,14} The mole fraction of

(13) B. J. Mair, A. R. Glasgow, Jr., and F. D. Rossini, *Bur. Standards J. Research*, **26**, 591 (1941).

(14) A. R. Glasgow, Jr., A. J. Streiff and F. D. Rossini, *ibid.*, **35**, 355 (1945).

impurity in a compound can be estimated by means of the equation

$$N = \frac{1 - r}{r} \frac{H_{f_0}(T_{z_0} - T_z)}{R(T_{f_0})^2}$$

where

N is the mole fraction of impurity

H_{f_0} is the molar heat of fusion on the pure compound

T_{z_0} is the observed freezing point of the compound in °K.

T_z is the observed temp., °K., of a freezing sample at a given time, z , when a fraction, r , of the total sample has frozen

R is the gas constant, 1.9864 cal./°C./mole

T_{f_0} is the freezing point of the pure compound in °K.

(Of these values, T_{z_0} and T_z were obtained from cooling curve data within 0.1°, and H_f was estimated within 0.1 kcal./mole from solubility data. In the absence of a known value for the absolute freezing point, the geometric method devised by Rossini¹⁴ was used for estimating T_{f_0} from cooling curve data. By this means values for T_{f_0} were obtained which are approximately 0.01° above the observed freezing points.

By such calculations it was found that the 2-tridecanone and 2-nonadecanone used in this investigation contained 0.0006 ± 0.0002 mole of impurity, depending upon the limits of experimental error of the pertinent data. Even allowing double the probable experimental error, it was concluded that these methyl alkyl ketones contained less than 0.001 mole per cent. impurity. Thus, the unsymmetrical ketones can be considered to possess a sufficiently high purity for the purposes of this investigation.

Of significance in the diagrams in Fig. 5 is the fact that in all the solvents investigated, except for acetonitrile, the solubility curves of the symmetrical 10-nonadecanone, after a short initial segment, are steeper than those of the unsymmetrical 2-nonadecanone. Thus, the symmetrical ketone is generally more soluble than its unsymmetrical isomer. This observation contradicts a previous report.³

Increased internal pressure and/or polarity, which might conceivably result from shifting the position of the carbonyl group from the center of the paraffin chain, would tend to increase the solubility of the unsymmetrical homolog, particularly

in the polar solvents, and therefore could not account for decreased solubilities. Several investigators¹⁵ have reported that the solubility behavior of the ketones could not be explained simply by assuming intermolecular association (such as dipole-dipole coupling) of the solute.

The results of the present investigation suggest that the decreased solubility of the unsymmetrical ketones might be attributed to some form of intermolecular hydrogen bonding. In the case of the methyl alkyl ketones, the higher electron density near one end of the chain would be expected to enhance the bonding activity of the hydrogen atoms of the methyl group attached to the carbonyl. Such active hydrogen atoms would readily form bonds either with the oxygen atoms of neighboring ketone molecules or with hydrogen acceptor atoms of the solvent molecules, depending upon the relative energies of the bonds involved.¹¹ Hydrogen bonding among solute molecules via C-H-O bonds would effectively increase the dielectric constants of the unsymmetrical ketones and thus would account for the decreased solubility of these ketones in the non-bonding, non-polar solvents such as hexane, benzene and carbon tetrachloride. Inability of the active hydrogen atom of the ketones to break the already-existing strong O-H-O bonds of the alcohols would explain the lesser solubility of the unsymmetrical ketones in such strongly bonded solvents. The greater solubility of 2-nonadecanone in acetonitrile than in methanol, despite the high internal pressure of acetonitrile, indicates that the active hydrogen atoms of the ketones disrupt the relatively weak N-H-O and N-H-N bonds of acetonitrile to form stronger C-H-O bonds between solvent and solute molecules. That there is extensive interaction between 2-nonadecanone and acetonitrile molecules is evidenced by the compatibility of this system over a wide range of concentrations, whereas the symmetrical 10-nonadecanone in acetonitrile forms an immiscible liquid region over an appreciable concentration range.

(15) G. Berger, *Rec. trav. chim.*, **57**, 1029 (1938); K. L. Wolf, H. Frahm and H. Harms, *Z. physik. Chem.*, **B36**, 237 (1937); G. Hugel, *Oel Kohle Erdöl Teer*, **15**, 27 (1939); *cf. C. A.*, **34**, 3164 (1940).

CHEMICAL REACTIVITY OF CF_4 AND C_2F_4 INDUCED BY ELECTRICAL DISCHARGE

BY PAUL B. WEISZ

Contribution from Socony-Vacuum Laboratories, A Division of Socony-Vacuum Oil Co., Inc., Research and Development Department, Paulsboro, N. J.

Received December 16, 1954

Electron activation in the electrical glow discharge is shown to result in extensive reaction of CF_4 with SiO_2 to CO , CO_2 , O_2 and SiF_4 at near room temperature. Similar activation of C_2F_4 leads to liquid, mono-olefinic condensation products. The reactions are attributed to the initial formation of CF_3^{++} and of C_2F_4^+ ions, respectively.

Introduction

In a low pressure glow discharge, because of the weak interaction of the electron and the molecular (gas) assemblies, the average energies of the two can differ by a large amount.¹ For example, in a particular case² of a discharge at 1 mm. pressure, the gas temperature was about 300° , the quasi-temperature of the electron assembly, at the same time, was nearly 5000° . In such a system a steady state of electron and molecular energies can be maintained, but the distribution of chemical products need not be limited by thermodynamic equilibrium values based on the gas temperature. Furthermore, in producing electronically excited as well as ionized molecular states, the low pressure discharge may provide reaction paths unavailable in the normal thermal reaction systems.

We have studied the induction of chemical reactivity by electron activation for two perfluorocarbons: 1, pyrolysis of tetrafluoromethane, CF_4 , a compound of unusual thermal and thermodynamic stability^{3,4}; 2, the polymerization reaction of tetrafluoroethylene to liquid range olefins which is thermodynamically feasible at low temperatures but has not been successfully achieved by chemical means.

Experimental Procedure

The flow reaction system was used. The reactor consisted of one-half inch diameter Vycor tubing. An electrodeless discharge was induced by application of a radiofrequency voltage to the external electrodes. The electrodes and thus the glow discharge had a length of 3 cm. The charge gases were available at near atmospheric pressure. A needle valve determined the flow rate. The products were frozen into a trap cooled by liquid nitrogen. A valve between reactor and trap controlled the desired pressure in the reactor. A moderate pumping speed was usually maintained on the trap to eliminate the building up of non-condensable gases.

A controllable amount of radio-frequency power was supplied to the reactor from an oscillator amplifier. It was measured by noting the d.c. power performance of the radio-frequency amplifier and calibrating this d.c. power against the power supplied to an inductively coupled incandescent bulb. The latter was determined by the method of matching brightness between it and a second and similar incandescent bulb supplied by ordinary a.c. power through a watt meter.

Carbon tetrafluoride was obtained as a by-product from the direct fluorination of hydrocarbons and purified by low temperature fractionation. Tetrafluoroethylene was ob-

tained from the pyrolysis of Teflon and subsequent low temperature fractionation.

Results

Carbon Tetrafluoride.— CF_4 was subjected to a cold glow discharge at a pressure of 10 mm. and a flow rate of 60 std. cc./min. Various amounts of radio-frequency power were admitted to the discharge by varying the potential across the electrodes. The glass surfaces of the reaction system remained uncoated. However, glass was etched from the reactor wall and rapid depletion of the silica wall became evident. The etching of the surface diminished to an unnoticeable amount within 0.5 cm. from the end of the gas discharge volume in the direction of gas flow. At room temperature, no visible liquid product remained in the trap. The gaseous products were analyzed by a Consolidated mass spectrometer. The analyses showed production of CO_2 , CO , SiF_4 and O_2 . The quantitative analyses are presented in Fig. 1 as a function of the electrical power input to the reactor in units of kcal. of energy input per mole of reactant. Aside from the products included in Fig. 1, traces of COF_2 and C_6F_6 at concentrations not exceeding 1% were identifiable by mass spectral analysis.

Tetrafluoroethylene.—After passing tetrafluoroethylene through the discharge reactor at pressures ranging from 40 to below 1 mm., liquid product remained in the collection trap after reaching room temperature. Production of liquids resulted in the "cold" discharge, while approach to arc discharge conditions (higher pressure, higher gas temperature) resulted in a sharp drop of liquid range products in favor of gaseous products with carbon number two and three. This is demonstrated by the results shown in Table I.

TABLE I

PERFORMANCE OF C_2F_4 IN FLOW DISCHARGE SYSTEM UNDER COLD DISCHARGE AND NEAR ARC CONDITIONS			
Pressure, mm.	10	40	
Energy input/mole of reactant, kcal./mole	109	322	
Color of discharge	Blue	Yellow	
Flow rate, std. cc./min.	62 ± 5	70 ± 10	
Liquid product yield, % of charge	14	2	
Gaseous product anal., % (fractionation and mass spectrometer)	$\left\{ \begin{array}{ll} \text{C}_2\text{F}_4 & 89.7 \\ \text{C}_2\text{F}_6 & 1.4 \\ \text{C}_3\text{F}_6 & 8.9 \end{array} \right.$		$\left\{ \begin{array}{ll} 7.4 \\ 61.7 \\ 30.9 \end{array} \right.$

Figure 2 shows the product yield obtained *versus* energy input supplied to the reactant. These data were obtained at a flow rate of 50 std. cc./min. by varying the electrical power to the reactor by varia-

(1) A. V. Engel and M. Steenbeck, "Elektrische Gasentladungen," Vol. I, Julius Springer, Berlin, 1932, p. 53.

(2) C. G. Found, *I.E.S. Trans.*, **33**, 161 (1938); J. D. Cobine, "Gaseous Conductors," McGraw-Hill Book Co., New York, N. Y., 1941, Chapter 9.

(3) O. Ruff and O. Bretschneider, *Z. anorg. allgem. Chem.*, **210**, 173 (1933).

(4) L. White, Jr., and O. K. Rice, *J. Am. Chem. Soc.*, **69**, 267 (1947).

TABLE II
PROPERTIES OF LIQUID REACTION PRODUCTS FROM C_2F_4 REACTION, OBTAINED BY MICRODISTILLATION

Cut label	"Pot" temp., °C.	Wt., g.	Total wt. distilled, g.	B. p., °C.	n_D^{20}	$n_D - n_C$ Read.	Remarks
B	70-80	0.0716	0.0716	Below R.T.	1.280	0.06055	
C	80-100	.1638	.2354	Below R.T.	1.280	.06055	
D	100-140	.1252	.3606	32	1.285	.05537	
E	140-195	.1367	.4973	72.2-73.3	1.293	.05611	
G	195-250	.0549	.5522	?	1.298	.05632	
I	120	.1176	.6698	140-145	1.3250	.05524	At $p = 1$ mm.
S	120-200	.0222	.6920	165-180	1.3427	.05469	At $p = 1$ mm.

tion of the electrode potential at two constant pressures, 0.2 and 1 mm. The reactor in this experiment consisted of two concentric cylindrical Pyrex tubes, 35 mm. and 87 mm. diameter, 175 mm. long.

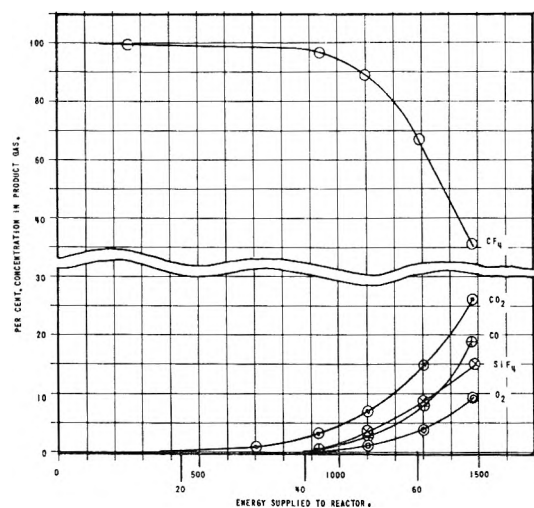


Fig. 1.— CF_4 reaction product concentration for various amount of energy supplied to the reactor per unit quantity of reactant in kcal./mole and in ev. molecule.

In contrast to the case of carbon tetrafluoride, no detectable reaction with silica occurred. Elemental analyses showed the liquid products to be perfluorocarbons of C_8 average carbon number.

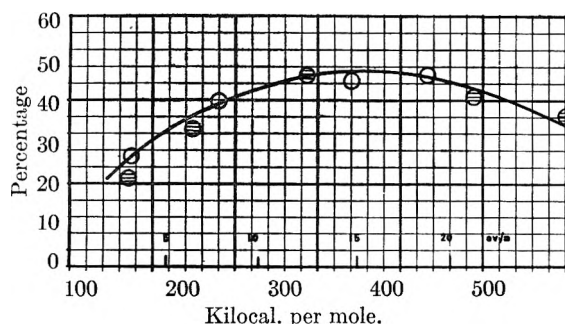


Fig. 2.—Weight percentage of C_2F_4 converted to liquid product for various amounts of energy supplied to the reactor per unit quantity of reactant.

A micro-distillation⁵ on a Craig⁶ column of ten theoretical plates on 1.5681 g. of liquid product resulted in the data summarized in Table II. It is possible to obtain a semi-quantitative picture of unsaturation by comparing boiling points and re-

(5) The author is indebted to I. A. Breger, Geology Dept., M.I.T., and his assistants for their indispensable help in obtaining these micro-distillation data.

(6) L. C. Craig, *Ind. Eng. Chem., Anal. Ed.*, **9**, 441 (1937).

fractive indices of the individual cuts from the micro-distillation with those of known compounds. This comparison is undertaken in Fig. 3. In the

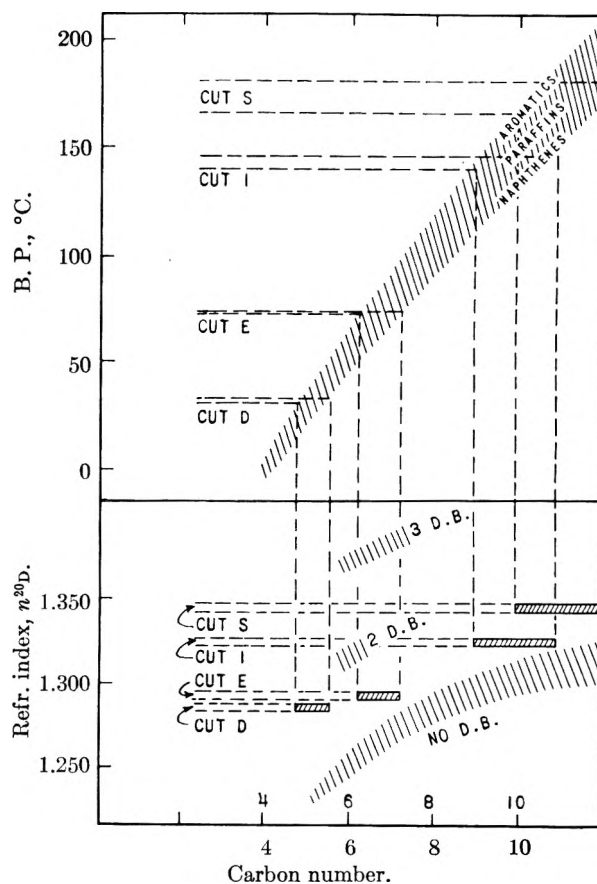


Fig. 3.—Deduction of degree of unsaturation of liquid products obtained from C_2F_4 , by comparing boiling points and refractive indices with those of known compounds. \parallel , known compounds; /// , properties of distillation cuts; D. B., double bonds.

upper portion, boiling points of four of the distillation cuts are used to derive their carbon number by comparison with known compounds. In the lower portion of the graph this information is combined with the values of the refractive index of the respective cuts. It will be seen that unsaturation of about one double bond per molecule is indicated. This mono-olefin character of the product was further confirmed by the nature of the mass spectrometer patterns and later by chlorination.

Discussion and Conclusions

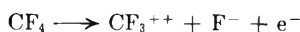
Carbon Tetrafluoride.—The product analyses shown in Fig. 1 show that CF_4 reacted with SiO_2

at up to 60% conversion during a molecular residence time of about 0.06 second in the discharge space at a temperature $\sim 100^\circ$. The over-all reaction can be described well by the formula



The analytical deficiency in SiF_4 is well explained by contact with traces of water previously observed in mass spectrometer analyses.

Mass spectrometer studies⁷ show that the ionization process of the parent molecule, *i.e.*, $\text{CF}_4 \rightarrow \text{CF}_4^+ + e^-$, does not occur. The first ion producing mechanism occurring at lowest electron energy (15.9 e.v.) yields CF_3^+ ions. Since an electrical discharge is produced only by virtue of an electron multiplication process accompanying molecular ionization, it follows *a priori* that chemical dissociation will necessarily accompany the occurrence of a discharge in CF_4 . There is evidence,⁷ furthermore, that the production of CF_3^+ ion does not generate an electron but occurs as $\text{CF}_4 \rightarrow \text{CF}_3^+ + \text{F}^-$. The first electron producing ionization process may be the reaction



requiring 43.8 e.v. electron energy, which would necessarily be the initial process of consumption of CF_4 molecules. The results in Fig. 1 show that

(7) V. H. Dibeler and F. L. Mohler, *J. Research Natl. Bur. Standards*, **40**, 25 (1948).

an appreciable fraction of CF_4 is indeed converted when the average electrical energy per molecule exceeds some 40 e.v., which supports the view that the initiating process is the highly energetic step indicated above.

Tetrafluoroethylene.—The cold electrical discharge successfully induces condensation reactions of C_2F_4 leading to liquid mono-olefins.

In case of C_2F_4 the production of the parent ion C_2F_4^+ is known to be the energetically lowest ion and electron producing process at 10.3 e.v. It must be held responsible for the sustenance of the glow discharge and for yielding C_2F_4^+ as the initial active species resulting in further chemical reaction. This view finds support in the observation of Fig. 3 that a large fraction of tetrafluoroethylene undergoes chemical conversion to products of three times the original molecular weight when the average energy supplied is as low as $10.3/3 \approx 3$ e.v. Absence of any reaction with SiO_2 speaks further for the absence of fragment ion production which would split off F or F_2 .

Ion neutralization in collision with the wall is a highly exothermic process accompanied by dissociation⁸ which can easily give rise to product molecules of odd carbon numbers, as are seen in the gas analysis shown in Table I.

(8) P. B. Weisz, *This Journal*, **52**, 578 (1948).

THE ELECTRICAL CONDUCTANCE OF WEAK ACIDS IN ANHYDROUS HYDRAZINE¹

BY LEON J. VIELAND² AND RALPH P. SEWARD

Contribution from College of Chemistry and Physics, The Pennsylvania State University, University Park, Pa.

Received December 23, 1954

The conductance of dilute solutions of phenol and four substituted phenols in hydrazine has been measured at 25° . Dissociation constants varying from 1.8×10^{-4} for *p*-cresol to 6.4×10^{-3} for *p*-chlorophenol were obtained. Conductance in the water-hydrazine system over the complete composition range was measured. For dilute aqueous solution a dissociation constant for hydrazine as a base of 9×10^{-7} was calculated. Water in nearly anhydrous hydrazine was found to be an extremely weak electrolyte.

Anhydrous hydrazine, having a liquid range similar to that of water, has a relatively high dielectric constant, 51.7 at 25° , according to Ulich and Nespital,³ and is known to be a good solvent for many salts. As it has not been employed as a solvent to any great extent, presumably because of its instability and rapid contamination when exposed to the atmosphere, it seemed worthwhile to investigate further its behavior as a solvent for electrolytes. Walden and Hilgert⁴ prepared anhydrous hydrazine having a specific conductance of $2\text{--}3 \times 10^{-6}$ ohm⁻¹ cm.⁻¹ and measured the conductance of a number of electrolytes in this solvent. These investigators found that salts in hydrazine, with due allowance for the difference in dielectric con-

stant, behaved much like they do in water. The strongly basic nature of the solvent, however, promoted such acids as benzoic, of $K = 6 \times 10^{-5}$ in water, to strong electrolytes in hydrazine.

For the present investigation, it was decided to study such weak acids that, even in hydrazine, dissociation would be incomplete, so that the change in dissociation constant accompanying the change in medium could be measured. For this purpose, phenol and four substituted phenols were selected. In addition, the conductance of water-hydrazine mixtures was measured over the complete range of composition, and the conductance of methyl alcohol in hydrazine was measured. Dissociation constants for the phenols in hydrazine have been evaluated, but the conductance of water and methyl alcohol was found to be too small for quantitative treatment. The conductance of dilute solutions of hydrazine in water was measured and its ionization constant calculated for comparison with previously reported values.

(1) This research was supported by the United States Air Force under contract No. AF(600)-448 monitored by the Office of Scientific Research.

(2) From the Ph. D. thesis of Leon J. Vieland, June, 1954.

(3) H. Ulich and W. Nespital, *Z. physik. Chem.*, **B16**, 221 (1932).

(4) P. Walden and H. Hilgert, *ibid.*, **A165**, 241 (1933).

Experimental

Materials.—Hydrazine was prepared by drying and distilling, starting with a commercial "anhydrous" product. After a preliminary distillation from potassium hydroxide the hydrazine was allowed to stand over barium oxide for several days and then distilled under reduced pressure into the apparatus. Calcium hydride was tried as a drying agent but abandoned. Although calcium hydride was undoubtedly effective in removing water, hydrazine of consistently low specific conductance was not obtained when it was used. When distilled from the barium oxide and once redistilled directly into the cell, hydrazine having a specific conductance of $1.7\text{--}3.0 \times 10^{-6}$ at 25° was obtained. This is about the same as the hydrazine used by Walden and Hilgert.⁴ The measurements on water and methyl alcohol solutions were made with this solvent. In the completely closed system, used for the phenol solutions, where repeated distillation and cycling through the cell was possible, hydrazine having a specific conductance $1.5\text{--}3.0 \times 10^{-7}$ was obtained.

Water from the laboratory triple still had a specific conductance of $1\text{--}2 \times 10^{-6}$ at 25° . Carbon dioxide-free nitrogen was bubbled slowly through the water before its use in making hydrazine solutions. After this treatment, its specific conductance was about 0.8×10^{-6} .

Phenol (m.p. 40.9°) and *p*-chlorophenol (m.p. 44.0°) were obtained by twice distilling under vacuum commercial purified materials.

o-Cresol (m.p. 31.0°), *m*-cresol (m.p. 11.3°) and *p*-cresol (m.p. 33.8°) were obtained from "Practical" grades by distilling through a fractionating column and redistilling *in vacuo*.

Apparatus.—The bridge consisted of a Leeds and Northrup Campbell-Shakelton shielded ratio box, a 100,000 ohm variable resistance box with parallel condenser, and the cell which was immersed in an oil-filled bath whose temperature was constant to $\pm 0.02^\circ$ at $25 \pm 0.1^\circ$. A variable audio frequency oscillator served as current source. Balance was detected with a telephone head set with the aid of an amplifier. The cells had non-platinized electrodes. When resistance readings were made at 1000 and 2000 cycles, differences of a maximum of 0.1% were observed. The values employed were obtained by extrapolation to infinite frequency. It is thought that the resistance measurements are accurate to $\pm 0.1\%$. This is probably a little better than the accuracy of the concentrations.

The cell used for the hydrazine water solutions was constructed from a 500-ml. round-bottom flask with an electrode chamber attached. Electrode leads through the glass were tungsten wires. A side tube from the flask permitted its evacuation or the passage of nitrogen through it. A ground joint at the top was used to connect the cell to the source of hydrazine. This cell had a constant of 0.429. In operation, the cell was first weighed empty, then connected and hydrazine distilled in at reduced pressure. After admitting dry nitrogen, the cell was disconnected from the hydrazine line while nitrogen passed through it and out the ground joint. The joint was then capped and the cell weighed. Water was added to the cell from a weight buret in various amounts in a similar way.

The measurements on the phenols were made in a way that was thought to be an improvement over the procedure described above, in that the solutions were made up and all dilutions carried out in a closed system, precluding possible contamination from the atmosphere. About 300 ml. of hydrazine was distilled into a flask which was equipped with a break off tube, the contents of the flask were frozen, and it was sealed as it was removed from the hydrazine line. After sealing onto the dilution system, the latter was evacuated and the tube leading to the hydrazine was broken off with the aid of a magnet. The solvent was then distilled into a storage bulb from which small amounts of liquid could be pushed, by raising the level of mercury at the bottom, into a U, where volumes and resistances were measured. The U extended into the oil bath with the cell near the bottom of one side. This cell had a constant of 0.02878. Above the cell was a 10-ml. buret where readings were made to obtain the volume of solution to ± 0.01 ml. Above the graduated portion, a side tube held a small ampoule of solute. The other side of the U consisted of a tube of 10-ml. volume. This volume, together with that of the cell (about 20 ml.) and the buret, had been calibrated by addi-

tion of water from a weight buret. Finally, at the top of both sides of the U were 50-ml. bulbs to facilitate mixing and on one side the entry tube for liquid solvent and on the other, a tube leading to the waste solution container from which the solvent was regenerated by distillation back to the solvent storage bulb.

In making a series of measurements, the cell was flushed with pure solvent until consistently low (less than 3×10^{-7} ohms⁻¹ cm.⁻¹) conductance was obtained. With a known volume of solvent in the U, the solute ampoule was broken with a magnetically operated breaker, and the solution pushed from one arm of the U to the other by pressure of dry, CO₂-free nitrogen until a constant resistance was observed. After pushing out part of the solution and noting the volume remaining, more solvent was added, the new volume recorded, and after mixing, the resistance of the new solution measured. In order to hold the number of dilutions to a reasonable maximum in covering the concentration range of interest, as the solvent volumes were small, it was necessary to use very small solute samples. Samples of 3 to 30 mg. were weighed in ampoules of about 0.3 g. on a microbalance to 1 microgram. Careful buoyancy corrections were made. The authors are indebted to Professor G. H. Fleming for making the weighings.

Experimental Results

The equivalent conductances at 25° of some dilute solutions of hydrazine in water of specific conductance 8.5×10^{-7} are presented in Table I, together with a dissociation constants calculated for each concentration.

TABLE I
SPECIFIC CONDUCTANCE OF DILUTE AQUEOUS HYDRAZINE SOLUTIONS AT 25°

<i>C</i> , mole/l. $\times 10^2$	0.201	0.635	1.000	2.454
Λ	5.71	3.21	2.55	1.64
<i>K</i> $\times 10^7$	8.55	9.15	9.16	9.48

The specific conductances of mixtures of water of specific conductance 8×10^{-7} and hydrazine of specific conductance 1.6×10^{-6} are shown in Table II.

TABLE II
SPECIFIC CONDUCTANCES (*L*) AT VARIOUS COMPOSITIONS IN THE WATER-HYDRAZINE SYSTEM AT 25°

Mole % N ₂ H ₄	$10^6 L$	Mole % N ₂ H ₄	$10^6 L$
0.25	97	43.5	56
3.8	299	53.2	29.1
8.1	325	64.6	12.7
14.0	335	74.6	6.09
19.2	247	84.0	3.14
25.6	179	93.0	1.99
36.5	90	98.3	1.64

The conductances of phenol and four substituted phenols were measured in dilute solution in anhydrous hydrazine. The values appearing in Table III for phenol are typical.

TABLE III
EQUIVALENT CONDUCTANCE OF PHENOL IN ANHYDROUS HYDRAZINE AT 25°

$10^4 C$, mole/l.	2.167	2.983	4.317	6.621	8.765
Λ	102.7	96.81	89.45	80.45	74.46

The data for the phenols were treated by Shedlovsky's⁵ method for incompletely dissociated electrolytes. At the lower concentrations, linear plots were obtained from which the limiting equivalent

(5) T. Shedlovsky, *J. Franklin Inst.*, **225**, 739 (1938).

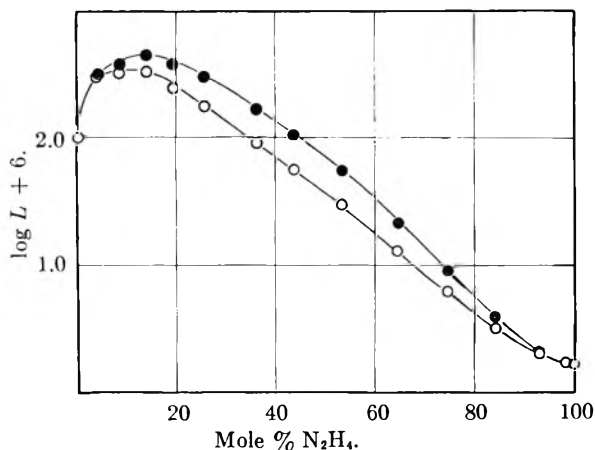


Fig. 1.—The specific conductance of hydrazine-water solutions at 25°: ○, measured; ●, corrected to uniform viscosity.

lent conductances and dissociation constants were calculated. The linearity of the plots was sufficient to fix the constant to about $\pm 1\%$. The solvent conductance did not exceed 0.3% of the measured conductance in any of the solutions and no correction was made for it. It was noted that the deviation from the straight lines began at lower concentrations than would be predicted from the value of 51.7 which is the reported dielectric constant of hydrazine. The behavior of the phenols is summarized in Table IV.

TABLE IV

LIMITING CONDUCTANCE AND DISSOCIATION CONSTANTS OF PHENOLS IN HYDRAZINE AT 25°

Solute	Concn. range, mole/l. $\times 10^4$	Λ_0	$10^4 K$	pK	pK in water ^d
Phenol	2-9	130.0	6.62	3.18	9.95
<i>c</i> -Cresol	3-27	129.0	3.60	3.44	10.20
<i>m</i> -Cresol	3-80	127.4	4.08	3.39	10.01
<i>p</i> -Cresol	7-70	128.5	1.79	3.75	10.17
<i>p</i> -Chlorophenol	2-25	127.4	64.2	2.18	9.38

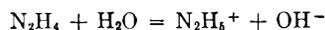
As it has been reported⁷ that methyl alcohol is more acidic than water, the conductance of a solution of methyl alcohol in hydrazine was measured. This conductance was so close to that of the solvent that the dissociation of methyl alcohol in hydrazine, like that of water, could not be estimated.

Discussion

In calculating the dissociation constants for hydrazine as a base, which appear in Table I, the solvent conductance was subtracted and corrections for the effect of the ionic atmosphere on conductance and activity coefficients made. The latter are relatively small, but in the most dilute solution the solvent conductance was 8% of the total and the calculated constants perhaps no more accurate than to $\pm 10\%$. The mean value of K , 9.1×10^{-7} , is in agreement within these limits with the potentiometrically determined constants, 9.84×10^{-7} , by Ware, Spulnik and Gilbert,⁸ 8.5×10^{-7} (20°) by

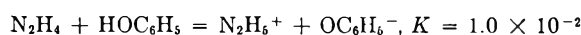
Schwarzenbach,⁹ and 8.63×10^{-7} by Yui¹⁰ but not with the earlier conductometric value, $2-3 \times 10^{-6}$, of Bredig.¹¹ Bredig, however, used 224 as the limiting conductance and his constants would have been smaller by about one-fourth had he used modern values of the limiting ion conductances, 59 for $N_2H_5^{+12}$ and 198 for OH^- , giving 257 as the limiting conductance for aqueous hydrazine.

The specific conductance over the complete water-hydrazine composition range is shown in Fig. 1. As the conductance is determined in part by the mobilities of the ions and the mobilities are, nearly at least, inversely proportional to the viscosity of the medium, assuming the current is carried by the same ions over the complete range of composition, the variation in conductance due to this factor may be eliminated by multiplying the measured values by the ratio of the viscosity at the given composition to the viscosity of water. This has been done using the viscosity data of Semishin,¹³ and the second curve shows the conductance corrected to equal viscosity as a function of composition. Points on this curve should be more nearly representative of ion concentrations in the various mixtures. It may be seen from the figure that whereas a small addition of hydrazine to water causes a very large increase in conductance, addition of a small amount of water to hydrazine causes a very small increase in conductance. It may be concluded that water in nearly anhydrous hydrazine is an extremely weak electrolyte. As it may be presumed that the ion forming reaction is



over the whole system, and as hydrazine has a lower dielectric constant, a decrease in the extent of this reaction with increasing hydrazine content should be expected. Lack of knowledge of the dielectric constants of the mixtures and activity coefficients of hydrazine and water at 25°, prevents a quantitative approach to the problem; but equilibrium constants calculated using molar concentrations, those for the ions obtained on the assumption of a constant Λ_0 , fall off so rapidly with decreasing dielectric constants, which were estimated by assuming a linear relation of dielectric constant with mole fraction, that an improbably small mean ionic radius is obtained from the Born equation.

For the phenols, the decreases in pK on going from water to hydrazine are roughly equal, varying from 6.4 to 7.2. The shift in pK not due to the difference in the basicity of the two solvents may be estimated, in the case of phenol, for example, by calculating for dilute aqueous solution from its ionization constant of 1.0×10^{-10} and the ionization constant of hydrazine as a base of 1.0×10^{-6} , that for



In hydrazine this reaction has a constant of 2.1×10^{-5} , obtained by dividing the constant 6.6×10^{-4}

(9) G. Schwarzenbach, *Helv. Chem. Acta*, **19**, 178 (1936).

(10) N. Yui, *Bull. Inst. Phys. Chem. Research (Tokyo)*, **20**, 256 (1941).

(11) G. Bredig, *Z. physik. Chem.*, **13**, 289 (1894).

(12) E. C. Gilbert, *J. Am. Chem. Soc.*, **53**, 3956 (1931).

(13) V. I. Semishin, *J. Gen. Chem. (USSR)*, **8**, 654 (1938).

(6) D. R. Boyd, *J. Chem. Soc.*, **107**, 1538 (1915).

(7) J. Hine and M. Hine, *J. Am. Chem. Soc.*, **74**, 5266 (1952).

(8) G. C. Ware, J. B. Spulnik and E. C. Gilbert, *ibid.*, **58**, 1605 (1936).

from Table IV by the concentration of hydrazine in the anhydrous solvent to put the constants on a comparable basis, and thus an increase of 2.66 in pK is attributable to the change in the nature of the medium. As is the case with water, this change is too large to be related satisfactorily to the dielectric constant of hydrazine by simple electrostatic theory.

Although phenol in hydrazine may be completely converted to a salt, there must be more than coul-

ombic interaction between the ions. For simple ion pair formation with a dissociation constant of 6.6×10^{-4} in a medium of dielectric constant 51.7 at 25°, a physically unlikely mean ionic diameter of 0.7×10^{-8} is obtained from the relation proposed by Fuoss and Kraus.¹⁴ It is likely that the ions and molecules in these solutions are more complex than those indicated in the equation above.

(14) R. M. Fuoss and C. A. Kraus, *J. Am. Chem. Soc.*, **55**, 1024 (1933).

SELF-DIFFUSION IN LIQUID *n*-PENTANE AND *n*-HEPTANE¹

BY ERWIN FISHMAN²

Department of Chemistry, Brown University, Providence, Rhode Island

Received December 27, 1954

The self-diffusion coefficients of *n*-pentane and *n*-heptane have been measured over most of their liquid temperature ranges. Tritium-tagged hydrocarbons served as the tracer for the capillary-type diffusion experiments. A gas phase sampling technique was employed after the diffusion. The results can be represented by the equations $D = 8.11 \times 10^{-4} e^{-1597/RT}$ (pentane) and $D = 1.35 \times 10^{-3} e^{-2246/RT}$ (heptane); however, some curvature is evident in the plots of $\log D$ vs. $1/T$. The molecular dimensions calculated with these data and viscosity data, using the Eyring theory, are in qualitative agreement with the known molecular dimensions.

Introduction

There now exists a rather extensive list of pure liquids whose self-diffusion coefficients have been determined. Some examples are water,³ sulfur,⁴ mercury⁵ and indium,⁶ and, of the organic liquids, carbon disulfide,⁷ benzene⁸ and ethanol.⁸ In this paper a study of the self-diffusion of normal pentane and heptane is presented. These liquids were chosen as being particularly amenable to treatment by the Eyring rate process theory of diffusion and viscosity⁹ because they are unassociated liquids and because their geometry should lead to diffusion preferentially along the carbon chain axis. This latter condition lends some significance to the various λ 's appearing in the Eyring equations, as will be seen later. Also, these liquids were chosen because they remain in the liquid state over a wide temperature range, allowing an accurate determination of the activation energy and its possible variation with temperature, and because the experimental procedure developed for them will be applicable to a large number of hydrocarbons in the C₅ to C₉ range. Thus, in future work, one may be able to obtain empirical relationships between self-diffusion coefficients, shapes, sizes and molecular weights of substances whose external force fields are quite

similar. These relationships could be a further lead in the development of an exact theory of liquids.

Experimental Procedure

Tritium-substituted hydrocarbons were used as tracers in this work. Phillips Petroleum Company "Pure Grade" pentene-2 and heptene-2 were reduced over platinum with a tritium-hydrogen mixture. The product was refluxed overnight with concentrated sulfuric acid, washed with sodium carbonate and water, then distilled in a Stedman fractionating column operating at a reflux ratio of about 10 to 1. The corresponding Phillips "Pure Grade" saturated hydrocarbons were used for the inactive constituent without further purification other than drying. The infrared spectra of all materials agreed exactly with the published spectra.¹⁰ The activity of the reduced material was adjusted to about 10¹⁰ counts per minute per mole.

The diffusion experiments were carried out by the capillary method of Anderson and Saddington¹¹ with the modification that the capillaries were fitted to a brass holder, permitting them to be closed off. The brass holder served the dual purpose of allowing manipulation of the capillary tubes before and after diffusion without loss of contents from evaporation and of providing a mechanism for introducing the contents to the vacuum system for sampling. Figure 1 illustrates the capillary holder. The circular disk of neoprene sealed the top of the capillary. The long handle and flattened base allowed the holder to be opened and closed in the reservoir where diffusion took place (Fig. 2) and in the vacuum system. The opener in the vacuum system consisted of two sections, one fitted to the base and one to the handle of the brass holder. These were connected by a standard taper glass joint so that rotation about the joint opened the holder.

The vibrations of the stirring motor in the constant temperature bath provided adequate stirring for the diffusion runs. This was demonstrated by the lack of dependence of the diffusion coefficients on time of diffusion or capillary length.

The temperature was controlled to $\pm 0.1^\circ$. An oil-bath thermostat was used for the runs at room temperature and above. In addition the following transition points were used for temperature control: (1) solid-liquid H₂O at 0°; (2) solid-liquid CCl₄ at -22.9° ; (3) solid-gas CO₂ at -78.5° . The Dry Ice thermostat contained a heating coil to expel the air, and a stirring motor was attached to

(1) Based on a Thesis submitted in partial fulfillment of the requirements for the Ph.D. degree, Brown University, 1954.

(2) Now at the Department of Chemistry and Chemical Engineering, University of Illinois, Urbana, Illinois.

(3) J. H. Wang, C. V. Robinson and I. S. Edelman, *J. Am. Chem. Soc.*, **75**, 466 (1953). This paper contains references to earlier papers on self-diffusion in liquid water by J. H. Wang.

(4) R. L. Saxton and H. G. Drickamer, *J. Chem. Phys.*, **21**, 1362 (1953); D. R. Cova and H. G. Drickamer, *ibid.*, **21**, 1364 (1953).

(5) R. E. Hoffman, *ibid.*, **20**, 1567 (1952).

(6) G. Careri, A. Paoletti and F. L. Salvetti, *Il Nuovo Cimento*, **11**, 399 (1954).

(7) R. C. Koeller and H. G. Drickamer, *J. Chem. Phys.*, **21**, 267 (1953).

(8) K. Graupner and E. R. S. Winter, *J. Chem. Soc.*, 1145 (1952).

(9) S. Glasstone, K. J. Laidler and H. Eyring, "The Theory of Rate Processes," McGraw-Hill Book Co., New York, N. Y., 1941.

(10) American Petroleum Institute Research Project 44 at National Bureau of Standards, Infrared Absorption Spectrograms.

(11) J. S. Anderson and K. Saddington, *J. Chem. Soc.*, S 381 (1949).

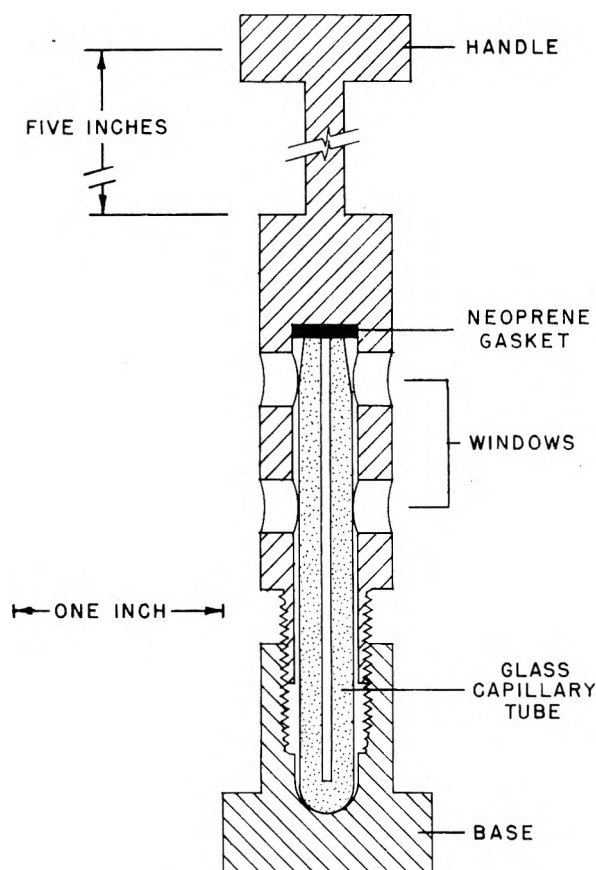


Fig. 1.—Capillary holder.

provide vibrational stirring for the diffusion cells, although no stirring was required for the thermostat. For the runs below room temperature, the diffusate was precooled to keep it from further contraction in the capillary tube when it was immersed in the cold reservoir.

After about 15 minutes had been allowed for temperature equilibration with the capillary holder closed, the diffusion runs were initiated by unscrewing the cover section and removing it from the reservoir. The cover was securely replaced to terminate the diffusion; then the entire holder was removed from the reservoir and placed into the opener in the vacuum system. Here the air and excess hydrocarbon were quickly pumped away. Then the brass holder was unscrewed and the contents of the capillary evaporated into an isolated section of the vacuum system. Next the hydrocarbon was frozen out in a small trap which was part of a mixing bulb. Argon was added to the mixing bulb and stirred with the hydrocarbon by a Teflon-coated magnetic stirrer. The resulting gas mixture was about 10% hydrocarbon to 90% argon. Some preliminary experiments demonstrated that this was a good counting gas mixture with either pentane or heptane. Actually any mixture of from 5 to 20% hydrocarbon in argon gave satisfactory results in our counter.¹²

After the mixing operation, the gas was expanded into the counter, yielding a final pressure of about 15 cm. The voltage on the counter was adjusted to provide a constant pulse height from experiment to experiment. The background was determined by filling the counter with a gas mixture prepared exactly as the active samples were prepared. There were no difficulties with memory effects as long as no free tritium or tritium oxide entered the counter. Only mercury float valves were employed in the portion of the vacuum system used for handling the hydrocarbon vapors. (A fritted glass "leak" incorporated in the valve leading from the mixing bulb allowed it to be opened, although a difference in pressure of 20 to 25 cm. existed at the time of opening.) Assuming good mixing, an aliquot sample

(12) Thin-walled β counter, purchased from the Eck and Krebs Company, Long Island City, New York.

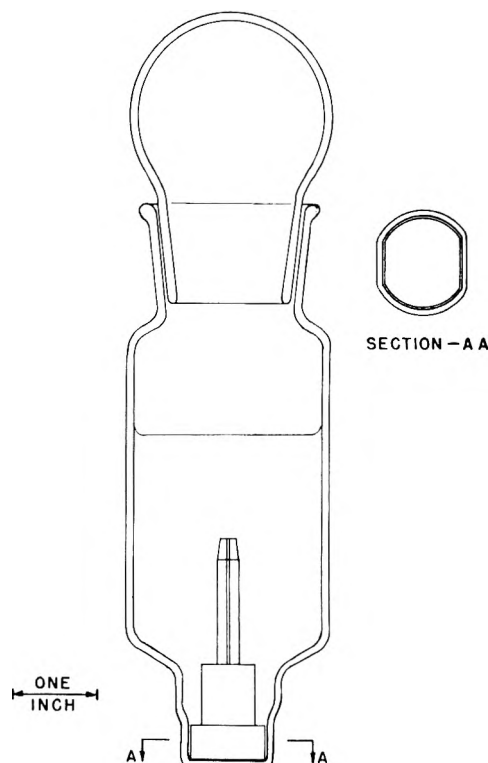


Fig. 2.—Diffusion reservoir with base of capillary holder.

of hydrocarbon was introduced into the counter each time; therefore, the specific activity of the hydrocarbon could be determined by the counting rate and the volume and density of the hydrocarbon in the capillary. This was not the true specific activity defined as counts per minute per gram of material, but some undetermined constant times the true value. This constant, however, canceled out of the diffusion calculations, since only the ratio of specific activities before and after diffusion appeared in them.

Results

The diffusion coefficients were calculated using the following solution to the diffusion equation

$$D = \frac{4 l^2}{\pi^2 t} \ln \frac{8 A_d}{\pi^2 A_0}$$

where

- D = diffusion coefficient in cm^2/sec .
- l = length of capillary in cm.
- t = time of diffusion in sec.
- A_d = av. specific activity in the capillary after diffusion
- A_0 = specific activity of the diffusate before diffusion

No systematic errors due to end effects could be observed by plotting length of capillary against the deviation from the average D , although capillaries varying in length from 1.5 to 5.0 cm. were used. (Only the shortest capillaries could be employed for the *n*-heptane at -78.5° , otherwise diffusion periods of several weeks would have been required to get sufficient accuracy.) The capillaries had an inside diameter of about 1 mm. Some preliminary work showed that this was the optimum size for obtaining experimental accuracy and minimizing end effects. Most of the observed scatter of about 5% must be attributed to random sampling errors or random end effects during diffusion.

Table I contains the experimental results. The error quoted is the probable error, so defined that there is a 50% probability that the true value

lies within the limits. As shown, a probable error was determined at each temperature.

Figure 3 contains a plot of $\log D$ vs. $1/T$ for both liquids. The vertical line drawn through each experimental point gives the extent of the probable error. The heavy solid lines are the best straight line representations obtained by the method of least squares (no weighting factor). The equations for these lines are

$$D = 8.11 \times 10^{-4} e^{-1597/RT} \text{ for pentane, and}$$

$$D = 1.35 \times 10^{-3} e^{-2246/RT} \text{ for heptane}$$

Also present is a dotted curve drawn to pass near the center of each experimental point. Its purpose is to emphasize the curvature of the $\log D$ vs. $1/T$ plot. It must be stated that the experiments are not accurate enough to decide unequivocally between the two representations; however, the decided curvature of those experimental points whose probable error is very small would lead one to favor the dotted line representation.

TABLE I
DIFFUSION COEFFICIENTS

Capillary length (cm.)	Time of diffusion (hr.)	Temp. (°C.)	$D \times 10^6$ (cm. ² /sec.)	D av. $\times 10^5$ (cm. ² /sec.)
<i>n</i> -pentane				
4.36	20.65	35.5	6.38	
3.58	21.90	35.5	6.45	
3.58	21.92	35.5	6.44	
5.12	22.50	35.5	5.70	6.29 ± 0.13
3.58	25.15	35.5	6.60	
5.12	26.00	35.5	6.19	
4.36	19.95	25.0	5.30	
3.58	28.52	25.0	5.49	
3.58	20.65	25.0	5.73	
4.36	20.50	25.0	5.20	5.62 ± .22
1.509	17.05	25.0	6.13	
3.58	20.12	25.0	5.62	
1.491	17.38	25.0	5.87	
3.58	23.32	0.0	4.24	
5.57	23.93	.0	4.45	
4.36	28.68	.0	4.46	
3.58	29.42	.0	4.19	
4.36	25.16	.0	3.64	4.14 ± .18
1.509	9.06	.0	4.25	
5.02	25.92	.0	3.95	
3.58	24.70	.0	3.98	
3.58	23.43	-22.9	2.26	
1.491	22.02	-22.9	3.18	2.97 ± .32
3.58	21.13	-22.9	3.26	
1.571	17.45	-22.9	3.19	
1.509	19.65	-78.5	1.45	
1.571	17.13	-78.5	1.52	1.38 ± .08
1.509	21.20	-78.5	1.26	
1.491	14.00	-78.5	1.28	
<i>n</i> -Heptane				
4.36	21.38	95.8	6.34	
5.12	22.23	95.8	6.58	6.56 ± .15
3.58	22.33	95.8	6.77	
4.36	20.06	80.2	5.59	
5.02	18.87	80.2	5.54	5.76 ± .20
5.12	19.33	80.2	5.72	
3.58	19.68	80.2	6.20	
4.36	20.06	56.6	4.07	
5.02	20.53	56.5	4.12	4.21 ± .10

5.12	20.82	56.5	4.32	
3.58	19.53	56.5	4.35	
5.12	20.10	32.5	3.06	
4.36	41.57	32.5	3.07	3.22 ± .13
5.12	42.77	32.5	3.33	
3.58	45.32	32.5	3.43	
5.12	42.09	0.0	2.08	
3.58	22.50	.0	1.95	
3.58	17.35	.0	2.08	
4.36	44.32	.0	2.11	2.08 ± .04
5.12	45.25	.0	2.15	
5.12	43.00	.0	2.14	
3.58	41.43	.0	2.08	
1.491	17.10	-22.9	1.45	
1.509	16.17	-22.9	1.54	1.52 ± .06
3.58	25.68	-22.9	1.63	
1.571	19.58	-22.9	1.46	
1.491	25.45	-78.5	0.596	
1.571	17.57	-78.5	.339	
1.571	38.63	-78.5	.444	0.415 ± .067
1.509	39.78	-78.5	.407	
1.571	45.09	-78.5	.317	
1.509	46.03	-78.5	.388	

Discussion

As stated in the introduction, these data will be discussed in terms of the Eyring theory, especially as contained in Chapter IX of ref. 9. There, the viscosity and self-diffusion coefficient of liquids are related by the equation

$$\frac{D\eta}{kT} = \frac{\lambda_1}{\lambda_2\lambda_3}$$

where λ_1 is the distance between layers of liquid molecules parallel to the concentration gradient for diffusion or the shearing force in viscosity. $\lambda_2\lambda_3$ is the area of the molecule whose normal is perpendicular to the concentration gradient or the shearing force. The quantities $D\eta/kT$ as a function of temperature have been calculated in Table II. The fifth and sixth columns of this table were calculated with the further assumption that $\lambda_1\lambda_2\lambda_3$ is equal to the volume per molecule in the liquid at each temperature.

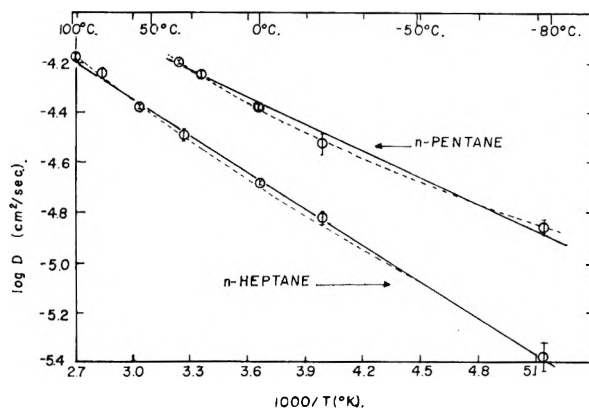


Fig. 3.—Temperature dependence of diffusion coefficient. Solid line is straight line fitted by method of least squares. Dotted line is drawn to emphasize curvature.

For comparison, the dimensions of a cylinder containing a freely rotating, extended molecule

are¹³: pentane, 4.9 Å. diameter \times 9.0 Å.; heptane, 4.9 Å. diameter \times 11.5 Å.

TABLE II
CALCULATION OF MOLECULAR DIMENSIONS FROM DIFFUSION AND VISCOSITY

T, °K.	η , cpoise ^a	$D\eta/kT$, cm. ⁻¹	ρ , g./cc. ^b	λ_1 , Å.	$(\lambda_2\lambda_3)^{1/2}$, Å.
Pentane					
308.7	0.195	2.88	0.6103	2.38	9.08
298.2	.215	2.43	.6210	2.16	9.43
273.2	.277	3.04	.6453	2.37	8.85
250.3	.355	3.05	.6662	2.34	8.75
194.7	.755	3.88	.7155	2.54	8.10
Heptane					
369.0	0.202	2.60	0.6167	2.64	10.2
353.4	.229	2.70	.6310	2.67	9.94
329.7	.282	2.61	.6517	2.58	9.95
305.7	.360	2.75	.6730	2.60	9.72
273.2	.525	2.90	.7004	2.62	9.50
250.3	.702	3.09	.7195	2.67	9.30
194.7	2.51	3.88	.7644	2.91	8.66

^a See reference 13. ^b G. Egloff, "Physical Constants of Hydrocarbons," Reinhold Publ. Corp., New York, N. Y.

Thus the agreement in absolute value between this theory and the known dimensions of the molecules is fairly good; there is perhaps more significance in the relative values of λ_1 and $(\lambda_2\lambda_3)^{1/2}$, showing diffusion taking place along the direction of least resistance, as anticipated.

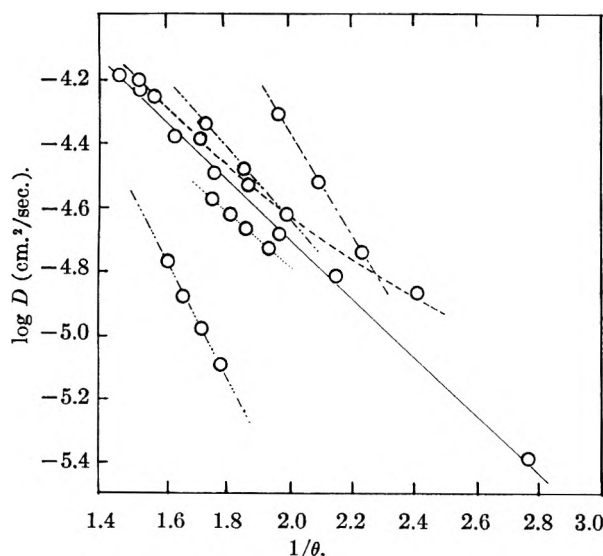


Fig. 4.—Plot of $\log D$ vs. $1/\theta$ for various liquids, where θ is the reduced temperature: —, *n*-pentane; ---, *n*-heptane; ·····, water; - · - · - ·, CS_2 , ·····, benzene; - · - · - ·, ethanol.

The diffusion itself is also treated in this theory,

(13) R. J. Moore, P. Gibbs and H. Eyring, *THIS JOURNAL*, **57**, 172 (1953). The writer would like to point out that the conclusions in this reference based on low temperature viscosities depend on extrapolated values obtained from F. D. Rossini, "Selected Values of the Properties of Hydrocarbons," N.B.S. Circular C 461, U. S. Government Printing Office, Washington, D. C., 1947. Near the freezing points, these extrapolated values are smaller than the measured values (E. B. Giller and H. G. Drickamer, *Ind. Eng. Chem.*, **41**, 2067 (1949)) by as much as a factor of two. The values given by Rossini and by Giller and Drickamer are in good agreement around -20° . The viscosities reported in Table II are those of Rossini at high temperatures and those of Giller and Drickamer at low temperatures.

resulting in the expression

$$D = e\lambda_2(kT/h) e^{\Delta S^\ddagger/R} e^{-E_{\text{act}}/RT}$$

where λ is the distance between equilibrium positions in the liquid lattice along the direction of diffusion. Using experimental values of D and E_{act} at 0° the following result is obtained: pentane, $\lambda e^{\Delta S^\ddagger/2R} = 0.81$ Å.; heptane, $\lambda e^{\Delta S^\ddagger/2R} = 0.92$ Å. The results obtained above on λ_1 , and $(\lambda_2\lambda_3)^{1/2}$ indicate that the mechanism of diffusion pictured by Eyring, namely, molecular jumps from an equilibrium position in the liquid lattice to a neighboring hole, is correct. In that case λ is approximately the molecular length, and ΔS^\ddagger is equal to -10.1 e.u. for both pentane and heptane. If, on the other hand, λ is taken as the length of a methylene group (1.3 Å.), then ΔS^\ddagger is -5.6 and -7.2 e.u. for pentane and heptane, respectively. This agrees with the values of ΔS^\ddagger obtained from pure viscosity data¹³: -5.08 and -7.24 e.u. Thus of the two postulates for the flow mechanism, jumps of the entire molecular length and jumps of the length of a single methylene group, the theory seems to favor the latter. Of course the real picture will be further complicated by the motion resulting from hindered rotation about the C-C bonds, lack of long range order in the liquid, and motion along other molecular coordinates.

Some correlations which can be drawn from the self-diffusion data already available are contained in Table III and Fig. 4. The ratio of the energy of evaporation to the activation energy for self-diffusion is about 3.7 for the "ideal" organic liquids, 2.1 for the hydrogen bonded liquids, and a much greater number for the liquid metals. Similar trends have been observed for these ratios using the activation energy for viscosity instead of diffusion.⁹ The plot of $\log D$ vs. $1/\theta$, where θ is the ratio of the temperature to the critical temperature, was drawn to see if a law of corresponding states applied to the self-diffusion of ideal liquids. To date there is inadequate experimental evidence for this.

TABLE III
COMPARISON OF RATIO OF ENERGY OF EVAPORATION TO ACTIVATION ENERGY FOR SELF-DIFFUSION FOR VARIOUS LIQUIDS

Substance	$\Delta E_{\text{vap.}}^a$, kcal./mole	$\Delta E_{\text{diff.}}^a$, kcal./mole	$\Delta E_{\text{vap.}}/\Delta E_{\text{diff.}}$
Pentane	5.7	1.6	3.6
Heptane	8.1	2.2	3.7
Benzene	7.7	2.1	3.7
CS_2	6.0	2.9 ^b	2.1
Ethanol	9.8	4.5	2.2
Water	9.4	4.6	2.0
Mercury	14.2	1.16	12
Indium	50.7 ^c	1.35	38

^a Evaluated at 25° where possible. ^b Based on extrapolated high pressure data from reference 7. ^c J. Anderson, *J. Chem. Soc.*, 141 (1943).

Acknowledgment.—The author would like to thank Dr. Henry A. Kierstead, who originally suggested this problem and offered guidance during the initial stages of the investigation. He would like to thank Dr. Edward F. Greene and Dr. Donald F. Hornig for many useful suggestions.

ON THE KINETICS OF CHEMISORPTION

BY GERT EHRLICH

*General Electric Research Laboratory, Schenectady, New York**Received January 3, 1955*

The presence of *physically* adsorbed molecules on solid surfaces, suggested by theory and experiment, is taken into account in formulating the kinetics of chemisorption. A rate law results which differs fundamentally from those derived on the assumption that only the molecules striking empty sites on impinging on a surface from the gas are chemisorbed, in that (1) the dependence of rate on temperature is determined by the difference between the activation energy for desorption of physically adsorbed molecules and that for chemisorption, rather than by the latter alone, (2) the rate of chemisorption, contrary to the predictions of the Langmuir relation, may be insensitive to changes in the extent of coverage (θ), (3) a rate law nonlinear in the gas pressure can arise if "deactivation" through binary collisions of molecules physically adsorbed on the surface becomes important.

Starting with Langmuir's classical investigation of the adsorption of gases on solids,¹ it has been generally assumed that chemisorption on clean surfaces is determined by the rate at which molecules from the gas encounter vacant sites on the substrate. Recently, however, in connection with his study of the adsorption of nitrogen on tungsten, Becker^{2,3} has emphasized that physical adsorption is a necessary prerequisite to chemisorption, and that it is the rate of collision of physically adsorbed molecules with the substrate rather than the direct impingement of gas upon the surface which limits the reaction. Direct experimental evidence for physical adsorption of molecules prior to chemisorption is scanty,⁴ but for gas-metal systems this was already suggested in 1932 by Lennard-Jones,⁵ and the interaction of physically and chemically bound species was later postulated by Rideal to account for the catalysis of the conversion of parahydrogen on metal surfaces⁶; the existence of such a layer of physically adsorbed gas is entirely in accord with present knowledge of interatomic forces. In this note we outline a formalism for the kinetics of chemisorption which, following Becker's suggestion, accounts for the presence of physically adsorbed species, and derive a rate law, based on a simple model, which differs significantly from those hitherto derived in its dependence upon the extent of chemisorption, temperature and pressure.

The Rate of Chemisorption.—We shall limit ourselves to the interaction of a gas with an initially clean solid surface, and consider the special case of a diatomic molecule of mass m for which we specify two states on the surface, distinguished by a sizeable difference in the heat of adsorption. On impinging upon the surface of a solid from the gas, the molecule can either suffer an elastic collision and return to the gas, or else interact weakly with the surface, to become "physically" adsorbed; the fraction of the molecules following the latter course is given by the condensation coefficient, which for gases other than hydrogen and helium appears to be unity.⁷ The physically adsorbed

molecules will, however, again return to the gas unless, during their sojourn on the surface, the duration of which is dictated by the ratio of the energy of desorption, E_1 , to the thermal energy, kT , they form a chemical bond with the surface and become "chemisorbed." In the kinetics of this process we can, just as in solution,⁸ distinguish between two extremes—control by the rate of transport to the site of the reaction and control through the rate of favorable collisions between the reactants, that is, between physically bound gas and a surface site. A decision concerning the limiting step must depend upon the circumstances of the individual experiment; here we shall consider only the latter possibility.

If we assume that chemisorption can occur at any one of the N_s , lattice sites available per unit area, and that this process is irreversible, then the rate is given by

$$\frac{N_s}{2} \times \frac{d\theta}{dt} = n_1 k_2 \quad (1)$$

where n_1 is the number of molecules physically adsorbed on unit area, k_2 ⁹ the rate constant for chemisorption, and θ the fraction of the sites occupied by chemisorbed species; the factor $1/2$ arises from the assumption that a chemisorbed molecule occupies two sites. We obtain n_1 from the condition of mass balance, which (assuming a condensation coefficient effectively equal to unity) requires that the rate of impingement from the gas be equal to the sum of the rates of the processes occurring on the surface—chemisorption, desorption of species 1, and growth of the physically adsorbed layer. The impingement rate, found from kinetic theory, is given by $p/(2\pi m\beta^{-1})^{1/2}$, p being the pressure and $\beta = 1/kT$. If we designate the rate constant for the desorption of the physically adsorbed molecules (species 1) by k_1 , then, if dn_1/dt is negligible compared to the other rates, that is, if we assume a steady state for the concentration of species 1, we obtain for the number of physically adsorbed molecules

$$n_1 = \frac{p}{(2\pi m\beta^{-1})^{1/2}} \frac{1}{k_1 + k_2} \quad (2)$$

and (1) becomes

$$\frac{N_s}{2} \times \frac{d\theta}{dt} = \frac{p}{(2\pi m\beta^{-1})^{1/2}} \times \frac{k_2}{k_1 + k_2} = \frac{p}{(2\pi m\beta^{-1})^{1/2}} \quad (3)$$

(8) R. H. Fowler and N. B. Slater, *Trans. Faraday Soc.*, **34**, 81 (1938).

(9) The constants k_i in this paper denote the specific rate for unit area of adsorbent and so incorporate terms for the number of sites available on the substrate.

(1) A recent review of the literature of chemisorption has been given by K. J. Laidler in Emmett's "Catalysis," Vol. 1, Reinhold Publ. Corp., New York, N. Y., 1953, chap. 3.

(2) J. A. Becker and C. D. Hartman, *This Journal*, **57**, 157 (1953).

(3) J. A. Becker in R. Gomer and C. S. Smith, "Structure and Properties of Solid Surfaces," University of Chicago, Chicago, Ill., 1953, p. 459.

(4) See, however, the work of R. Gomer and J. K. Hulm, *J. Am. Chem. Soc.*, **75**, 4114 (1953).

(5) J. E. Lennard-Jones, *Trans. Faraday Soc.*, **28**, 333 (1932).

(6) E. K. Rideal, *Proc. Cambridge Phil. Soc.*, **35**, 130 (1939).

(7) F. Knauer and O. Stern, *Z. Physik*, **53**, 779 (1929).

s , the sticking coefficient, denoting the fraction of the impinging molecules that is chemisorbed. Equation 3, it should be noted, is quite general for the mechanism of chemisorption postulated, provided the condition of irreversibility for chemisorption and of a steady state for species 1 is satisfied. To attain a greater insight into the consequences of physical adsorption on the rate, we shall derive a rate law for a very simple, restricted model. We assume a single, perfect crystallographic plane, above which the physically adsorbed molecules are presumed to form a 2-dimensional gas; the expression for the rate constants in terms of a crude collision mechanism is then obtained as follows.

In the transfer of physically adsorbed molecules into the chemisorbed state, the number of successful events will depend on the number of collisions with the substrate, $\nu_2 \exp(-E_2\beta)$, in which the energy exceeds E_2 , the barrier to chemisorption, upon a factor f which accounts for the availability of free sites, and on the probability κ_2 that such a collision with a free site will be successful, so that

$$k_2 = f\kappa_2\nu_2 \exp(-E_2\beta) \quad (4)$$

For diatomic molecules which dissociate upon chemisorption, and in which the chemisorbed species 2, are randomly distributed, $f = (1 - \theta)^2$. The assumption of random distribution is equivalent to assuming both surface diffusion for chemisorbed material and also negligibly small interactions between the individual species; the factor f is only insignificantly altered for an immobile film of non-interacting diatomic molecules, however.¹⁰

In considering the rate of desorption of the physically adsorbed molecules, we do *not* take account of the fact that once chemisorption has occurred even a perfect crystal plane becomes heterogeneous, inasmuch as filled and empty sites may differ in respect to physical adsorption. We specify the rate of evaporation of species 1 as

$$k_1 = \kappa_1\nu_1 \exp(-E_1\beta) \quad (5)$$

Here κ_1 denotes the probability factor in desorption, corresponding to κ_2 of eq. 4, ν_1 the frequency of vibration perpendicular to the surface, and E_1 the activation energy for desorption.

Substituting (4) and (5) in eq. 3, we obtain for the rate of chemisorption

$$\frac{N_s}{2} \times \frac{d\theta}{dt} = \frac{p}{(2\pi m\beta^{-1})^{1/2}} \times \frac{1}{1 + \frac{1}{(1-\theta)^2} \frac{\kappa_1\nu_1}{\kappa_2\nu_2} \exp[(E_2 - E_1)\beta]} \quad (6)$$

Dependence upon Macroscopic Variables T , P , θ .—If we assume that only the exponential terms of eq. 6 are functions of the temperature, *i.e.*, if we neglect variations in κ and ν as minor,¹¹ then the change in rate with temperature is most readily found by plotting the logarithm of the ratio of the rate constant k_2 to k_1 against $1/kT$, since from eq. 6 it follows that

(10) A. R. Miller, "The Adsorption of Gases on Solids," Cambridge University Press, New York, N. Y., 1949, chap. 4.

(11) For ν , this approximation is justified by the calculations of J. E. Lennard-Jones and A. F. Devonshire, *Proc. Roy. Soc. (London)*, **A156**, 6 (1936).

$$\left(\frac{\partial \ln s/(1-s)}{\partial \beta} \right)_\theta = E_1 - E_2 \quad (7)$$

It is apparent that the temperature dependence of the experimentally accessible quantity $s/(1-s)$ is thus dictated by the *difference* in the activation energies of the two processes on the surface that compete for species 1—incorporation of physically adsorbed molecules into a chemisorbed layer on the one hand, and evaporation into the surrounding gas on the other. A rise in temperature can result in either an increase or a decrease in the rate, depending on the relative magnitudes of the activation barriers to these two processes. The activation energy for the transformation from the physically to the chemically bound state can be derived from the variation of rate with temperature only if the magnitude of E_1 is known or if it can be shown that $E_2 \gg E_1$. It is particularly noteworthy that chemisorption can occur even at very low temperatures, provided that $E_1 > E_2$; this qualitative conclusion has been anticipated by Halsey.¹² Moreover, as the temperature is lowered until $E_2 > kT$, the rate of chemisorption becomes negligible, but physical adsorption will then itself be irreversible, if E_1 indeed exceeds E_2 . The situation $E_2 > E_1$, on the other hand, results in an increase in the rate of chemisorption as temperature increases; at low temperature, however, we may encounter a situation in which there are physically bound molecules reversibly adsorbed and yet none chemisorbed.

Becker³ has deduced by the route we have adopted in the previous section, an expression for s equivalent to eq. 6, but he arbitrarily equated the pre-exponential factor for chemisorption, that is, $(1-\theta)^2 \kappa_2\nu_2$ to that for desorption of physically adsorbed species, $\kappa_1\nu_1$, thus obtaining an equation for the sticking coefficient involving only the heat terms E_1 and E_2 as unknowns. This approximation appears to be unjustified and does not yield correct values of the activation energies.

A second point of interest is provided by the dependence of s upon θ , the extent of chemisorption. If for the moment we assume the activation energies to be independent of θ then, according to eq. 6, the dependence of s is of the form

$$s = \frac{1}{1 + \delta \frac{1}{(1-\theta)^2}} \quad (8)$$

where

$$\delta = \frac{\kappa_1 \nu_1}{\kappa_2 \nu_2} \exp[(E_2 - E_1)\beta]$$

Although $1/(1-\theta)^2$ increases rapidly with θ , this will not affect the sticking coefficient s , and therefore the rate, if δ is small compared to unity. For $k_2 > k_1$ (*i.e.*, presumably $E_1 > E_2$), the condition $1 \gg \delta$ prevails, and s will become a function of θ only for values of θ approaching unity at which $\delta[1/(1-\theta)^2] \sim 1$. If $E_2 \gg E_1$, however, that is if the activation energy for chemisorption is large compared with that for desorption, we may expect that $1 \sim \delta$, and that s will be a sensitive function of θ .

The third macroscopic variable, the pressure p ,

(12) G. D. Halsey, *Trans. Faraday Soc.*, **47**, 649 (1951).

appears to enter only through the expression for the rate of impingement upon the surface. This, however, is a consequence of our neglect of collisions between species 1 physically adsorbed on the surface. Upon increasing the pressure, and therefore n_1 , an additional route for the depletion of species 1 will eventually have to be taken into account—evaporation resulting from a collision between two physically adsorbed molecules—and this introduces a term into s explicitly dependent upon n_1 . This mechanism need be considered only at high pressures at which the number of binary collisions per molecule becomes comparable with the frequency of oscillation ν_1 of physically adsorbed molecules with respect to the surface. Before this becomes important, we can foresee that binary collisions may affect the rate at which physically adsorbed species are chemisorbed, inasmuch as a collision of an *active* molecule, one that is otherwise capable of surmounting the activation barrier to chemisorption, with another molecule physically adsorbed on the surface may be expected to result in deactivation. If $n_1^2 k_{-2}$ denotes the rate of deactivation through such collision, then the expression for the sticking coefficient becomes

$$s = \frac{k_2 - n_1 k_{-2}}{k_1 + k_2} \quad (9)$$

provided $k_1 \gg n_1 k_{-2}$, and a plot of sticking coefficient against pressure should yield a curve with an initial slope

$$\left(\frac{\partial s}{\partial p}\right)_\theta = -\frac{k_{-2}}{(k_1 + k_2)^2 (2\pi m \beta^{-1})^{1/2}} \quad (10)$$

Binary collisions will affect the rate provided $n_1 k_{-2} = c$, c being an arbitrary constant, of the order of a tenth, the exact value of which depends upon the precision to which a non-linearity of the rate in pressure can be detected. Non-linearity will thus be observed at a pressure

$$p_c = c \frac{k_2}{k_{-2}} (k_1 + k_2) (2\pi m \beta^{-1})^{1/2} \quad (11)$$

Deviations from a linear dependence of rate on pressure will, under these assumptions, occur at lower pressures the smaller the rate constants for physical desorption (k_1) and chemisorption (k_2) and the greater the probability of deactivation during passage over the potential barrier to chemisorption (k_{-2}). To find the temperature dependence of p_c , we assume as a first approximation that k_{-2} , through the rate of surface diffusion, varies directly with the square root of the temperature. Substituting eq. 3 and 4 into eq. 11, we obtain the relation

$$\left(\frac{\partial \ln p_c^{-1}}{\partial \beta}\right)_\theta = E_2 [1 + (s)_{p=0}] + E_1 [1 - (s)_{p=0}] \quad (12)$$

that is, with increasing temperature, the deviations from a rate law linear in the pressure diminish. At pressures much greater than p_c , binary collisions will have to be considered in both the desorption of physically adsorbed molecules and in the activation for chemisorption; eq. 9 will no longer be valid under these conditions.

The mechanism proposed to account for a non-linear rate arises directly from the assumption of the presence of physically adsorbed gas on the surface; it should be noted that on this model a

dependence on a power of the pressure other than the first does *not* require the postulate that chemisorption occurs through collision of *atoms* with the surface.

The Effect of Surface Heterogeneity.—Underlying the formalism presented above are three *fundamental* assumptions: (1) the rate of chemisorption is determined by the frequency of successful collisions of physically adsorbed gas with substrate, (2) the physically adsorbed molecules are in a steady state, and (3) chemisorption occurs at fixed sites on a surface not subjected to thermal disordering.¹³ The first condition must indeed correspond to the situation of physical interest if in the limit of zero coverage ($\theta \rightarrow 0$) the rate of impingement exceeds the rate of chemisorption, provided it can be established that chemisorption is not confined to a small number of sites. The latter situation should be readily recognizable, inasmuch as once these sites are filled, chemisorption, if it proceeds at all, will be limited by a new step, the diffusion of chemisorbed species away from these sites. The second and third conditions appear to be satisfied by initially clean metal surfaces. The rate law embodied by eq. 6 and the consequences deduced from it are, however, based on further assumptions, of which the one most obviously in conflict with reality is that of a perfect crystallographic surface, two sites of which are required for chemisorption, and for which the physical adsorption is not dependent upon θ . As already pointed out, the very act of chemisorption will create a heterogeneous surface; this can be expected to affect the distribution of physically adsorbed molecules over the surface, and therefore both k_1 and k_2 . To take account of this, as well as of the possible presence of different crystal planes, grain boundaries, etc., we would have to specify both the distribution of sites as well as the kinetics of chemisorption and physical desorption peculiar to each. This demands a detailed knowledge of surface structure and the details of the chemisorption process not yet achieved; formally, we can accommodate a multiplicity of site types by writing, instead of eq. 6

$$s = \frac{k_2}{k_1 + k_2} = \frac{\sum_i f_i \Theta_i w_i \exp(-E_i \beta)}{\sum_j f_j \Theta_j w_j \exp(-E_j \beta) + \sum_i f_i \Theta_i w_i \exp(-E_i \beta)} \quad (13)$$

f gives the fraction of the surface taken up by a specified set of sites, Θ accounts for the dependence upon the fraction of such sites already covered, and the term w incorporates both the necessary steric and frequency factors; the subscripts i and j distinguish chemisorption and physical desorption, respectively. The dependence of rate upon temperature thus becomes

$$\left(\frac{\partial \ln s/(1-s)}{\partial \beta}\right)_\theta = \langle E_j \rangle_k - \langle E_i \rangle_k$$

where

$$\langle E_j \rangle_k = \frac{\sum_j E_j k_j - \sum_j \frac{\partial \ln \Theta_j k_j}{\partial \beta}}{\sum_j k_j}$$

(13) F. F. Volkenshtein, *Zhur. Fiz. Khim.*, **23**, 917 (1949).

$$\langle E_i \rangle_k = \frac{\sum_i E_i k_i - \sum_i \frac{\partial \ln \Theta_i k_i}{\partial \beta}}{\sum_i k_i}$$

It is apparent that the term $\langle E_j \rangle_k - \langle E_i \rangle_k$ which dictates the temperature variation of s for a heterogeneous surface may itself be a function of the temperature, as well as of the extent of chemisorption. A value of $\langle E_j \rangle_k - \langle E_i \rangle_k$ independent of T may be a good indication that the reaction is occurring on sites energetically equivalent, but we are still unable to predict an explicit variation with θ . Thus the restrictions under which eq. 6 was derived make it appear unlikely that it can afford a quantitative description of the kinetics of chemisorption in actual experimental systems. The qualitative predictions concerning the dependence of rate upon T , p and θ , which follow from the three basic assumptions do retain their validity; however, the temperature dependence is dictated by the difference of two activation terms relating, respectively, to chemisorption and physical desorption, the dependence upon coverage by the extent to which the decrease in the probability of a successful chemisorption collision with increasing θ is compensated either by an increase in the concentration of physically adsorbed molecules or by a decrease in the activation barrier E_2 (or an increase in $\kappa_2\nu_2$), and the dependence upon pressure by the details of the activation process occurring in the physically adsorbed layer.

Comparison with Classical Theory and with Experiments.—The predictions of the rate equation derived above differ significantly from those that follow from the assumption that transport from the gas to vacant sites is rate determining. Thus, for the chemisorption of diatomic molecules, Roberts¹⁴ assumed that surface diffusion was negligible, and proposed that the sticking coefficient for a mobile film without interactions would simply be equal to

$$s = (1 - \theta)^2 a_2 \quad (14)$$

where a_2 , the probability that a molecule condenses on striking two neighboring sites that are vacant, is of the form $A \exp(-E_2\beta)$. We would, on this model, expect an increase in s with temperature, and a very significant decrease with θ ; a dependence on a power of the pressure other than the first cannot be accommodated.¹⁵ Qualitatively, the disparity between the predictions of eq. 6 and 14 are immediately understandable. If we recognize the possibility of physical adsorption, a molecule which on impinging from the gas does not make a successful encounter with an empty site is no longer immediately eliminated—it may still be chemisorbed at any time during its period of existence τ in the physically adsorbed layer. In the limit of $\tau \rightarrow 0$ we again revert to kinetics of the classical type.

(14) Reference 10, p. 61.

(15) It has been suggested¹⁶ that if dissociation is completed before the "activated state" is reached the rate of chemisorption will depend on $p^{1/2}$. This cannot, however, account for a change in the pressure dependence as p increases.

(16) Reference 1, p. 200; S. Glasstone, K. J. Laidler and H. Eyring, "The Theory of Rate Processes," McGraw-Hill Book Co., Inc., New York, N. Y., 1941, p. 357.

The fact that the presence of such a layer would significantly affect the rate of chemisorption has already been pointed out by Morrison and Roberts¹⁷ in their work on oxygen films on tungsten. They proposed to account for the possibility of surface diffusion in a layer of molecular oxygen by assuming that chemisorption occurs when a molecule encounters a vacant site, and that desorption of a physically adsorbed molecule takes place if it does not encounter such a site. If during its lifetime τ in the physically adsorbed state a molecule migrates to a total of n sites, then the probability of evaporation is θ^n , the probability of chemisorption $1 - \theta^n$. Upon increasing the temperature, τ , and with it n , will decrease, and this, according to Patterson,¹⁸ would lead to a decrease in s at smaller values of θ . We cannot, however, without modification of this model account for a decrease in s with increasing temperature on a bare surface. This is a consequence of the fact that this formalism is rigorously dependent on the assumption that the rate of encounter of physically adsorbed molecules and vacant sites (as distinguished from the actual collisions) is limiting, and that each such encounter, if it occurs, is successful. As θ approaches zero, the rate of chemisorption should thus be given by the rate of impingement; if this condition is not met, then the formalism presented above is the more appropriate.

Becker and Hartman² have carried out quantitative measurements of the kinetics of chemisorption of nitrogen on tungsten, a system that satisfies the requirements of an initially clean surface for which the creation of thermal defects is of negligible importance, and it is interesting to examine some of their results in terms of the concepts we have advanced. From the decrease in the sticking coefficient with T observed by Becker, we conclude that the barrier to evaporation is greater than that to chemisorption. Figure 1 shows a plot of the data as in eq. 7; straight lines are found with slopes yielding $E_1 - E_2$ of 2.3 kcal./mole for $\theta = 0.25$, and 4.4 kcal./mole for $\theta = 1.25$. Inasmuch as the condition $E_2 \gg E_1$ does not appear to be satisfied, we cannot, in the absence of data concerning the exact magnitude of E_1 , establish either the activation energy for chemisorption, or assign the cause of the variation of the heat term with θ . An increase in E_1 with θ may be implied by the work of Roberts,^{19,20} who found an increase in the accommodation coefficient of neon on tungsten upon chemisorption of H_2 , N_2 and O_2 . Such an increase may also account for the curvature apparent in the temperature dependence at $\theta = 0.75$, shown in Fig. 1.

However this may be, it is evident that the simple rate law, eq. 6, which does not envisage a dependence of $E_1 - E_2$ upon θ , cannot account quantitatively for the kinetics. The variation of s with θ found by Becker is, however, in qualitative accord with our formalism. At $T = 300^\circ K.$, the sticking coefficient only decreases with increasing

(17) Reference 10, p. 100.

(18) D. Patterson, *Nature*, **173**, 1184 (1954).

(19) Reference 10, pp. 12, 96.

(20) J. K. Roberts, *Nature*, **137**, 659 (1938).

θ at values of θ approaching unity; for smaller values of θ the change in $E_1 - E_2$ compensates for the decreasing availability of empty sites for chemisorption. Upon increasing the temperature, to 600°K., the sticking coefficient decreases since the concentration of species 1 is decreased; the increase in the rate of desorption of species 1 being greater than that in the rate of conversion of species 1 into 2, the compensation for the filling up of sites is less effective and the dependence upon θ commences at lower values of the coverage. A more than qualitative agreement with experiment is not to be expected, even for a detailed kinetic theory, since it must be recalled that θ is not a quantity readily amenable to direct measurement, and that its value rests on an arbitrary assignment of the monolayer area.

The pressure dependence predicted by eq. 10 involves, in addition to the rate constants k_1 and k_2 , the specific rate of deactivation. At present, neither the collision frequency of a physically adsorbed molecule, nor the lifetime of an activated complex on a surface, both of which enter into the constant k_{-2} is known. Information on both must be obtained before a decision concerning even the qualitative validity of the mechanism proposed for a rate law non-linear in the pressure can be made.

Chemisorption Equilibrium.—In the preceding it has been stressed that the kinetic formalism for chemisorption is fundamentally changed when the presence of physically adsorbed molecules suggested by theory and experiment is properly taken into account. That this does not necessarily affect the equilibrium state significantly should be apparent from the fact that the model for the chemisorbed film has not been altered; this can be appreciated from a continuation of the kinetic argument, by taking into account the desorption of chemisorbed material, which we have so far neglected.

We postulate that at equilibrium the mechanism of chemisorption is that presented above; for evaporation we therefore need only consider the combination of two chemisorbed atoms and their transfer to the physically adsorbed layer, the rate of which, again assuming no interaction between chemisorbed species, and only a single homogeneous crystal surface, is

$$-\frac{1}{2} \frac{dn_2}{dt} = \theta^2 N_s^2 Z \exp(-E_3\beta) \quad (15)$$

Here the term Z accounts for both collision and steric factors and is independent of n_1 ; E_3 is the

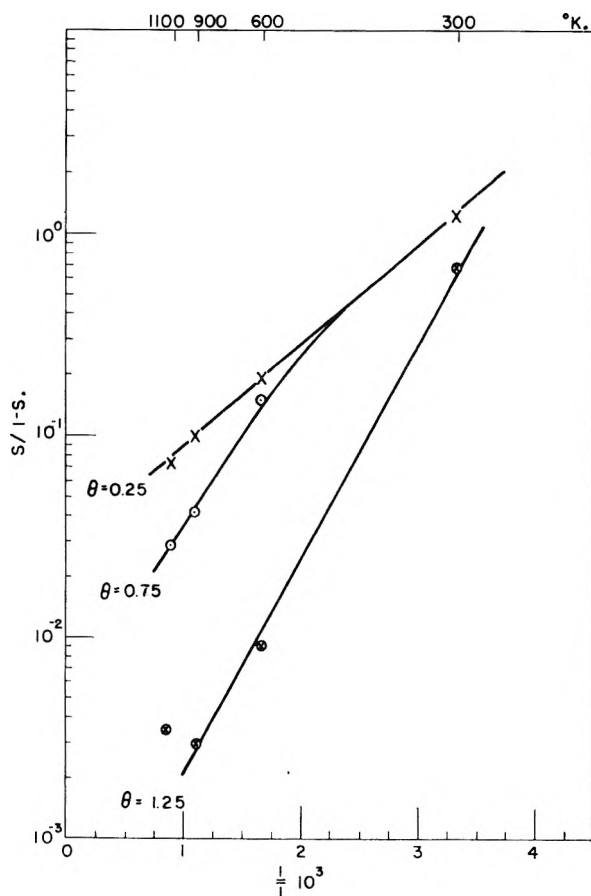


Fig. 1.—The temperature dependence of the rate of chemisorption of N_2 on tungsten ($\theta = 1$ for 1.25×10^{14} molecules/cm.²).

activation energy for desorption. At equilibrium, we equate the rate of chemisorption to that for desorption, so that

$$\frac{\theta^2}{(1 - \theta)^2} = \frac{n_1 \nu_2 \kappa_2}{N_s^2 Z} \exp[(E_3 - E_2)\beta] \quad (16)$$

Moreover, detailed balancing also gives us

$$n_1 = \frac{p}{(2\pi m\beta^{-1})^{1/2}} \frac{1}{\kappa_1 \nu_1} \exp(E_1\beta) \quad (17)$$

Substituting eq. 17 in 16, we obtain

$$\frac{\theta^2}{(1 - \theta)^2} = Kp \quad K = \frac{\nu_2 \kappa_2 \exp[(E_3 + E_1 - E_2)\beta]}{\nu_1 \kappa_1 Z N_s^2 (2\pi m\beta^{-1})^{1/2}} \quad (18)$$

which, except for differences in the constant of proportionality K , is precisely the Langmuir equation for adsorption of a dissociable diatomic gas.²¹

(21) Reference 10, p. 82.

NOTE

THE EXCHANGE REACTION BETWEEN DEUTERIUM AND METHYLAMINES ON IRON POWDER¹

BY JOEL R. GUTMANN

Israel Atomic Energy Commission, Rehovoth, Israel

Received January 25, 1955

Kinetic studies have established that the iron-catalyzed exchange of hydrogens between ammonia and deuterium comes about by the interaction of strongly adsorbed ammonia (or of the products of the surface dissociation of ammonia, namely, M—NH₂, M—NH or M—N) with either D atoms or gaseous D₂ molecules.²

The rates of exchange between the methylamines and deuterium have now been measured on a pure iron powder. By comparing these exchange rates with the rate of exchange of ammonia and deuterium an attempt is made to identify the intermediates in all these exchange reactions.

Apparatus and Materials.—The exchange rates were determined in a slightly modified version of the apparatus previously described by the author.³ Ammonia, hydrogen and deuterium were prepared as described before. Methylamine, dimethylamine and trimethylamine were liberated from their respective hydrochlorides by concentrated potassium hydroxide solution, dried by passage through a column of potassium hydroxide pellets, distilled in vacuum from -80° into a receiver cooled in liquid air and finally stored in bulbs covered with freshly distilled sodium films.

Experimental Procedure.—Reduced iron (May and Baker, 65 mg.) was used as a catalyst, after initial exhaustive reduction in a stream of dry hydrogen at 350° . Before each experiment the catalyst was flushed with deuterium and outgassed at 350° for about half an hour through liquid air traps. The reaction mixtures of about 85 mm. deuterium with the same amount of either ammonia, methylamine or dimethylamine were introduced into the catalyst chamber through an ice-cooled trap after the catalyst had been brought to the appropriate temperature. The exchange reactions were followed by extracting small samples of gas from the catalyst chamber, freezing out the condensable gases in a liquid air trap and measuring the atom fraction of the heavy isotope in the hydrogen (the "D" content) in a thermal-conductivity gage. The rates of exchange in the different runs are given in terms of the initial rates of change of the "D" content^{3a} (*i.e.*, the rate when the "D" content is 1), which were evaluated either from the first-order constant of the exchange and the "D" content when isotopic equilibrium had been established⁴ or directly from the slope of the reaction plot at zero time. In order to detect variations in catalyst activity from time to time, all exchange runs whose rates were compared were "bracketed" by standard exchange experiments between ammonia and deuterium. The sequence of runs where the rates of these control reactions were not reasonably constant, were rejected.

(1) This work forms part of a thesis submitted to the Hebrew University, Jerusalem, in partial fulfillment of the requirements for a Ph.D. degree.

(2) K. J. Laidler, "Catalysis," Ed. by P. H. Emmett, Vol. 1, Reinhold Publ. Corp., Inc., New York, N. Y., 1954, p. 174.

(3) J. R. Gutmann, *THIS JOURNAL*, **57**, 309 (1953); for details of modifications made see Thesis, 1954, The Hebrew University, Jerusalem.

(3a) Since the different runs were made in the same reaction vessel and at a fixed deuterium pressure, the number of hydrogen atoms exchanged in unit time in the different runs are proportional to these rates.

(4) J. Singleton, E. Roberts and E. Winter, *Trans. Faraday Soc.*, **47**, 1318 (1951).

Results

The exchange of methylamine and dimethylamine with deuterium at 242 and 289° followed a first-order law. From this and from the distribution of the isotopes between the amines and the hydrogen when isotopic equilibrium had been established it appears that only the N-bound hydrogens of the amines exchange rapidly; methylamine giving CH₃NHD and CH₃ND₂ and dimethylamine giving (CH₃)₂ND. A similar conclusion had been reached before by Roberts, Emeleus and Briscoe, for the reaction between methylamine and deuterium on a nickel catalyst.⁵

In the exchange run of dimethylamine and deuterium at 331° a continual slow change of the "D" content, at the practically constant rate of 6.6×10^{-4} min.⁻¹, was superimposed on the fast first-order change and measured after isotopic equilibrium for the N-bound hydrogen of the dimethylamine should have been established. (The rate of exchange of the N-bound hydrogen in this run was 0.05 min.⁻¹. This was evaluated from the reaction plot after subtracting from each reaction point the amount due to the slow change.) The same slow dilution of deuterium was measured, unmasked by the faster initial change, in the interaction of (CH₃)₂ND with deuterium. The slow change in "D" content was found to be due to hydrogen gas produced in the slight decomposition of dimethylamine on the catalyst at this temperature and no exchange of hydrogens of the methyl groups was involved. The catalytic decomposition of dimethylamine, which was found to give hydrogen with about 5% of methane as the sole non-condensable products, is in contrast to the homogeneous decomposition of dimethylamine which yields mainly methane and some polymerized nitrogenous material.⁶

The rates of exchange of NH₃, CH₃NH₂ and (CH₃)₂NH, respectively, with deuterium at 242° were found to be 2.9, 3.0 and 2.5×10^{-3} min.⁻¹. The corresponding rates at 289° were 0.023, 0.022 and 0.021 min.⁻¹. At 331° the rates for the NH₃ and (CH₃)₂NH exchanges, respectively, were 0.050 and 0.042 min.⁻¹. The rates are seen to be essentially equal, with the dimethylamine runs slower by 10–15% at all temperatures. The values for each single temperature refer to the catalyst at a constant activity as determined by control reactions. However changes in activity occurred between groups of runs at different temperatures and the values recorded should not be used to determine activation energies. A separate determination of the activation energy for the ammonia-deuterium exchange on a different batch of the same catalyst, gave a value of 17.5 kcal./mole.²

No change of the "D" content was found on in-

(5) E. R. Roberts, H. J. Emeleus and E. V. A. Briscoe, *J. Chem. Soc.*, 41 (1939).

(6) A. G. Carter, P. A. Bosanquet, C. G. Silcocks, M. W. Travers and A. F. Wilshire, *J. Chem. Soc.*, 495 (1939); compare, however, the iron-catalyzed decomposition of monomethylamine, P. H. Emmett and R. W. Harkness, *J. Am. Chem. Soc.*, **54**, 538 (1932).

teracting trimethylamine with deuterium at low temperatures. At 331° a slow continual change of D content was observed (decomposition). The rate of this change was about one third of the corresponding rate measured with dimethylamine. The exchange rate of an ammonia-deuterium mixture at 331° was unchanged by the addition of trimethylamine to it (equal rates of $0.055 \pm 0.002 \text{ min.}^{-1}$ for $\text{NH}_3 + \text{D}_2$ and $\text{NH}_3 + (\text{CH}_3)_3\text{N} + \text{D}_2$ mixtures). The slow decomposition of trimethylamine on the catalyst which had been observed before at this temperature was not found in the presence of ammonia.

Discussion

The rates of exchange of methylamine and dimethylamine with deuterium have been found to be essentially the same as those of ammonia with deuterium at 242, 289 and 331°. It follows that the Arrhenius parameters of the three reactions are similar and therefore the rate-determining steps are also similar. This fact enables us to obtain further insight into the nature of the reaction intermediates and their participation in the rate determining process.

It is known⁷ that the rate-determining step in the ammonia exchange is not associated with the activation or desorption of deuterium but rather involves the reaction of chemisorbed ammonia or one of its surface dissociation products. By analogy therefore the rate-determining step in the exchange of any of the amines will involve the reaction of the chemisorbed amine or one of its surface dissociation products. A further requirement is that the participating chemisorbed species in both the ammonia and amine exchange reactions occupy about the same surface area on the catalyst.

We may now be more specific about the role of the surface dissociation products in these reactions. In the case of ammonia adsorption on iron it is known⁸ that extensive dissociation can occur on the surface, leading to products M-NH_2 , M-NH and M-N . In the case of the adsorption of an amine the corresponding dissociative surface processes, involving the rupture of a C-N bond, cannot be a stage in an exchange reaction since such steps would be irreversible and lead to decomposition of the amine concerned. (Such decomposition was detected only at the highest temperatures used.) It follows that the exchange reaction of dimethyl-

amine, for example, proceeds either through undissociated adsorbed molecule, $\text{M} \dots \text{NH}(\text{CH}_3)_2$, or through the chemisorbed radical $\text{M-N}(\text{CH}_3)_2$ but not through a more dissociated species. Since methylamine and ammonia exchange their N-bound hydrogens at the same rate and by the same mechanism as does dimethylamine it follows that in both cases the reaction intermediates are the corresponding adsorbed molecules, $\text{M} \dots \text{NH}_2\text{CH}_3$ and $\text{M} \dots \text{NH}_3$, or the radicals M-NHCH_3 and M-NH_2 , respectively (*cf.* also Kemball's conclusion on the $\text{NH}_3\text{-D}_2$ reaction⁹). A decision between the two alternatives may be reached on the basis of the experiment involving exchange in the presence of trimethylamine. As expected $(\text{CH}_3)_3\text{N}$ is strongly adsorbed on surfaces on which NH_3 is adsorbed without dissociation¹⁰ and will partially displace ammonia from such sites. The fact that addition of trimethylamine has no effect on the rate of ammonia-deuterium exchange on iron suggests that the rate-determining step of this exchange does not involve adsorbed undissociated molecules of ammonia. We may therefore conclude that the exchange rate of ammonia with deuterium is determined by the rate of reaction of the M-NH_2 radical and analogously the rates of exchange of methylamine and dimethylamine, respectively, with deuterium are determined by the rate of reaction of the species M-NHCH_3 and $\text{M-N}(\text{CH}_3)_2$.

The results obtained furthermore show that no appreciable part of the catalyst surface is covered by the more dissociated species of ammonia (surface imides or nitrides) under the conditions prevailing during the exchange reaction of ammonia with deuterium. For the presence of these species, which have been found not to be intermediates, would inhibit the exchange reaction by blocking part of the catalyst surface and thus depress the rate of the ammonia exchange relative to that of the two amines.

Acknowledgment.—The helpful guidance of Dr. I. Dostrovsky in the course of this work is gratefully acknowledged. The author wishes to thank the Research Director, Israeli Atomic Energy Commission, for permission to publish these results and the Weizmann Institute of Science, Rehovoth, for its hospitality extended for the duration of this work.

(9) Ch. Kemball, *Proc. Roy. Soc. (London)*, **A214**, 413 (1952).

(10) W. A. Felsing and C. T. Ashley, *J. Am. Chem. Soc.*, **56**, 2226 (1934).

(7) A. Farkas, *Trans. Faraday Soc.*, **32**, 417 (1936).

(8) Ch. Kemball and H. Wahba, *ibid.*, **49**, 1351 (1953).

COMMUNICATION TO THE EDITOR

MONOLAYER STRUCTURE AS REVEALED BY ELECTRON MICROSCOPY

Sir:

The electron micrographs of Ries and Kimball¹ of films of *n*-hexatriacontanoic acid at various stages of compression are very interesting and recall the ultra microscopical investigations of Zocher and Stiebel.²

Their explanation, however, presents certain difficulties which must be explained if the observations are not to be attributed to artefacts introduced by this novel technique. For example, Fig. 1B apparently shows islands of film, which the authors calculate to be one molecule thick, covering only about half the surface and surrounded either by a clean surface or a very attenuated monolayer, the whole system exerting a surface pressure of 15 dynes/cm. While the force-area curves are not given, it is obvious that at this pressure the film area must be less than 20.4 Å.² per molecule, *i.e.*, the extrapolated area corresponding to a close packing of the hydrocarbon chains. There seem to be two possible explanations of this anomaly: Either (1) the island structure has been introduced during

(1) Ries and Kimball, *J. Phys. Chem.*, **59**, 94 (1955).

(2) Zocher and Stiebel, *Z. physik Chem.*, **147A** 401 (1930).

the process of transferring the monolayer from the water to collodion support, which could be simply tested by comparing the area of the film on the collodion support with the decrease in area of the film, at constant surface pressure, on the Langmuir-Adam trough, or (2) assuming that there has been no change in film area during transfer, the islands may not, in fact, be monomolecular and that some collapse has already begun. This explanation receives some support from the authors' observation that the surface pressures are unstable in this region. On this assumption, Fig. 1C presents no difficulty since the multimolecular islands might be expected to grow and cohere on further compression until the whole system ultimately crumples into *quasi* fibers as in Fig. 1D.

Electron micrographs of films at areas larger than 20.4 Å.² per molecule might be very informative since here patches of coherent monolayer in a circumambient gaseous monolayer are known to exist and can be demonstrated by fluctuations in surface potential from point to point.

BRITISH LEATHER MANUFACTURERS'
RESEARCH ASSOCIATION
MILTON PARK, EGHAM
SURREY, ENGLAND

KENNETH G. A. PANKHURST

RECEIVED FEBRUARY 7, 1955

FOR EASIER, SURER ACCESS
TO RECORDED INFORMATION
IN CHEMICAL ABSTRACTS

*Place Your Order to One Or
More Of The ACS Indexes*

27-Year Collective Formula Index to Chemical Abstracts

Over half a million organic and inorganic compounds listed and thoroughly cross referenced for 1920–1946. In 2 volumes of about 1000 pages each.

Paper bound \$80.00

Cloth bound \$85.00

10-Year Numerical Patent Index to Chemical Abstracts

Over 143,000 entries classified by countries in numerical order with volume and page references to Chemical Abstracts for 1937–1946. Contains 182 pages.

Cloth bound \$6.50

Decennial Indexes to Chemical Abstracts

Complete subject and author indexes to Chemical Abstracts for the 10-Year periods of 1917–1926, 1927–1936, and 1937–1946.

2nd Decennial Index (1917–1926)	Paper bound	\$100.00
3rd Decennial Index (1927–1936)	Paper bound	150.00
4th Decennial Index (1937–1946)	Paper bound	120.60

(Foreign postage on the Decennial Indexes is extra)

order from: **Special Publications Department**
American Chemical Society
1155 Sixteenth Street, N.W.
Washington 6, D.C.

ANNOUNCING

New Schedule of Back Issue Prices

Effective January 1, 1955

American Chemical Society Journals

RATES FOR SINGLE COPIES OF CURRENT ISSUES AND BACK NUMBERS

Single copies or complete volumes of nearly all the ACS journals listed below may be purchased at these prices.

NOTE: In the event an issue appears in two or more parts, a special issue price will apply.

Journal	Current Year	Back Years	Foreign Postage	Canadian Postage
ANALYTICAL CHEMISTRY (formerly Analytical Edition)				
Volumes 1-4.....	...	\$2.00	\$0.15	\$0.05
Volumes 5-8.....	...	1.25	.15	.05
Volume 9 et seq.....	\$1.00	1.50	.15	.05
CHEMICAL ABSTRACTS, Volumes 11-30				
Numbers 1-22.....	...	1.25	.15	.05
Numbers 23 and 24 (Author & Subject Index).....	...	3.00	.45	.15
CHEMICAL ABSTRACTS, Volume 31 et seq.				
Numbers 1-22.....	2.00	2.25	.15	.05
Number 23 (Author Index).....	12.00*	12.00*	free	free
Number 24 (Subject Index).....	24.00*	24.00*	free	free
CHEMICAL AND ENGINEERING NEWS, Vols. 1-2425	.05	free
CHEMICAL AND ENGINEERING NEWS, Vol. 25 et seq.40	.50	.05	free
INDUSTRIAL AND ENGINEERING CHEMISTRY	1.50	2.00	.15	.05
JOURNAL OF AGRICULTURAL AND FOOD CHEMISTRY	1.00	1.25	.15	.05
JOURNAL OF THE AMERICAN CHEMICAL SOCIETY				
Volumes 32-73.....	...	1.75	.15	.05
Volume 74 et seq.....	1.00	1.50	.15	.05
JOURNAL OF PHYSICAL CHEMISTRY				
Volume 56 et seq.....	1.00	1.75	.15	.05

* A special rate of 50% of these amounts applies to orders from ACS members for personal use.

RATES FOR VOLUMES OF BACK NUMBERS

Journal	Current Year	Foreign Postage	Canadian Postage
ANALYTICAL CHEMISTRY (formerly Analytical Edition)			
Volumes 1-8.....	\$7.50	\$0.75	\$0.25
Volume 9, et seq.....	15.00	.75	.25
CHEMICAL ABSTRACTS			
Volumes 11-30.....	25.00	2.40	.80
Volume 31, et seq.....	65.00	2.40	.80
CHEMICAL AND ENGINEERING NEWS			
Volumes 1-24.....	5.00	2.25	.75
Volume 25 et seq.....	20.00	2.25	.75
INDUSTRIAL AND ENGINEERING CHEMISTRY			
Volume 1 et seq.....	20.00	2.25	.75
JOURNAL OF AGRICULTURAL AND FOOD CHEMISTRY			
Volume 1 et seq.....	10.00	1.50	.50
* JOURNAL OF THE AMERICAN CHEMICAL SOCIETY			
Volume 32 et seq.....	20.00	1.50	.50
* JOURNAL OF PHYSICAL CHEMISTRY			
Volume 56 et seq.....	15.00	1.20	.40

* Prior Volumes—Order from Walter Johnson, 125 East 23rd Street, New York 10, N. Y.

American Chemical Society

Back Issue Department

1155 Sixteenth Street, N.W.

Washington 6, D.C.